DISSERTATION

ENGINEERING IN VITRO MODELS OF NON-ALCOHOLIC FATTY LIVER DISEASE

Submitted by

Matthew David Davidson

Graduate Degree Program in Bioengineering

In partial fulfillment of the requirements

For the Degree of Doctor of Philosophy

Colorado State University

Fort Collins, Colorado

Spring 2017

Doctoral Committee:

Advisor: Salman R. Khetani

Adam J. Chicco
Seth W. Donahue
Arun K. Kota

ABSTRACT

ENGINEERING IN VITRO MODELS OF NON-ALCOHOLIC FATTY LIVER DISEASE

Decreased resources and a scarcity of affordable, healthy food is contributing to rising obesity rates throughout the world. Consequentially, non-alcoholic fatty liver disease (NAFLD), which is highly correlated with obesity, rates are also increasing with greater than 30% of the US population currently diagnosed. NAFLD starts as a benign state of fat accumulation within liver hepatocytes but often progresses to more detrimental conditions such as non-alcoholic steatohepatitis (NASH), fibrosis/cirrhosis and hepatocellular carcinoma (HCC). There is no cure for NAFLD or its downstream complications and questions still remain about what factors contribute to disease progression. Specifically, the cause(s) of insulin resistance, lipid accumulation, inflammation, and fibrosis are not completely understood. Many of these questions cannot be elucidated in animal models due to confounding contributions from other organs, differences in animal disease pathology (relative to humans) and dietary restrictions. Additionally, if therapies are to be identified for NALFD, human-relevant systems will need to be used due to species differences in drug metabolism enzymes.

Primary human hepatocytes (PHHs) are the gold standard for assessing drug metabolism *in vitro*, but these cells rapidly lose their liver phenotype *in vitro*. Here we show that micropatterned co-cultures (MPCCs) of PHHs and stromal cells maintain glucose and lipid metabolism in hepatocytes, which suggests their utility for *in vitro* disease models of NAFLD. Major advances in culturing methods were developed to increase the insulin sensitivity and overall health of hepatocytes in MPCCs prior to carrying out studies regarding NAFLD-related

insulin resistance. The highly insulin sensitive MPCC model was then used to develop models of fatty acid-induced NAFLD and hepatic stellate cell induced NASH phenotypes. Potential disease mechanisms and treatments for fatty acid-induced insulin resistance and NASH disease progression were identified using these models.

ACKNOWLEDGEMENTS

I would like to acknowledge my advisor, Dr. Salman Khetani, my committee members Dr. Adam Chicco, Dr. Seth Donahue, and Dr. Arun Kota. Thank you for your knowledge, guidance and thoughtful questions.

I would like to thank the faculty and staff at Colorado State University and the University of Illinois at Chicago for collaborations, training, and equipment use, Mrs. Sara Mattern, Mr. Lukasz Zientara, Dr. Melissa Reynolds, Dr. Michael Pagliassotti , Dr. Ketul Popat, and Dr. Terry Unterman. I would like to thank Dr. David Eddington for developing the micropatterned protein plasma etching process I used for every experiment in this dissertation. I would also like thank the undergraduate students that significantly contributed to the experimental work reported here, Josh Pickrell, Adam LeJeune, Michael Lehrer, and Jaron Thompson.

I would like to thank current and past members of the group, particularly my good friends, Dustin Berger, for always being so generous, and providing thoughtful feedback and advice, Brent Ware, for always being someone I can count on, Christine Lin, for helping me logically think things through, and Kim Ballinger, for helping me grow as a mentor and keeping me on my toes. I would like to also acknowledge my funding sources, without which none of this would be possible, Colorado State University and the University of Illinois at Chicago. I would like to thank my family, Mom, Dad, Katie, Bubba, Brittney, and friends, especially Sherlock, for their support throughout this endeavor.

Last, I have to thank Alyssa for always being there for me, believing in me and keeping our relationship strong through anything. We will be together again soon!

TABLE OF CONTENTS

Chapter 1

Introduction

1.1 Liver composition and homeostasis

The liver is composed of multiple cells that make up a functional unit called the sinusoid, where specific tasks are carried out along the functional unit (1). Hepatocytes make up the majority of the cells in the liver (~60%) where their functions along the liver sinusoid are zonated. Specifically, hepatocytes produce proteins and glucose in the periportal region, while they metabolize xenobiotics and store/synthesize lipids in the perivenous region (Fig. 1). Lining the blood vessels of the liver are the hepatic stellate cells (HSCs), which make up approximately 5% of the cells in the liver, store vitamin A, and aid in regeneration (Fig. 1) (2).

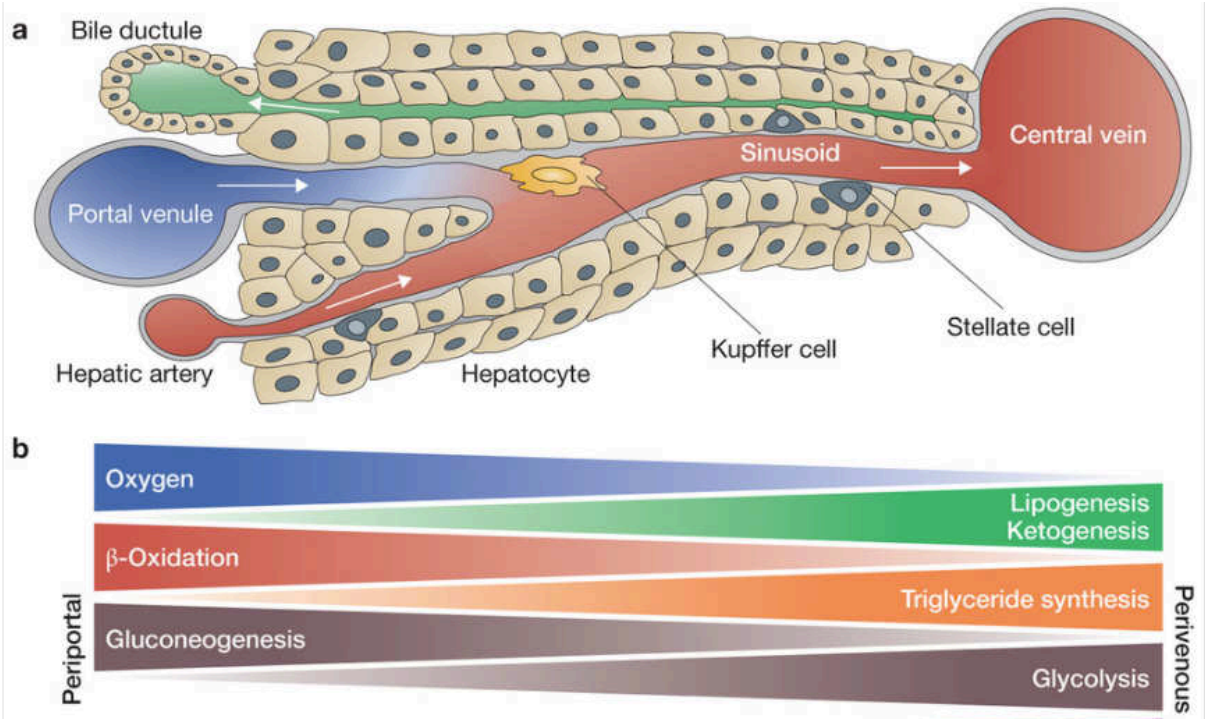

Figure 1.1. Liver composition and zonated functions across the sinusoid. Oxygenated and nutrient-rich blood flows into the periportal region (right) where hepatocytes generally have a

secretory phenotype. The perivenous region (right) has oxygen-depleted blood and mainly metabolizes xenobiotics and produces/stores lipids. Adapted from Birchmeirer, W. Nat. Cell. Bio. 18, 463-465, License granted by Nature Publishing Group Copyright © 2016.

There are other non-parenchymal cells found in the liver such as endothelial cells, immune cells (Kuppfer macrophages and natural killer cells), fibroblasts and biliary epithelial cells, which play various roles in liver health and disease (Fig. 1).

Hepatocytes and stellate cells play interdependent roles in maintaining liver functions. During regeneration, stellate cells produce extracellular matrix (ECM) and growth factors, which induce hepatocyte expansion (3). Alternatively, hepatocytes produce retinol binding protein and albumin, which facilitate the uptake of retinol by stellate cells (4). Furthermore, stellate cells regulate the mechanical properties of the liver by modifying the ECM to maintain a soft (1-6 kPa) substrate for hepatocytes to reside (5). These two cell types act in unison to respond to adverse nutritional stimuli (ie. Excess glucose, fatty acids) and liver damage, although chronic liver insults can make this relationship go awry.

1.2 Nutrition related liver disease

Nutritional homeostasis is crucial for the prevention of metabolic disorders such as non-alcoholic fatty liver disease (NAFLD) and Non-alcoholic steatohepatitis (NASH). NAFLD is characterized by ectopic lipid accumulation within hepatocytes, where more than 5% of the cells have visible lipids (Fig. 2). This fat accumulation or steatosis is considered benign, but it predisposes patients to detrimental downstream complications such as insulin resistance (IR), NASH, cirrhosis and hepatocellular carcinoma (HCC) (6). NAFLD currently affects more than 30% of the US population and is generally found in obese or type 2 diabetic patients. There is no

cure for this disease and massive efforts are underway to identify potential therapies to reduce the symptoms of NAFLD.

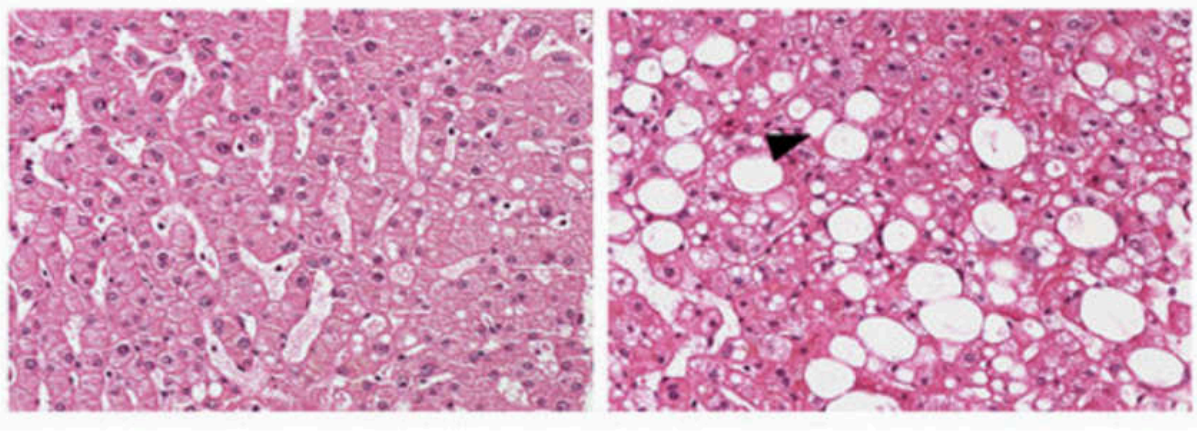

Figure 1.2. Histology of a normal and fatty liver. H+E stain showing normal (left) and NAFLD (right) liver histology in human liver. Arrow points to lipid accumulation. Adapted from Wruck, W. et al. Scientific Data (2), 150068, which is free to disseminate under the CC-BY license.

1.3 Hepatocyte nutrient metabolism and insulin signaling

Upon ingesting a meal, there is a spike in blood glucose as well as lipid levels, which triggers the release of insulin from the pancreas. Insulin stimulates adipose tissue to take up excess fats, while also stimulating the liver to store excess glucose (7). Hepatocytes will store glucose as a polymer, glycogen, as well as fatty acids after glucose has been broken down through glycolysis. The liver also has an enormous capability to produce glucose from glycolytic intermediates, as well as amino acid and lipid precursors during fasting. This process of glucose production, or gluconeogenesis, is activated by another pancreatic hormone, glucagon, and shut off by the action of insulin (8). During times of starvation, the liver can provide glucose for the entire body, although gluconeogenesis can also be overactive in diabetic patients with insulin resistance (9). Interestingly, diabetic patients have a unique signature in their type of insulin

resistance, termed ‘selective insulin resistance’ where insulin fails to shut down glucose production in the liver while still stimulating the production of lipids (1,10). This leads to a state of hyperglycemia, with increasing lipid accumulations in the liver; a vicious cycle that can only be overcome with exercise and or serious surgical intervention.

Vitamin A aids in normal hepatocyte signaling with regard to drug metabolism and lipid homeostasis (2,11,12). Additionally, vitamin A has been shown to prevent hepatic stellate cell activation, which occurs in chronic liver disease (3,13). Although, tissue vitamin A levels have been shown as one of the first nutrients to decrease in the liver as humans become obese, which could have detrimental effects on hepatocytes (4,14).

1. 4 Hepatocyte lipid metabolism

The majority of the dietary fat is absorbed by adipose tissue, while the liver mainly takes up lipids lysed from inflamed fat tissue (5,15). Additionally, excess glucose is also converted to lipids via the protein Fatty Acid Synthase. The liver also takes up LDL, HDL, and chylomicrons, which contain free fatty acids, triglycerides and cholesterol. Fatty acids can be used for energy production through beta-oxidation, while triglycerides need to be broken down into fatty acids prior to use for energy production. Additionally, fatty acids and cholesterol can be incorporated into cell membranes to adjust membrane fluidity. Once energy and membrane-associated needs of the cell are fulfilled, excess lipids, as well as cholesterol sources, combine to form lipid droplets within hepatocytes (6,16). Healthy hepatocytes package triglycerides and cholesterol esters into VLDL particles and secrete them for use by the rest of the body. In animal models of nonalcoholic fatty liver disease, this function is significantly decreased (7,17). The production of

lipids within hepatocytes from precursors such as glucose is also increased in NAFLD (18). Specific hepatic lipids, such as diacylglycerol and ceramides, have been shown to decrease hepatic insulin signaling pathway proteins, which contributes to type II diabetes progression in patients with NAFLD (9,19). Steatotic hepatocytes have also been shown to activate local stromal cells via exosomal and paracrine signaling, which can further exacerbate disease progression (20). Within the progressive stages of non-alcoholic steatohepatitis, excessive cholesterol and lipid peroxides build up in hepatocytes and have been shown to contribute to hepatocyte malfunction and apoptosis (21). New potential therapies that show efficacy in reducing or preventing NAFLD in animal models are published often. Unfortunately, there are key differences between animal disease models and the human progression of NAFLD, which limits the translation of therapies developed using animal models.

All NAFLD animal disease models have the basic requirement to recapitulate the abnormal lipid accumulation, ≥5% of hepatocytes containing visible lipids, seen in NAFLD patients, but there are major differences between animal and human disease progression. One major difference is the location within the liver sinusoid where lipids first begin to accumulate. In humans, steatosis starts in the perivenous region, and then makes its way to the periportal region before it fills the liver parenchyma completely. Rodent NAFLD models show an opposite trend, with steatosis starting in the periportal region (22). Additional discrepancies between animal models and human disease can also be seen when considering metabolic and disease severity differences. The most common animal model to study non-alcoholic steatohepatitis (NASH), a progressive stage of NAFLD, is developed by feeding mice a methionine and choline deficient (MCD) diet (22,23). This causes a massive infiltration of inflammatory cells, fibrosis, steatosis, and liver injury, similar to NASH (Fig. 3). Alternatively, the animals on this diet

actually become more insulin sensitive, lose weight and never become hyperglycemic. It is thought that the lack of methionine and choline inhibits phosphatidyl choline production and subsequent release of VLDL particles out of hepatocytes (17). The MCD diet might allow the researcher to study the damage of steatohepatitis, although there is little relevance of this diet on human pathophysiology since a lack of these molecules in most NAFLD patient diets is not a significant issue.

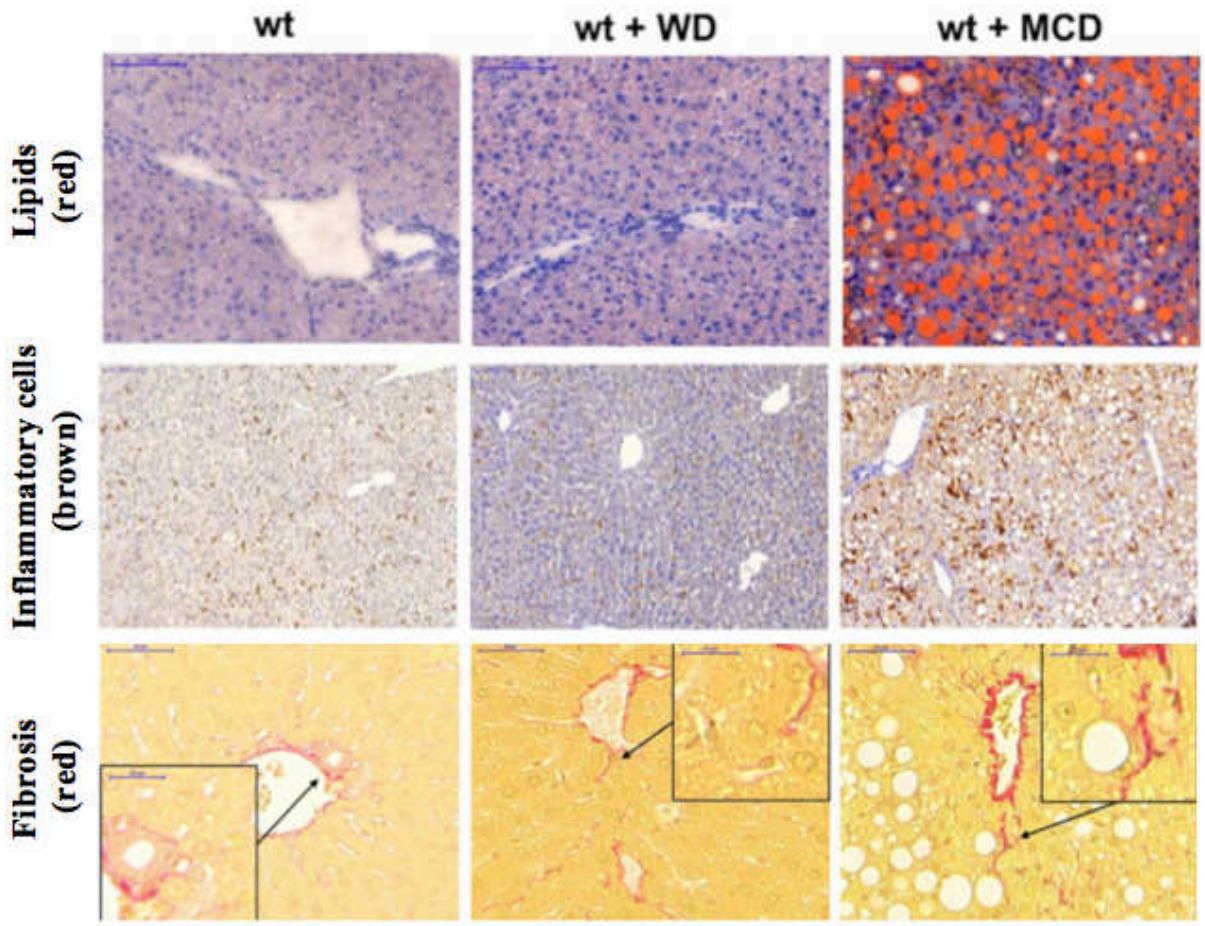

Figure 1.3. Comparison of different diets effects on liver histology. Normal chow (wt), western diet (wt+WD) and MCD diet (wt+MCD) were given to mice for 7 weeks and their lipid, inflammatory cell infiltrate and fibrosis levels were visualized in histology slides. Adapted from Schierwaen et al. Sci Reports. 2016.doi:1038/srep12931 which is free to disseminate under the CC-BY license.

The high-fat diet, as well as genetically altered hyperphagic mouse models, have also been used to a great extent in NAFLD research. Hyperinsulinemia, weight gain, hyperglycemia and liver fat accumulation are all found in these models, although the level of disease severity is nowhere near that of NASH patients or the MCD diet (23). Specifically, these models generally show less fibrosis, inflammation and liver damage (Fig. 3). Additionally, similar levels of lipid accumulation found in human NAFLD patients have only been attained in rodent models by gavage, or forced feeding of high-fat diets. Fortunately, some recently developed diet-induced models are bridging the gap between human and rodent NAFLD by including components found in most obese westerner diets, such as high amount of cholesterol, the western diet, and even the addition of artificial trans-fatty acids, the fast food diet (24). Using these advanced diets, researchers are able to obtain mouse models with severe fibrosis, steatosis, inflammation, and liver cell damage. Even so, there still remains the challenge of recapitulating the distinct differences between rodent and human drug metabolism pathways in order to enable translatable results on the efficacy of compounds for treating human disease (25).

1.5 Bile acids, transporters, and nuclear receptors

Cholesterol is converted to bile acids, cholic acid (CA) and chenodeoxycholic acid (CDCA), via the actions of CYP7A1 and CYP8B1 (Fig. 4). This pathway constitutes ~75% of the bile acids produced in the liver, although an alternative pathway that is regulated by CYP27A1, also shows significant contributions to bile acid production (26). Importantly, there are distinct differences between human and rodent bile acids pools. While CA and CDCA make up the majority of bile acids in humans, mouse bile acids are made up of mostly Beta-muricholic

acid and to a lesser extent CA (27). These differences may play a role in drug development as bile acids are now recognized as key intracellular signaling molecules that regulate hepatocyte metabolism (28). Either way, CYP450 enzymes are the major regulators of bile acid production.

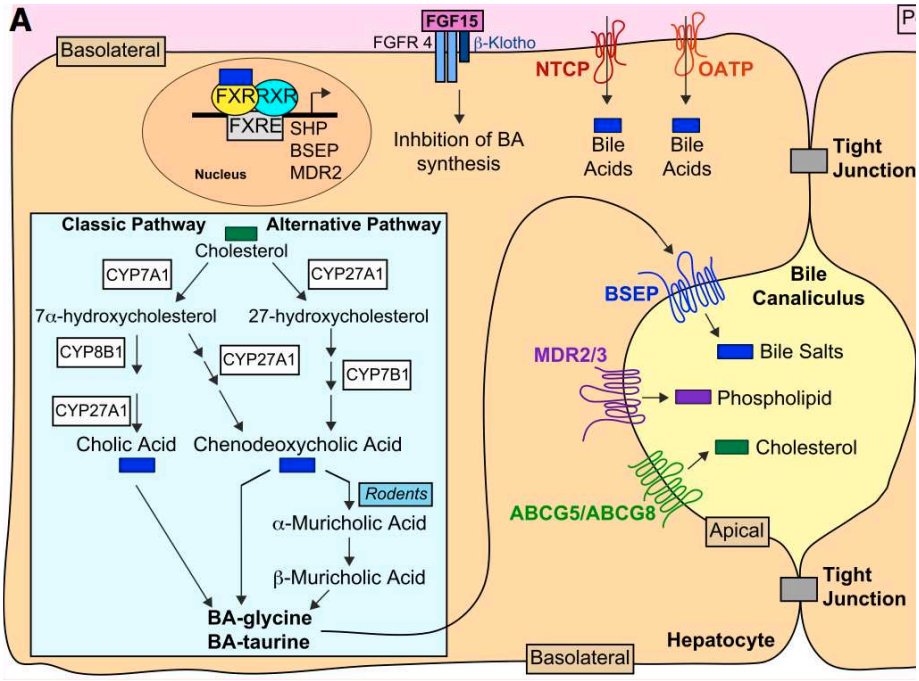

Figure 1.4. Bile acid production, regulation and excretion in hepatocytes. Hepatocytes take up bile acids from the portal blood circulation and also produce them through CYP 450 mediated pathways. FXR acts to shut down bile production pathways and increase bile excretion pathways. Adapted from de Aguiar Vallim, TQ et al. Cell Metab. 17 (5):657-69. 2013, License granted by Elsevier Inc Copyright © 2013.

Bile acids, such as CA and CDCA, can freely move in and out of the cell membrane, although most bile acids are amidated with taurine or glycine to increase their pKa and their ability to form micelles within the acidic duodenum of the small intestine. Within the intestine, the amphipathic nature of bile salts enables the absorption of lipids and fat-soluble vitamins, such as vitamin A (29). Bile salts play a role in nutrient absorption as well as regulating negative feedback loops on bile acid production within hepatocytes. Unlike bile acids, these conjugated

bile salts need transporters to get them in and out of the cell, and their build up within the liver can cause damage to organelles and subsequent oxidative stress (30).

Common diseases, such as primary biliary and liver -cirrhosis, are characterized by cholestasis or the buildup of bile within the liver. Additionally, it is now recognized that NASH patients have abnormal bile as well other biotic and xenobiotic accumulations within the liver and associated altered transporter expression in the liver (31). Na^+-taurocholate cotransporting polypeptide (NTCP), and to a lesser extent the solute carrier organic anion transporter family of proteins (SLCOs), mediate the uptake of conjugated bile salts, drugs and biological waste products such as bilirubin, into the liver (Fig. 4). Multidrug resistant-like proteins (MRPs 1,3 and 4) excrete these same components back into the blood when levels are too high in hepatocytes. Additionally, MRP2 and the bile salt export pump (BSEP) coordinate the major excretion of conjugated bilirubin and drugs as well as bile acids into the apical (canalicular) lumen. All of the aforementioned transporters have been shown to be downregulated, except for MRP4, in human NASH or fibrotic livers (32). Although, animal disease models have shown opposite trends in transporter expression (33). Since there is a coordinated down regulation of these transporters, some believe that NASH mediators, such as inflammation, act on master transcription factors, such as nuclear receptors, to orchestrate this effect (34).

The farnesoid x receptor (FXR), pregnane x receptor (PXR) and constitutive androstane receptor (CAR) are all bile-sensitive nuclear receptors found in hepatocytes that act to maintain normal homeostatic functions of the liver such as elimination of toxins and metabolites and regulation of drug, glucose and lipid metabolism (28). FXR appears to mostly be affected by bile acids, while PXR and CAR are also modulated by xenobiotics (35). FXR is activated by a variety of bile acids and acts as an intracellular bile acid rheostat by downregulating bile acid production

pathways, such as CYP7A1, as well as bile uptake proteins, such as NTCP, and increasing the expression of bile export transporters, such as MRP2 and BSEP (Fig. 4) (29). Additionally, FXR can rehabilitate lipid and glucose metabolism in fatty livers by shutting down lipid production and repressing excessive glucose production. A synthetic form of the natural agonist, CDCA, for FXR, called obeticholic acid (OCA) has a much higher affinity for FXR than any natural ligand and has been shown to recapitulate the beneficial effects of FXR activation (36). Additionally, OCA has shown beneficial effects for type II diabetic NASH patients by positively regulating the aforementioned pathways as well as decreasing inflammation (37). PXR and CAR are also activated by increases in bile acids and respond by increasing bile metabolism and excretion pathways. PXR, specifically acts by increasing enzymes, such as CYP3A4, and transporters to increase the removal of bile acids from hepatocytes (35). Importantly, FXR, PXR and CAR have all been shown to be downregulated in NAFLD/NASH and therefore have been critical targets for treatment. Human-relevant models will undoubtedly aid the development of therapies that target these pathways.

1.6 Drug metabolism/toxicity

Along with bile acid regulation, nuclear receptors also control drug metabolism enzymes that are a part of the cytochrome P450 family. Accordingly, drug metabolism pathways are altered in NALFD and NASH in humans and animal disease models. Although, studies regarding the trends in CYP450 have differed tremendously, and the only consistent effects of this disease have been shown in late stage NASH and associated fibrosis (38). These studies have shown a general decrease in CYP450 activity, especially for CYP3A4. By administering midazolam, a

substrate for CYP 3A4, to biopsy-proven NASH patients, it has been shown that the degree of fibrosis as well as inflammation and hepatocyte ballooning negatively correlate with midazolam turnover (39). *In vitro* studies with primary hepatocyte as well as hepatocyte cell lines have shown that lipid overloading with the saturated fatty acid, palmitic acid, causes steatosis and a concomitant decrease in CYP3A4. Additionally, Donato et al. also found that NAFLD patient hepatocytes generally had decreased CYP3A4 enzyme levels (40). However, Niemelä et al. found CYP3A4 to be upregulated and Fisher et al. found it to be unchanged in patients with NAFLD. Due to the enormous amount of factors that can contribute to NAFLD pathogenesis, it is not surprising that conflicting results have been reported. Recent reviews have suggested that we should stop considering the old NAFLD dogma, termed the 'two-hit hypothesis', and consider NAFLD as a disease where multiple events can simultaneously induce NASH rather than steatosis being the primary symptom prior to disease progression (41). With this line of thought, one could imagine that very different results would be obtained by assessing patients solely based on their hepatic lipid profile and suggest that specific biomarkers need to be developed in order to identify the main etiology of NASH development. Model systems, either *in vitro* or *in vivo*, that can recapitulate NASH based on specific manipulated etiologies may help elucidate different subsets of NASH and also identify new targets for disease therapy.

1.7 Hepatic stellate cells

Hepatic stellate cells (HSCs), the mesenchymal vitamin-A storing cells of the liver, aid in liver regeneration in health, while they contribute to fibrosis and hepatocellular carcinoma progression in disease (42-44). HSCs have a quiescent phenotype in the normal liver, but upon

stimulation, they become activated and secrete various molecules (collagen, MMPs, TIMPs, growth factors and cytokines) that can engender the organ to an altered functional state (Fig. 5) (2). Some diseases associated with activated HSCs include viral infection, drug-induced liver injury, and the most prominent ailment non-alcoholic fatty liver disease (NAFLD), which affects ~30% of the general population (45).

Non-alcoholic steatohepatitis (NASH) is considered the progressive stage of NAFLD and fibrosis usually accompanies this disease. NASH is increasing in prevalence (5-10% of NAFLD patients) and the lack of treatment options makes this disease the second highest etiology for a liver transplant (46). Resident liver and bone marrow-derived hematopoietic cells (Kupffer macrophages, natural killer T cells etc) have rightly gained the spotlight in the pathogenesis of NASH due to their well-known pro-inflammatory capabilities and characteristic accumulation in NASH livers (47).

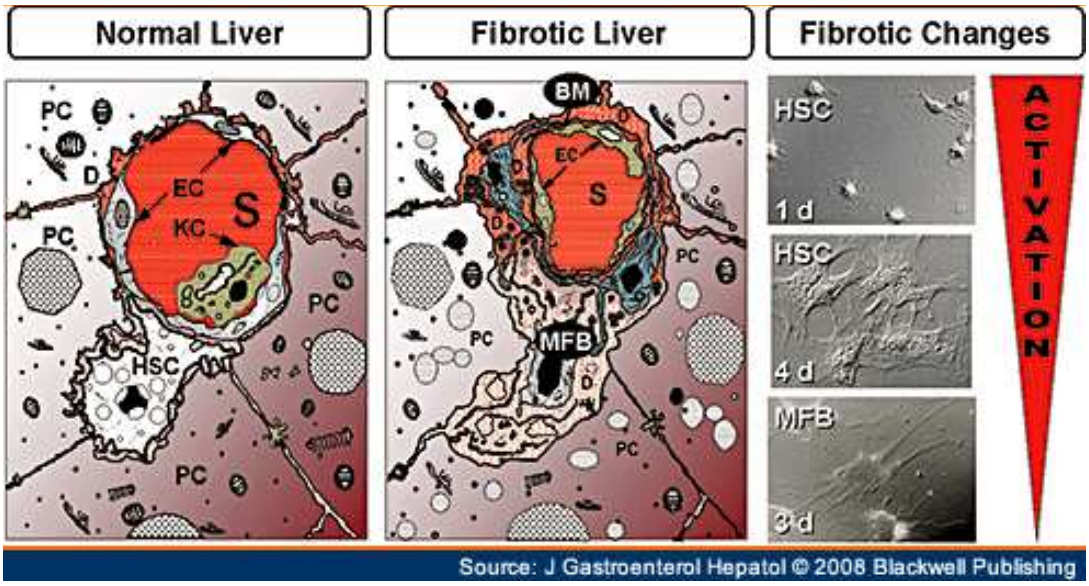

Figure 1.5. Quiescent and activated HSCs. HSCs in the normal liver reside between the endothelial cells (EC) and parenchymal hepatocytes (PC) in the space of disse (D). These HSCs are quiescent and store vitamin A. In the fibrotic liver, activated HSCs assume a myofibroblast phenotype (MFB) while inflammatory cells (blue) infiltrate the parenchyma and significant extracellular matrix (BM) accumulates. (Right) HSCs become activated in culture. Adapted from Gressner, O A, et al. J. Gastroenterol Hepatol. 23(7):1024-35. 2008, License granted by The

Although, fibrosis, not inflammation, has recently been identified as the major predictor of the long-term outcomes for patients with NASH (48). Therefore, it is plausible that other liver cell types capable of promoting an immune response and fibrosis could be involved in the development of human NASH symptoms.

HSCs are generally thought of as innocent bystanders that are activated as a response to factors first produced by immune cells and hepatocytes during NASH (49). This may not always be the case, since HSCs can not only initiate inflammation, by secreting cytokines (ie: TNFa and IL-6), but also become activated by non-hepatocyte/immune cell stimuli such as tissue compliance and hormonal/nutrient signaling. Specifically, increased substrate stiffness, insulin, and a loss of vitamin A have been shown to activate HSCs *in vitro*, all of which are common symptoms in fibrosis, NASH, and obesity (5,14,50,51). In line with the 'multiple parallel hit' hypothesis, HSCs could play a role in initiating NASH, or yet to be defined subsets of the disease, as well as sustaining the disease phenotype as obese patient livers progress to an insulin resistant, and inflamed/fibrotic state (6,41). Although the effects of activated primary HSCs on hepatocytes have scarcely been addressed (52-55). Moving forward, in vitro models of NASH will need to incorporate hepatic stellate cells, as well as other inflammatory cells.

1.8 Current *in vitro* liver models

Hepatocytes rapidly dedifferentiate outside of the body when cultured *in vitro* (56). They change from having a characteristic cuboidal epithelial morphology, to a flattened, well-spread

fibroblast-like phenotype (57). Additionally, these hepatocytes secrete many growth factors, such as TGFβ, and cytokines associated with liver disease such as fibrosis (58,59). Even when they are cultured in a way that maintains hepatocyte functions, they still do not proliferate, which presents a difficult problem for sourcing these cells. Therefore maintaining their phenotype and function *in vitro* is critical to the study of human hepatocytes. Accordingly, many attempts have been made to identify methods that increase the retention of hepatocyte phenotype *in vitro* (60). Sandwich cultures, which sandwiches hepatocytes between two collagen gels, have been shown to extend the phenotype of hepatocytes *in vitro*, which could be due to the maintenance of a 3D environment and or a compliant substrate that mimics the *in vivo* stiffness (57). Unfortunately, hepatocytes in this format have a limited lifetime and do not retain all hepatocyte functions such as glucose metabolism (61). Considering compliance and three-dimensions as important parameters, many attempts have been made to create long-term hepatocyte cultures by fabricating cell spheroids (60). Briefly, hepatocytes are seeded into non-adherent wells so that they self-organize into spherical 'organoids.' This method allows for the introduction of other cell types found in the liver and can maintain hepatocyte phenotype for about 4 weeks *in vitro*. There are practical limitations to this system since imaging organoids requires sectioning and the small number of cells makes it difficult to detect changes in hepatocyte secretions. Therefore a high throughput system based on this method will be difficult to attain.

1.9 Micropatterned co-cultures

In the 1980s Begue et al. fortunately found that co-culturing hepatocytes with supportive cells extends their lifetime and improves their functions *in vitro* (62). The major drawback to this

co-culture format was that the cells were randomly distributed, which decreased consistency from well to well and made it difficult to elucidate the role of cell-cell interactions in maintaining hepatocyte phenotype (63). Bhatia et al. overcame this limitation by micropatterning collagen domains using lithographic techniques, which can be subsequently patterned with hepatocytes (64). This improved the control over the number of hepatocytes that can attach and the level of homotypic, same cell, and heterotypic interactions in co-cultures. Khetani et al. then identified the mouse embryonic 3T3-J2 clone as an optimal supportive cell for hepatocytes from multiple species, by comparing the ability of other similar cells to support hepatocyte functions (65). This specific mouse fibroblast clone has been compared to other human liver non-parenchymal cells (endothlial, Kupffer, and stellate cells) in our lab, and it supports hepatocytes at significantly higher levels than any cells we tested. Eventually Khetani and Bhatia published a high throughput micropatterned co-culture (MPCC) platform for human hepatocytes with an optimized geometry for maintaining hepatocyte functions (66). The architecture of this system does not reflect the liver sinusoid, but the circular patterns used retain their shape for an extended period of time while other geometries may become altered. Additionally, hepatocyte transporters, polarity, and glucose metabolism, key determinants of disease progression in NASH, are retained at higher levels in the MPCCs than any other model available (61). The MPCC provides the field with exceptionally long-lived cultures (3-4 weeks), but the suggested lifetime of a hepatocyte in a healthy liver is about 1 year and therefore there is still room for improvement.

1.10 Motivation for this dissertation

There is a clear need to develop a better understanding of how metabolic disease affects the liver as the metabolic syndrome is now spreading throughout the world. With the latter issue in mind, *in vitro* models of the liver that retain the aspects of liver physiology (glucose, lipid and drug metabolism as well as transporters and bile production) that are important for normal liver health and altered in pathologic conditions in the liver, such as NAFLD and NASH, are in great need. Models that retain these functions of the liver will undoubtedly aid researchers ranging from tissue engineers to molecular biologists who's interests lie in the field of metabolic disease. Inspired by the lack of effort put forth by the bioengineering community to aid type II diabetes research, this dissertation has been dedicated to developing tools to further our understanding of this disease, its related complications in the liver and eventually developing new treatments for diabetic complications in the liver by making the first *in vitro* disease models of fatty liver disease. Major technological hurdles must be overcome to achieve this goal. A human liver model that retains hepatocyte glucose metabolism and insulin sensitivity must first be developed. This model will need to have an extended lifetime and durability so that chronic treatments, necessary for disease development, can be administered. Additionally, non-parenchymal liver cells will need to be incorporated into this system to recapitulate the critical cell-cell interactions that occur in NAFLD and NASH.

References

1. Gebhardt R, Matz-Soja M. Liver zonation: Novel aspects of its regulation and its impact on homeostasis. **20**(26), 8491, 2014.

2. Friedman SL. Hepatic Stellate Cells: Protean, Multifunctional, and Enigmatic Cells of the Liver. Physiological Reviews. **88**(1), 125, 2008.

3. Ding B-S, Cao Z, Lis R, Nolan DJ, Guo P, Simons M, et al. Divergent angiocrine signals from vascular niche balance liver regeneration and fibrosis. **505**(7481), 97, 2014.

4. Vicente CP, Fortuna VA, Margis R, Trugo L, Borojevic R. Retinol uptake and metabolism, and cellular retinol binding protein expression in an in vitro model of hepatic stellate cells. Mol. Cell. Biochem. **187**(1-2), 11, 1998.

5. Olsen AL, Bloomer SA, Chan EP, Gaça MDA, Georges PC, Sackey B, et al. Hepatic stellate cells require a stiff environment for myofibroblastic differentiation. AJP: Gastrointestinal and Liver Physiology. **301**(1), G110, 2011.

6. Birkenfeld AL, Shulman GI. Nonalcoholic fatty liver disease, hepatic insulin resistance, and type 2 diabetes. Hepatology. **59**(2), 713, 2014.

7. Samuel VT, Liu ZX, Qu X, Elder BD, Bilz S, Befroy D, et al. Mechanism of Hepatic Insulin Resistance in Non-alcoholic Fatty Liver Disease. Journal of Biological Chemistry. **279**(31), 32345, 2004.

8. Puigserver P, Rhee J, Donovan J, Walkey CJ, Yoon JC, Oriente F, et al. Insulin-regulated hepatic gluconeogenesis through FOXO1-PGC-1alpha interaction. Nature. **423**(6939), 550, 2003.

9. Boden G, Chen X, Stein TP. Gluconeogenesis in moderately and severely hyperglycemic patients with type 2 diabetes mellitus. American Physiological Society; **280**(1), E23, 2001.

10. Brown MS, Goldstein JL. Selective versus Total Insulin Resistance: A Pathogenic Paradox. Cell Metabolism. **7**(2), 95, 2008.

11. Amengual J, Ribot J, Bonet ML, Palou A. Retinoic acid treatment enhances lipid oxidation and inhibits lipid biosynthesis capacities in the liver of mice. Cellular physiology and biochemistry : international journal of experimental cellular physiology, biochemistry, and pharmacology. **25**(6), 657, 2010.

12. Kim SC, Kim C-K, Axe D, Cook A, Lee M, Li T, et al. All-trans-retinoic acid ameliorates hepatic steatosis in mice by a novel transcriptional cascade. Hepatology.

59(5), 1750, 2014.

13. Taghdouini El A, Najimi M, Sancho-Bru P, Sokal E, van Grunsven LA. In vitro reversion of activated primary human hepatic stellate cells. Fibrogenesis & Tissue Repair. Fibrogenesis & Tissue Repair; 1, 2016.

14. Trasino SE, Tang X-H, Jessurun J, Gudas LJ. Obesity Leads to Tissue, but not Serum Vitamin A Deficiency. Sci. Rep. Nature Publishing Group; 1, 2016.

15. Samuel VT, Shulman GI. Mechanisms for Insulin Resistance: Common Threads and Missing Links. Cell. **148**(5), 852, 2012.

16. Walther TC, Farese RV Jr. Lipid Droplets and Cellular Lipid Metabolism. Annual Review of Biochemistry. **81**(1), 687, 2012.

17. Rinella ME, Elias MS, Smolak RR, Fu T, Borensztajn J, Green RM. Mechanisms of hepatic steatosis in mice fed a lipogenic methionine choline-deficient diet. The Journal of Lipid Research. **49**(5), 1068, 2008.

18. Postic C, Girard J. Contribution of de novo fatty acid synthesis to hepatic steatosis and insulin resistance: lessons from genetically engineered mice. Journal of clinical Investigation. **118**(3), 829, 2008.

19. Perry RJ, Samuel VT, Petersen KF, Shulman GI. The role of hepatic lipids in hepatic insulin resistance and type 2 diabetes. Nature. **510**(7503), 84, 2014.

20. Wobser H, Dorn C, Weiss TS, Amann T, Bollheimer C, Büttner R, et al. Lipid accumulation in hepatocytes induces fibrogenic activation of hepatic stellate cells. Cell Res. Nature Publishing Group; **19**(8), 996, 2009.

21. Chalasani N, Deeg MA, Crabb DW. Systemic levels of lipid peroxidation and its metabolic and dietary correlates in patients with nonalcoholic steatohepatitis. Am J Gastroenterology. **99**(8), 1497, 2004.

22. Takahashi Y, Soejima Y, Fukusato T. Animal models of nonalcoholic fatty liver disease/nonalcoholic steatohepatitis. WJG. **18**(19), 2300, 2012.

23. Winzell MS, Ahren B. The High-Fat Diet-Fed Mouse: A Model for Studying Mechanisms and Treatment of Impaired Glucose Tolerance and Type 2 Diabetes. Diabetes. American Diabetes Association; **53**(Supplement 3), S215, 2004.

24. Charlton M, Krishnan A, Viker K, Sanderson S, Cazanave S, McConico A, et al. Fast food diet mouse: novel small animal model of NASH with ballooning, progressive fibrosis, and high physiological fidelity to the human condition. AJP: Gastrointestinal and Liver Physiology. **301**(5), G825, 2011.

25. Martignoni M, Groothuis GMM, de Kanter R. Species differences between mouse, rat, dog, monkey and human CYP-mediated drug metabolism, inhibition and

induction. Expert Opin Drug Metab Toxicol. Taylor & Francis; **2**(6), 875, 2006.

26. Schwarz M, Lund EG, Setchell KD, Kayden HJ, Zerwekh JE, Björkhem I, et al. Disruption of cholesterol 7alpha-hydroxylase gene in mice. II. Bile acid deficiency is overcome by induction of oxysterol 7alpha-hydroxylase. The Journal of Biological Chemistry. **271**(30), 18024, 1996.

27. Sayin SI, Wahlström A, Felin J, Jäntti S, Marschall HU, Bamberg K, et al. Gut microbiota regulates bile acid metabolism by reducing the levels of tauro-beta-muricholic acid, a naturally occurring FXR antagonist. Cell Metabolism. **17**(2), 225, 2013.

28. Schaap FG, Trauner M, Jansen PLM. Bile acid receptors as targets for drug development. Nat Rev Gastroenterol Hepatol. **11**(1), 55, 2014.

29. de Aguiar Vallim TQ, Tarling EJ, Edwards PA. Pleiotropic Roles of Bile Acids in Metabolism. Cell Metabolism. Elsevier Inc; **17**(5), 657, 2013.

30. Sokol RJ, Winklhofer-Roob BM, Devereaux MW, McKim JM Jr. Generation of hydroperoxides in isolated rat hepatocytes and hepatic mitochondria exposed to hydrophobic bile acids. Gastroenterology. **109**(4), 1249, 1995.

31. Okushin K, Tsutsumi T, Enooku K, Fujinaga H, Kado A, Shibahara J, et al. The intrahepatic expression levels of bile acid transporters are inversely correlated with the histological progression of nonalcoholic fatty liver disease. J. Gastroenterol. **51**(8), 808, 2016.

32. Nakai K, Tanaka H, Hanada K, Ogata H, Suzuki F, Kumada H, et al. Decreased Expression of Cytochromes P450 1A2, 2E1, and 3A4 and Drug Transporters Na+-Taurocholate-Cotransporting Polypeptide, Organic Cation Transporter 1, and Organic Anion-Transporting Peptide-C Correlates with the Progression of Liver Fibrosis in Chronic Hepatitis C Patients. Drug metabolism and disposition. **36**(9), 1786, 2008.

33. Canet MJ, Hardwick RN, Lake AD, Dzierlenga AL, Clarke JD, Cherrington NJ. Modeling Human Nonalcoholic Steatohepatitis-Associated Changes in Drug Transporter Expression Using Experimental Rodent Models. Drug metabolism and disposition. **42**(4), 586, 2014.

34. Ogura J, Terada Y, Tsujimoto T, Koizumi T, Kuwayama K, Maruyama H, et al. The Decrease in Farnesoid X Receptor, Pregnane X Receptor and Constitutive Androstane Receptor in the Liver after Intestinal Ischemia-Reperfusion. J Pharm Pharm Sci. **15**(5), 616, 2012.

35. Musso G, Cassader M, Gambino R. Non-alcoholic steatohepatitis: emerging molecular targets and therapeutic strategies. Nature Publishing Group. Nature Publishing Group; 1, 2016.

36. Verbeke L, Farre R, Trebicka J, Komuta M, Roskams T, Klein S, et al. Obeticholic acid, a farnesoid X receptor agonist, improves portal hypertension by two distinct pathways in cirrhotic rats. Hepatology. **59**(6), 2286, 2014.

37. MD PBAN-T, MD RL, MD PAJS, MD PJEL, Van Natta MHS ML, MD MFA, et al. Farnesoid X nuclear receptor ligand obeticholic acid for non-cirrhotic, non-alcoholic steatohepatitis (FLINT):a multicentre, randomised, placebo-controlled trial. The Lancet. Elsevier Ltd; **385**(9972), 956, 2015.

38. Fisher CD, Lickteig AJ, Augustine LM, Ranger-Moore J, Jackson JP, Ferguson SS, et al. Hepatic cytochrome P450 enzyme alterations in humans with progressive stages of nonalcoholic fatty liver disease. Drug metabolism and disposition. **37**(10), 2087, 2009.

39. Woolsey SJ, Mansell SE, Kim RB, Tirona RG, Beaton MD. CYP3A Activity and Expression in Nonalcoholic Fatty Liver Disease. Drug metabolism and disposition. **43**(10), 1484, 2015.

40. Donato MT, Jimenez N, Serralta A, Mir J, Castell JV, Gomez-Lechon MJ. Effects of steatosis on drug-metabolizing capability of primary human hepatocytes. Toxicology in Vitro. **21**(2), 271, 2007.

41. Buzzetti E, Pinzani M, Tsochatzis EA. The multiple-hit pathogenesis of non-alcoholic fatty liver disease (NAFLD). Metabolism. 2016.

42. Ji J, Eggert T, Budhu A, Forgues M, Takai A, Dang H, et al. Hepatic stellate cell and monocyte interaction contributes to poor prognosis in hepatocellular carcinoma. Hepatology. **62**(2), 481, 2015.

43. Kang N, Gores GJ, Shah VH. Hepatic stellate cells: Partners in crime for liver metastases? Hepatology. **54**(2), 707, 2011.

44. Yin C, Evason KJ, Asahina K, Stainier DYR. Hepatic stellate cells in liver development, regeneration, and cancer. Journal of clinical Investigation. **123**(5), 1902, 2013.

45. Chalasani N, Younossi Z, Lavine JE, Diehl AM, Brunt EM, Cusi K, et al. The diagnosis and management of non-alcoholic fatty liver disease: practice Guideline by the American Association for the Study of Liver Diseases, American College of Gastroenterology, and the American Gastroenterological Association. Hepatology. p. 2005–23, 2012.

46. Wong RJ, Aguilar M, Cheung R, Perumpail RB, Harrison SA, Younossi ZM, et al. Nonalcoholic steatohepatitis is the second leading etiology of liver disease among adults awaiting liver transplantation in the United States. Gastroenterology. **148**(3), 547, 2015.

47. Wree A, Broderick L, Canbay A, Hoffman HM, Feldstein AE. From NAFLD to

NASH to cirrhosis-new insights into disease mechanisms. Nature Publishing Group. **10**(11), 627, 2013.

48. Angulo P, Kleiner DE, Dam-Larsen S, Adams LA, Bjornsson ES, Charatcharoenwitthaya P, et al. Liver Fibrosis, but No Other Histologic Features, Is Associated With Long-term Outcomes of Patients With Nonalcoholic Fatty Liver Disease. Gastroenterology. **149**(2), 389, 2015.

49. Nati M, Haddad D, Birkenfeld AL, Koch CA, Chavakis T, Chatzigeorgiou A. The role of immune cells in metabolism-related liver inflammation and development of non-alcoholic steatohepatitis (NASH). Rev Endocr Metab Disord. **17**(1), 29, 2016.

50. Svegliati-Baroni G, Ridolfi F, Di Sario A, Casini A, Marucci L, Gaggiotti G, et al. Insulin and insulin-like growth factor-1 stimulate proliferation and type I collagen accumulation by human hepatic stellate cells: differential effects on signal transduction pathways. Hepatology. **29**(6), 1743, 1999.

51. Hellemans K, Grinko I, Rombouts K, Schuppan D, Geerts A. All-trans and 9-cis retinoic acid alter rat hepatic stellate cell phenotype differentially. Gut. **45**(1), 134, 1999.

52. Jeong W-I, Osei-Hyiaman D, Park O, Liu J, Bátkai S, Mukhopadhyay P, et al. Paracrine Activation of Hepatic CB1 Receptors by Stellate Cell-Derived Endocannabinoids Mediates Alcoholic Fatty Liver. Cell Metabolism. **7**(3), 227, 2008.

53. Chen L, Charrier A, Zhou Y, Chen R, Yu B, Agarwal K, et al. Epigenetic regulation of connective tissue growth factor by MicroRNA-214 delivery in exosomes from mouse or human hepatic stellate cells. Hepatology. **59**(3), 1118, 2014.

54. Qian H, Deng X, Huang Z-W, Wei J, Ding C-H, Feng R-X, et al. An HNF1a-regulated feedback circuit modulates hepatic fibrogenesis via the crosstalk between hepatocytes and hepatic steallate cells. Cell Res. Nature Publishing Group; **25**(8), 930, 2015.

55. Leite SB, Roosens T, Taghdouini El A, Mannaerts I, Smout AJ, Najimi M, et al. Novel human hepatic organoid model enables testing of drug-induced liver fibrosis in vitro. Biomaterials. Elsevier Ltd; **78**(C), 1, 2015.

56. Richert L, Liguori MJ, Abadie C, Heyd B, Mantion G, Halkic N, et al. Gene expression in human hepatocytes in suspension after isolation is similar to the liver of origin, is not affected by hepatocyte cold storage and cryopreservation, but is strongly changed after hepatocyte plating. Drug metabolism and disposition. **34**(5), 870, 2006.

57. Desai SS, Tung JC, Zhou VX, Grenert JP, Malato Y, Rezvani M, et al. Physiological Ranges of Matrix Rigidity Modulate Primary Mouse Hepatocyte Function in Part Through Hepatocyte Nuclear Factor 4 Alpha. Hepatology. **64**(1), 261, 2016.

58. Nanthakumar CB, Hatley RJD, Lemma S, Gauldie J, Marshall RP, Macdonald SJF. Dissecting fibrosis: therapeutic insights from the small-molecule toolbox. Nat Rev Drug Discov. **14**(10), 693, 2015.

59. Cicchini C, Amicone L, Alonzi T, Marchetti A, Mancone C, Tripodi M. Molecular mechanisms controlling the phenotype and the EMT/MET dynamics of hepatocyte. Liver Int. **35**(2), 302, 2014.

60. Khetani SR, Berger DR, Ballinger KR, Davidson MD, Lin C, Ware BR. Microengineered liver tissues for drug testing. J Lab Autom. **20**(3), 216, 2015.

61. Davidson MD, Lehrer M, Khetani SR. Hormone and Drug-Mediated Modulation of Glucose Metabolism in a Microscale Model of the Human Liver. Tissue Engineering Part C: Methods. **21**(7), 716, 2015.

62. Begue JM, Guguen-Guillouzo C, Pasdeloup N, Guillouzo A. Prolonged Maintenance of Active Cytochrome P-450 in Adult Rat Hepatocytes Co-Cultured with Another Liver Cell Type. Hepatology. W.B. Saunders; **4**(5), 839, 1984. t

63. March S, Ramanan V, Trehan K, Ng S, Galstian A, Gural N, et al. Micropatterned coculture of primary human hepatocytes and supportive cells for the study of hepatotropic pathogens. Nature Protocols. **10**(12), 2027, 2015.

64. Bhatia SN, Yarmush ML, Toner M. Controlling cell interactions by micropatterning in co-cultures: hepatocytes and 3T3 fibroblasts. Journal of biomedical materials research. **34**(2), 189, 1997.

65. Khetani SR, Szulgit G, Del Rio JA, Barlow C, Bhatia SN. Exploring interactions between rat hepatocytes and nonparenchymal cells using gene expression profiling. Hepatology. **40**(3), 545, 2004.

66. Khetani SR, Bhatia SN. Microscale culture of human liver cells for drug development. Nat Biotechnol. **26**(1), 120, 2007.

Chapter 2

Utilizing a microengineered hepatocyte co-culture system to retain hormone responsiveness and glucose metabolism in vitro[1]

Summary:

In order to begin developing in vitro disease models for NAFLD, we first had to establish protocols and assays as well as a culture system to assess hormonal responses and glucose metabolism *in vitro.* The requirements for this systems were that it needed to be scalable, for high throughput applications, human-relevant, have an extended lifetime and be amendable for quick readouts to give mechanistic as well as efficacy information. The most basic hepatocyte culture systems, 2D pure hepatocyte monolayers, rapidly dedifferentiate in vitro and most importantly lose their glucose metabolism and hormonal responsiveness. This is unfortunate because many high-throughput technologies have been developed using 2D systems. The micropatterned co-culture (MPCC) stays within this "2D" realm of culturing systems while maintaining high levels of hepatocyte functions for weeks in vitro. Here we investigated the ability of the MPCC to retain glucose metabolism and hormonal responsiveness towards enabling drug efficacy screening for anti-diabetic drugs. Importantly, this work lays the groundwork for developing more complex and carefully designed systems to start developing NAFLD disease models.

[1]This chapter has been adapted from Davidson, M. D. et al. 2015. Hormone and drug-mediated modulation of glucose metabolism in a microscale model of the human liver. Tissue engineering Part C. 21 (7): 716-725. With permission from Mary Ann Liebert, Inc, which does not require authors of the content being used to obtain a license for their personal reuse of full article, charts/graphs/tables, or text excerpt**.**

2. 1 Introduction

Relative insulin deficiency due to declining pancreatic functions coupled with insulin resistance in target tissues (i.e. liver, muscle) can lead to high levels of glucose in the blood or type 2 diabetes mellitus (T2DM), which accounts for ~95% of total diabetes cases with over 285 million people affected globally (World Health Organization). Insulin resistance has also been implicated in the pathogenesis of metabolic syndrome, non-alcoholic fatty liver disease (NAFLD), non-alcoholic steatohepatitis and cardiovascular disease (1-5). The liver plays a central role in glucose homeostasis (6). Hepatocytes in the liver can regulate blood glucose levels within 3.9 to 6.1 mM by preventing hyperglycemia in the fed state by storing excess glucose as glycogen, and avoiding hypoglycemia in the fasting state by releasing glucose via glycogen breakdown and/or gluconeogenesis. Therefore, with the rise of obesity, T2DM and metabolic syndrome, the liver has become an important organ for fundamental investigations of metabolic disorders and for developing novel drugs to treat T2DM and NAFLD (7-10).

While studies in animals are useful for elucidating mechanisms underlying the aforementioned diseases, there are significant differences across species in liver pathways (11-13). Thus, *in vitro* models of the human liver, such as liver slices, cell lines and primary human hepatocytes (PHHs) are now used to supplement animal data (14-15). However, liver slices suffer from a rapid (hours to days) decline in liver functions while immortalized/cancerous cell lines contain abnormal levels of liver functions (14-17). Thus, PHHs are ideal for constructing *in vitro* human liver models since they maintain an intact cell architecture and can be used *in vitro* for medium-to-high throughput experimentation, including drug screening (18). However, conventional culture models that expose confluent PHH monolayers to extracellular matrix (ECM) coatings/gels ignore other key liver microenvironmental cues (i.e. stromal contact), and

display a precipitous decline in liver functions, which makes them inadequate for accurate prediction of human physiology (15). While three-dimensional culture of hepatocytes in aggregates has been demonstrated, many studies have been restricted to animal hepatocytes (14-15,18-19), which can display different functional responses as compared to PHHs (11-12). Furthermore, most studies that culture hepatocytes in engineered platforms have not evaluated glucose metabolism or responsiveness to hormones over long-term (weeks) culturing (19).

Co-culture with liver- and non-liver-derived stromal cells can stabilize several functions of primary hepatocytes from both animal and human livers (20-21). Further organization of homotypic interactions between hepatocytes and heterotypic interactions between hepatocytes and specific stromal cells can significantly augment the levels and longevity of liver functions. Indeed, such micropatterned co-cultures (MPCCs) between PHHs and 3T3-J2 murine embryonic fibroblasts have been shown to be higher functioning with respect to major liver functions than pure hepatocyte cultures and randomly distributed co-cultures of the same two cell types (22). However, it remains unclear whether co-culture approaches, including MPCCs, can stabilize glucose handling capacity and hormonal responsiveness over several weeks *in vitro*. Thus, here we assessed gene expression relevant for glucose metabolism, gluconeogenesis and glycogen dynamics in MPCCs in the presence or absence of hormones over several weeks. Glucose output and responsiveness to hormones in MPCCs were compared to those obtained in conventional monolayers using the same donor of cryopreserved PHHs. Lastly, we explored two glucose-related applications of MPCCs: one for screening small molecules to modulate gluconeogenesis and another to model hyperglycemia-induced fat (lipid) accumulation *in vitro* as occurs in NAFLD.

2.2 Methods

2.2.1 Culture of primary human hepatocytes (PHHs)

Cryopreserved PHHs were purchased from vendors permitted to sell products derived from human organs procured in the United States by federally designated Organ Procurement Organizations (BioreclamationIVT, Baltimore, MD; Triangle Research Laboratories, Durham, NC). Lots used were EJW (Age: 29, Caucasian, female) from BioreclamationIVT and Hum4011 (Age: 26, Caucasian, male) from Triangle Research Laboratories. PHHs were thawed, counted and viability was assessed as previously described (23). Conventional monolayer cultures and sandwich cultures were created as previously described (22-23). Briefly, ~350,000 PHHs were seeded in each collagen-coated (rat tail type I, Corning Biosciences) well of a 24-well plate in serum-supplemented hepatocyte medium. For creation of sandwich cultures, cultures were overlaid with ~0.25 mg/mL Matrigel™ (Corning Life Sciences, Tewksbury, MA) the next day after seeding. Conventional cultures were maintained in serum-free culture medium (500 µL/well) with daily replacement of medium as previously described (22-23).

Micropatterned co-cultures (MPCCs) were created as previously described (22-23). Briefly, adsorbed collagen was lithographically patterned in each well of a multi-well plate to create 500 µm diameter circular domains spaced 1200 µm apart, center-to-center. Hepatocytes selectively attached to the collagen domains leaving ~30,000 attached hepatocytes on ~85 collagen-coated islands within each well of a 24-well plate or ~4,500 hepatocytes attached on ~13 collagen-coated islands within each well of a 96-well plate. 3T3-J2 murine embryonic

fibroblasts (24) were seeded 12 to18 hours later in each well to create MPCCs. Culture medium was replaced every 2 days (~50 μL/well for 96-well format or ~300 μL/well for 24-well format).

2.2.2 Gene expression profiling

Total RNA was isolated and purified using the RNeasy mini kit (Qiagen, Valencia, CA) and genomic DNA was digested using the Optizyme™ recombinant DNase-I digestion kit (Fisher BioReagents, Pittsburgh, PA). Approximately 10 uL of purified RNA was reverse transcribed into cDNA using the high capacity cDNA reverse transcription kit (Life Technologies Applied Biosystems, Foster City, CA). Approximately 250 ng of cDNA was added to each qPCR reaction along with Solaris™ master mix and pre-made primer/probe sets according to manufacturers' protocol (GE Healthcare Dharmacon, Lafayette, CO). RT-qPCR was performed on a Mastercycler Realplex instrument (Eppendorf, Hamburg, Germany), and data were analyzed using the comparative C(T) method (25). Gene expression was normalized to the housekeeping gene, glyceraldehyde 3-phosphate dehydrogenase (GAPDH).

2.2.3 Biochemical assays

Urea concentration in supernatants was assayed using a colorimetric endpoint assay utilizing diacetyl monoxime with acid and heat (Stanbio Labs, Boerne, TX). Albumin levels were measured using an enzyme-linked immunosorbent assay (MP Biomedicals, Irvine, CA) with horseradish peroxidase detection and 3,3',5,5'-tetramethylbenzidine (TMB, Fitzgerald Industries, Concord, MA) as the substrate (21). ATP in cell lysates was quantified using the

Celltiter-Glo® kit (Promega, Madison, WI). Glucose levels were measured using the Amplex Red glucose/glucose-oxidase assay kit (Life Technologies Molecular Probes, Eugene, OR).

2.2.4 Staining assays

Cultures were fixed with 4% paraformaldehyde (Electron Microscopy Sciences, Hatfield, PA) for 15 minutes at room temperature (RT), washed three times with 1X PBS (phosphate buffered saline, Mediatech, Manassas, VA), and stained for intracellular lipids with Nile Red (AAT Bioquest, Sunnyvale, CA). Briefly, cultures were incubated in Nile Red solution (10 μM in 1X PBS) for 10 minutes, washed 3 times with 1X PBS, and then imaged using a GFP light cube (excitation/emission: 470/510 nm) on an EVOS® FL Imaging System (Life Technologies). Hepatic glycogen content was visualized using the Periodic Acid-Schiff (PAS) staining kit (Sigma-Aldrich, St. Louis, MO).

2.2.5 Gluconeogenesis and glycogen assays

To assess gluconeogenesis, cultures were first washed 3 times with 1X PBS, and then incubated with glucose-free and serum-free Dulbecco's Modified Eagle's Medium (DMEM, Life Technologies) containing 100 nM glucagon for ~24 hours to rapidly deplete glycogen stores. Then, cultures were washed 3 times with 1X PBS and incubated with glucose-free DMEM for an additional ~24 hours to deplete residual intracellular glycogen. After this 48-hour starvation period, cultures were washed 3 times with 1X PBS and incubated for up to 24 hours with specific culture media as detailed below. Control cultures were incubated in glucose-free DMEM while

other cultures were incubated in glucose-free DMEM mixed with substrates for gluconeogenesis, specifically 2 mM pyruvate (GE Healthcare Hyclone, Logan UT) and 20 mM sodium DL-Lactate (Sigma-Aldrich). For some conditions, insulin (100 nM, Sigma-Aldrich) or glucagon (100 nM, Sigma-Aldrich) were added to the glucose-free culture medium with or without gluconeogenic substrates. Culture supernatants were collected between 4 and 24 hours post incubation and assayed for glucose levels as described above.

To assess glycogen lysis, cultures were first incubated with high glucose DMEM (25 mM) for several days to build up hepatic glycogen stores. Next, cultures were incubated in glucose-free DMEM with or without hormones (100 nM glucagon or 100 nM insulin) for 24 hours. To assess glycogen synthesis, hepatocyte cultures were first depleted of glycogen with the ~48 hour starvation protocol as described above. Then, cultures were incubated with or without hormones (100 nM glucagon or 100 nM insulin) in glucose-supplemented (5 mM) medium for 24 hours. Glycogen content was assessed using PAS staining as described above.

2.2.6 Drug studies

Hepatic glycogen was depleted for 24 hours as described above. Then, cultures were washed 3 times with 1X PBS and incubated with gluconeogenic substrates as described above and increasing concentrations of metformin (10.4, 52, 104, 208 μM, Sigma-Aldrich) for 24 hours or 3-mercaptopicolinic acid (50, 100, 250, 500 μM, 3-MPA, Santa Cruz Biotechnology, Santa Cruz, CA) for 4 hours. Culture supernatants were assayed for glucose levels as described above.

2.2.7 Data analysis

Each experiment was carried out at least 3 times in duplicate or triplicate wells for each condition. Two different cryopreserved primary human hepatocyte donors identified above were used to confirm trends. Microsoft Excel was used for data analysis and GraphPad Prism 5.0 (La Jolla, CA) was used for plotting data. Statistical significance of the data was determined using the Student's *t*-test or one-way ANOVA with Tukey's post-hoc test ($p < 0.05$).

2.3 Results

2.3.1 Morphology, gene expression and gluconeogenesis in conventional hepatocyte cultures

We created conventional confluent monolayers of PHHs on adsorbed collagen and also overlaid select cultures with a Matrigel™ overlay (i.e. sandwich cultures) (**Fig. 1a**), a commonly employed ECM for hepatocyte culture (15). PHH morphology declined over time in conventional cultures with presence of very few bile canaliculi between hepatocytes (**Fig. 1b**). However, the cultures maintained low levels (relative to MPCCs) of albumin and urea secretion over 1 week of culture, suggesting that overall hepatic phenotype was not entirely degraded (**Fig. 1c-d**). Next, we evaluated expression of transcripts involved in glucose regulation, including glucose 6-phosphatase (G6PC), phosphoenolpyruvate carboxykinase-1 (PCK1), solute carrier family 2 (facilitated glucose transporter) member 2 (SLC2A2), and glycogen synthase 2 (GYS2) (**Fig. 1e**). After 1 week of culture, PCK1 transcript levels in conventional monolayers decreased ~85% while G6PC transcript levels increased 270% relative to expression levels in 3-day-old

cultures. On the other hand, expression levels of GYS2 and SLC2A2 were relatively stable during the time-points tested (93% GYS2 and 134% SLC2A2 after 1 week of culture relative to expression levels in 3-day-old cultures).

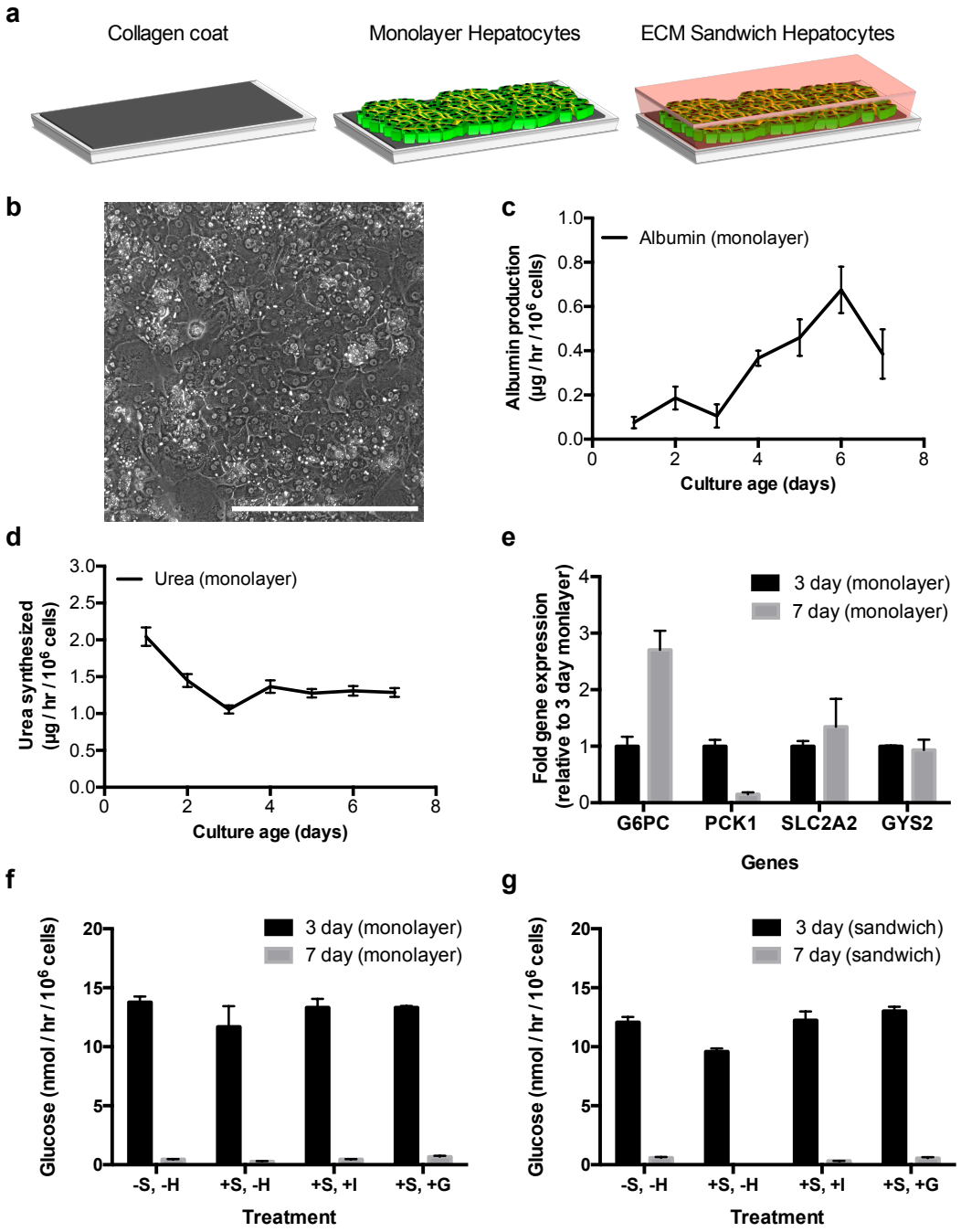

Figure 2.1. Functional characterization of conventional pure cultures of primary human hepatocytes (PHHs). (**a**) Schematic of conventional culture formats. Hepatocytes were seeded on top of a thin adsorbed collagen coat on tissue culture plastic to make monolayers, which were

then overlaid with Matrigel™ to create extracellular matrix (ECM) sandwich cultures. Such conventional cultures were maintained in high glucose medium prior to incubation in glucose-free medium for data shown in panels 'f' and 'g' below. (**b**) Morphology of PHHs in confluent monolayer after 7 days of culture. (**c,d**) Albumin production and urea synthesis over 1 week in monolayer format. (**e**) Expression of transcripts related to glucose metabolism and transport on day 7 of culture, normalized to day 3 monolayer gene expression. (**f**) Glucose release in supernatants (24-hour time-point, incubation in glucose-free medium) from 3-day- and 7-day-old monolayer cultures on adsorbed collagen in the presence or absence of gluconeogenic substrates (lactate, pyruvate) and effects of hormones, insulin and glucagon, on glucose output. +S and -S refer to incubation with or without gluconeogenic substrates, respectively; -H refers to incubation without hormones, while +I and +G refer to incubation with insulin and glucagon, respectively. (**g**) Same as panel 'f' but with sandwich cultures. In all panels, data from a single representative cryopreserved PHH donor is shown, whereas trends were seen in at least 2 donors. Error bars represent SD. Scale bar is 400 μm. G6PC (Glucose 6-phosphatase, catalytic subunit); PCK1 (phosphoenolpyruvate carboxykinase-1); SLC2A2 (solute carrier family 2, member 2, facilitated glucose transporter); and, GYS2 (glycogen synthase 2).

Conventional monolayers released glucose into supernatants in all conditions tested (+/- gluconeogenic substrates, +/- hormones) after 3 days of culture, but this level dropped by ~95-97% after 7 days of culture (**Fig. 1f**). When incubated in glucose-free culture medium in the presence of gluconeogenic substrates (pyruvate, lactate), monolayers that were 3 days old did not produce more glucose over control cultures in glucose-free medium alone. Furthermore, glucose output was not responsive to insulin and glucagon stimulation in conventional monolayers at either of the time-points tested (3 or 7 days). Lastly, overlaying the confluent monolayers on adsorbed collagen with a Matrigel™ overlay (sandwich cultures) did not significantly alter the gluconeogenesis results obtained with conventional monolayers (**Fig. 1g**).

2.3.2 Morphology, gene expression and gluconeogenesis in MPCCs

MPCCs were created as described in methods using the same PHH donors as that used for conventional monolayers of Fig. 1 (**Fig. 2a**). PHHs in MPCCs maintained a prototypical

hepatic morphology such as polygonal shape, distinct nuclei/nucleoli and bile canaliculi between hepatocytes (**Fig. 2b**). Furthermore, albumin and urea secretion levels in MPCCs were relatively stable for at least 3 weeks and several fold higher (~3 fold for albumin, ~9 fold for urea) than observed in conventional monolayers (**Fig. 2c-d**). In contrast to conventional monolayers, MPCCs maintained expression of mRNA transcripts (G6PC, PCK1, SLC2A2, GYS2), between 88% and 220% of week 1 levels by the end of the second week of culture (**Fig. 2e**). By the third week, we observed down-regulation of these transcripts in MPCCs to 52-70% of week 1 levels (data not shown), though such down-regulation was significantly less than that observed in the first week of conventional culture.

Glucose production by 1-week-old MPCCs increased by ~310% upon stimulation with gluconeogenic substrates. MPCCs that were 2 weeks old had a similar gluconeogenic response as that observed after 1 week of culture (**Fig. 2f**). Furthermore, incubation with insulin decreased gluconeogenesis in MPCCs by ~40% and 60%, while incubation with glucagon increased glucose output in MPCCs by ~310% and 340% after 1 and 2 weeks of culture, respectively, relative to hormone-free cultures (**Fig. 2g**). Glucose output in MPCCs was also responsive to different concentrations of insulin and glucagon (**Supplemental Fig. 1**). After 3 weeks of culture, MPCCs continued to display gluconeogenesis and respond to hormones with physiologically relevant trends, although glucose production levels dropped by ~51% (**Supplemental Fig. 2**). Lastly, MPCCs that were stimulated to undergo gluconeogenesis could be put back in serum-containing maintenance culture medium and re-stimulated several days later without loss of glucose output nor insulin responsiveness, thereby showing an ability to evaluate such functions in MPCC wells over multiple time-points (**Supplemental Fig. 3).**

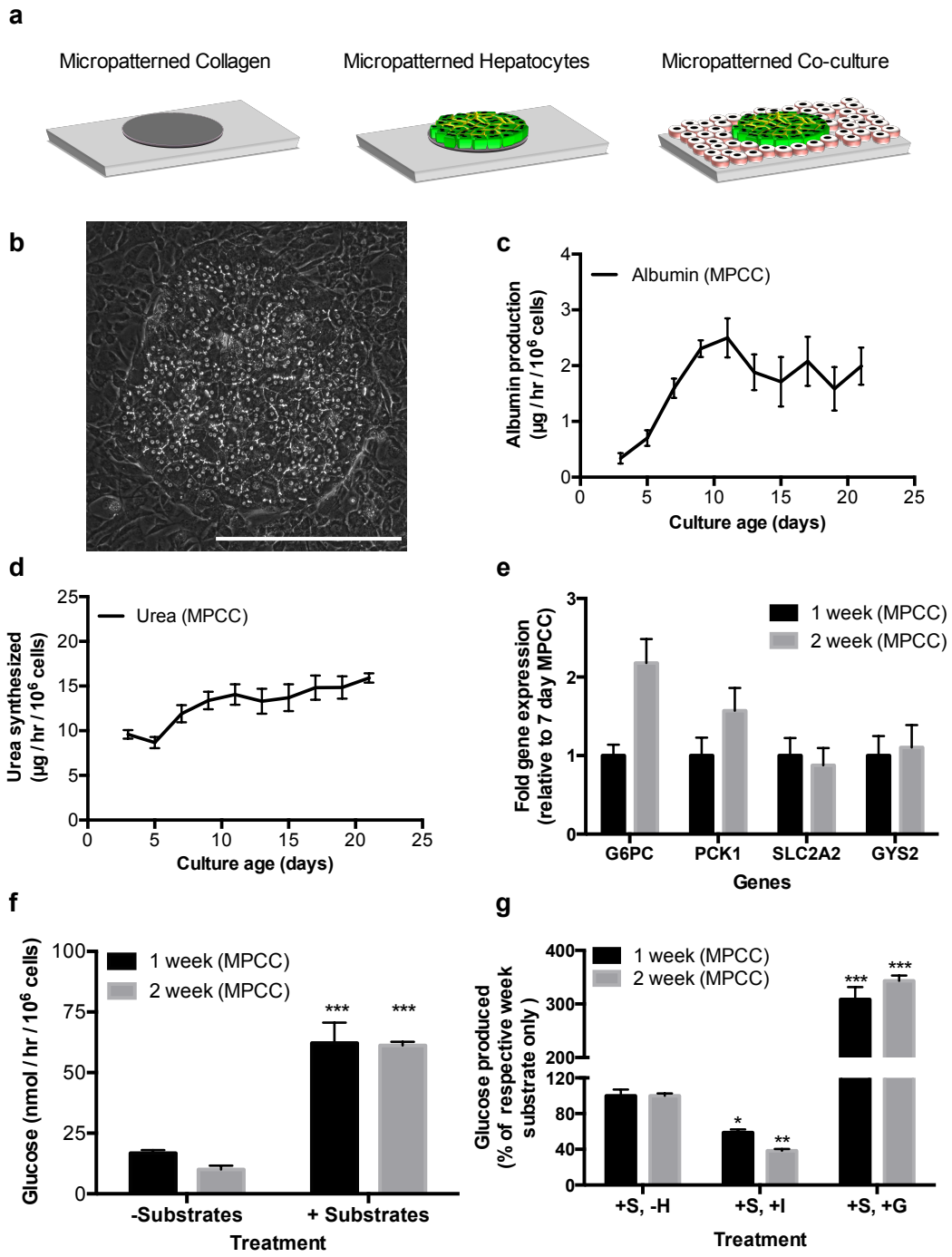

Figure 2.2. Functional characterization of micropatterned co-cultures (MPCCs) containing primary human hepatocytes (PHHs). (**a**) Schematic of MPCCs starting with collagen patterned on tissue culture plastic. MPCCs were maintained in high glucose medium prior to incubation in glucose-free medium for data shown in panels 'f' and 'g' below. (**b**) Morphology of PHHs in MPCCs after 7 days of co-culture. (**c-d**) Albumin production and urea synthesis over 3 weeks in MPCCs. (**e**) Glucose metabolism gene expression on day 14 normalized to day 7 MPCC gene expression. (**f**) Glucose release in supernatants (24-hour time-point, incubation in glucose-free medium) from 1 week and 2-week-old MPCCs in the presence or absence of gluconeogenic

substrates (lactate, pyruvate). (**g**) Effects of hormones, insulin and glucagon, on MPCC glucose output displayed as a percentage of the substrate-only control at 1 and 2 weeks of culture. Statistical significance was determined by comparing each condition to its respective hormone-free control for that week. Data from 1- and 2-week-old MPCCs is shown; however, similar trends were seen for 3 weeks of culture. +S refers to incubation with gluconeogenic substrates; -H refers to incubation without hormones, while +I and +G refer to incubation with insulin and glucagon, respectively. In all panels, data from a single representative cryopreserved PHH donor is shown, whereas trends were seen in at least 2 donors. Error bars represent SD. Scale bar is 400 μm. G6PC (Glucose 6-phosphatase, catalytic subunit); PCK1 (phosphoenolpyruvate carboxykinase-1); SLC2A2 (solute carrier family 2, member 2, facilitated glucose transporter); and, GYS2 (glycogen synthase 2). Asterisks represent statistical significance (*, **, *** denote p-values $\leq$ 0.05, 0.01 and 0.001, respectively).

2.3.3 Glycogen dynamics in hepatocytes in MPCCs

MPCCs were allowed to build intracellular glycogen stores via incubation in culture medium containing high glucose (25 mM) for 1-2 weeks in culture. Hepatic glycogen content was visualized using the PAS stain as described in methods. Next, MPCCs were incubated in glucose-free culture medium for 24 hours in the presence or absence of hormones, insulin or glucagon. In the absence of hormones, some of the hepatic glycogen content was depleted during this timeframe. However, glucagon induced significant lysis of glycogen in PHH islands (**Fig. 3a**), which appeared as glucose in the culture medium (data not shown). Insulin, on the other hand, inhibited glycogen lysis in MPCCs relative to the glucagon-treated cultures. Lastly, MPCCs were first starved for 2 days (as described in methods) to deplete the glycogen almost entirely in the PHHs. Then, a physiologic concentration of glucose was introduced into the culture medium (5 mM) and cultures were stained for glycogen after 24 hours. In the presence of glucose, PHH islands in MPCCs stored glycogen, which was significantly enhanced in the presence of insulin (**Fig. 3b**). However, glucagon prevented any glycogen storage and even stimulated lysis of residual glycogen in PHHs following the starvation period.

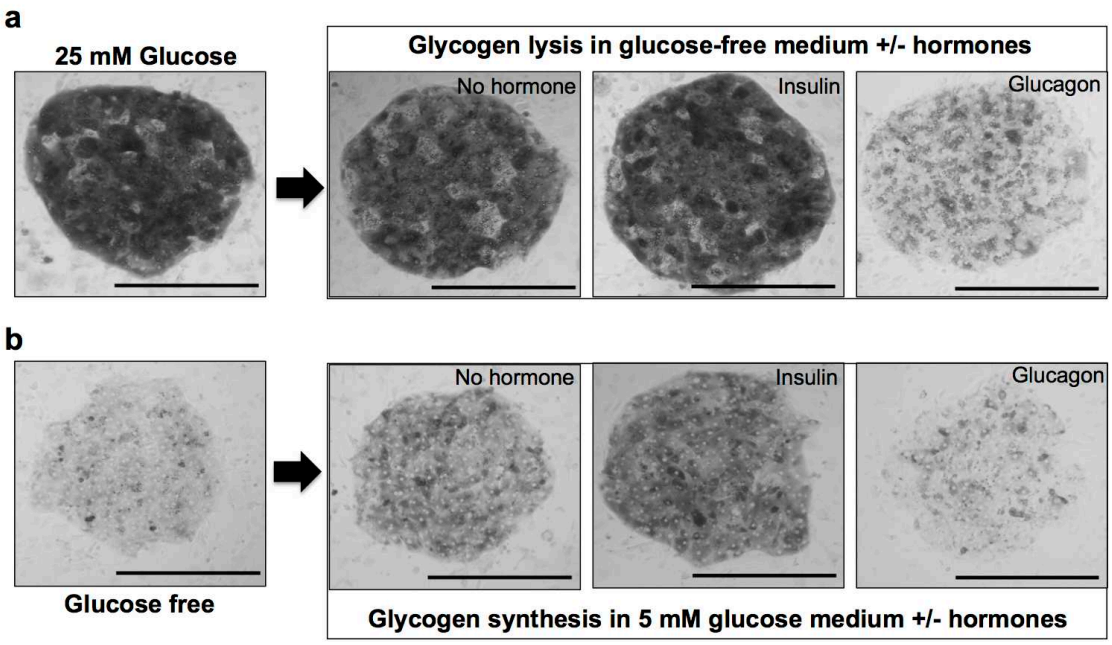

Figure 2.3. Glycogen lysis and synthesis in MPCCs. (**a**) Representative images of glycogen lysis in fed (with high glucose) MPCCs over 24 hours of incubation in glucose-free culture medium in the presence or absence of hormones, insulin or glucagon. (**b**) Representative images of glycogen synthesis in starved (in glucose-free medium) MPCCs over 24 hours of incubation in glucose-supplemented (5 mM) culture medium in the presence or absence of hormones, insulin or glucagon. Images from 2-week-old MPCCs are shown but similar trends were seen after 1 week of culture. In all panels, data from a single representative cryopreserved PHH donor is shown, whereas trends were seen in at least 2 donors.

2.3.4 Small molecule-based inhibition of hepatic gluconeogenesis in MPCCs

We stimulated gluconeogenesis in MPCCs as described above while incubating them with different concentrations of metformin, a type 2 diabetes mellitus drug known to inhibit glucose output from the liver (7). Concentrations of metformin at 17.5 µg/mL or higher were capable of inhibiting gluconeogenesis in 1-week-old MPCCs (14-30% inhibition relative to vehicle-only controls), without causing loss of cell viability at the same doses as assessed by ATP in cell lysates (**Fig. 4a-b**). Next, we incubated MPCCs with 3-mercaptopicolinic acid (3-MPA), a specific inhibitor of phosphoenolpyruvate carboxykinase, an enzyme that carries out the

rate-controlling step in gluconeogenesis (26). Concentrations of 3-MPA at 9.58 µg/mL or higher were capable of inhibiting gluconeogenesis in 1-week-old MPCCs (12-63% inhibition relative to vehicle-only controls), without causing significant depletion of ATP (**Fig. 4c-d**). Both metformin and 3-MPA inhibited gluconeogenesis in 2-week-old MPCCs as well (**Supplemental Fig. 4).**

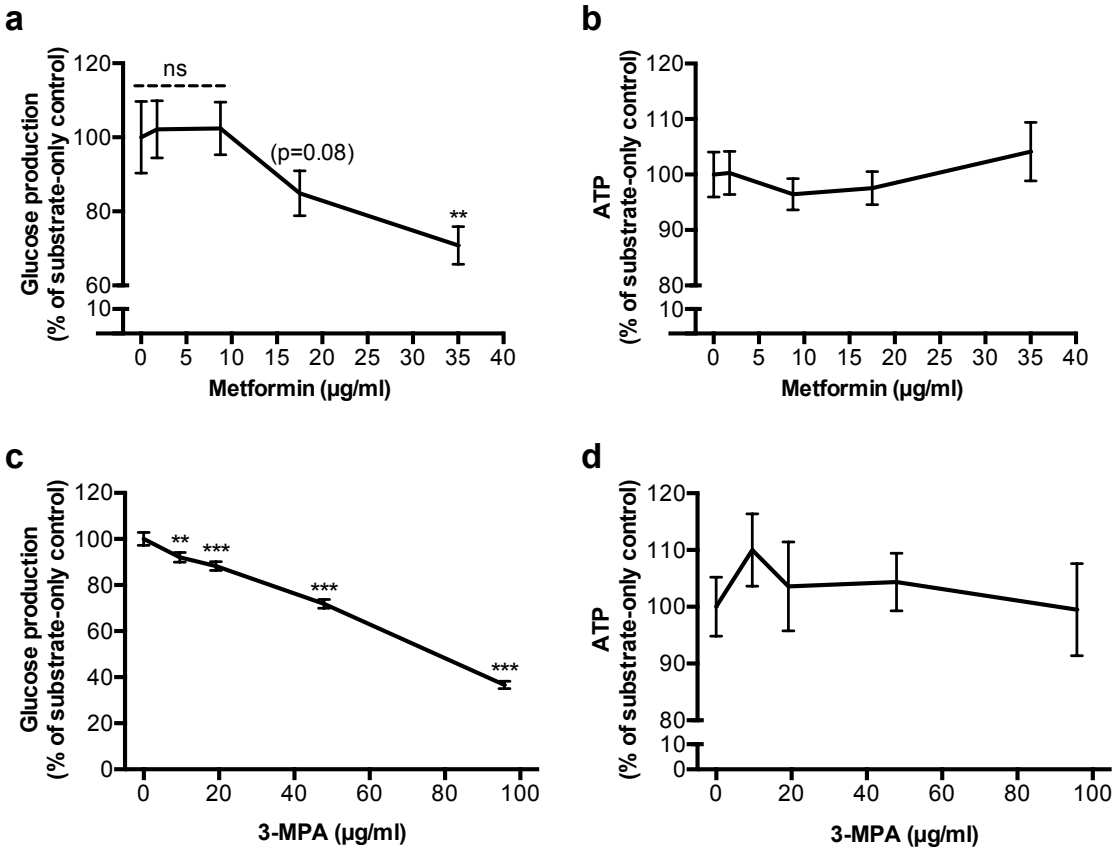

Figure 2.4. Utility of MPCCs for screening of small molecules that effect hepatic glucose metabolism. (**a**) Inhibition of gluconeogenesis in MPCCs upon incubation with increasing doses of metformin over 24 hours. (**b**) ATP levels in MPCC lysates after dosing with metformin. (**c**) Inhibition of gluconeogenesis in MPCCs upon incubation with increasing doses of phosphoenolpyruvate carboxykinase (PCK) inhibitor, 3-mercaptopicolinic acid (3-MPA), over 4 hours. (**d**) ATP levels in MPCC lysates after dosing with 3-MPA. Statistical significance was determined by comparing each drug-treated condition to its drug-free control. Data from 1-week-old MPCCs is shown here, but trends were seen for 2 weeks as seen in supplemental figure 4. In all panels, data from a single representative cryopreserved PHH donor is shown, whereas trends were seen in at least 2 donors. Error bars represent SD. Asterisks represent statistical significance (*, **, *** denote p-values ≤ 0.05, 0.01 and 0.001, respectively).

2.3.5 Hyperglycemia-induced hepatic lipid accumulation in MPCCs

We incubated MPCCs for 6 days with increasing concentrations of glucose (5, 25, 50, 100 mM). Lipid accumulation in PHH islands was then visualized using the Nile Red fluorescent stain, which was quantified using ImageJ software (http://imagej.nih.gov/ij/) (27). Nile Red displays a characteristic shift in emission from red to yellow when bound to neutral lipids such as triglycerides and cholesterol (28). PHHs in MPCCs increased their intracellular lipid content with increasing glucose concentrations in the culture medium (**Fig. 5a**).

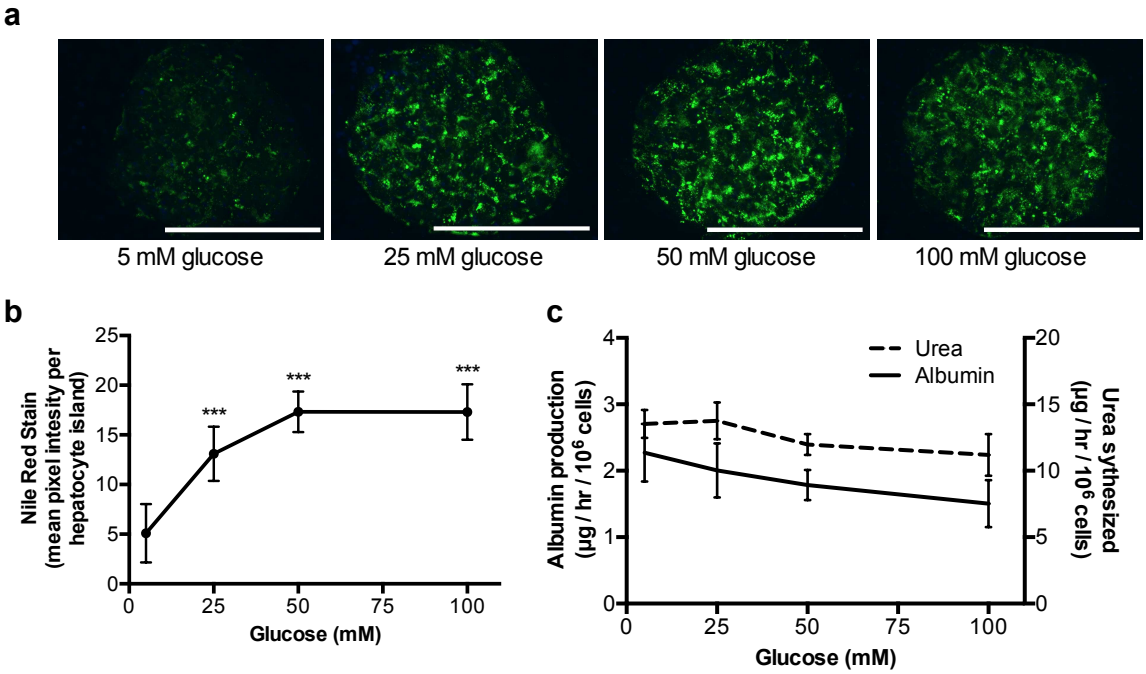

Figure 2.5. Hyperglycemia-induced lipid accumulation in MPCCs. (**a**) Representative images of Nile Red staining in PHH island in 2-week-old MPCCs following treatment with increasing levels of glucose for 6 days (started when cultures were 1 week old). (**b**) Quantification of Nile Red fluorescence observed in panel 'a'. (**c**) Urea and albumin production in MPCCs following dosing with glucose as in panel 'a'. In all panels, data from a single representative cryopreserved PHH donor is shown, whereas trends were seen in at least 2 donors. Error bars represent SD. Scale bar is 400 µm. Asterisks represent statistical significance (*, **, *** denote p-values ≤ 0.05, 0.01 and 0.001, respectively).

Quantitatively, PHHs treated with 25 mM glucose accumulated ~256% more lipids, which saturated at 340% in 50 mM and 100 mM glucose as compared to 5 mM glucose treated cultures

(**Fig. 5b**). Furthermore, albumin secretion by MPCCs was decreased by 12% after incubation with 25 mM glucose, 22% with 50 mM glucose and 34% with 100 mM glucose relative to 5 mM glucose treated cultures. Urea secretion by MPCCs was decreased by 12% after incubation with 50 mM glucose and 18% with 100 mM glucose relative to incubation with 5 mM glucose (**Fig. 5c**).

2.4 Discussion

Due to its central role in glucose homeostasis, the liver is often at risk for developing diseases related to over-nutrition, such as NAFLD, which has been linked to fibrosis, cirrhosis, hepatocarcinoma, and T2DM (4, 29-30). Primary human hepatocytes (PHHs) cultured *in vitro* can provide a powerful tool to better understand the role of the human liver in the aforementioned diseases relative to their animal counterparts. Here, we demonstrate that micropatterned co-cultures (MPCCs) containing cryopreserved PHHs and 3T3-J2 murine embryonic fibroblasts can be induced to undergo gluconeogenesis (i.e. *de novo* production of glucose from precursor substrates) for at least 3 weeks *in vitro* and that such responses are sensitive to insulin and glucagon with *in vivo*-like trends. In contrast, commonly employed conventional cultures created from the same PHH donor and under identical dosing conditions lost gluconeogenesis and hormonal responsiveness after only 3 days in culture, which is in agreement with other studies, and thus limits utility of such models for evaluating the chronic aspects of drug treatments and disease progression (19,31). Furthermore, even absolute glucose output from conventional cultures declined by 95-97% after 7 days in culture whereas such output remained relatively stable in MPCCs for 2 weeks. The stable expression of

phosphoenolpyruvate carboxykinase-1 (PCK-1) in MPCCs as opposed to its declining expression in conventional cultures may underlie these differences in glucose output. Indeed, inhibiting PCK-1 using 3-mercaptopicolinc acid (26), reduced MPCC glucose output.

Culturing MPCCs in a high glucose (25 mM) culture medium (feeding) led to significant stores of intracellular glycogen in PHH islands. Incubating these fed MPCCs in glucose free medium (i.e. starvation) then in the presence of insulin inhibited glycogen lysis, while the presence of glucagon allowed the PHHs to lyse most of their glycogen stores. Once the hepatic glycogen stores were depleted following a ~48 hour starvation period in glucose-free medium, PHHs in MPCCs cultured in glucose containing medium (re-feeding) synthesized glycogen when stimulated with insulin, whereas such synthesis was severely inhibited in the presence of glucagon relative to hormone-free controls. Thus, these results show that glycogen dynamics were observed in MPCCs with *in vivo*-relevant fasting and feeding trends.

A reduction in hepatic glucose production has been shown to be an effective treatment of hyperglycemia in patients with T2DM (32). Metformin in particular treats hyperglycemia mainly by decreasing gluconeogenesis (7). Here, metformin reduced gluconeogenesis in MPCCs in a dose dependent manner; however, doses of 10 times the maximal concentration of metformin observed in human blood (i.e. C_{max}) were needed to elicit statistically significant down-regulation of gluconeogenesis. The need for such a higher dose could be due to down-regulation of key pathways in MPCCs being modulated by metformin and/or due to a higher concentration of metformin in the liver *in vivo* as a result of transporter-mediated uptake (33). Nonetheless, it is not uncommon during drug screening to use doses as high as 100 fold of a drug's anticipated C_{max} in order to account for variability across individual patients in drug concentrations in the liver due to polymorphisms in drug metabolism enzymes and transporters (23,34). Such a

strategy still allows effective rank ordering of structural analog drugs based on efficacy and toxicity and prioritization for further development. The effects of metformin on ATP levels in MPCCs were minimal, suggesting that it was efficacious without causing loss of cell viability. However, increasing doses of metformin decreased urea synthesis in MPCCs (data not shown), which merits further investigation since detoxification of ammonia into urea is a key liver function. Nonetheless, our data shows that MPCCs provide the dual advantage of evaluating both the efficacy and toxicity of T2DM drug candidates due to the retention of glucose metabolism functions but also high activities of drug metabolism enzymes and transporters (22, 35). Furthermore, the use of cryopreserved PHHs in MPCCs allows on-demand creation of cultures for drug screening applications.

Once glycogen stores in hepatocytes are saturated, glucose is shifted into pathways leading to fatty acid synthesis (36), thereby leading to accumulation of intracellular triglycerides and diacylglycerol. Such fat accumulation in hepatocytes has been linked to pathways involved in inducing insulin resistance (37). Abnormal lipid accumulation is defined as more than 5% of hepatocytes in the liver containing visible lipids (38). Here, majority of the PHHs in MPCCs accumulated neutral lipids when incubated with increasing concentrations of glucose, up to 340% more lipids in high glucose conditions (50-100 mM) as compared to incubation in a physiologic level of glucose (5 mM). Other liver functions (albumin, urea) were also affected upon incubation with high levels of glucose; however, the effects on lipid accumulation were significantly greater (i.e. 256% increase in lipid content vs. 12% reduction in albumin secretion and no effect on urea secretion with 25 mM glucose incubation relative to 5 mM glucose control). These results suggest that MPCCs are capable of responding to hyperglycemia with *in vivo* relevant trends while displaying basic liver functions, as would be the case in a live patient.

While our results show that, in contrast to conventional culture techniques, MPCCs have robust utility in the study of glucose metabolism, hormonal responsiveness, drug screening to reduce hepatic glucose output and effects of hyperglycemia on PHHs, the culture method has limitations. In particular, we observed down-regulation of gluconeogenesis by the third week of culture, which limits the ability to evaluate effects of over-nutrition, drugs and other stimuli over several months. Furthermore, PHHs in MPCCs produce ~2.8 fold lower glucose following stimulation with glucagon than observed *in vivo* (39-40), which is likely due to the reduction in PCK1 transcript expression in MPCCs relative to thawed hepatocytes immediately prior to plating (data not shown). We also needed to use supra-physiologic concentrations of insulin to see robust down-regulation of gluconeogenesis (i.e. 1 nM vs. 100 nM). Such deviations from physiological outcomes are likely due to incomplete presentation of micro-environmental cues in MPCCs that play modulatory roles *in vivo* (i.e. complex mixtures of ECM, liver stromal cells) (41). For instance, Kupffer macrophages have been implicated in metabolic disorders (42-43).

We chose 3T3-J2 fibroblasts as the support cell type in MPCCs because of ease of propagation, contact inhibition of growth in culture, lack of detectable liver functions, and induction of liver phenotype in hepatocytes from multiple species (22, 44). Nonetheless, our preliminary studies indicate that the fibroblast monolayer can be mixed with Kupffer macrophages and liver sinusoidal endothelial cells (data not shown), which may ultimately improve PHH glucose metabolism. While the use of static media allows us to create MPCCs in industry-standard multi-well formats (i.e. 24- and 96-well plates) for higher throughput experimentation than larger formats (i.e. petri dishes, glass slides), perfusion of culture medium in the future will allow subjecting PHHs and stromal cells in MPCCs to gradients of hormones, among other factors (i.e. oxygen), that are implicated in zonal liver functions *in vivo* (45).

In conclusion, PHHs cultured in MPCCs displayed high levels of gluconeogenesis and glycogen lysis/synthesis, which were responsive to hormones (insulin, glucagon) with *in vivo*-relevant trends for at least 3 weeks. In contrast, gluconeogenesis and modulation with hormones were lost within 3 days in conventional PHH cultures. Furthermore, using prototypical drugs, we showed that MPCCs could be potentially useful for screening novel drug candidates that modulate gluconeogenesis in PHHs. Hyperglycemia induced significant lipid accumulation in PHHs in MPCCs, suggesting utility of this model to explore mechanisms underlying effects of T2DM on the human liver. Ultimately, the longevity of MPCCs for several weeks allows for the study of effects of repeat drug dosing and over-nutrition on PHH functions, including glucose metabolism and insulin sensitivity.

2.5 Supplemental Figures

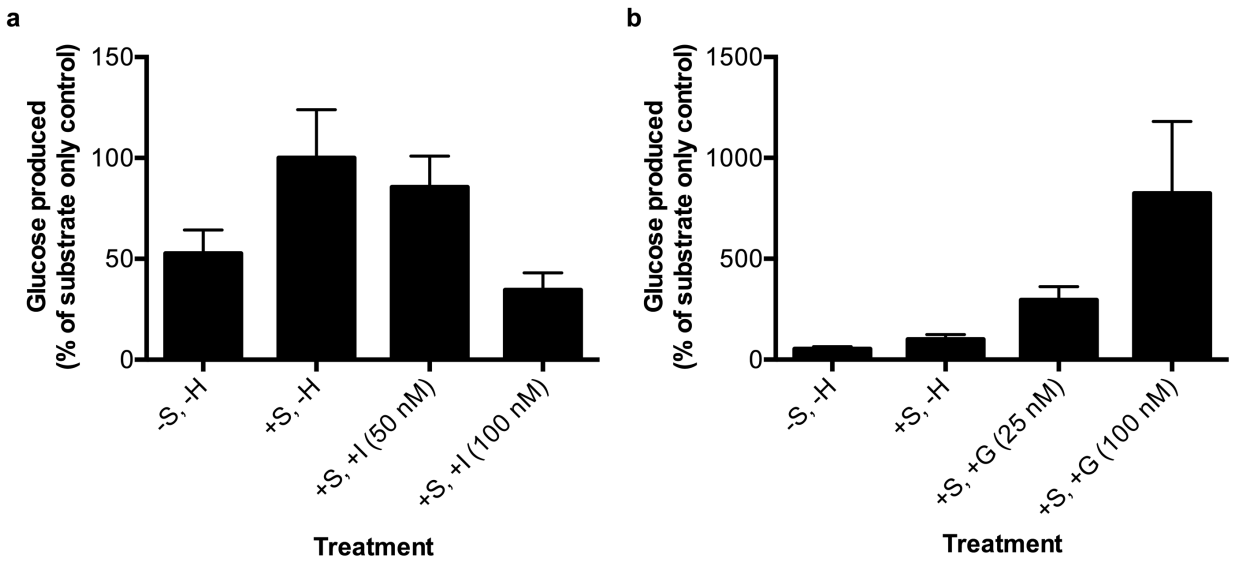

Supplemental Figure 2.5.1. Glucose released from MPCCs in response to various concentrations of insulin or glucagon. (**a**) Glucose release in supernatants (24-hour time-point, incubation in glucose-free medium) from 1-week-old MPCCs in the presence or absence of gluconeogenic substrates (lactate, pyruvate) and effects of insulin (50nM or 100nM) on glucose output. (**b**) Same as panel 'a' but with response to glucagon (25nM or 100nM). +S and -S refer to incubation with or without gluconeogenic substrates, respectively. -H refers to incubation without hormones, while +I and +G refer to incubation with insulin and glucagon, respectively. Error bars represent SD.

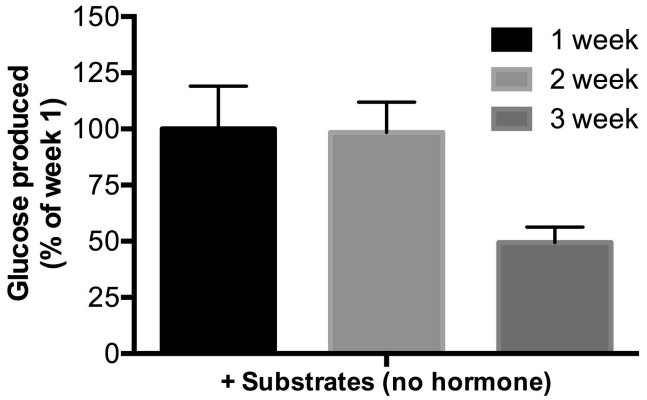

Supplemental Figure 2.5.2. Gluconeogenesis in MPCCs over time relative to 1-week-old MPCCs. By the third week in culture, glucose output from MPCCs declines by ~50% relative to the first 2 weeks in culture. Error bars represent SD.

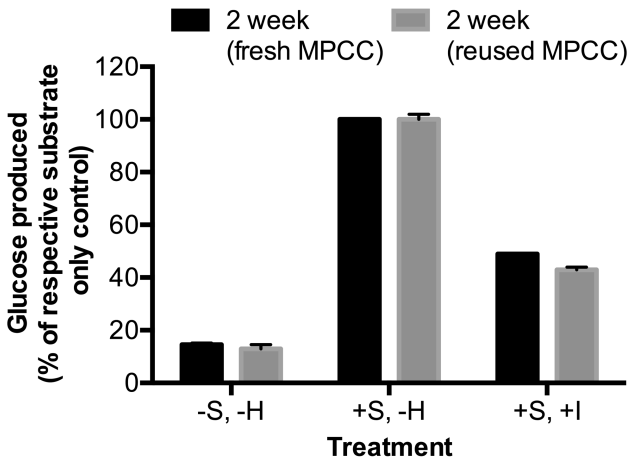

Supplemental Figure 2.5.3. Glucose release in fresh (naïve) or reused MPCCs. Fresh MPCCs were first cultured in maintenance medium (high glucose, serum-supplemented) for 2 weeks and then stimulated once to secrete glucose into supernatants at 2 weeks of culture age. Re-used MPCCs, on the other hand, were cultured in maintenance medium for 1 week, stimulated to produce glucose, put back in maintenance culture medium (high glucose, serum-supplemented) for ~1 more week, and then finally re-stimulated (i.e. re-use) concurrently with fresh MPCCs above to secrete glucose into supernatants at 2 weeks of culture age. +S and -S refer to incubation with or without gluconeogenic substrates, respectively. -H refers to incubation without hormones, while +I refers to incubation with insulin. Error bars represent SD.

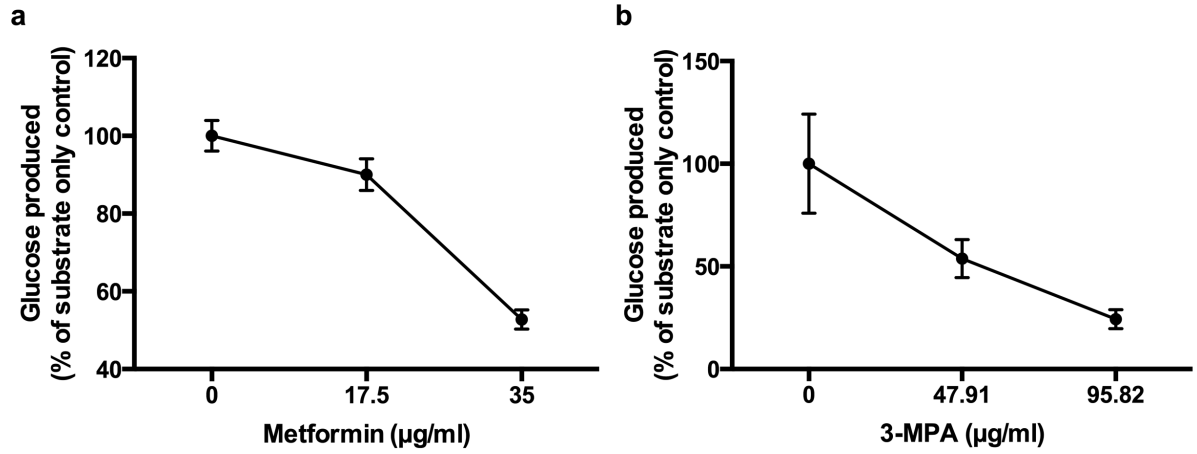

Supplemental Figure 2.5.4. Small molecule inhibition of glucose production in MPCCs after 2 weeks of culture. (**a**) Inhibition of gluconeogenesis in 2-week-old MPCCs upon incubation with increasing doses of metformin over 24 hours. (**b**) Inhibition of gluconeogenesis in MPCCs upon incubation with increasing doses of phosphoenolpyruvate carboxykinase (PCK) inhibitor, 3-mercaptopicolinic acid (3-MPA), over 4 hours. Error bars represent SD.

References

1. Haffner, S.M., D'Agostino, R., Mykkänen, L., Tracy, R., Howard, B., Rewers, M., Selby, J., Savage, P.J., and Saad, M.F. Insulin sensitivity in subjects with type 2 diabetes. Relationship to cardiovascular risk factors: the Insulin Resistance Atherosclerosis Study. Diabetes Care **22**, 562, 1999.

2. Hanley, A.J.G., Williams, K., Festa, A., Wagenknecht, L.E., D'Agostino, R.B., and Haffner, S.M. Liver Markers and Development of the Metabolic Syndrome: The Insulin Resistance Atherosclerosis Study. Diabetes **54**, 3140, 2005.

3. Sanyal, A.J., Campbell-Sargent, C., Mirshahi, F., Rizzo, W.B., Contos, M.J., Sterling, R.K., Luketic, V.A., Shiffman, M.L., and Clore, J.N. Nonalcoholic steatohepatitis: association of insulin resistance and mitochondrial abnormalities. Gastroenterology **120**, 1183, 2001.

4. Cusi, K. Nonalcoholic fatty liver disease in type 2 diabetes mellitus. Curr Opin in Endocrinol Diabetes Obes **16**, 141, 2009.

5. Samuel, V.T., and Shulman, G.I. Mechanisms for Insulin Resistance: Common Threads and Missing Links. Cell **148**, 852, 2012.

6. Sherwin, R.S. Role of Liver in Glucose Homeostasis. Diabetes Care **3**, 261, 1980.

7. Viollet, B., and Foretz, M. Revisiting the mechanisms of metformin action in the liver. Ann Endocrinol (Paris) **74**, 123, 2013.

8. Tahrani, A.A., Bailey, C.J., Del Prato, S., and Barnett, A.H. Management of type 2 diabetes: new and future developments in treatment. Lancet **378**, 182, 2011.

9. Perry, R.J., Samuel, V.T., Petersen, K.F., and Shulman, G.I. The role of hepatic lipids in hepatic insulin resistance and type 2 diabetes. Nature **510**, 84, 2014.

10. Tao, H., Zhang, Y., Zeng, X., Shulman, G.I., and Jin, S. Niclosamide ethanolamine–induced mild mitochondrial uncoupling improves diabetic symptoms in mice. Nat Med **20**, 1263, 2014.

11. Olson, H., Betton, G., Robinson, D., Thomas, K., Monro, A., Kolaja, G., Lilly, P., Sanders, J., Sipes, G., Bracklen, W., Dorato, M., Van Deun, K., Smith, P., Berger, B., and Heller, A. Concordance of the toxicity of pharmaceuticals in humans and in animals. Regul Toxicol Pharmacol **32**, 56, 2000.

12. Shih, H., Pickwell, G.V., Guenette, D.K., Bilir, B., and Quattrochi, L.C. Species differences in hepatocyte induction of CYP1A1 and CYP1A2 by omeprazole. Human & experimental toxicology **18**, 95, 1999.

13. Raman, P., Donkin, S.S., and Spurlock, M.E. Regulation of hepatic glucose metabolism by leptin in pig and rat primary hepatocyte cultures. Am J Physiol Regul Integr Comp Physiol **286**, R206, 2004.

14. Guillouzo, A., and Guguen-Guillouzo, C. Evolving Concepts in Liver Tissue Modeling and Implications for In Vitro Toxicology. Expert Opin Drug Metab Toxicol **4,** 1279, 2008.

15. LeCluyse, E.L., Witek, R.P., Andersen, M.E., and Powers, M.J. Organotypic liver culture models: meeting current challenges in toxicity testing. Crit Rev Toxicol **42**, 501, 2012.

16. Wilkening, S., Stahl, F., and Bader, A. Comparison of primary human hepatocytes and hepatoma cell line Hepg2 with regard to their biotransformation properties. Drug Metab Dispos **31**, 1035, 2003.

17. Hariparsad, N., Carr, B.A., Evers, R., and Chu, X. Comparison of immortalized Fa2N-4 cells and human hepatocytes as in vitro models for cytochrome P450 induction. Drug Metab Dispos **36**, 1046, 2008.

18. Godoy, P., Hewitt, N.J., Albrecht, U., Andersen, M.E., Ansari, N., Bhattacharya, S., Bode, J.G., Bolleyn, J., Borner, C., Böttger, J., Braeuning, A., Budinsky, R.A., Burkhardt, B., Cameron, N.R., Camussi, G., Cho, C-S., Choi, Y-J., Craig Rowlands, J., Dahmen, U., Damm, G., Dirsch, O., Donato, M.T., Dong, J., Dooley, S., Drasdo, D., Eakins, R., Ferreira, K.S., Fonsato, V., Fraczek, J., Gebhardt, R., Gibson, A., Glanemann, M., Goldring, C.E.P., Gómez-Lechón, M.J., Groothuis, G.M.M., Gustavsson, L., Guyot, C., Hallifax, D., Hammad, S., Hayward, A., Häussinger, D., Hellerbrand, C., Hewitt, P., Hoehme, S., Holzhütter, H-G., Houston, J.B., Hrach, J., Ito, K., Jaeschke, H., Keitel, V., Kelm, J.M., Kevin Park, B., Kordes, C., Kullak-Ublick, G.A., LeCluyse, E.L., Lu, P., Luebke-Wheeler, J., Lutz, A., Maltman, D.J., Matz-Soja, M., McMullen, P., Merfort, I., Messner, S., Meyer, C., Mwinyi, J., Naisbitt, D.J., Nussler, A.K., Olinga, P., Pampaloni, F., Pi, J., Pluta, L., Przyborski, S.A., Ramachandran, A., Rogiers, V., Rowe, C., Schelcher, C., Schmich, K., Schwarz, M., Singh, B., Stelzer, E.H.K., Stieger, B., Stöber, R., Sugiyama, Y., Tetta, C., Thasler, W.E., Vanhaecke, T., Vinken, M., Weiss, T.S., Widera, A., Woods, C.G., Xu, J.J., Yarborough, K.M., and Hengstler, J.G. Recent advances in 2D and 3D in vitro systems using primary hepatocytes, alternative hepatocyte sources and non-parenchymal liver cells and their use in investigating mechanisms of hepatotoxicity, cell signaling and ADME. Arch Toxicol **87**, 1315, 2013.

19. Lu, Y., Zhang, G., Shen, C., Uygun, K., Yarmush, M.L., and Meng, Q. A novel 3D liver organoid system for elucidation of hepatic glucose metabolism. Biotechnol Bioeng **109**, 595, 2012.

20. Bhatia, S.N., Balis, U.J., Yarmush, M.L., and Toner, M. Effect of cell-cell interactions in preservation of cellular phenotype: cocultivation of hepatocytes and nonparenchymal cells. FASEB J **13**, 1883, 1999.

21. Guguen-Guillouzo, C., Clément, B., Baffet, G., Beaumont, C., Morel-Chany, E., Glaise, D., and Guillouzo, A. Maintenance and reversibility of active albumin secretion by adult rat hepatocytes co-cultured with another liver epithelial cell type. Exp Cell Res **143**, 47, 1983.

22. Khetani, S.R., and Bhatia, S.N. Microscale culture of human liver cells for drug development. Nat Biotechnol **26**, 120, 2008.

23. Khetani, S.R., Kanchagar, C., Ukairo, O., Krzyzewski, S., Moore, A., Shi, J., Aoyama, S., Aleo, M., and Will, Y. Use of Micropatterned Co-cultures to Detect Compounds that Cause Drug induced Liver Injury in Humans. Toxicol Sci **132**, 107, 2012.

24. Rheinwald, J.G., and Green, H. Serial cultivation of strains of human epidermal keratinocytes: the formation of keratinizing colonies from single cells. Cell **6**, 331, 1975.

25. Schmittgen, T.D., and Livak, K.J. Analyzing real-time PCR data by the comparative C(T) method. Nat Protoc **3**, 1101, 2008.

26. Robinson, B.H., and Oei, J. 3-Mercaptopicolinic acid, a preferential inhibitor of the cytosolic phosphoenolpyruvate carboxykinase. FEBS Letters **58**, 12, 1975.

27. Collins, T.J. ImageJ for microscopy. BioTechniques **43 (1 Suppl)**, 25, 2007.

28. Diaz, G., Melis, M., Batetta, B., Angius, F., and Falchi, A.M. Hydrophobic characterization of intracellular lipids in situ by Nile Red red/yellow emission ratio. Micron 39, 819, 2008.

29. Smith, B.W., and Adams, L.A. Nonalcoholic fatty liver disease and diabetes mellitus: pathogenesis and treatment. Nat Rev Endocrinol **7**, 456, 2011.

30. Koppe, S.W.P. Obesity and the liver: nonalcoholic fatty liver disease. Transl Res **164,** 312, 2014.

31. Yamada, S., Otto, P.S., Kennedy, D.L., and Whayne, T.F. The effects of dexamethasone on metabolic activity of hepatocytes in primary monolayer culture. In Vitro **16**, 559, 1980.

32. Wu, C., Okar, D.A., Kang, J., and Lange, A.J. Reduction of hepatic glucose production as a therapeutic target in the treatment of diabetes. Curr Drug Targets Immune Endocr Metabol Disord **5**, 51, 2005.

33. Wang, D-S., Jonker, J.W., Kato, Y., Kusuhara, H., Schinkel, A.H., and Sugiyama, Y. Involvement of organic cation transporter 1 in hepatic and intestinal distribution of metformin. J Pharmacol Exp Ther **302,** 510, 2002.

34. Xu, J.J., Henstock, P.V., Dunn, M.C., Smith, A.R., Chabot, J.R., and de Graaf, D.

Cellular Imaging Predictions of Clinical Drug-Induced Liver Injury. Toxicol Sci **105**, 97, 2008.

35. Ploss, A., Khetani, S.R., Jones, C.T., Syder, A.J., Trehan, K., Gaysinskaya, V.A., Mu, K., Ritola, K., Rice, C.M., and Bhatia, S.N. Persistent hepatitis C virus infection in microscale primary human hepatocyte cultures. Proc Natl Acad Sci USA **107**, 3141, 2010.

36. Postic, C., and Girard, J. Contribution of de novo fatty acid synthesis to hepatic steatosis and insulin resistance: lessons from genetically engineered mice. J Clin Invest **118**, 829, 2008.

37. Nagle, C.A., Klett, E.L., and Coleman, R.A. Hepatic triacylglycerol accumulation and insulin resistance. J Lipid Res **50 Suppl**, S74, 2009.

38. Kleiner, D.E., Brunt, E.M., Van Natta, M., Behling, C., Contos, M.J., Cummings, O.W., Ferrell, L.D., Liu, Y-C., Torbenson, M.S., Unalp-Arida, A., Yeh, M., McCullough, A.J., and Sanyal, A.J. Design and validation of a histological scoring system for nonalcoholic fatty liver disease. Hepatology **41**, 1313, 2005.

39. Sohlenius-Sternbeck, A-K. Determination of the hepatocellularity number for human, dog, rabbit, rat and mouse livers from protein concentration measurements. Toxicol In Vitro **20**, 1582, 2006.

40. Rothman, D.L., Magnusson, I., Katz, L.D., Shulman, R.G, and Shulman, G.I. Quantitation of hepatic glycogenolysis and gluconeogenesis in fasting humans with 13C NMR. Science **254**, 573, 1991.

41. Kmieć, Z. Cooperation of liver cells in health and disease. Adv Anat Embryol Cell Biol **161**, III, 2001.

42. Baffy, G. Kupffer cells in non-alcoholic fatty liver disease: the emerging view. J Hepatol **51**, 212, 2009.

43. Huang, W., Metlakunta, A., Dedousis, N., Zhang, P., Sipula, I., Dube, J.J., Scott, D.K., and O'Doherty, R.M. Depletion of liver Kupffer cells prevents the development of diet-induced hepatic steatosis and insulin resistance. Diabetes **59**, 347, 2010.

44. Ukairo, O., Kanchagar, C., Moore, A., Shi, J., Gaffney, J., Aoyama, S., Rose, K., Krzyzewski, S., McGeehan, J., Anderson, M.E., Khetani, S.R., and LeCluyse, E.L. Long-Term Stability of Primary Rat Hepatocytes in Micropatterned Cocultures. J Biochem Mol Toxicol **27**, 204, 2013.

45. Jungermann, K., and Kietzmann, T. Zonation of parenchymal and nonparenchymal metabolism in liver. Annu Rev Nutr **16**, 179, 1996.

Chapter 3

Optimizing available glucose in hepatocyte culture medium towards enabling studies of lipid accumulation and insulin resistance[2]

Summary:

In chapter 2 we clearly demonstrated that the MPCC system retains highly functional hepatocytes that can undergo various metabolic functions that would be important for developing healthy and diseased liver mimics. One major drawback to the MPCC used in chapter 1 was that over time, the hepatocyte cultures became lipid-laden and insulin resistant, similar to a NAFLD patient liver. Although this is the disease model we were looking for, we needed a healthy control to compare our disease model to. The most basic aspect of type II diabetes is the development of hyperglycemia, or high glucose, which can predispose the liver, as well as other organs, to increased lipid production and insulin resistance. Taking a closer look at the medium formulation used in chapter 1, we can see that we are giving our cultures excessive, hyperglycemic, levels of glucose. Therefore here we first assessed the possibility of culturing MPCCs in normoglycemic levels of glucose and then characterized the potential benefits of using normoglycemic medium towards eventually developing an *in vitro* model of NAFLD. Specifically, we wanted to know if glucose alone could cause any changes in drug metabolism, insulin resistance and lipid accumulation in our MPCC model.

[2] This chapter has been adapted from Davidson, M. D. et al. 2016. Long-term exposure to abnormal glucose levels alters drug metabolism pathways and insulin sensitivity in primary human hepatocytes. Scientific Reports **6**, 28178**.** Which is freely available to disseminate under the Creative Commons CC-BY license. URL for CC 4.0 agreement https://creativecommons.org/licenses/by/4.0/legalcode ,

3.1 Introduction

The liver maintains blood glucose levels in a tight range (~3.9-7.2 mM glucose) by carefully balancing its own glucose output with the absorption of glucose in peripheral tissues. In type 2 diabetes mellitus (**T2DM**), blood glucose levels rise into the hyperglycemic range (>7.2 mM blood glucose), which is associated with many detrimental effects throughout the body(1). In the liver itself, the prominent effect of high glucose is ectopic lipid accumulation in hepatocytes called steatosis(2). Steatosis is the prominent symptom of non-alcoholic fatty liver disease (**NAFLD**), which is currently the most prevalent liver aliment and has been implicated in causing altered drug metabolism(3) and non-alcoholic steatohepatitis (**NASH**)(4). Conversely, the liver can experience hypoglycemia (<3.9 mM blood glucose) from fasting, cancer and T2DM drugs (i.e. oral hypoglycemic drugs). Fasting induces changes in cytochrome P450 (**CYP450**) pathways, which could alter drug efficacy and toxicity(5,6). Importantly, the liver is the main site for cancer metastases, which places this tissue at risk for local glucose deprivation(7,8). Furthermore, hypoglycemia is common in T2DM patients on drugs and is associated with cardiovascular disease(9,10).

Owing to its critical role in glucose homeostasis, the liver is emerging as an essential target for metabolic disorder therapies(11,12). Animal models of metabolic disease, such as diabetic (db/db) and high fat diet fed mice, have provided important details on disease pathogenesis(13,14). However, there are important differences in the progression of metabolic disease and drug metabolism pathways between animals and humans(15,16). Thus, animal data needs to be supplemented with assays designed using *in vitro* models of the human liver, which include liver slices, cell lines and isolated primary human hepatocytes (**PHHs**) cultured on adsorbed or gelled extracellular matrices (**ECM**) such as collagen and Matrigel(17). Liver slices

are known to rapidly lose viability *in vitro* and are not amenable to high-throughput drug screening(17). Cancerous and immortalized hepatic cell lines contain abnormal levels of drug metabolism enzymes and display an improper metabolism of energy sources(18,19). On the other hand, untransformed PHHs are relatively simple to use in a medium-to-high throughput culture format for fundamental investigations and drug screening(20). However, in the presence of ECM manipulations alone, PHHs display a precipitous decline in liver functions such as CYP450 activities, glucose metabolism and responsiveness to insulin and glucagon(21,22). The aforementioned limitations with *in vitro* models of the human liver have thus hampered the investigation of how various stimuli (i.e. hypo- and hyperglycemia) affect cellular phenotypes in ways that have implications for the progression and treatment of diseases such as T2DM, NAFLD, and NASH.

Microfabrication tools can be utilized to control the extent of both homotypic interactions between PHHs and their heterotypic interactions with supportive nonparenchymal cells (**NPCs**), which has been shown to significantly enhance the functions and lifetime of PHHs *in vitro*(17). Indeed, micropatterned co-cultures (**MPCCs**) of PHHs and 3T3-J2 murine embryonic fibroblasts can maintain prototypical hepatic morphology, secrete albumin and urea, and display high levels of CYP450 activities for 4-6 weeks(21,23). In this model, PHHs are first organized onto collagen-coated circular domains of empirically optimized dimensions in 24- or 96-well plates using semiconductor-driven soft-lithographic tools and then surrounded by 3T3-J2 fibroblasts. More recently, we have shown that MPCCs created using cryopreserved PHHs maintain glucose metabolism and sensitivity to insulin and glucagon for several weeks(22). In particular, MPCCs retained the ability to store glycogen and produce glucose (via gluconeogenesis or glycogen

lysis) under the nutritional states of feeding and fasting, respectively. Furthermore, such glucose metabolism in MPCCs responded robustly to insulin and glucagon with *in vivo*-like trends.

In this study, we utilized MPCCs to investigate for the first time the effects of chronic stimulation (~3 weeks) with pathophysiologic glucose levels (hypo- and hyperglycemia) on several aspects of the PHH phenotype, which included: hepatocyte morphology, gene expression, albumin secretion, urea synthesis, CYP450 activities, hepatic lipid accumulation, and the effects of insulin on glucose output. We compared our results to a normoglycemic control condition.

3.2 Methods

3.2.1 Cell culture

Cryopreserved primary human hepatocytes (PHHs) were purchased from vendors permitted to sell products derived from human organs procured in the United States of America by federally designated Organ Procurement Organizations (BioreclamationIVT, Baltimore, MD; Triangle Research Laboratories, Durham, NC). Work with human cells was conducted at Colorado State University and University of Illinois at Chicago with the approval of the Institutional Biosafety Committees at each institution. PHHs were thawed, counted and viability was assessed as previously described(23). Micropatterned co-cultures (MPCCs) were created as previously described(21). Briefly, adsorbed rat tail collagen I (Corning Life Sciences, Tewksbury, MA) was lithographically patterned in each well of a 24-well or 96-well plate to create 500 μm diameter circular domains spaced 1200 μm apart, center-to-center. PHHs selectively attached to the collagen domains leaving ~30,000 attached PHHs on ~85 collagen-

coated islands within each well of a 24-well plate or ~4,500 attached PHHs on ~13 collagen-coated islands within each well of a 96-well plate. 3T3-J2 murine embryonic fibroblasts were seeded 18 to 24 hours later at ~90,000 cells per well in a 24-well plate or ~15,000 cells per well in a 96-well plate to create MPCCs. Culture medium containing ~5 mM D-glucose (Fisher BioReagents, Pittsburgh, PA) in a DMEM base (Dulbecco's Modified Eagle's Medium, Corning Life Sciences) was replaced on MPCCs every 2 days (300 μL/well for 24-well plate and 50 μL/well for 96-well plate). Other components of the MPCC culture medium have been described previously(51). Four days after establishment of the contact-inhibited fibroblast monolayer adjacent to the confluent PHH clusters, MPCCs were treated with varying D-glucose levels, including hypoglycemia (~0.4-0.5 mM), normoglycemia (~5 mM) and hyperglycemia (~25 mM). For the hypoglycemic culture medium, no additional glucose was supplemented in the culture medium except for what was present in the 10% vol/vol serum used.

3.2.2 Gene expression profiling

Total RNA was isolated and purified using the RNeasy mini kit (Qiagen, Valencia, CA) and genomic DNA was digested using the Optizyme recombinant DNase-I digestion kit (Fisher BioReagents). Approximately 10 μL of purified RNA was reverse transcribed into complementary DNA (cDNA) using the high capacity cDNA reverse transcription kit (Applied Biosystems, Foster City, CA). Then, 250 ng of cDNA was added to each qPCR (quantitative polymerase chain reaction) reaction along with the Solaris™ master mix and pre-made human-specific primer/probe sets according to manufacturer's protocol (GE Healthcare Dharmacon, Lafayette, CO). The primer and probe sequences provided by GE Healthcare Dharmacon are

provided in **Supplemental Table 1**. Additionally, for some genes that included: *SREBF1* (ID: HS01088691_m1), *FASN* (ID: HS01005622_m1), *GK1* (ID: HS04235340_s1), *NFE2L2* (ID: HS00975961_g1), *CYP1A2* (ID: HS00167927_m1), *CYP2C19* (ID: HS00426380_m1), *CYP2E1* (ID: HS00559368_m1), *CYP2B6* (ID: HS03044636_m1), *CYP2D6* (ID: HS00164385_m1), *HNF4A* (ID: HS00230853_m1), *NR1I2* (ID: HS01114267_m1) *and NR1I3* (ID: HS00901571_m1), Taqman™ (Thermo Fisher Scientific) master mix and primer/probe sets were used according to manufacturer's protocol. The Taqman primer/probe sets were selected to be human-specific without cross-reactivity to mouse DNA; however, primer/probe sequences are proprietary to the manufacturer. The primer/probe sets were also tested with pure mouse 3T3-J2 fibroblast cDNA and found to not cross-react. qPCR was performed on a Mastercycler Realplex instrument (Eppendorf, Hamburg, Germany), and data were analyzed using the comparative C(T) method. Gene expression was normalized to the housekeeping gene, glyceraldehyde 3-phosphate dehydrogenase (*GAPDH*), the expression of which did not vary in MPCCs as a function of glucose levels over at least 18 days of exposure (data not shown).

3.2.3 Biochemical assays

Urea concentration in collected cell culture supernatants was assayed using a colorimetric endpoint assay utilizing diacetyl monoxime with acid and heat (Stanbio Labs, Boerne, TX). Albumin levels were measured using an enzyme-linked immunosorbent assay (MP Biomedicals, Irvine, CA) with horseradish peroxidase detection and 3,3',5,5'-tetramethylbenzidine (TMB, Fitzgerald Industries, Concord, MA) as the substrate as previously described(21).
CYP450 enzyme activities were measured by first incubating cultures in substrates for 1 hour at

37°C and then detecting either the luminescence or fluorescence of metabolites using previously described protocols(23). In particular, CYP1A2 was measured by cleavage of ethoxyresorufin into fluorescent resorufin (Sigma-Aldrich, St. Louis, MO); CYP2A6 was measured by modification of coumarin to fluorescent 7-hydroxy-coumarin (Sigma-Aldrich); and, CYP3A4 was measured by cleavage of luciferin-IPA into luminescent luciferin (Promega, Madison, WI).

In order to assess glucose output in MPCC supernatants, hypo-, normo- or hyperglycemic cultures were first incubated in hormone-free PHH culture medium for 24 hours, washed 3 times with 1X phosphate buffered saline (PBS, Corning Cellgro, Manassas, VA), and then incubated for 4 to 8 hours in glucose-free and serum-free culture medium containing +/- gluconeogenic substrates (2 mM pyruvate from Corning Cellgro and 20 mM L-lactate from Sigma-Aldrich) and +/- recombinant human insulin (1 to 100 nM, Sigma-Aldrich). Finally, glucose levels in collected cell culture supernatants were measured using the Amplex Red glucose/glucose-oxidase assay kit (Life Technologies Molecular Probes, Eugene, OR).

3.2.4 Cell staining

Cultures were fixed with 4% (vol/vol) paraformaldehyde (Alfa Aesar, Ward Hill, MA) for 15 minutes at room temperature (RT), washed three times with 1X PBS, and nuclei and intracellular lipids were stained. Briefly, cultures were incubated in a 300 nM 4',6-diamidino-2-phenylindole (DAPI, MP Biomedicals, Solon, OH) solution for 10 minutes at RT, followed by incubation in a 10 μM Nile Red (AAT Bioquest, Sunnyvale, CA) solution for 10 minutes at 37°C. Cultures were then washed 3 times with 1X PBS and imaged using a DAPI light cube (excitation/emission: 357/447 nm) and GFP (green fluorescent protein) light cube

(excitation/emission: 470/510 nm) on an EVOS FL Imaging System (Life Technologies). Nile red staining was quantified by measuring the pixel intensity per island of PHHs using the ImageJ software(52).

FOXO1 immunofluorescent staining was carried out on normo- or hyperglycemic cultures after they had first been treated with hormone-free, serum-containing, 5 mM glucose medium for 24 hours and then treated with serum-free, glucose-free medium with +/- various concentrations of recombinant human insulin as described above. Cultures were fixed 1 hour after adding the aforementioned medium using 4% PFA in 1X PBS. Fixed cultures were first blocked for 1 hour at RT with blocking solution containing 5% (vol/vol) goat serum (Thermo Fisher Scientific) and 0.3% (vol/vol) Triton-X 100 in 1X PBS. Next, rabbit anti-human FOXO1 antibody (Thermo Fisher Scientific) was diluted in blocking solution at a concentration of 4 µg/mL and incubated with cells overnight at 4°C. Cells were washed three times with 1X PBS, and then a secondary goat anti-rabbit IgG Alexa Fluor™ 555 conjugated antibody (Thermo Fisher Scientific) was added at a concentration of 20 µg/ml diluted in blocking buffer for 2 hours at RT. Cultures were then washed three times with 1X PBS, nuclei were counter-stained with DAPI, and cells were imaged using the EVOS FL Imaging System as described above. N:C ratios of FOXO1 labeling were obtained using image J software.

Viability staining of fibroblasts and MPCCs were carried out using ReadyProbes® Cell Viability Imaging Kit (Thermo Fisher Scientific) and the EVOS FL Imaging System according to manufacturer's protocol. Briefly, 2 drops of live cell, NucBlue®, reagent (Hoechst 33342) and dead cell, propidium iodide, reagent were added per mL of cell culture medium needed and then incubated with cultures for 15 minutes at 37°C. Cell viability was assessed via the incorporation of propidium iodide into the nucleus and imaged using the EVOS FL Imaging System.

Propidium iodide only incorporates into cells with a compromised cell membrane, while Hoechst 33342 can permeate the membranes of live cells and bind to the DNA in the nucleus.

Glycogen was visualized in fixed cells using the periodic acid-Schiff (PAS) kit (Sigma Aldrich) according to manufacturer's recommendations. Briefly, fixed cultures were incubated with periodic acid solution for 5 minutes at RT. Cells were then washed time times with dH_2O and Schiff's reagent was added for 15 minutes at RT. Cells were then rinsed under tap water for 5 minutes continuously. Cultures were imaged with bright field microscopy and a color camera using the EVOS XL Core Cell Imaging System.

3.2.5 Statistical analysis

Each experiment was carried out in duplicate or triplicate wells for each condition. Three cryopreserved PHH donors were used when available to confirm trends. Error bars represent standard deviation (SD). Microsoft Excel and GraphPad Prism 5.0 (La Jolla, CA) were used for data analysis and plotting data. Statistical significance of the data was determined using the Student's *t*-test or one-way ANOVA with Dunnett's multiple comparison test for post hoc analysis.

3.3 Results

PHHs in MPCCs were initially stabilized in a normoglycemic culture medium (5 mM glucose) for 4 days to enable fibroblasts to reach a confluent monolayer across all conditions, and then exposed for up to 18 days to culture media supplemented with different glucose levels.

In order to induce a hypoglycemic state, no additional glucose was added to the culture medium except for the amount of glucose (0.4-0.5 mM) that was present in the 10% vol/vol bovine serum used. In order to mimic a hyperglycemic state, glucose was added to the serum-supplemented culture medium to yield a concentration of 25 mM, which was also chosen as a comparator to the high glucose culture media typically utilized for hepatocyte culture(24).

The glucose concentrations in the spent culture supernatants were measured every 2 days at the fresh medium exchange. MPCCs in the hypo- and normoglycemic culture media consistently consumed glucose over 3 weeks in culture with average glucose fluctuations from ~0.5 mM down to 0.03 mM (**Fig. 1A**) and ~5 mM down to 3.11 mM (**Fig. 1B**), respectively.

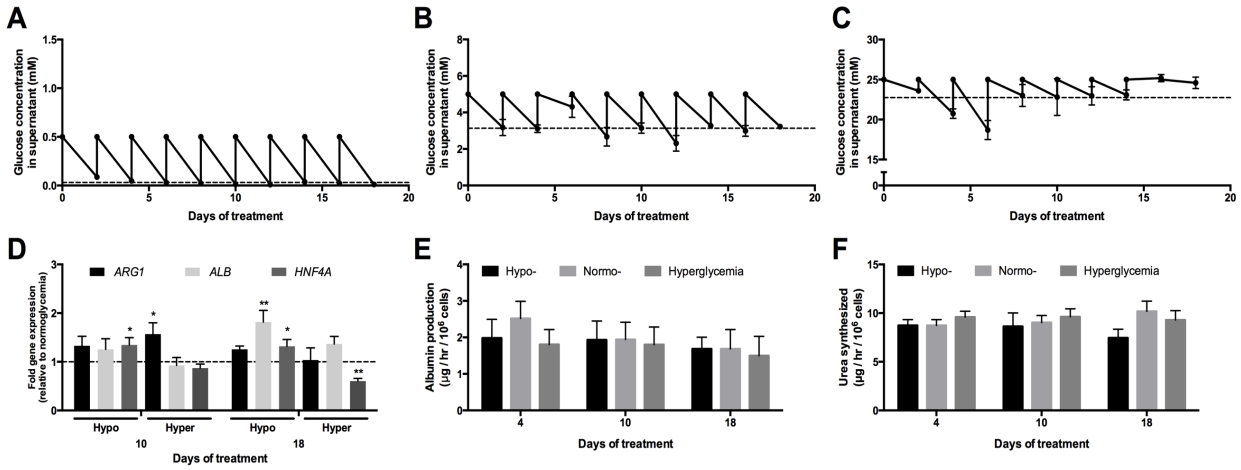

Figure 3.1. Albumin and urea secretion in MPCCs treated with varying levels of glucose. Fluctuations in culture medium glucose concentration in hypo- (**A**), normo- (**B**) and hyperglycemic (**C**) MPCCs over 3 weeks of culture. All cultures were initially cultured in a normoglycemic (5 mM glucose) culture medium for 4 days and then switched to their respective glycemic conditions (0.4-0.5 mM glucose for hypoglycemic and 25 mM glucose for hyperglycemic). Glucose levels in the depleted culture medium were measured with every 2-day culture media exchange. Dashed lines indicate average depleted glucose levels. Levels of albumin (*ALB*), arginase 1 (*ARG1*) and hepatocyte nuclear factor 4 α (*HNF4A*) mRNA transcripts (**D**) in MPCCs treated with hypo- and hyperglycemic culture media for either 10 or 18 days. Data is normalized to a normoglycemic control. Albumin (**E**) and urea secretion (**F**) in MPCCs incubated for up to 18 days in the varying glucose levels. Error bars represent SD. * $p \leq 0.05$ and ** $p \leq 0.01$. Trends were observed in multiple hepatocyte donors.

On the other hand, hyperglycemic cultures showed more erratic glucose consumption over three weeks with minor fluctuations in glucose levels at terminal time points and an average drop from ~25 mM down to 22.74 mM (**Fig. 1C)**. The use of propidium iodide (stains nuclei of dead cells) coupled with Hoechst 33342 (stains nuclei of live cells) showed no significant differences in PHH or 3T3-J2 viability in MPCCs treated with the various glucose concentrations for ~3 weeks (data not shown). Furthermore, 3T3-J2 fibroblast numbers, as measured by counting DAPI (4',6-diamindino-2-phenylindole)-stained fibroblast nuclei after 3 weeks of culture in MPCCs, were not significantly altered in the 3 different glucose concentrations (**Fig. S1**). The 3T3-J2 fibroblasts are required for maintenance of PHH functions in MPCCs(21,23). However, these non-liver and murine fibroblasts do not express the *human* mRNA transcripts measured here nor do they display liver functions, such as albumin secretion, urea synthesis and CYP450 activities(21).

3.3.1 Albumin and urea in MPCCs is not affected by the glycemic state

At the gene expression level, *ARG1* (arginase 1, urea cycle enzyme) was not significantly affected in hypoglycemic MPCCs, and only *transiently* upregulated in hyperglycemic MPCCs (~1.6 fold after 10 days of exposure) relative to the normoglycemic control (**Fig. 1D**). *ALB* (albumin) in hypoglycemic MPCCs was upregulated ~1.8 fold after 18 days of exposure relative to the normoglycemic control, while it was not affected to any significant degree in hyperglycemic MPCCs. *HNF4A* (hepatocyte nuclear factor 4 alpha) was upregulated ~1.3 fold in MPCCs after 10-18 days of exposure to a hypoglycemic culture medium, while it showed a downregulation (by ~40%) in hyperglycemic MPCCs after 18 days of exposure as compared to the normoglycemic control.

In spite of the aforementioned gene expression changes, neither the secretion of albumin (**Fig. 1E**) nor urea by MPCCs (**Fig. 1F**) was affected significantly in any of the glycemic states. These markers are used to monitor the overall 'health' and phenotypic stability of hepatocytes *in vitro*(24). On the other hand, the removal of serum from the culture medium caused PHH functions to decline irrespective of glucose levels (**Fig. S2**).

3.3.2 CYP450 pathways are modulated by glycemic states

At the gene expression level, *CYP1A2*, *CYP2B6*, *CYP2C19* and *CYP3A4* expression were significantly increased by ~2.7 fold, 3.1 fold, 1.8 fold, and 3.7 fold after 10 days of treatment with a hypoglycemic culture medium, respectively, as compared to a normoglycemic control (**Fig. S3**). Similar trends were observed after 18 days of treatment with a hypoglycemic culture medium such that *CYP1A2, CYP2D6*, *CYP2E1* and *CYP3A4* were increased by ~1.6 fold, 1.3 fold, 1.5 fold and 1.3 fold, respectively, relative to normoglycemic MPCCs. *CYP2A6* expression in hypoglycemic MPCCs remained within the range of the normoglycemic control.

In hyperglycemic MPCCs, we measured a ~1.5 fold increase in *CYP2A6* transcript, while the other CYP450 transcripts (*CYP1A2, CYP2B6, CYP2C19, CYP2D6, CYP2E1*, and *CYP3A4)* were not significantly affected after 10 days of treatment relative to the normoglycemic control (**Fig. S3**). However, after 18 days of treatment, hyperglycemic cultures showed upregulation of *CYP1A2* (~1.3 fold) and *CYP2D6* (~1.4 fold), while *CYP2E1* was downregulated (by ~43%) as compared to the normoglycemic cultures.

When we measured CYP450 enzyme activities in MPCCs using prototypical substrates, we observed a ~1.7 fold increase in CYP3A4 activity after 4 and 10 days of treatment, and ~2.3

fold increase after 18 days of treatment with a hypoglycemic culture medium relative to the normoglycemic control (**Fig. 2A**). CYP3A4 activity was decreased (by ~40%) in hyperglycemic cultures after 4 days of treatment, but such a decrease was diminished after 10 and 18 days of treatment compared to the normoglycemic cultures. On the other hand, neither CYP1A2 activity (**Fig. 2B**) nor CYP2A6 activity (**Fig. 2C**) in MPCCs was significantly affected as a function of glucose levels in the culture medium over 18 days of exposure.

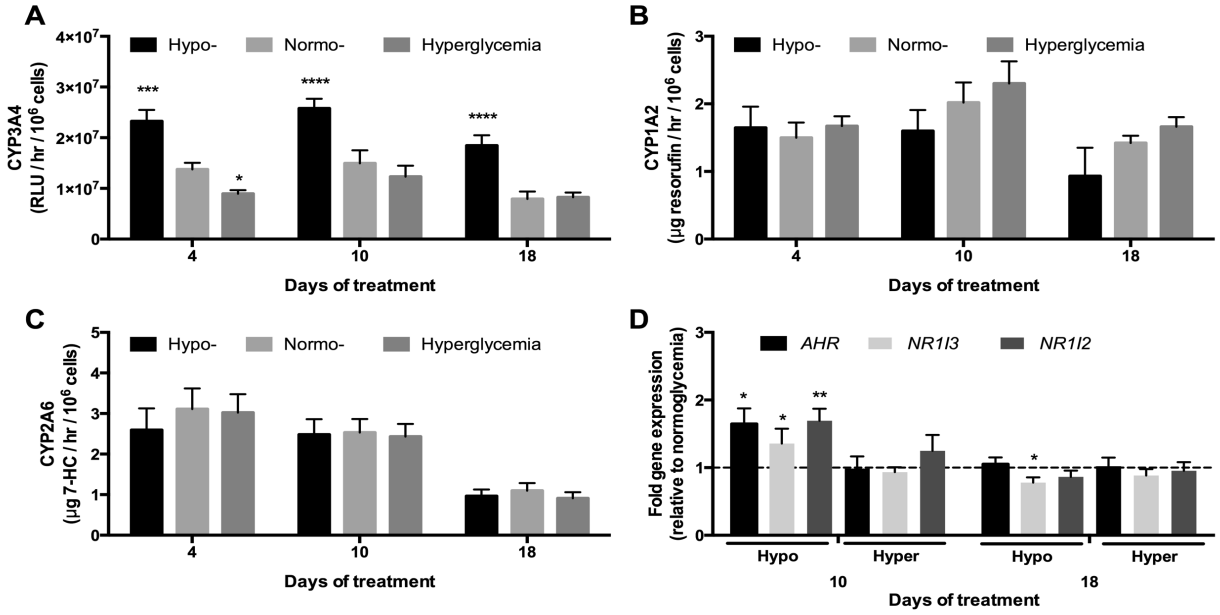

Figure 3.2. Glucose-induced modulation of CYP450 pathways in MPCCs. (A) CYP3A4 enzyme activity in MPCCs (as measured by cleavage of luciferin-IPA into luciferin) treated with hypo-, normo- and hyperglycemic culture media for up to 18 days. (**B**) CYP1A2 activity (as measured by cleavage of ethoxyresorufin into resorufin) in MPCCs treated as in panel (**A**). (**C**) CYP2A6 activity (as measured by conversion of coumarin into 7-hydroxycoumarin) in MPCCs treated as in panel (**A**)**.** (**D**) Levels of aryl hydrocarbon receptor (*AHR*), constitutive androstane receptor (*NR1I3*) and pregnane X receptor (*NR1I2*) mRNA transcripts in MPCCs treated with hypo- and hyperglycemic culture media for 10 or 18 days. Data is normalized to a normoglycemic control. Error bars represent SD. * $p \leq 0.05$, ** $p \leq 0.001$, *** $p \leq 0.01$, and **** $p \leq 0.0001$. Trends were observed in multiple hepatocyte donors.

The aforementioned increase in CYP3A4 activity in hypoglycemic MPCCs relative to the normoglycemic control could potentially be due to the up-regulation of *NR1I2* (nuclear receptor subfamily 1, group I, member 2, also known as pregnane X receptor or *PXR)* and *NR1I3* (nuclear

receptor subfamily 1, group I, member 3, also known as constitutive androstane receptor or *CAR*) transcripts(25) by ~1.7 fold and ~1.4 fold, respectively, after 10 days of exposure (**Fig. 2D**). Interestingly, the up-regulation of *AHR* (aryl hydrocarbon receptor) transcripts measured in hypoglycemic MPCCs by ~1.6 fold relative to the normoglycemic control after 10 days of exposure did not correlate with the lack of modulation observed in CYP1A2 enzyme activity(26) (Fig. 2B). However, such upregulation of nuclear receptors at the gene expression level in MPCCs was diminished after 18 days of exposure to a hypoglycemic culture medium. None of the aforementioned nuclear receptors' transcripts were modulated to any significant degree in hyperglycemic MPCCs as compared to the normoglycemic control.

3.3.3 Hepatic lipid accumulation in MPCCs increases under hyperglycemia

Under all glucose treatments, PHHs cultured in MPCCs remained attached to the distinct micropatterned collagen islands and maintained prototypical *in vivo*-like morphology (i.e. polygonal shape, distinct nuclei/nucleoli, visible bile canaliculi) over ~3 weeks of treatment (**Fig. S4**). Additionally, we did not observe any overt changes in the morphology and spreading of fibroblasts in MPCCs as a function of glucose concentrations. However, PHHs exposed to a hyperglycemic culture medium in the presence of insulin over a prolonged culture duration accumulated vesicles in their cytoplasm at a greater rate/level than PHHs exposed to hypo- and normoglycemic media (**Fig. 3A-C, Fig. S5A-C**). The vesicles that accumulated in the hepatic cytoplasm were found to be neutral lipids (i.e. triacylglycerol and cholesterol esters) via Nile red staining (**Fig. 3D-F, Fig. S5D-F**). Some lipid accumulation was also observed in PHHs exposed to a normoglycemic culture medium, while PHHs exposed to a hypoglycemic culture medium

accumulated little or no lipids throughout the culture duration even in the presence of insulin. Quantification of the Nile Red fluorescence intensities revealed that there were ~1.7 and ~2.1 fold more lipids after 10 days and 18 days of exposure to a hyperglycemic culture medium, respectively, when compared to a normoglycemic control (**Fig. 3G**). In contrast, hypoglycemic MPCCs had ~50% of the hepatic lipids found in normoglycemic MPCCs.

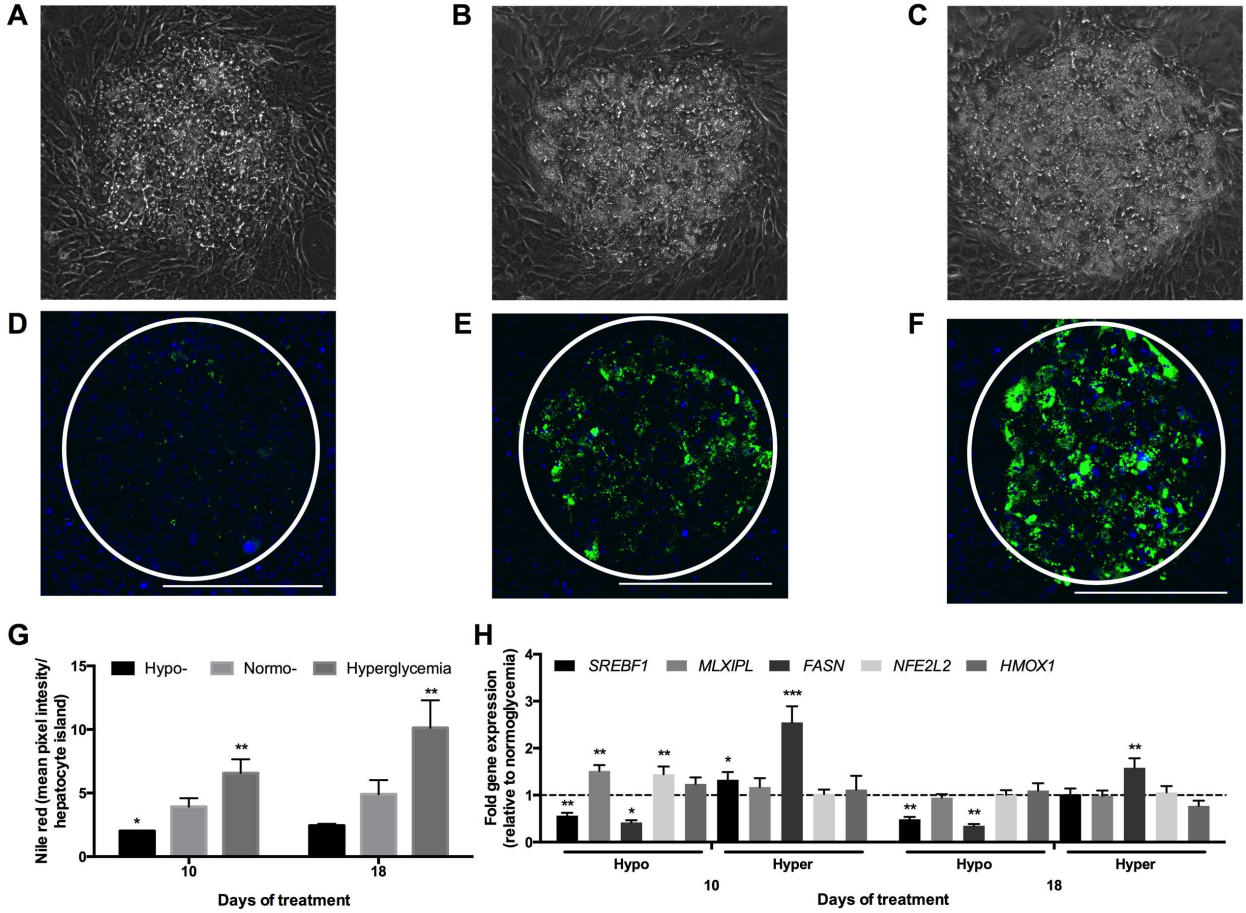

Figure 3.3. Glucose-induced accumulation of neutral lipids in MPCCs. Phase contrast images of MPCCs treated for 18 days with a hypo- (**A**), normo- (**B**) and hyperglycemic (**C**) culture medium. Nile red (neutral lipids) staining of MPCCs treated for 18 days with a hypo- (**D**), normo- (**E**) and hyperglycemic (**F**) culture medium. Scale bars represent 400 µm. (**G**) Quantification of Nile Red staining in hepatocyte islands in MPCCs subjected to hypo-, normo- or hyperglycemic culture media for 10 or 18 days. (**H**) Levels of sterol regulatory element binding protein (*SREBF1*), carbohydrate response element binding protein (*MLXIPL*), fatty acid synthase (*FASN*), nuclear factor (erythroid-derived 2)-like 2 (*NFE2L2)* and heme oxygenase 1 (*HMOX1*) mRNA transcripts in MPCCs treated with hypo- and hyperglycemic culture media for 10 or 18 days. Data is normalized to a normoglycemic control. Error bars represent SD. * $p \leq 0.05$, ** $p \leq 0.01$, and *** $p \leq 0.001$. Trends were observed in multiple hepatocyte donors.

Consistent with the aforementioned lipid profile, *FASN* (fatty acid synthase) and *SREBF1* (sterol regulatory element binding transcription factor 1) mRNA transcripts were upregulated ~2.5 fold and ~1.3 fold, respectively, in hyperglycemic MPCCs relative to a normoglycemic control after 10 days of exposure (**Fig. 3H**). After 18 days of exposure, only *FASN* remained upregulated by ~1.6 fold in hyperglycemic MPCCs relative to normoglycemic cultures. In contrast, expression levels of *MLXIPL* (MLX-interacting protein-like, also known as carbohydrate responsive element binding protein or ChREBP), *HMOX1* (heme oxygenase 1, oxidative stress marker), and *NFE2L2* (nuclear factor (erythroid-derived 2)-like 2, oxidative stress marker) were not affected to any significant degree in hyperglycemic MPCCs when compared to a normoglycemic control.

In hypoglycemic MPCCs, *FASN* and *SREBF1* were downregulated by ~58% and ~44% after 10 days of exposure, and by ~65% and ~51% after 18 days of exposure, respectively, as compared to normoglycemic levels (**Fig. 3H**). Surprisingly, *MLXIPL* expression in hypoglycemic MPCCs was increased by ~1.5 fold after 10 days of exposure, although this diminished after 18 days of exposure. *HMOX1* was not increased significantly in hypoglycemic MPCCs relative to the normoglycemic control. Finally, *NFE2L2* was increased by ~1.4 fold in hypoglycemic MPCCs relative to the normoglycemic control after 10 days of exposure; however, such an increase diminished after 18 days of exposure.

3.3.4 Hyperglycemic MPCCs become less sensitive to insulin's effects on glucose output

We first probed the expression levels of genes involved in glucose metabolism in MPCCs treated with varying glucose concentrations in the culture medium. *PCK1* (phosphoenolpyruvate

carboxykinase 1) gene expression was upregulated by ~1.4 fold in hypoglycemic cultures as compared to the normoglycemic control after 10 days of exposure (**Fig. 4A**). However, after 18 days of exposure, *PCK1* expression was downregulated in hypoglycemic cultures by ~31% of normoglycemic transcript levels. *SLC2A2* (solute carrier family 2, facilitated glucose transporter member 2) gene expression was similar between hypo- and normoglycemic cultures. On the other hand, *G6PC* (glucose-6-phosphatase, catalytic subunit) expression was downregulated in hypoglycemic cultures by ~50% and ~70% of normoglycemic levels after 10 and 18 days of exposure, respectively. Finally, *GK1* (glycerol kinase) expression was not significantly altered in hypoglycemic MPCCs as compared to normoglycemic MPCCs.

In hyperglycemic MPCCs, *PCK1* gene expression was upregulated by ~1.4 fold relative to normoglycemic controls after 10 days of exposure (**Fig. 4A**). However, after 18 days of exposure, *PCK1* expression was downregulated in hyperglycemic cultures by ~57% of normoglycemic transcript levels. *SLC2A2* gene expression was upregulated by ~1.5 fold in hyperglycemic cultures relative to the normoglycemic control after 10 days of exposure. Following 18 days of exposure, *SLC2A2* expression became similar across normo- and hyperglycemic MPCCs. In contrast to hypoglycemic MPCCs, *G6PC* gene expression was upregulated in hyperglycemic cultures at 10 and 18 days of exposure to ~2.5 fold and ~1.8 fold of the normoglycemic control, respectively. Lastly, *GK1* expression showed a slight downregulation in hyperglycemic MPCCs by ~28% of normoglycemic controls, but only after 18 days of exposure.

Next, we assessed the effects of insulin doses on glucose secretion from MPCCs treated with varying glucose levels. In particular, normo- and hyperglycemic MPCCs exposed to the respective glucose levels for 10 days were subsequently incubated for 1 day in hormone-free (but

5 mM glucose-supplemented) culture medium, and then placed in glucose-free and serum-free culture medium containing substrates for gluconeogenesis (20 mM L-lactate and 2 mM pyruvate) in the presence or absence of different doses of recombinant human insulin.

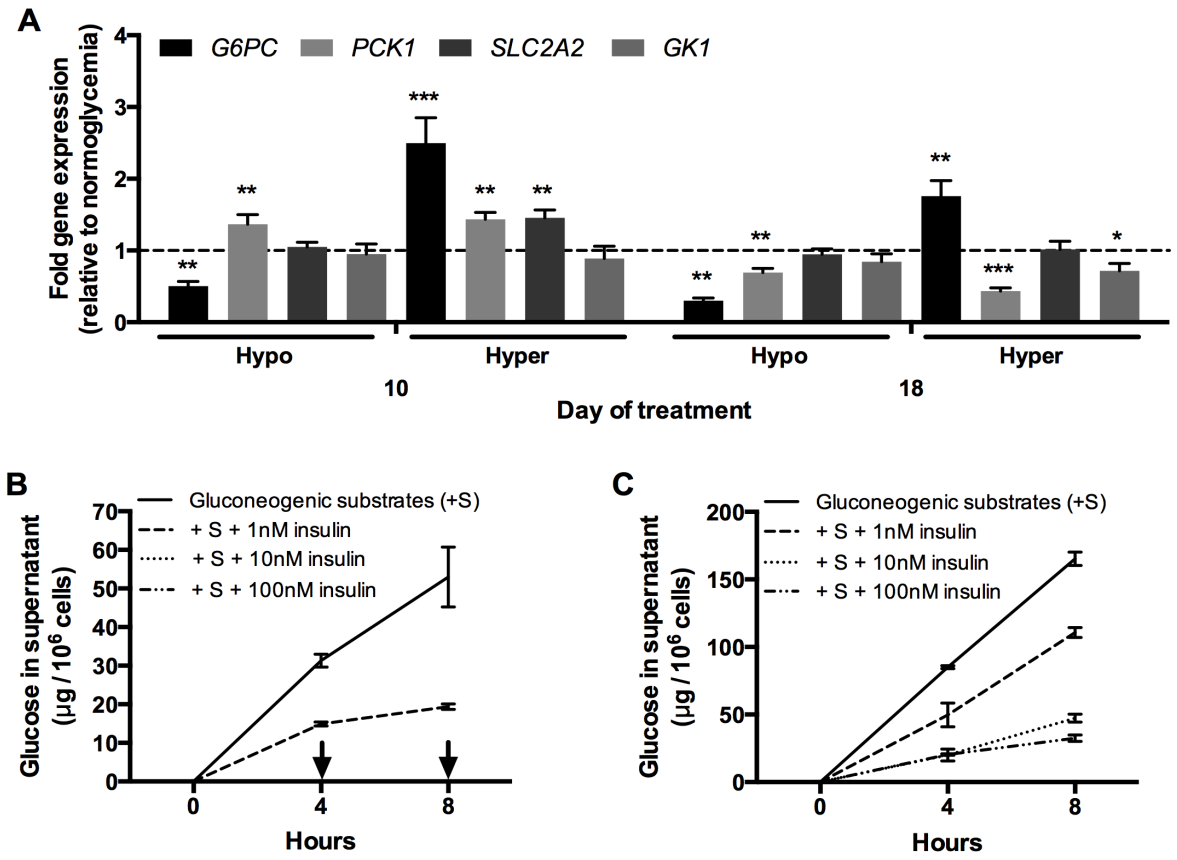

Figure 3.4. Glucose-induced modulation of glucose metabolism pathways and insulin sensitivity in MPCCs. (**A**) Levels of glucose-6-phosphatase catalytic subunit (*G6PC*), phosphoenolpyruvate carboxykinase-1 cytosolic (*PCK1*), glucose transporter 2 (*SLC2A2*) and glycerol kinase (*GK1*) mRNA transcripts in MPCCs treated with hypo- and hyperglycemic culture media for 10 or 18 days. Data is normalized to a normoglycemic control. (**B**) Glucose output in supernatants of normoglycemic MPCCs (10 days of treatment) treated with gluconeogenic substrates (20 mM lactate and 2 mM pyruvate) in the presence or absence of different levels of insulin (see methods for additional details). Arrows indicate no detectable glucose in supernatants. (**C**) Glucose output as in panel (**B**) except hyperglycemic MPCCs were used. Error bars represent SD. * $p \leq 0.05$, ** $p \leq 0.01$, and *** $p \leq 0.001$. Similar results were observed in another primary hepatocyte donor.

After 8 hours of stimulation, normoglycemic hepatocytes produced ~53 µg of glucose per million hepatocytes in supernatants (**Fig. 4B**), while hyperglycemic hepatocytes produced 165 µg

of glucose per million hepatocytes (**Fig. 4C**). When incubated with a 1 nM dose of insulin, glucose output from normoglycemic and hyperglycemic MPCCs was reduced by ~64% and ~33% of insulin-free controls, respectively. Increasing the insulin doses to 10 and 100 nM completely inhibited glucose output from normoglycemic MPCCs. On the other hand, glucose output was still detected at high levels (32-47 μg/million hepatocytes) in supernatants from hyperglycemic MPCCs treated with 10 and 100 nM insulin, suggesting an insulin resistant phenotype in hyperglycemic MPCCs relative to the normoglycemic control.

A time-course assessment showed that the aforementioned insulin resistance trends started appearing in hyperglycemic MPCCs after 6 days of exposure (but not after 2 days) and persisted through the exposure period of 18 days (**Fig. S6**). Furthermore, reducing the glucose concentration in a hyperglycemic culture medium down to 12.5 mM led to a similar amount of lipid accumulation as observed in the 25 mM glucose concentration. However, significant insulin resistance was only observed in the 25 mM glucose culture medium when compared to the normoglycemic control. Lastly, insulin resistance was also observed in hyperglycemic MPCCs relative to the normoglycemic control when the PHHs were allowed to produce glucose in supernatants in the *absence* of gluconeogenic substrates (**Fig. S7**). Without gluconeogenic substrates, PHHs can presumably produce glucose due to potential gluconeogenesis from other sources (i.e. free amino acids and glycerol) and/or the lysis of built-up glycogen stores, which were found to be similar across the normo- and hyperglycemic MPCCs *prior* to incubation with the hormone-free culture medium as mentioned above (**Fig. S7**).

As an alternative measure of altered insulin signaling in hyperglycemic MPCCs relative to their normoglycemic counterparts, we assessed FOXO1 (forkhead box O1) levels in the nucleus and cytoplasm of cultures after stimulation with different doses of insulin for 1 hour.

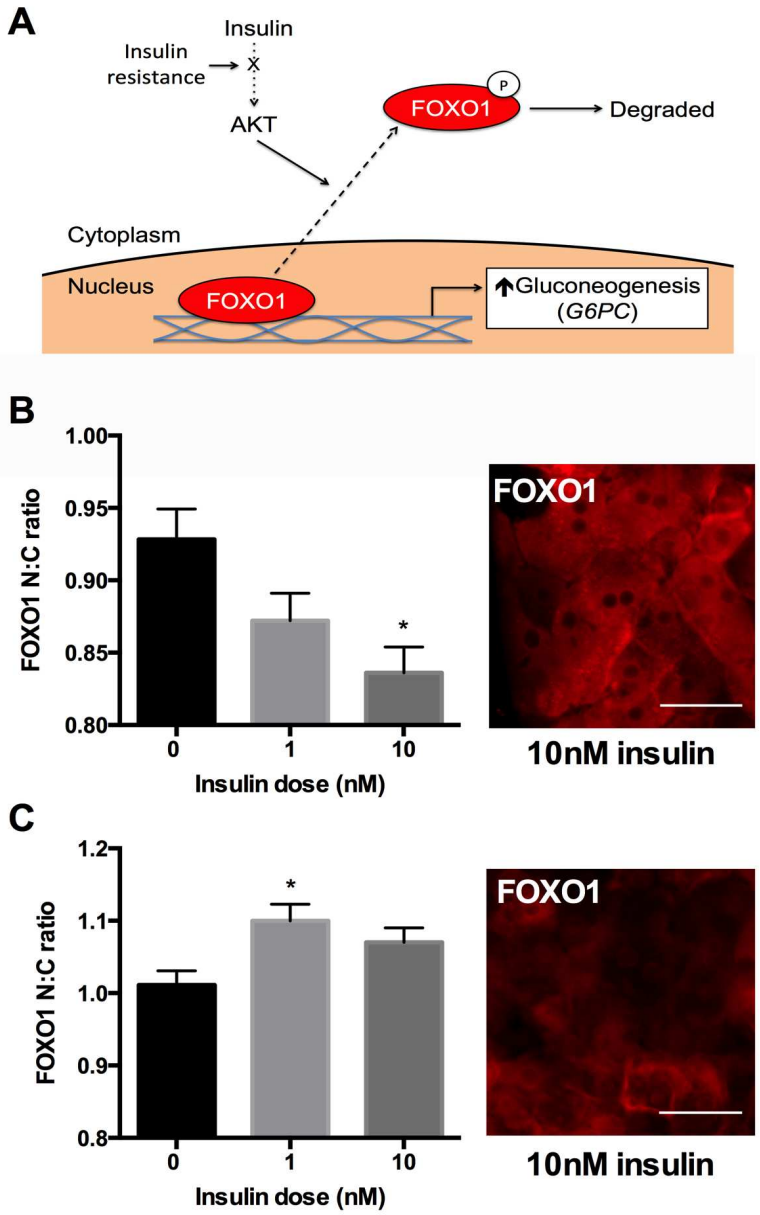

Figure 3.5. Insulin-induced translocation of FOXO1 in hepatocytes. (**A**) Schematic illustrating the effect of insulin on translocation of transcription factor, FOXO1 (forkhead box O1) from the nucleus to the cytoplasm. FOXO1 typically stimulates gluconeogenic gene expression in the nucleus; however, in the presence of insulin, Akt phosphorylates FOXO1, thereby causing its translocation from the nucleus to the cytoplasm where it is degraded. MPCCs treated with a hyperglycemic or normoglycemic culture medium for 10 days were treated for 1 hour with 0, 1 or 10 nM insulin and then FOXO1 protein localization was visualized via immunostaining (see methods for additional details). (**B**) Quantification of nuclear to cytoplasmic (N:C) ratio of FOXO1 labeling in primary human hepatocytes within normoglycemic MPCCs after stimulation with or without insulin doses (n= 205 cells per treatment). Representative image of the FOXO1 labeling is shown to the right. (**C**) Quantification of N:C ratio of FOXO1 and representative image of the FOXO1 labeling in

hyperglycemic MPCCs (n= 205 cells per treatment). Scale bars are 30 μm. Error bars represent SD. * $p \leq 0.05$, ** $p \leq 0.01$, and *** $p \leq 0.001$.

FOXO1 is a transcription factor involved in the transcription of gluconeogenic genes. Normal insulin signaling leads to the translocation of FOXO1 from the nucleus to the cytoplasm where it is degraded, thereby decreasing gluconeogenesis(27) (**Fig. 5A**). The nuclear to cytoplasmic ratio (N:C) of FOXO1 has been previously used to assess FOXO1 sensitivity to insulin stimulation(28). Here, we found that normoglycemic PHHs in MPCCs showed a reduction in the FOXO1 N:C ratio from 0.93 in an insulin-free control down to 0.87 and 0.84 with a 1 nM and 10 nM insulin stimulation, respectively (**Fig. 5B**). On the other hand, hyperglycemic PHHs in MPCCs showed an increase in the FOXO1 N:C ratio from 1.01 in an insulin-fee control up to 1.1 and 1.07 in 1 nM and 10 nM insulin simulation, respectively (**Fig 5C**).

3.4 Discussion

Hyperglycemia in T2DM has been implicated in the development of NAFLD, which can further exacerbate insulin resistance and progress to NASH, fibrosis/cirrhosis and hepatocellular carcinoma(29). Conversely, hypoglycemia in the liver due to fasting, cancer or the effects of T2DM drugs can induce changes in drug metabolism pathways, which can potentially alter drug efficacy and/or toxicity(5-8). *In vitro* models of the human liver can supplement animal studies for investigating the progression of disease profiles and drug outcomes given species-specific differences in drug metabolism(15,24). PHHs are considered to be the 'gold standard' for creation of such models; however, these cells rapidly decline in their phenotypic functions in conventional monolayers, including sensitivity to insulin and glucagon(22). Such a functional

decline can be mitigated for a few weeks when PHHs are placed in MPCCs(22). Here, we incubated MPCCs in a hypo- or hyperglycemic culture medium for ~3 weeks and compared phenotypic changes to those observed in a normoglycemic control. We observed for the first time that PHHs in MPCCs: a) maintain albumin and urea secretions at similar levels across all glycemic states; b) significantly upregulate CYP3A4 activity under hypoglycemia; and, c) accumulate neutral lipids while becoming less sensitive to insulin-mediated reduction in glucose output under hyperglycemia as compared to a normoglycemic control.

Surprisingly, we found that besides what was found in serum (~0.4-0.5 mM glucose in medium containing 10% vol/vol serum), no additional glucose supplementation in the culture medium was required to enable the survival of 3T3-J2 fibroblasts as well as the survival and major functions (i.e. albumin and urea secretion) of PHHs in such hypoglycemic MPCCs after ~3 weeks of treatment as compared to other glycemic states. Additionally, oxidative stress markers (*HMOX1* and *NFE2L2* gene expression) did not vary significantly across MPCCs treated with varying glucose levels, except for a transient upregulation in hypoglycemic MPCCs (~1.4 fold relative to a normoglycemic control). However, removal of serum from the culture medium caused PHH functions to decline irrespective of glucose concentrations, which is likely due to the lack of fibroblast spreading and growth in serum-free medium, along with other unidentified factors in serum that may be beneficial for PHHs. Thus, our results suggest that the levels of glucose (10-25 mM) present in many culture media bases (i.e. Williams E, DMEM, Alpha-MEM)(21,30) might not be necessary for high functions of *stable* PHHs in co-culture with stromal cells; however, serum is a required supplement.

While albumin and urea secretion were not affected in hypoglycemic MPCCs, expression of CYP450 transcripts (*1A2, 2B6, 3A4, 2C19*) consistently showed significant upregulation

relative to a normoglycemic control. Such increases in CYP450 gene expression are likely due to the measured upregulation of NR gene expression (*AHR, PXR, CAR)* in hypoglycemic MPCCs. Specifically, PXR and CAR activation induce hepatic CYP3A4 expression(25), while AHR activation induces CYP1A2 expression(26). NRs are also sensitive to cellular energy status and can thus mediate glucose metabolism(31). At the enzyme activity level, CYP1A2 and CYP2A6 were not affected under hypoglycemia as compared to normoglycemia; however, hypoglycemia led to a significant (up to 2.3 fold) increase in CYP3A4 activity, an enzyme involved in the metabolism of >50% of drugs on the market(32). Such an upregulation in CYP3A4 activity could have clinical implications for altered drug efficacy and/or toxicity. While our results in PHHs over long-term culture are novel, they are consistent with the activation of PXR and upregulation of CYP3A11 (ortholog of CYP3A4) during fasting of rodents(5,6,33).

As with hypoglycemia, hyperglycemia did not affect albumin and urea secretion as compared to a normoglycemic control. However, expression of some CYP450 transcripts (*2A6, 1A2*, *2D6)* showed a slight (~1.3-1.5 fold) upregulation, while *2E1* was downregulated when MPCCs were exposed to a hyperglycemic culture medium as compared to a normoglycemic control. In spite of the aforementioned gene expression changes, CYP1A2 and CYP2A6 activities were not affected in hyperglycemic MPCCs relative to the other glycemic states. Consistent with its gene expression, CYP3A4 activity was similar between hyperglycemic and normoglycemic MPCCs. The lack of changes in measured CYP450 activities in hyperglycemic MPCCs are not always consistent with changes in CYP450 activities observed in patients with NAFLD, such as decreased CYP3A4/3A5 activity(34-36), decreased CYP1A2 activity(35,37,38) and increased CYP2A6 activity(38). However, statistical confidence is not always reached in clinical studies due to significant donor-to-donor variabilty(38). While our CYP450 results could

be due to variability in response across PHH donors, they could also suggest that hyperglycemia and ensuing lipid accumulation are not responsible for all the changes in drug metabolism enzymes seen in NAFLD patients. In addition to any lipid accumulation due to hyperglycemia, fatty acids delivered to the liver from adipose tissue also contribute to NAFLD(39). Therefore, the effects of different types of fatty acids on long-term drug metabolism changes in PHHs merits further investigation.

Similar to T2DM patients, a hyperglycemic state induced between 1.7 fold and 2.1 fold greater accumulation of neutral lipids (i.e. triacylglycerol and cholesterol esters) in PHHs relative to a normoglycemic control. Furthermore, hyperglycemic cultures had elevated *FASN* and *SREBF1* gene expression, whereas the expression of *MLXIPL* was unchanged by hyperglycemia as compared to normoglycemic cultures. The *SREBF*1 gene encodes for SREBP-1c, an insulin-responsive transcription factor that regulations *de novo* lipogenesis, including the expression of *FASN*(40). Thus, it is likely that the increased lipid accumulation observed in hyperglycemic MPCCs is due to the excess glucose being shuttled into insulin-stimulated lipogenesis pathways(41). On the other hand, hypoglycemic MPCCs showed significant downregulation (~50%) of *FASN* and *SREPF1* expression and neutral lipid accumulation relative to normoglycemic MPCCs.

Hyperglycemic MPCCs became less sensitive to insulin's effects on gluconeogenesis over time relative to the normoglycemic control (i.e. insulin resistance). Such a trend was also observed in the absence of supplemented gluconeogenic substrates. The increase in glucose output from hyperglycemic MPCCs correlated with significantly higher expression of *G6PC* as compared to the normoglycemic control. Interestingly, *HMOX1*, a positive predictor of insulin resistance in obese individuals(42), was not altered in hyperglycemic PHHs at the gene

expression level. While we cannot rule out differential protein activity, the lack of changes in transcript potentially suggest a different mechanism by which hyperglycemia induces insulin resistance in PHHs relative to the insulin resistance observed in individuals whose livers are being affected by both *de novo* lipogenesis and delivery of fatty acids from adipocytes. Importantly, we found that FOXO1 displacement from the nucleus following stimulation with insulin, which normally inhibits gluconeogenesis, was significantly decreased in hyperglycemic PHHs relative to the normoglycemic PHHs. Since insulin-stimulated pathways, namely AKT-mediated phosphorylation, cause the translocation of FOXO1 from the nucleus to the cytoplasm(43), it is conceivable that this arm of the insulin signaling pathway is inhibited under hyperglycemia in MPCCs. However, further cell signaling studies would be required to probe such mechanisms in greater detail.

To our knowledge, our study constitutes the first time that 'selective' insulin resistance has been observed in hyperglycemic PHHs such that insulin continued to simulate lipid accumulation (steatosis) but did not reduce glucose output to the same extent as the normoglycemic control. Complete loss of insulin signaling (i.e. lipogenesis and glucose production) can be achieved using liver-specific insulin receptor knockout mice(44). However, the selective insulin resistance we observed in PHHs is more akin to a T2DM state in humans in which insulin fails to suppress gluconeogenesis but continues to activate lipogenesis, thereby leading to hyperglycemia, hypertriglyceridemia and steatosis(45). Hypertriglyceridemia has been linked to lipotoxicity in multiple organs, including NASH(46). Furthermore, the resulting hyperglycemia due to selective insulin resistance continues to stimulate insulin production from the pancreas, which causes the classic triad of hyperinsulinemia, hyperglycemia, and hypertriglyceridemia in patients with T2DM.

While our results provide fundamental insights into how varying glucose levels affect the PHH phenotype, the liver also contains non-parenchymal cells (**NPCs**), such as Kupffer macrophages (**KMs**), sinusoidal endothelial cells and stellate cells, that can modulate NAFLD/NASH progression(47,48). The MPCC platform is 'modular' in that controlled interactions between PHHs and different NPCs can be studied without significant changes to PHH homotypic interactions on the micropatterned ECM domains. In our experience, 3T3-J2 fibroblasts induce higher levels of functions in PHHs than liver NPCs (manuscript in preparation). However, liver NPCs can be cultured within or on top of the fibroblast layer to provide a better physiological context while retaining high hepatic functions. For instance, KMs can be cultured atop pre-established MPCCs to study the effects of KM activation on hepatic CYP450s(49). This model can also be useful to study how PHHs and KMs interact when cultured in a NAFLD/NASH-like milieu (i.e. hyperglycemia). Other groups are pursuing inclusion of stellate cells into PHH models(50), which could be useful to understand the role of these cells in liver diseases.

In conclusion, we show the utility of long-term PHH cultures for understanding how energy sources lead to changes in glucose metabolism and hormonal responsiveness that have been implicated in T2DM, NAFLD and NASH. In the future, MPCCs could be useful for novel drug discovery efforts for such diseases. Ultimately, coupling MPCCs with other tissue types on a microfluidic chip can allow a systems level exploration of disease progression.

3.5 Supplemental Figures

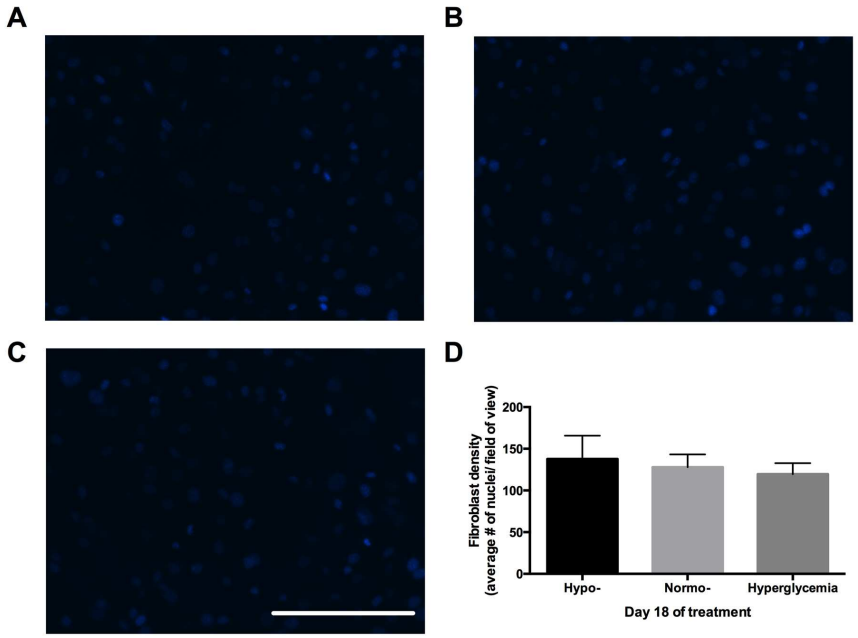

Supplemental Figure 3.5.1. Effects of glucose concentration on fibroblast numbers in MPCCs. MPCCs were fixed after 18 days of treatment with various glucose concentrations and stained with DAPI for cell counting. Images of 3T3-J2 fibroblasts between hepatocyte islands cultured in hypo- (0.4- 0.5 mM) (**A**), normo- (5 mM) (**B**) and hyperglycemic (25 mM) (**C**) culture medium on day 18 of treatment. Scale bar is 200 µm. (**D)** Average number of cells per field of view quantified using ImageJ software. Error bars represent SD.

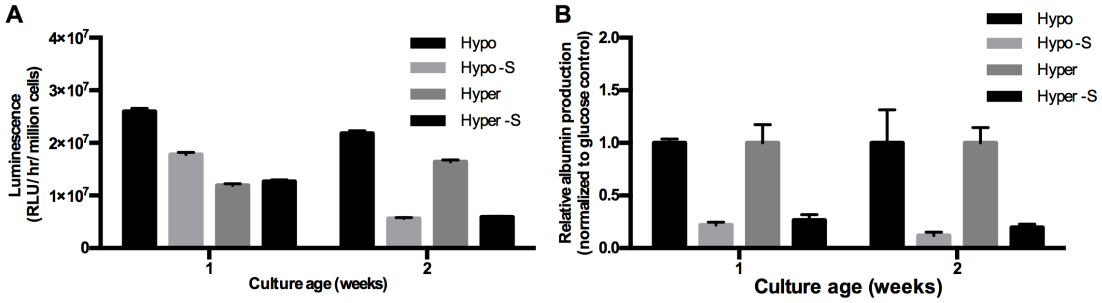

Supplemental Figure 3.5.2. Serum removal decreases hepatocyte functions in MPCCs. MPCCs were established for 4 days and then serum was removed from culture media. **(A)** CYP3A4 activity measured with Luciferin-IPA in hypo- and hyperglycemic medium with or without 10% (vol/vol) serum (-S). (**B)** Relative albumin production in hypo- and hyperglycemic medium with or without serum (-S). Data is normalized to the serum-containing control for each glucose level. Error bars represent SD across 3 wells. Similar results were observed in another primary hepatocyte donor.

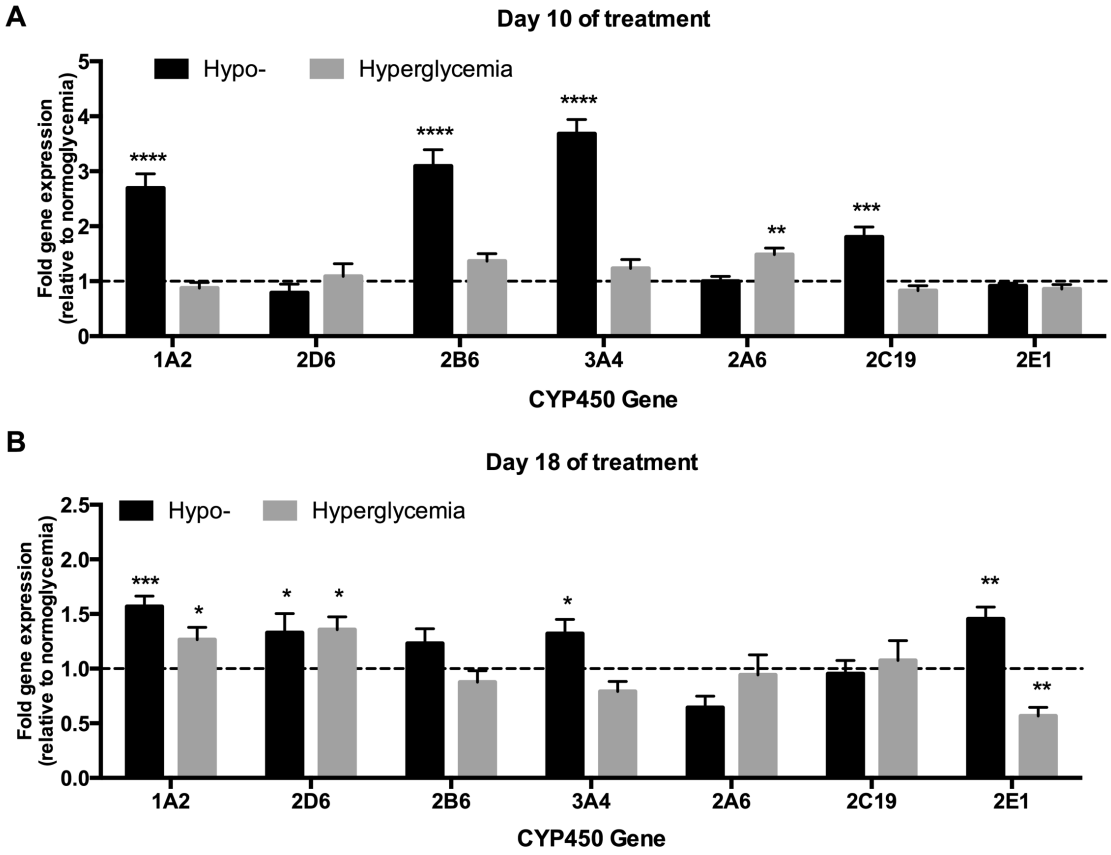

Supplemental Figure 3.5.3. Glucose-induced modulation of CYP450 gene expression in MPCCs. Levels of CYP1A2 *(1A2),* CYP2D6 (*2D6*), CYP2B6 (*2B6*), CYP3A4 *(3A4)*, CYP2A6 (*2A6*), CYP2C19 (*2C19*), and CYP2E1 (*2E1*) mRNA transcripts in MPCCs treated with hypo- and hyperglycemic culture media for 10 days (**A**) and 18 days (**B**). Data is normalized to the normoglycemic control. Error bars represent SD. * $p \leq 0.05$, ** $p \leq 0.01$, *** $p \leq 0.001$, and **** $p \leq 0.0001$.

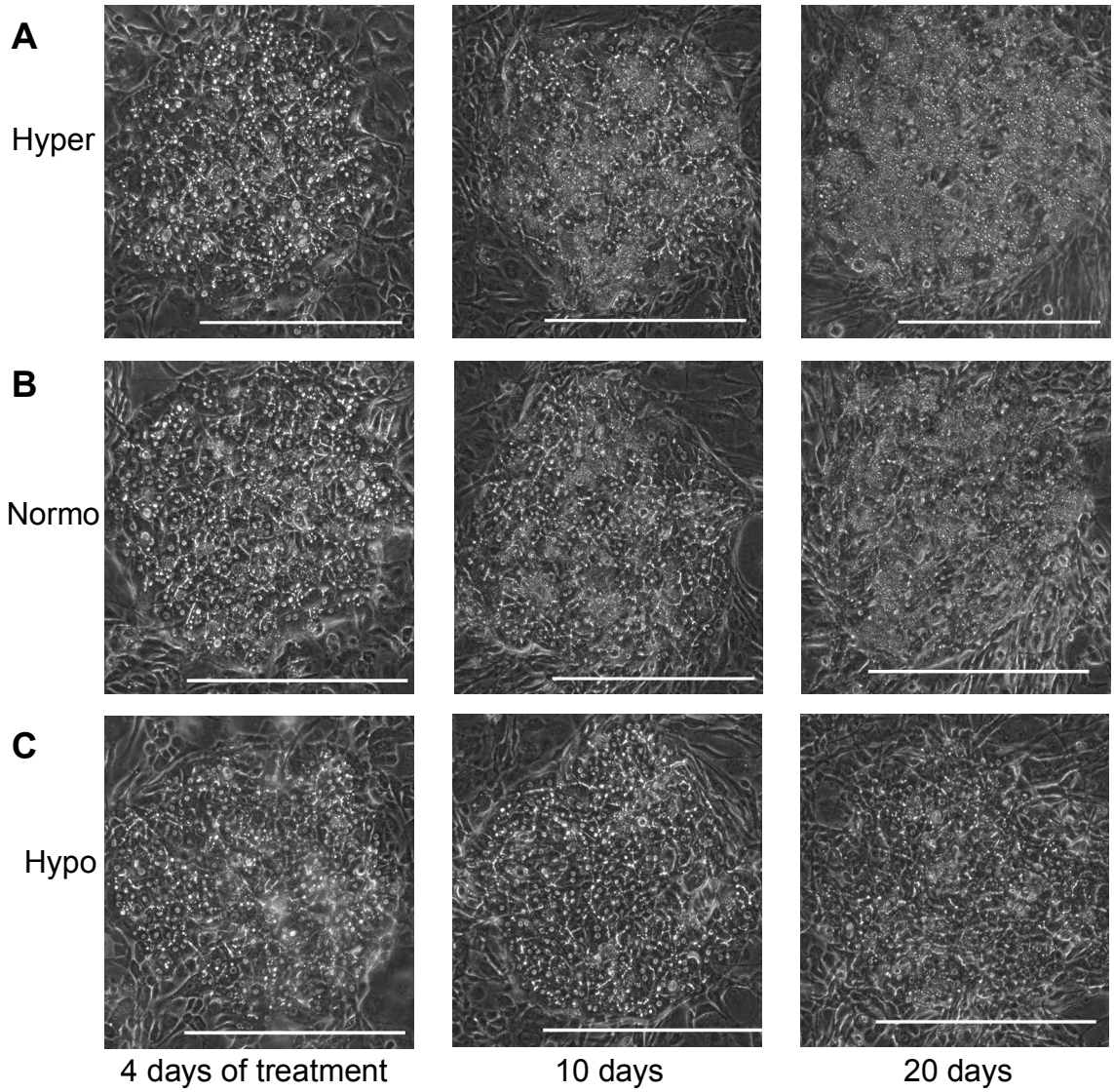

Supplemental Figure 3.5.4. Glucose-induced changes in hepatocyte morphology in MPCCs. Phase contrast image of PHHs in MPCCs treated over time with a hyper- (**A**), normo- (**B**), and hypoglycemic (**C**) culture medium. Scale bars represent 400 μm.

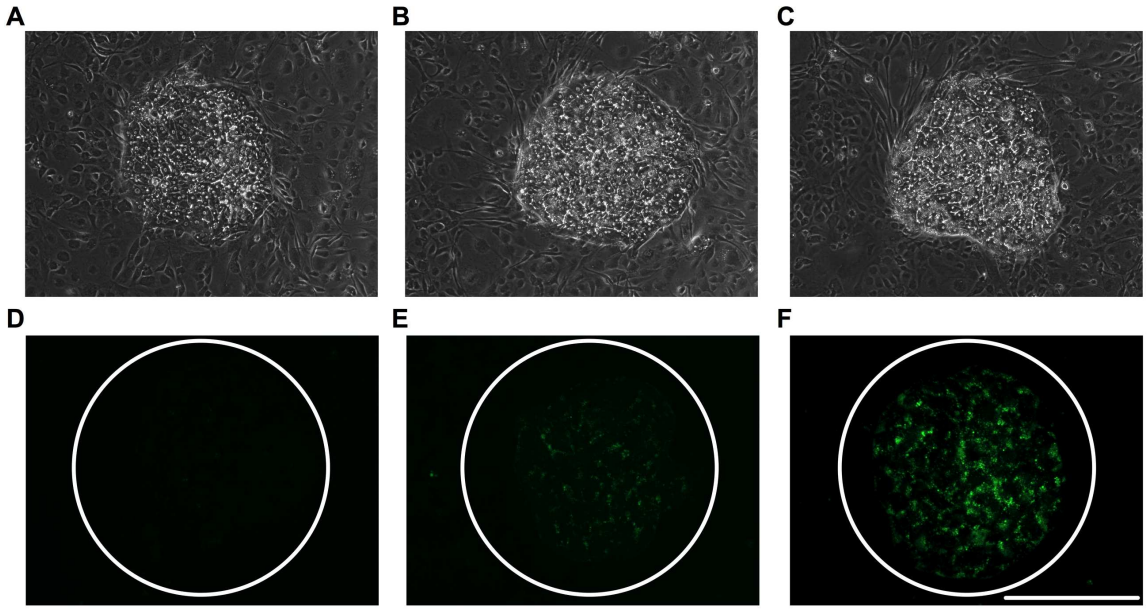

Supplemental Figure 3.5.5. Glucose-induced accumulation of neutral lipids in MPCCs after 10 days of treatment. Phase contrast images of MPCCs in hypo- (**A**), normo- (**B**) and hyperglycemic (**C**) culture medium after 10 days of treatment. Nile red (neutral lipids) staining of MPCCs in hypo- (**D**), normo- (**E**) and hyperglycemic (**F**) culture medium after 10 days of treatment. Circles highlight hepatocyte island location and scale bar is 400 μm.

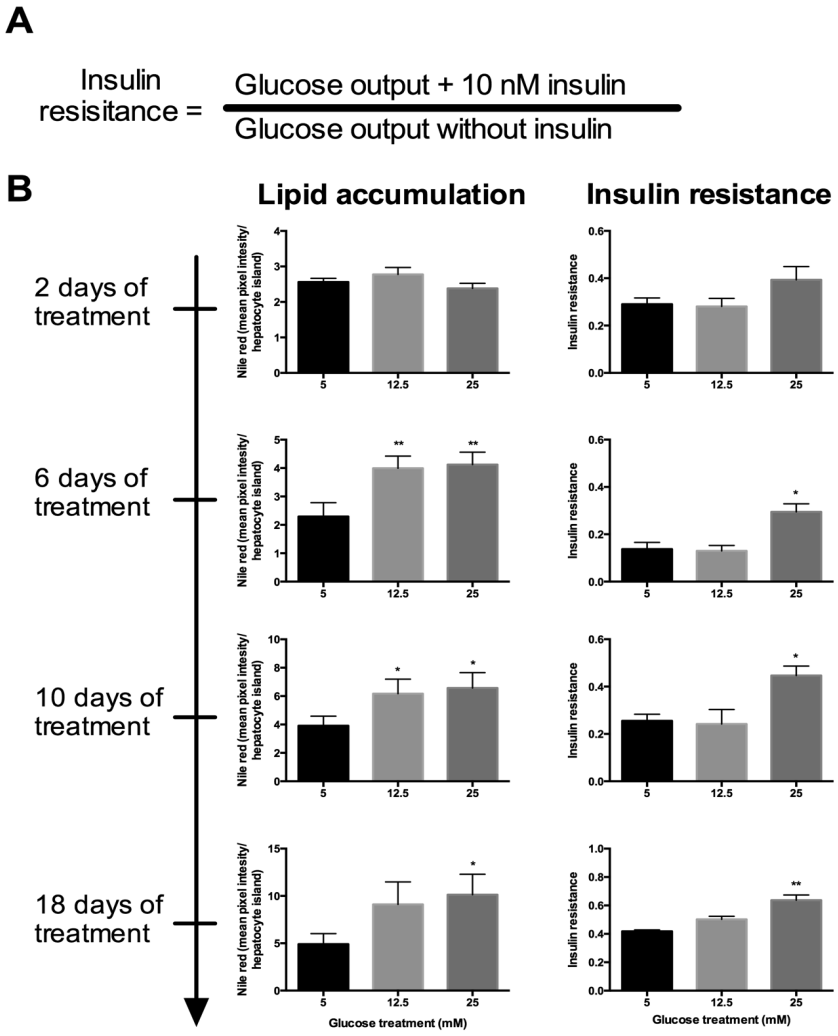

Supplemental Figure 3.5.6. Lipid accumulation and insulin resistance in MPCCs treated with varying glucose levels. (**A**) Insulin resistance is calculated by dividing the MPCC glucose output under insulin stimulation (10 nM) by the glucose output without insulin ("0" means complete inhibition of glucose output by insulin, while "1" means no effect of insulin on glucose output). (**B**) Time course of lipid accumulation, assessed via Nile Red fluorescence quantification (9 hepatocyte islands quantified per treatment), in MPCCs continuously treated with culture media containing 5 mM (normoglycemic), 12.5 mM or 25 mM (hyperglycemic) glucose. (**C**) Insulin resistance development over time in MPCCs treated as in panel (**B**). Error bars represent SD. * $p \leq 0.05$, and ** $p \leq 0.01$.

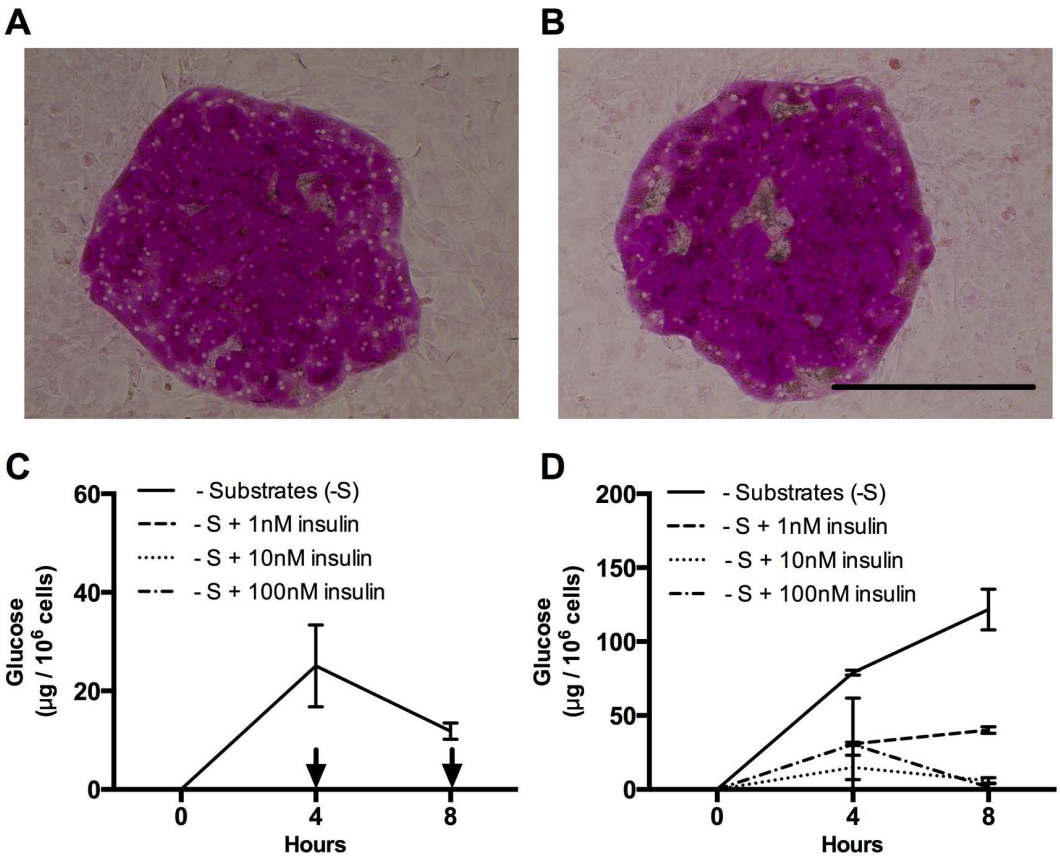

Supplemental Figure 3.5.7. Glucose-induced modulation of insulin sensitivity in MPCCs. PAS (glycogen) staining of MPCCs treated with either normo- (**A**) or hyperglycemic (**B**) culture medium for 10 days *prior* to assessing glucose output in the supernatants as in the subsequent panels of this figure. Scale bar is 400 µm. (**C**) Glucose output over time in supernatants of normoglycemic MPCCs (10 days of treatment) treated *without* any gluconeogenic substrates in the presence or absence of different levels of insulin (see methods for additional details). Arrows indicate no detectable glucose in supernatants. (**D**) Glucose output as in panel (**C**) except hyperglycemic MPCCs were used. Error bars represent SD across 3 wells. Similar results were observed in another primary hepatocyte donor.

SUPPLEMENTAL TABLE 1: Sequences for the GE Healthcare Dharmacon Solaris™ brand primer/probe sets used in this study.

Gene: GAPDH
Forward Primer: GCCTCAAGATCATCAGCAATG
Reverse Primer: CTTCCACGATACCAAAGTTGTC
Probe: GCCAAGGTCATCCATGA

Gene: ARG1
Forward Primer: ACTTGCATGGACAACCTGT
Reverse Primer: ATCCTGGCACATCGGGAAT
Probe: GAACTAAAAGGAAAGATTC
Gene: ALB
Forward Primer: AATGTTGCCAAGCTGCTGA
Reverse Primer: TCATCCCGAACTTCATC
Probe: CTGTTGCCAAAGCTCGATG
Gene: AHR
Forward Primer: CGTCTAAGGTGTCTGCTGGATA
Reverse Primer: CCCTTGGAAATTCATTGC
Probe: TCATCTGGTTTTCTGGCAA
Gene: CYP3A4
Forward Primer: CCTCATCCCAATTCTTGAAG
Reverse Primer: GCTGAAGGAAATCCACTC
Probe: GAAGATACACAAAAGCACCG
Gene: CYP2A6
Forward Primer: GATGACCACGTTGAACCT
Reverse Primer: ATGGACCTTGGCCTCCAC
Probe: ATGAAGCACCCAGAGGT
Gene: MLXIPL
Forward Primer: GTTTGATGACTACGTCCGAAC
Reverse Primer: GCCGGATGAGGATGCTG
Probe: AAGTTCTGGGTGTTCAG
Gene: HMOX1

Forward Primer: ATTGCCAGTGCCACCAAGTTC
Reverse Primer: CTCCTCAAAGAGCTGGATGT
Probe: AGACTGCGTTCCTGCTCAA
Gene: G6PC
Forward Primer: CCTACAGATTTCGGTGCTTG
Reverse Primer: TTCGTGACAGACAGACATTCAG
Probe: TTCTGGGCTGTGCAGCT
Gene: PCK1
Forward Primer: TCGAGAATAACGCTGAGCTGTG
Reverse Primer: TGAGAGCCAACCAGCAGTT
Probe: CTGAAGAAGTATGACAAC
Gene: SLC2A2
Forward Primer: GCTCAACTAATCACCATGCTCTG
Reverse Primer: GCTACTAACATGGCTTTGATTCTTC
Probe: CTTGGGGACACACTTGG

References

1. Yan L-J. Pathogenesis of Chronic Hyperglycemia: From Reductive Stress to Oxidative Stress. Journal of Diabetes Research. **2014**(4), 1, 2014.

2. Parks EJ. Dietary carbohydrate's effects on lipogenesis and the relationship of lipogenesis to blood insulin and glucose concentrations. BJN. **87**(S2), S247, 2002.

3. Merrell MD, Cherrington NJ. Drug metabolism alterations in nonalcoholic fatty liver disease. Drug Metab. Rev. **43**(3), 317, 2011.

4. Smith BW, Adams LA. Nonalcoholic fatty liver disease and diabetes mellitus: pathogenesis and treatment. Nat Rev Endocrinol. **7**(8), 456, 2011.

5. Buler M, Aatsinki S-M, Skoumal R, Hakkola J. Energy sensing factors PGC-1α and SIRT1 modulate PXR expression and function. Biochemical Pharmacology. **82**(12), 2008, 2011.

6. van den Bosch HM, Bu nger M, de Groot PJ, van der Meijde J, Hooiveld GJ, Mu ller M. Gene expression of transporters and phase I/II metabolic enzymes in murine small intestine during fasting. BioMed Central Ltd; 2007.

7. Tsuburaya A, Blumberg D, Burt M, Brennan MF. Energy Depletion in the Liver and in Isolated Hepatocytes of Tumor-Bearing Animals. Journal of Surgical Research. **59**(4), 421, 1995.

8. Qiu SL, Xiao ZC, Piao CM, Xian YL, Jia LX, Qi YF, et al. AMP-activated Protein Kinase 2 Protects against Liver Injury from Metastasized Tumors via Reduced Glucose Deprivation-induced Oxidative Stress. Journal of Biological Chemistry. **289**(13), 9449, 2014.

9. Khunti K, Davies M, Majeed A, Thorsted BL, Wolden ML, Paul SK. Hypoglycemia and risk of cardiovascular disease and all-cause mortality in insulin-treated people with type 1 and type 2 diabetes: a cohort study. Diabetes Care. **38**(2), 316, 2015.

10. Snell-Bergeon JK, Wadwa RP. Hypoglycemia, Diabetes, and Cardiovascular Disease. Diabetes Technology & Therapeutics. **14**(S1), S, 2012.

11. Tahrani AA, Bailey CJ, Del Prato S, Barnett AH. Management of type 2 diabetes: new and future developments in treatment. The Lancet. Elsevier; **378**(9786), 182, 2011.

12. Tao H, Zhang Y, Zeng X, Shulman GI, Jin S. Niclosamide ethanolamine–induced mild mitochondrial uncoupling improves diabetic symptoms in mice. Nature Medicine. Nature Publishing Group; **20**(11), 1263, 2014.

13. Hebbard L, George J. Animal models of nonalcoholic fatty liver disease. Nat Rev Gastroenterol Hepatol. **8**(1), 35, 2011.

14. King A, Bowe J. Animal models for diabetes: Understanding the pathogenesis and finding new treatments. Biochemical Pharmacology. **99**, 1, 2016.

15. Olson H, Betton G, Robinson D, Thomas K, Monro A, Kolaja G, et al. Concordance of the toxicity of pharmaceuticals in humans and in animals. **32**(1), 56, 2000.

16. Shih H, Pickwell GV, Guenette DK, Bilir B, Quattrochi LC. Species differences in hepatocyte induction of CYP1A1 and CYP1A2 by omeprazole. Hum Exp Toxicol. **18**(2), 95, 1999.

17. Lin C, Ballinger KR, Khetani SR. The application of engineered liver tissues for novel drug discovery. Expert opinion on drug discovery. **10**(5), 519, 2015.

18. Wilkening S, Bader A. COMPARISON OF PRIMARY HUMAN HEPATOCYTES AND HEPATOMA CELL LINE HEPG2 WITH REGARD TO THEIR BIOTRANSFORMATION PROPERTIES. Drug metabolism and disposition. **31**(8), 1035, 2003.

19. Gerets HHJ, Tilmant K, Gerin B, Chanteux H, Depelchin BO, Dhalluin S, et al. Characterization of primary human hepatocytes, HepG2 cells, and HepaRG cells at the mRNA level and CYP activity in response to inducers and their predictivity for the detection of human hepatotoxins. Cell biology and toxicology. **28**(2), 69, 2012.

20. Godoy P, Hewitt NJ, Albrecht U, Andersen ME, Ansari N, Bhattacharya S, et al. Recent advances in 2D and 3D in vitro systems using primary hepatocytes, alternative hepatocyte sources and non-parenchymal liver cells and their use in investigating mechanisms of hepatotoxicity, cell signaling and ADME. Arch Toxicol. **87**(8), 1315, 2013.

21. Khetani SR, Bhatia SN. Microscale culture of human liver cells for drug development. Nat Biotechnol. **26**(1), 120, 2007.

22. Davidson MD, Lehrer M, Khetani S. Hormone and Drug-mediated Modulation of Glucose Metabolism in a Microscale Model of the Human Liver. Tissue Engineering Part C: Methods. 141217055135006, 2014.

23. Lin C, Shi J, Moore A, Khetani SR. Prediction of Drug Clearance and Drug-Drug Interactions in Microscale Cultures of Human Hepatocytes. Drug metabolism and disposition: the biological fate of chemicals. **44**(1), 127, 2016.

24. Khetani SR, Berger DR, Ballinger KR, Davidson MD, Lin C, Ware BR. Microengineered liver tissues for drug testing. J Lab Autom. **20**(3), 216, 2015.

25. Rushmore TH, Kong A-NT. Pharmacogenomics, regulation and signaling pathways of phase I and II drug metabolizing enzymes. Current Drug Metabolism [Internet].

3(5), 481, 2002.

26. Yoshinari K, Takagi S, Sugatani J, Miwa M. Changes in the expression of cytochromes P450 and nuclear receptors in the liver of genetically diabetic db/db mice. Biological & pharmaceutical bulletin. **29**(8), 1634, 2006.

27. Puigserver P, Rhee J, Donovan J, Walkey CJ, Yoon JC, Oriente F, et al. Insulin-regulated hepatic gluconeogenesis through FOXO1-PGC-1alpha interaction. Nature. **423**(6939), 550, 2003.

28. Wimmer RJ, Liu Y, Schachter TN, Stonko DP, Peercy BE, Schneider MF. Mathematical modeling reveals modulation of both nuclear influx and efflux of Foxo1 by the IGF-I/PI3K/Akt pathway in skeletal muscle fibers. American Journal of Physiology - Cell Physiology. **306**(6), C570, 2014.

29. Cusi K. Nonalcoholic fatty liver disease in type 2 diabetes mellitus. Curr Opin Endocrinol Diabetes Obes. **16**(2), 141, 2009.

30. LeCluyse EL. Human hepatocyte culture systems for the in vitro evaluation of cytochrome P450 expression and regulation. European journal of pharmaceutical sciences : official journal of the European Federation for Pharmaceutical Sciences. **13**(4), 343, 2001.

31. Gao J, Xie W. Pregnane X Receptor and Constitutive Androstane Receptor at the Crossroads of Drug Metabolism and Energy Metabolism. Drug metabolism and disposition. **38**(12), 2091, 2010.

32. Zanger UM, Schwab M. Cytochrome P450 enzymes in drug metabolism: regulation of gene expression, enzyme activities, and impact of genetic variation. Pharmacology & therapeutics. **138**(1), 103, 2013.

33. Finck BN. PGC-1 coactivators: inducible regulators of energy metabolism in health and disease. Journal of clinical Investigation. **116**(3), 615, 2006.

34. Weltman MD, Farrell GC, Hall P, Ingelman-Sundberg M, Liddle C. Hepatic cytochrome P450 2E1 is increased in patients with nonalcoholic steatohepatitis. Hepatology (Baltimore, Md). **27**(1), 128, 1998.

35. Donato MT. Potential Impact of Steatosis on Cytochrome P450 Enzymes of Human Hepatocytes Isolated from Fatty Liver Grafts. Drug metabolism and disposition. **34**(9), 1556, 2006.

36. Donato MT, Jimenez N, Serralta A, Mir J, Castell JV, Gomez-Lechon MJ. Effects of steatosis on drug-metabolizing capability of primary human hepatocytes. Toxicology in Vitro. **21**(2), 271, 2007.

37. Greco D, Kotronen A, Westerbacka J, Puig O, Arkkila P, Kiviluoto T, et al. Gene expression in human NAFLD. Am. J. Physiol. Gastrointest. Liver Physiol. **294**(5),

G1281, 2008.

38. Fisher CD, Lickteig AJ, Augustine LM, Ranger-Moore J, Jackson JP, Ferguson SS, et al. Hepatic cytochrome P450 enzyme alterations in humans with progressive stages of nonalcoholic fatty liver disease. Drug metabolism and disposition. **37**(10), 2087, 2009.

39. Gentile CL, Gentile CL, Frye MA, Frye MA, Pagliassotti MJ, Pagliassotti MJ. Fatty acids and the endoplasmic reticulum in nonalcoholic fatty liver disease. BioFactors (Oxford, England). **37**(1), 8, 2011.

40. Horton JD, Goldstein JL, Brown MS. SREBPs: activators of the complete program of cholesterol and fatty acid synthesis in the liver. Journal of clinical Investigation. **109**(9), 1125, 2002.

41. Sanders FWB, Griffin JL. De novo lipogenesis in the liver in health and disease: more than just a shunting yard for glucose. Biological reviews of the Cambridge Philosophical Society. **91**(2), 452, 2016.

42. Jais A, Einwallner E, Sharif O, Gossens K, Lu TT-H, Soyal SM, et al. Heme Oxygenase-1 Drives Metaflammation and Insulin Resistance in Mouse and Man. Cell. Elsevier Inc; **158**(1), 25, 2014.

43. Kang S, Tsai LT-Y, Rosen ED. Nuclear Mechanisms of Insulin Resistance. Trends in Cell Biology. **26**(5), 341, 2016.

44. O-Sullivan I, Zhang W, Wasserman DH, Liew CW, Liu J, Paik J, et al. FoxO1 integrates direct and indirect effects of insulin on hepatic glucose production and glucose utilization. Nat Commun. **6**, 7079, 2015.

45. Brown MS, Goldstein JL. Selective versus Total Insulin Resistance: A Pathogenic Paradox. Cell Metabolism. **7**(2), 95, 2008.

46. Ioannou GN. The Role of Cholesterol in the Pathogenesis of NASH. Trends Endocrinol. Metab. **27**(2), 84, 2016.

47. Baffy G. Kupffer cells in non-alcoholic fatty liver disease: The emerging view. Journal of Hepatology. Elsevier; **51**(1), 212, 2009.

48. Leclercq IA, Da Silva Morais A, Schroyen B, Van Hul N, Geerts A. Insulin resistance in hepatocytes and sinusoidal liver cells: Mechanisms and consequences. Journal of Hepatology. **47**(1), 142, 2007.

49. Nguyen TV, Ukairo O, Khetani SR, McVay M, Kanchagar C, Seghezzi W, et al. Establishment of a hepatocyte-kupffer cell coculture model for assessment of proinflammatory cytokine effects on metabolizing enzymes and drug transporters. Drug metabolism and disposition: the biological fate of chemicals. **43**(5), 774, 2015.

50. Barbero-Becerra VJ, Giraudi PJ, Chavez-Tapia NC, Uribe M, Tiribelli C, Rosso N. The interplay between hepatic stellate cells and hepatocytes in an in vitro model of NASH. Toxicology in Vitro. Elsevier Ltd; **29**(7), 1753, 2015.

51. March S, Ramanan V, Trehan K, Ng S, Galstian A, Gural N, et al. Micropatterned coculture of primary human hepatocytes and supportive cells for the study of hepatotropic pathogens. Nature Protocols. **10**(12), 2027, 2015.

52. Collins TJ. ImageJ for microscopy. Biotechniques. **43**(1 Suppl), 25, 2007.

Chapter 4

Mimicking the dynamics of fasting and feeding cycles to improve the in vitro lifetime and NAFLD disease profile of hepatocytes in micropatterned co-cultures[3]

Summary:

In chapter 3 we showed that glucose is a major determinant of hepatocyte lipid metabolism as well as insulin resistance and overall health. Unfortunately, MPCCs maintained in physiologic glucose still develop steatosis and some insulin resistance over time. This significantly limits the long-term studies we can do with our MPCC model if we intend on studying lipid accumulation and insulin signaling. The development of lipid accumulation and insulin resistance in MPCCs is likely due to a lack of some cue normally found in the body that prevents the hepatocytes from accumulating excess fats. One aspect we had not previously considered is the dynamic fasting and feeding cycles that occur in the body, which results in fluctuations in nutrient availability and hormone signals at the cell level. At first, we were not sure if the MPCC system could handle dramatic changes in medium supplements, but once we found that cultures could withstand periodic serum removal we developed a simple method for mimicking the fasting and feeding process in our static cell culture system. Specifically, we periodically removed serum and hormones from our cell culture medium and then assessed the potential benefits this may have on hepatocyte drug metabolism enzymes, disease profile and longevity and utility.

[3]A manuscript similar to the work described in this chapter is in preparation and will be submitted for publication shortly.

4.1 Introduction

Current research and development efforts to bring a drug to market are increasing and have an average cost of $2.9 billion (1). Post market withdraws are also common and have detrimental impacts on society and the economy (2). Hepatotoxicity is a leading cause for post market withdraws of FDA approved compounds, and this can be attributed to a lack of proper *in vitro* screening tools. Additionally, lack of drug efficacy is a major issue for therapies once they reach the clinic due to decreased relevancy of the models tested prior to trials in humans (3). Since many new therapies for metabolic, viral and parasitic disease are being developed to target the liver, screening platforms are desperately needed. Ideally we could preemptively identify efficacious and safe compounds prior to clinical trials, but major hurdles still remain in developing the best preclinical systems to streamline drug development.

Species-specific differences in drug metabolism require the use of human relevant systems prior to clinical screens to assess liver toxicity (4). Additionally, disease mechanisms and progression are significantly different between animals and humans (5,6). Therefore human systems, ranging from least to most complex, such as microsomes, cell lines, primary hepatocytes, and liver slices have been utilized to complement animal data (7). The gold standard for the pharmaceutical industry is the use of primary human hepatocytes (PHHs) since they retain all of the normal liver enzymes and functions right after they are isolated from the body(8). Unfortunately, pure cultures of PHHs rapidly decline *in vitro*, which limits their utility in long term applications such as drug screening. Recently, tissue-engineering methods, such as 3D culturing, cell patterning and co-culture systems, have been shown to significantly prolong the lifetime of hepatocytes *in vitro*. The goal of these platforms is to enable stable liver functions over time to allow for a diseased state to develop (9-11) or enable chronic drug dosing (12). Even

in these engineered systems, hepatocytes fail to maintain stable liver functions over extended periods of time, which limits their utility in the aforementioned applications.

Increasing the lifetime of liver cultures is an increasingly important and necessary goal for liver cell models since this will enable the development of disease models and toxicity screening systems that require prolonged exposure. No culture system has been able to recapitulate the lifetime of hepatocytes that is observed in vivo, >1 year(13), which suggests that significant advances in culturing systems can still be made. Therefore, any modifications to hepatocyte culturing conditions that lead to increased functionality or lifetime over existing models should be widely applicable to the various existing *in vitro* liver culture systems.

One factor that has not been addressed with liver cell culture is the impact of nutrient/hormonal fluctuations, or starvation, on hepatocyte lifetime, which is likely due to the lack of long-term models to properly address this question. In the body, there are dynamic fasting and feeding cycles that regulate normal processes within cells and may be responsible for the prolonged lifetime of hepatocytes *in vivo* (14). Current culture systems, even advanced 3D, and co-culturing platforms, utilize a consistent culture medium schedule that provides a steady supply of nutrients every few days. The liver is sensitive to changes in hormones and nutrients and the lack of these dynamic stimuli may partially explain the premature decline in hepatocyte functions observed *in vitro* (15).

Serum starvation and hormone fluctuations have been shown to initiate fasting-stimulated signaling pathways in cell cultures as well as maintain normal oscillations in gene expression in hepatocytes, respectively (16,17). Here we hypothesized that periodically starving hepatocyte cultures of serum and hormones could prolong their *in vitro* functional lifetime. We utilized a robust co-culturing system, the micropatterned co-culture (MPCC) that maintains high

hepatocyte functions for multiple weeks, to address this question and prevent confounding variables from declining pure hepatocyte cultures(18). Hepatocytes do not proliferate in this system and their patterned architecture allows us to easily visualize loss of cells over time. Additionally hepatocyte cell-cell interactions have been optimized so that liver transporters and drug enzyme activity can be monitored. We assessed hepatocyte morphology, drug enzyme activity/induction, hepato-specific protein production, transporter function and the ability to accurately identify liver toxins/non-toxins after multiple, three to five, weeks of serum/hormone starvation.

4.2 Methods

4.2.1 Cell culture and MPCC fabrication

MPCCs were fabricated using the same methods described in chapter 2 and 3. One main difference with this chapter was the use of growth arrested fibroblasts in place of the usual non-growth arrested fibroblasts. For growth arrested fibroblast cultures we passaged fibroblasts until they reached 90% confluency and then we treated them with mitomycin C the day of seeding with micropattenred hepatocytes. Specifically, cultures were first washed with 1x PBS, to removed residual medium, and then incubated with 1 μg/ml mitomycin C in fibroblast maintenance medium (10% bovine serum, 1 % penicillin/streptomycin, and high glucose DMEM) for ~ 4 hours in the cell culture incubator. Mitomycin C containing medium was then removed and replaced with fibroblast maintenance medium for at least 30 minutes prior to splitting and seeding fibroblasts into cultures containing patterned hepatocytes.

4.2.2 Starvation protocol and experimental timeline

Once MPCCs were fabricated, they were cultured in 5 mM glucose containing maintenance medium for 2 weeks. Cultures were treated with various starvation treatments, 1 hour, 1 day, 2 day and 3 days. To start the starvation, cultures were washed once with 1x PBS, and then incubated in 5 mM glucose containing serum free medium for the specified time. This medium was also supplemented with 1% penicillin/streptomycin and 1.5% HEPES buffer. After the starvation period, cultures were then placed back in maintenance medium for 5-8 days, depending on the previous starvation period. This was continued for 4 weeks, including the initial starvation. To mimic starvation, we treated cultures with metformin, which activates AMPK, at a concentration of 250 μg/ml in hepatocyte maintenance medium during the same period, 2 days, where cultures were starved.

4.2.3 Biochemical assays

Biochemical assays (albumin production, urea synthesis) and enzyme activity assays (CYP2A6, CYP3A4 and CYP1A2) were carried out in the same fashion as described in chapter 3. Additionally, CYP2C9 enzyme activity was assessed in these studies and this was carried out by incubating cultures with the CYP2C9 specific substrate Luciferin-H for 3 hours in serum free/phenol red free medium. Culture medium was collected after this incubation period and analyzed according to manufacturer protocols (Promega, Madison, WI).

4.2.4 Live cell imaging and staining

Hepatocyte island morphology was monitored over time using phase contrast imaging. Additionally, we assessed bile canaliculi over time using CDCFDA fluorescent staining and Hoechst 33342 to visualize cell nuclei. Specifically, cultures were washed 1 time with serum free medium containing 5 mM glucose, 1% penicillin/streptomycin and 1.5% HEPES buffer and glucose free DMEM containing 4 mM supplemented L-glutamine. CDCFDA and Hoechst 33342 were added to this same serum free culture medium at a concentration of 2 μM and 1 μM, respectively, immediately before treating cultures, and then cultures were treated for 15 minutes in the cell culture incubator. This staining medium was then removed and cultures were washed 3 times with serum free medium, and the third wash was left in the culture dish. Cultures were then imaged using the EVOS FL microscope, where the CDCFDA (bile) stain was imaged using the GFP light cube, and the nuclear stain was imaged using the DAPI light cube.

4.2.5 Drug screening and enzyme induction

To assess drug toxicity, cultures were incubated with increasing multiples of the specific drug's C_{max}, the average maximal concentration the drug reaches in patients after administration. Specifically, compounds were first dissolved in DMSO at 100,000 times their C_{max}, and then added to serum free culture medium (containing 5 mM glucose, 1% ITS+ (Corning) 1% penicillin/streptomycin and 1.5% HEPES buffer, 100 nM dexamethasone, 2 nM glucagon and glucose free DMEM containing 4 mM supplemented L-glutamine) at a concentration of 25*C_{max} or 100*C_{max}. By diluting compounds at 100,000* C_{max}, we could maintain a concentration of

0.1% w/v DMSO in the culture medium. Accordingly, 0.1% DMSO was used as the vehicle control for these studies. Cultures were treated 3 times with compounds, every 2 days, for a total of 6 days of treatment.

For enzyme induction, cultures were treated with prototypical enzyme inducers (rifampin for CYP2C9, phenobarbital for CYP3A4 and omeprazole for CYP1A2) or their vehicle control, over 4 days, which consisted of 2 treatments every 2 days. Specifically, rifampin, phenobarbital, and omeprazole or the vehicle control was added to the same medium used for drug toxicity screening at a concentration of 25 μM, 1 mM, and 10 μM. We assessed enzyme induction by first incubating induced or vehicle treated control cultures with respective enzyme specific substrates and then secondly quantifying the amount of substrate turnover that occurred over 1-3 hours, depending on the specific enzyme tested.

4.2.6 Statistical analyses

Each experiment was carried out in 2 or more wells for each condition. Two to three cryopreserved PHH donors were used to confirm observed trends. Microsoft Excel and GraphPad Prism 5.0 (La Jolla, CA) were used for data analysis and plotting data. Error bars on average values represent standard deviation (SD) across wells. Statistical significance of the data was determined using the average and SD across wells in representative experiments using the Student's *t*-test or one-way ANOVA with Dunnett's multiple comparison tests for post hoc analysis.

4.3 Results

4.3.1 Periodic starvation prolongs hepatocyte lifetime *in vitro*

To mimic a starved state, we developed a protocol where cultures are first washed with PBS, to remove residual proteins and nutrients, and then incubated with a starvation medium that has no hormones or serum. This starvation protocol was carried out weekly for 5 weeks and started 2 weeks after cultures were initially seeded (Fig. 1). To assess any benefit of starvation on hepatic cultures, we measured albumin production and urea synthesis, two major functions of the liver, as well as drug metabolism enzyme activity and transporter function after 5 weeks of starvation (Supplemental Fig. 1). We tried a range of starvation periods and found that a two-day starvation had the overall highest liver functions when compared to one hour, one day, three day or no starvation. Consequently, throughout the remainder of the studies we utilized the two-day starvation period.

Once the optimal starvation time was identified, we then assessed how starvation retained hepatocyte morphology and survival in culture using phase contrast imaging over 6 weeks *in vitro* (Fig. 1). In MPCCs, hepatocytes are patterned into circular domains, and do not proliferate, so we can easily assess the loss of cells over time. Surprisingly, we found that hepatocyte island morphology was strongly retained over 6 weeks in starved cultures, whereas non-starved culture island morphology diminished over time and was almost indistinguishable from the surrounding fibroblast population by 6 weeks in culture. These results suggest that periodic starvation helps maintain liver cells in a co-culture model.

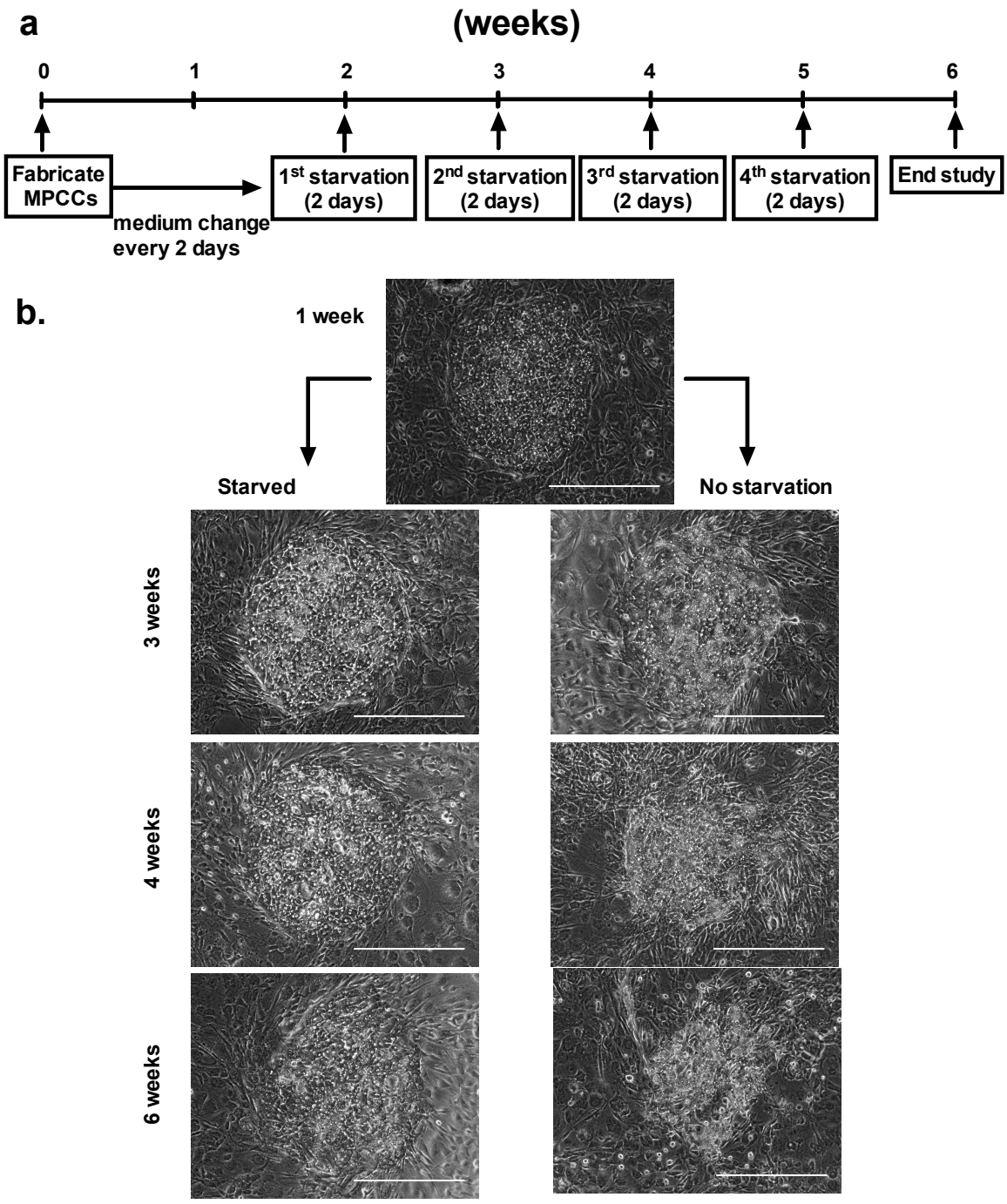

Figure 4.1. Experimental timeline and MPCC morphology over time. (a) Experimental timeline and procedures for periodically starving cultures. (b) Representative phase contrast images of MPCC hepatocyte islands before (1 week) and after periodic starvation (left column) or without starvation (right column). Scale bars represent 400 μm.

4.3.2 Starvation prolongs hepatocyte functional lifetime *in vitro*

After observing the drastic difference in hepatocyte lifetime mediated by periodically starving cultures, we assessed how these changes were reflected in hepatocyte functions over time. We found that albumin production and urea synthesis were on average 3 fold and 4.6 fold higher in starved cultures for 6 weeks, after initiating the starvation protocol (Fig. 2).

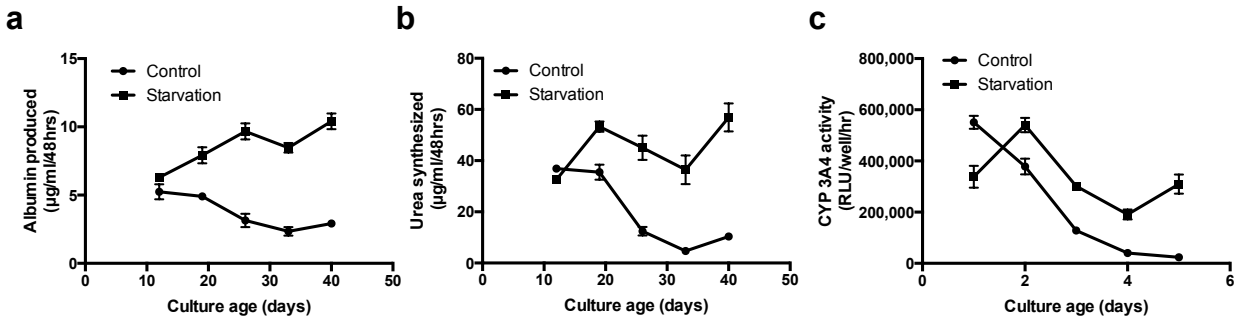

Figure 4.2. MPCC functions over time with and without starvation. Albumin production (a), urea synthesis (b) and CYP3A4 enzyme activity (c) in starved and non-starved cultures over 5-6 weeks of culture. Error bars represent SD.

Additionally, we measured drug enzyme activity levels in starved and non-starved cultures over time. CYP2A6, CYP2C9 and CYP1A2 enzyme activity levels over 5 weeks of starvation were on average 2 fold, 1.8 fold and 1.3 fold higher in starved cultures (Supplemental Fig. 2). Importantly, CYP3A4 activity was on average 5.4 fold higher than non-starved cultures when compared over 5 weeks of culture (Fig. 2). Additionally, at the terminal time point of 6 weeks, transporter activity was retained in starved cultures, as shown by live cell imaging of transporter specific dye excretion, compared to the loss of transporter functions in non-starved cultures (Supplemental Fig. 1). These results suggest that periodic starvation helps retain liver cell functions over time in an already stable model.

4.3.3 Periodic starvation keeps supportive fibroblast numbers in check while activating AMPK in MPCCs

Besides the hepatocyte specific changes we observed between starved and non-starved cultures, we also noticed changes in fibroblast morphology during starvation and subsequent density after starvation (data not shown). Fibroblasts assumed a rounded-up morphology suggesting they may be detaching, which would lower the overall fibroblast number during starvation, and accordingly the density of nuclear DAPI staining was also lower (Fig. 3). To confirm fibroblast density was decreased after starvation, we assessed the effects of the starvation protocol on pure fibroblast double stranded DNA (dsDNA) concentration. We found that dsDNA in starved fibroblasts was significantly (p value ≤ 0.0001) reduced to 20% of the non-starved control after 1 starvation at 1 week of culture.

Serum starvation is known to activate adenosine monophosphate (AMP) activated kinase (AMPK), and is associated with longevity. To probe the possibility that our starvation protocol may stimulate AMPK activation, we used a human specific phosphorylated AMPK (p-AMPK) enzyme linked immunosorbent assay (ELISA), which recognizes the phosphorylation that occurs on threonine 183 (T183) in the AMPK amino acid sequence. We found that the starvation protocol lead to a 1.5 fold higher concentration of p-AMPK (p value ≤ 0.01) than the non-starved MPCCs after 2 starvations. These results suggest that the starvation protocol reduces fibroblast numbers, while concomitantly activating AMPK in hepatocytes.

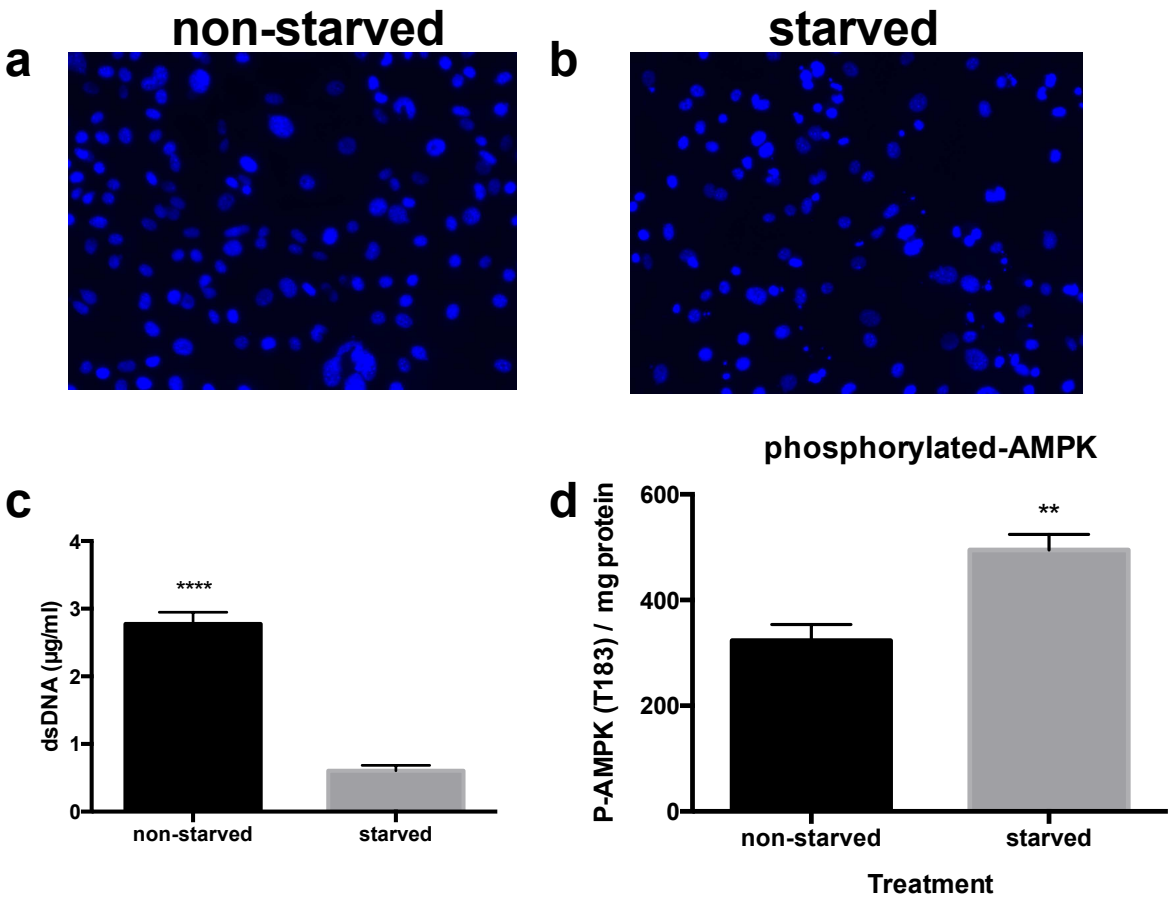

Figure 4.3. Starvation decreases fibroblasts density and increases adenosine monophosphate activated kinase (AMPK) activation. Pure fibroblasts were not-starved (a) or starved (b) after 1 week of culture, fixed and stained with DAPI to visualize nuclei, and DNA was isolated and quantified (c) (n=4). After 3 weeks of culture and 2 starvation treatments, total protein was isolated from MPCCs and the level of activated, phosphorylated-T183, AMPK was quantified and normalized to the total amount of protein (n=3). Error bars represent SD. **, and **** represent $p<0.01$ and <0.0001, respectively, assessed via t-test between non-starved and starved cultures.

4.3.4 Maintaining optimal fibroblast numbers as well as activating AMPK benefits hepatocyte *in vitro* lifetime, but not to the same extent as starvation

Since fibroblasts can continuously repopulate the culture once starvation medium is removed, we counted fibroblast nuclei between hepatocyte islands after 5 weeks of starvation

using Hoechst 33342 to confirm fibroblast numbers were in fact reduced. Image J analysis of cell nuclei showed that starvation significantly (p value ≤0.05) reduced fibroblast numbers between hepatocyte islands in starved cultures when compared to non-starved cultures (Fig. 4). To assess the effects of reduced fibroblast numbers on hepatocyte functions alone, we growth arrested fibroblasts using mitomycin C prior to incorporation into MPCCs and assessed their effects on hepatocytes without serum starvations. Accordingly, we found that fibroblast numbers were significantly reduced (p value ≤0.0001) when compared to non-starved cultures (Fig. 4). Surprisingly we found that MPCCs with growth arrested fibroblasts had on average 2, 2.9, 1.5 and 1.5 fold higher levels of CYP3A4 activity, CYP2A6 activity, as well as albumin and urea production, respectively, over time when compared to non-starved cultures. The magnitude of these functional markers was still below starved culture levels. Transporter activity and hepatocyte morphology were also better retained in MPCCs with growth-arrested fibroblasts, although not to the same extent as starved cultures. These results suggest that periodic starvation may prolong hepatocyte functions by maintaining an optimal level of fibroblasts in culture and preventing their overgrowth.

To address the effects of AMPK activation on hepatocyte functions alone, we periodically treated our cultures with metformin during the normal starvation period every week for 5 weeks in serum-containing medium. Importantly, fibroblasts numbers were not significantly reduced in metformin treated cultures. We found that on average metformin treated MPCCs had 1.7, 2.6, 1.5 and 1.6 fold higher levels of CYP3A4 activity, CYP2A6 activity, as well as albumin and urea production, respectively, over time when compared to non-starved cultures. The magnitude of these functional markers was still below starved culture levels. Transporter activity and hepatocyte morphology were also better retained in MPCCs treated with

metformin, although not to the same extent as starved cultures. These results suggest that periodic starvation may prolong hepatocyte functions by increasing AMPK activation.

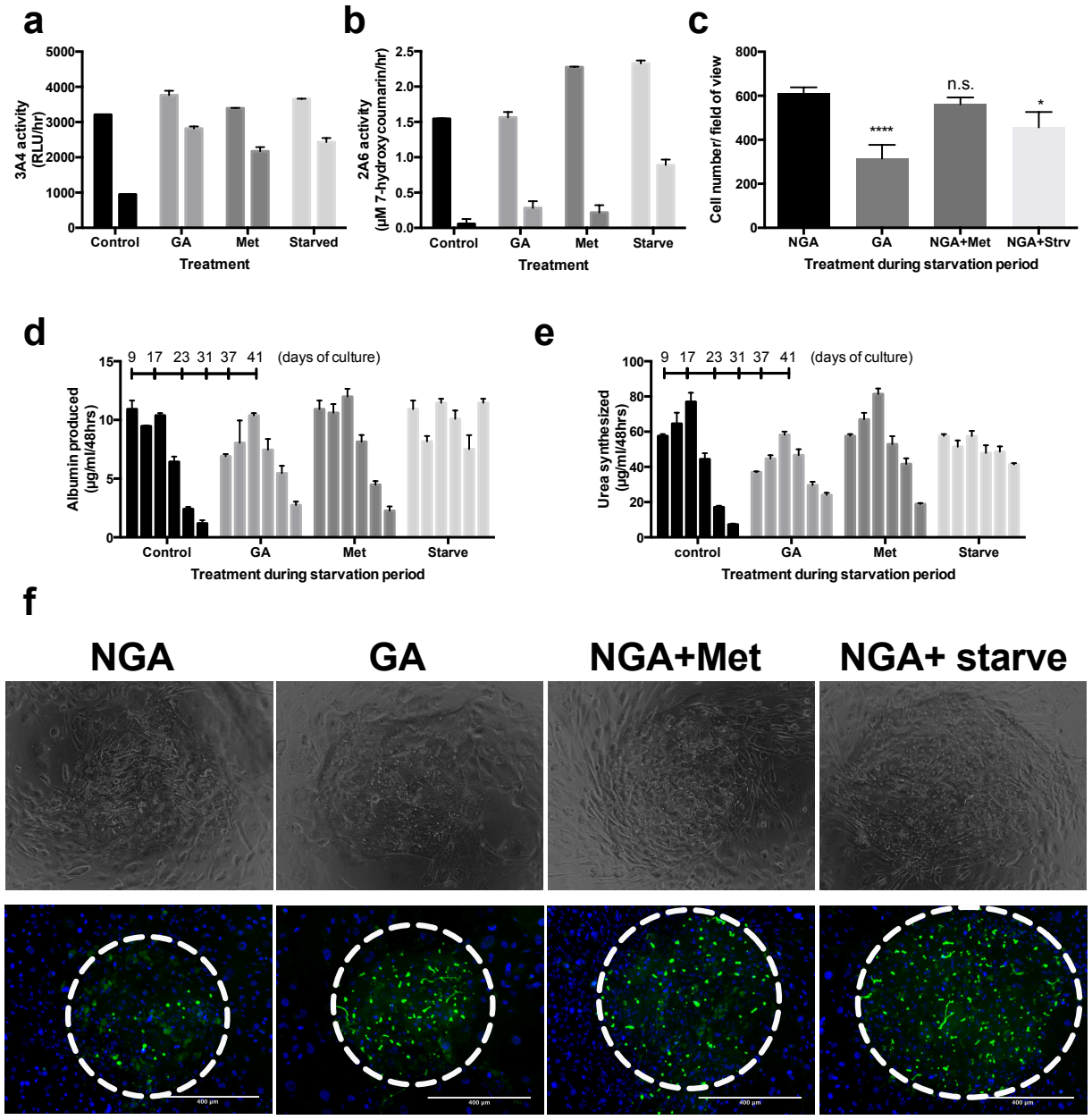

Figure 4.4. Effects of growth arresting (GA) fibroblasts and metformin (Met) treatment on MPCC longevity/functions compared to starvation. MPCCs were created with non-growth arrested (NGA) or GA fibroblasts and then cultured for ~6 weeks. CYP3A4 (a) and CYP2A6 (b) activity in MPCCs with various treatments at 4 (first bar) and 6 (second bar) weeks of culture. (c) Fibroblast numbers, assessed via live cell imaging of nuclei using Hoechst 33342 staining, between hepatocyte islands were obtained after 6 weeks of treatment. Albumin production (d) and urea synthesis (e) in MPCCs in the various treatments over 6 weeks of culture. (f)

Representative phase contrast images and respective bile canaliculi staining of MPCCs with various treatments. Circles outline hepatocyte islands. Scale bars represent 400 μm. Error bars represent Sd. *, and **** represent $p<0.05$ and <0.0001, respectively, assessed via one way ANOVA across treatments.

4.3.5 Serum starvation prevents identification of false positive compounds in toxicity screens

To assess the potential utility of the starvation protocol for drug toxicity screening after prolonged culture, we treated starved and non-starved MPCCs with 5 toxins and 5 non-toxins after 3 weeks of starvation. To prevent potential drug-protein interactions, we dosed cultures with compounds in serum free medium. Cultures were treated 3 times over a period of 6 days (i.e. every 2 days), with multiples of the maximum concentration observed in the blood after administration to humans, C_{max}. Specifically, cultures were treated with 25* C_{max}, 100* C_{max} or a vehicle, Dimethyl sulfoxide (DMSO), control. Albumin and urea production were used to identify hepatospecific toxicity since fibroblast ATP cannot be distinguished from hepatocyte ATP and could therefore show non-specific toxicity of cultures. Additionally, albumin and urea have been shown to be more sensitive markers of hepatotoxicity than ATP in micropatterned co-cultures (19). Accordingly, when albumin or urea levels dropped below 50% of the DMSO control, the compound was considered toxic, and the toxic concentration that reduced the response by 50% (TC_{50}) was interpolated from the dose response curves between DMSO and 25* $C_{max,}$, if the latter value fell below 50%, or between 25* C_{max} and 100* $C_{max,}$ and graphed (Fig. 5).

To screen for toxicity, we treated starved or non-starved cultures with compounds that have been extensively shown to be hepatotoxins (20). Using toxic compounds we can assess the sensitivity of the system to identify toxic and non-toxic compounds. Sensitivity is calculated by

dividing the total number of compounds identified as toxic by the total number of toxic compounds tested. Diclofenac, troglitazone, piroxicam, amiodarone and clozapine, all of which are considered liver toxins, were all identified as toxins in both starved and non-starved cultures and had similar TC_{50} values for albumin and urea outputs (Fig. 5, and Supplemental Fig. 3, 4).

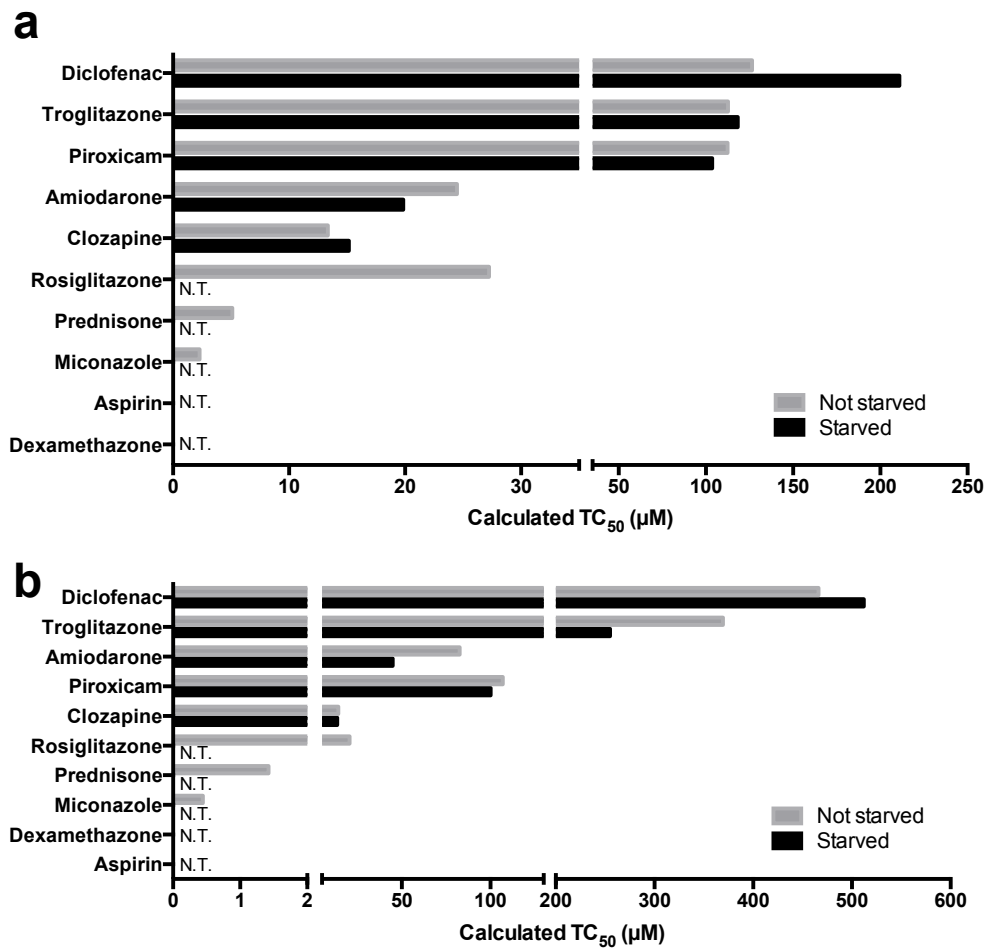

Figure 4.5. Interpolated TC_{50} values for known hepatotoxins and non-toxins in starved and non-starved MPCCs. MPCCs were maintained or starved for 4 weeks of culture and then assessed for the ability to predict toxicity. Albumin (a) and urea (b) based TC_{50} calculations for starved and non-starved cultures. Top 5 compounds are known hepatotoxins and bottom five are not considered hepatotoxins. N.T. represents not toxic.

TC_{50} values for urea were higher than the values obtained for albumin, regardless of culture treatment. These results suggest that starved and non-starved cultures have a high level of sensitivity.

To assess starved and non-starved cultures specificity, we treated cultures with non-liver toxins at increasing concentrations of the C_{max}. Specificity is defined as the ability of the system to correctly distinguish non-toxic compound from toxic compounds. This is calculated by dividing the number of compound identified as non-toxic by the total number of compounds tested. Starved cultures did not identify any of the non-toxins as toxic even at the 100*C_{max} dose, whereas non-starved cultures identified 3 of the 5 non-toxins as potentially toxic (ie: albumin and urea levels fell below 50% of the control with increasing doses of the compound) (Fig.5 and Supplemental Fig. 3). Specifically, rosiglitazone, prednisone and miconazole were all identified as toxic in non-starved cultures. This suggests that the specificity of starved cultures is 100%, while non-starved cultures have a specificity of 40%.

4.3.6 Small molecule based drug enzyme activity induction is better preserved in periodically starved cultures over time

To assess the potential utility of the starvation protocol to identify drug-drug interactions after prolonged culture, we treated starved and non-starved MPCCs with known enzyme inducers and then assessed drug enzyme activity. Induction of CYP3A4, CYP1A2 and CYP2C9 was carried out with 2 treatments of phenobarbital, omeprazole or rifampin over 4 days in serum free medium, respectively. Enzyme induction was assessed by comparing the enzyme activity of cultures treated with either the inducer or the vehicle control after 4 days of treatment.
Major differences in the level of enzyme induction were observed between starved and non-starved cultures. Non-starved culture CYP2C9 induction was 4.8 (± 1.2) fold, while starved CYP2C9 induction was 7.3 (± 2.5) fold (Fig. 6). Non-starved culture CYP23A4 induction was

3.7 (± 1.6) fold, while starved CYP3A4 induction was 10.2 (± 5.8) fold. CYP1A2 induction was similar between starved, 2.6 (± 0.12) fold, and non-starved cultures, 2.2 (± 0.3) fold. These results suggest that periodic starvation prolongs the ability of hepatocytes to respond to enzyme inducers.

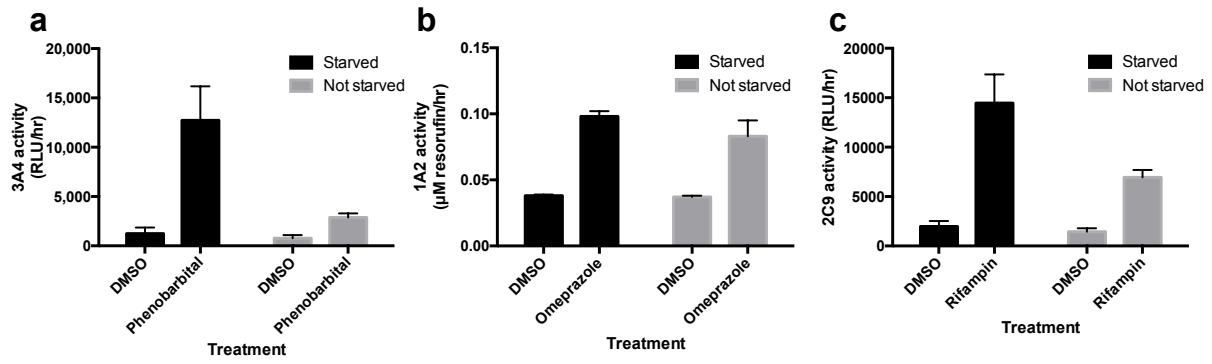

Figure 4.6. Enzyme induction in starved and non-starved MPCCs. MPCCs were maintained or starved for 4 weeks and then assessed for enzyme induction capabilities. CYP3A4 (a), CYP1A2 (b), and CYP 2C9 (c) induction in starved (black bars) and non-starved (grey bars) cultures. Error bars represent SD.

4.4 Discussion

Hepatocytes are notoriously difficult to maintain *in vitro* using conventional methods, although recent advances have made it possible to prolong the lifetime of hepatocytes outside the body (21). Successful efforts have taken inspiration from *in vivo* microenvironmental cues and physiological processes (22). One dynamic physiologic process that has not been investigated for its impact on hepatocyte longevity is nutrient and hormonal fluctuations. Here we sought to address the potential benefits of mimicking the fasting and feeding cycles in the body on hepatocyte *in vitro* lifetime. We developed a protocol where cell culture medium components, specifically serum and hormones, are periodically removed to mimic some aspects of fasting and

feeding in the liver, which we termed starvation (23). We found that cyclic starvation every week had profound effects on hepatocytes ranging from morphologic stability to prolonged hepatocyte function.

Since hepatocytes are already difficult to maintain *in vitro*, we utilized the micropatterned co-culture (MPCC) platform which has been shown to sustain hepatocytes for at least 3 weeks *in vitro* for various applications (9). Importantly, we have recently shown that hepatocytes in this system retain their ability to respond to hormones and nutrients, which is necessary to investigate the potential utility of dynamic culturing methods such as periodic starvations (10,24). Since our goal was to increase the functional lifetime of liver cells, the MPCC platform is a great system to assess this since liver cell secretions and hepatocyte colonies can be tracked over time to assess the loss of cells using simple phase contrast microscopy. Another aspect that motivates the use of the MPCC system to address how starvation impacts liver cell lifetime, is that it requires the use of hormones and serum to support long-term functions, which allows us to modulate those parameters to more accurately mimic a starved or fasted state. During fasting, nutrients and insulin levels decrease significantly and we can easily mimic this by removing serum and insulin from our culture medium (25). Specifically, after 2 weeks of culture stabilization in maintenance medium, we washed cultures with saline to remove excess nutrients, and then incubated MPCCs with a base medium lacking any serum or hormones.

Surprisingly, we found that starvation drastically increased the lifetime and function of hepatocytes in our system. Even a one-hour starvation seemed to benefit hepatocyte functions, although a 2-day starvation period was found to be the optimal starvation time with respect to multiple hepatocyte functions. MPCCs that were periodically starved for 5 weeks had similar morphology and island size as 2-week old cultures. Accordingly, liver cell functions such as

albumin and urea production were sustained at similar or higher levels to 2-week old cultures whereas non-starved culture function rapidly declined after 3 weeks of culture. Additionally, drug metabolism, which is notoriously difficult to retain in liver cells, was retained to at least 50% of the 2-week values in starved cultures after 5 weeks of culture, while non-starved cultures lost almost all drug metabolism capabilities by 5 weeks in culture. Since hepatocyte homotypic interactions (i.e. hepatocyte island integrity) was retained, we found a corresponding retention of hepatocyte transporter function in starved cultures, which was visualized with live cell imaging of a fluorescent transporter specific dye export, while this was mostly lost in non-starved cultures (26).

Since altered feeding schedules, abnormal hormone levels and an abundance of nutrients are associated with altered liver function, the buildup of toxins and metabolic related disease, we suggest that our periodic starvation prevents these deleterious effects from occurring and prolongs hepatocyte lifetime in our cultures(14-16,23). The maintenance of liver transporters we observed should enable proper removal of toxins that build up in hepatocytes over time(27). Additionally, the retention of drug metabolism enzymes after starvation could allow for turnover of any toxic biologic compounds unknowingly present in cell culture medium. Lastly, hepatocytes accumulate less lipid droplets when exposed to the starvation protocol, which could limit the buildup of toxic lipids and prevent premature apoptosis (28).

Periodic fasting is associated with increased lifetime in species ranging from yeast all the way up to rodents and humans, and has been classically attributed to the activation of the energy sensing enzyme adenosine monophosphate (AMP) activated kinase (AMPK) (29,30). Serum starvation is a simple way to activate this protein in cell cultures, and we found that our starvation protocol led to increased levels of activated AMPK(17). AMPK activation is also

associated with increased hepatic nuclear receptor activation, transporters, and lipid turnover, which may explain why starved cultures had less lipid accumulation when compared to nonstarved cultures (31). Interestingly, we found that the starvation protocol reduced the number of fibroblast numbers, either in pure fibroblast or micropatterned co-cultures, when compared to non-starved cultures. Although this has not been thoroughly investigated, it is well known that supportive fibroblasts in co-culture with epithelial cells must be prevented from overgrowing the epithelial population to prevent a decline in epithelial cell colony integrity(32). Taken together, the starvation protocol likely prolongs hepatocyte functions in co-cultures by activating AMPK and preventing overgrowth of supportive fibroblasts.

To mechanistically investigate this hypothesis, we carried out experiments where we artificially activated AMPK using a nontoxic AMPK activator, metformin, and prevented fibroblast overgrowth, by growth arresting the fibroblast population with mitomycin c, in place of starvation and assessed how these perturbations affect hepatocyte longevity and functions (33). Metformin treatment or growth arresting fibroblasts in MPCCs significantly prolonged the functional lifetime of hepatocytes over an untreated control, although not to the same extent as the starvation protocol. These studies further suggest that the starvation protocol may prolong hepatocyte lifetime by activating AMPK and preventing fibroblast overgrowth, although other factors are clearly involved in prolonging longevity. Since many other liver culture systems and engineered tissues utilize serum and hormones as culture medium components we suspect that this protocol will benefit other platforms since it is inspired by a natural dynamic process that affects the entire body.

To appraise the potential impact of a longer functioning culture, we assessed the impact of starvation on hepatocyte drug toxicity screening capabilities and identification of potential

drug-drug interactions via enzyme induction. MPCCs have been rigorously tested and successfully utilized for the aforementioned applications, although this utility has not been characterized at later time points (i.e. >3 weeks) (18,19). MPCCs were fabricated in 96 well plates for drug toxicity screens and the starvation protocol worked equally well in this format. After 4 weeks in culture, we found that without starvation MPCCs could still identify hepatotoxins with 100% accuracy and showed significant enzyme induction. Although non-starved MPCCs incorrectly identified 3 out of the 5 non-liver toxins as toxic and also had much lower levels of induction when compared to starved cultures. Importantly, starved cultures correctly identified all toxic and non-toxic compounds at the drug concentrations tested. The results from these screening studies highlight the overall benefit of periodic starvation and suggest that it could be an essential component for the maintenance of proper function of engineered tissues in drug toxicity studies, which are highly needed (34).

As engineered tissues and cell culture devices continue to evolve we must constantly question the relevance of our practices towards physiology and pathophysiology. We have highlighted the impact of dynamic nutrient availability and hormone signaling with hepatocyte *in vitro* longevity, both of which are normally fluctuating in the body, but have not gained much importance in long term cell culture protocols to date (7). Importantly, we show that starvation not only prolongs hepatocyte lifetime, but it also improves overall cell health to help give proper responses for important applications such as distinguishing toxic drugs accurately.

4.5 Supplemental Figures

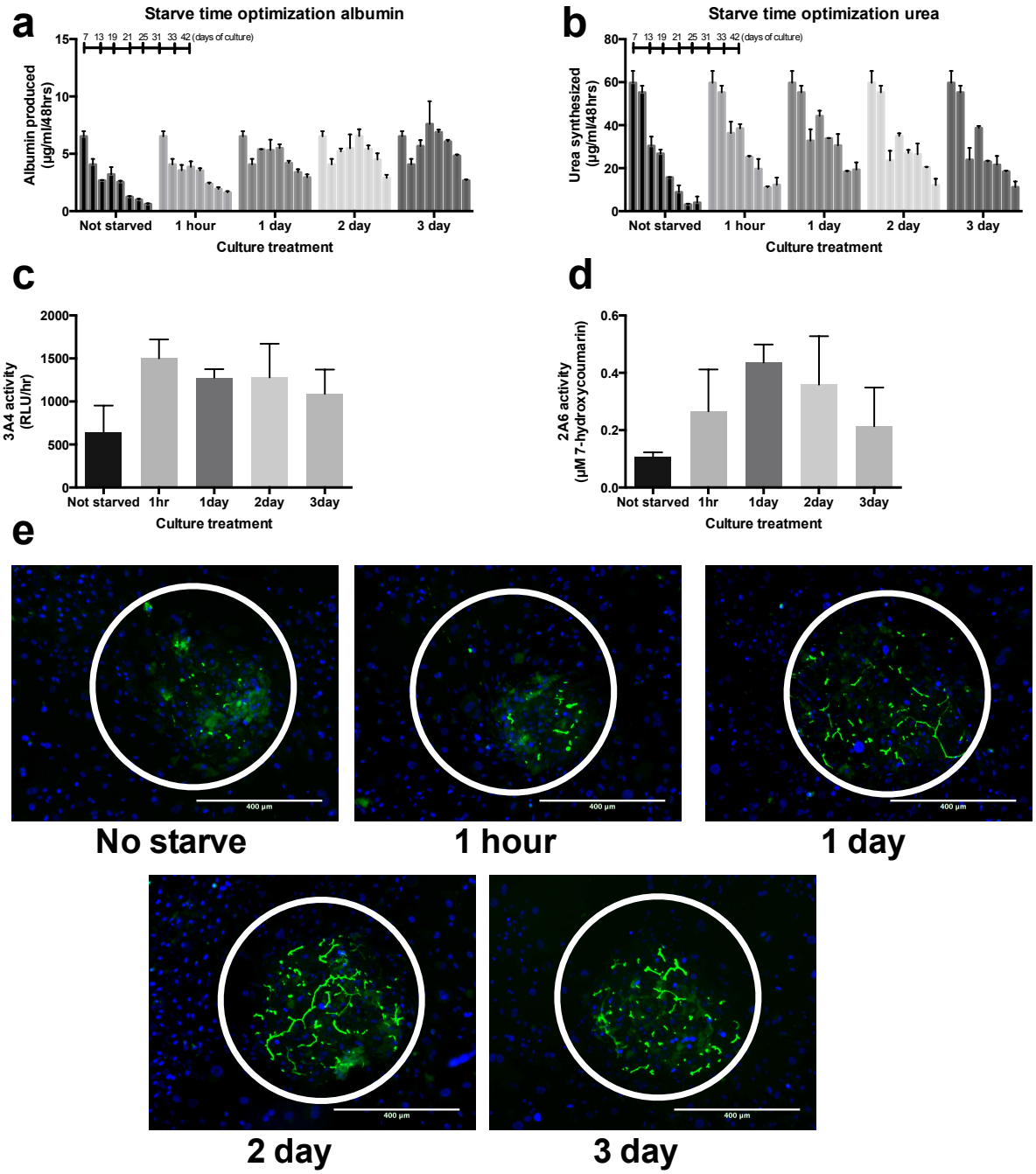

Supplemental Figure. 4.5.1. Starvation time optimization based on functional outputs from MPCCs. MPCCs were starved for 1 hour, 1-, 2 - or 3- days or not starved and assessed for albumin production (a), urea synthesis (b) over time and CYP3A4 (c) and CYP2A6 (d) enzyme activity at the terminal 6 week time point. Error bars represent SD. (e) Bile canaliculi staining after 6 weeks of culture. Circles outline hepatocyte islands and scale bars represent 400 µm.

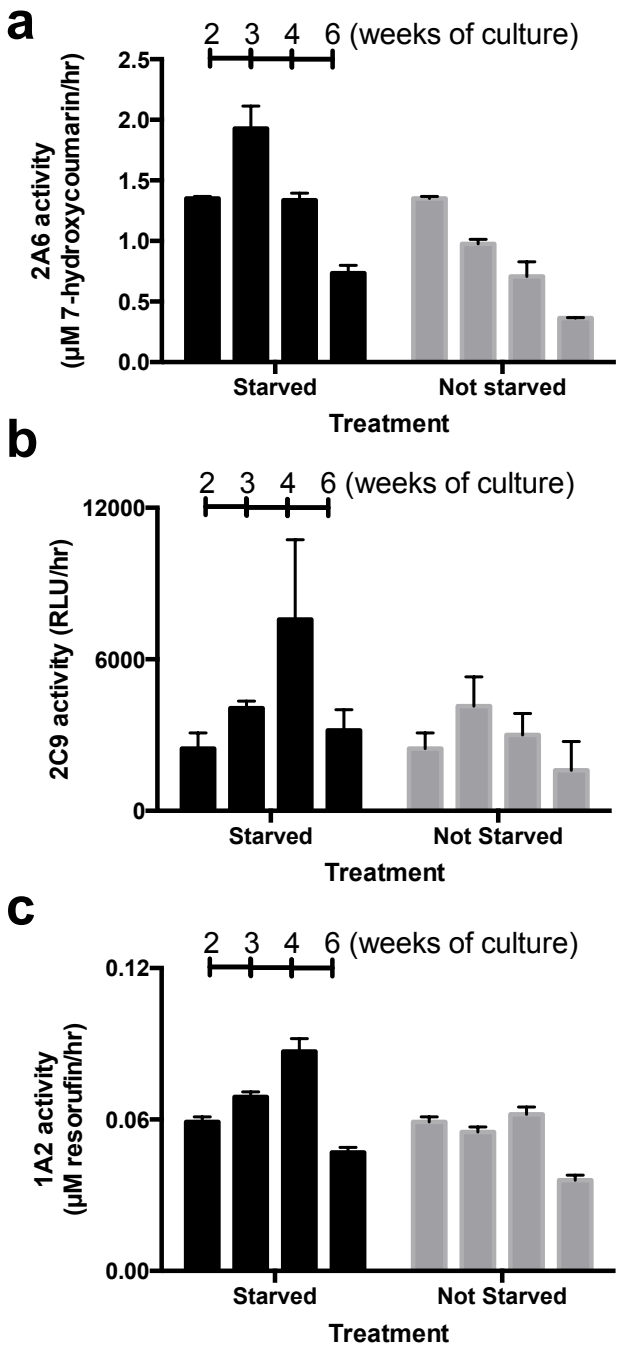

Supplemental Figure. 4.5.2 CYP450 enzyme activity over time in 2-day starved or non-starved cultures. MPCCs were starved or not starved for 6 weeks and assessed for CYP2A6 (a), CYP2C9 (b) and CYP1A2 (c) enzyme activity. Error bars represent SD.

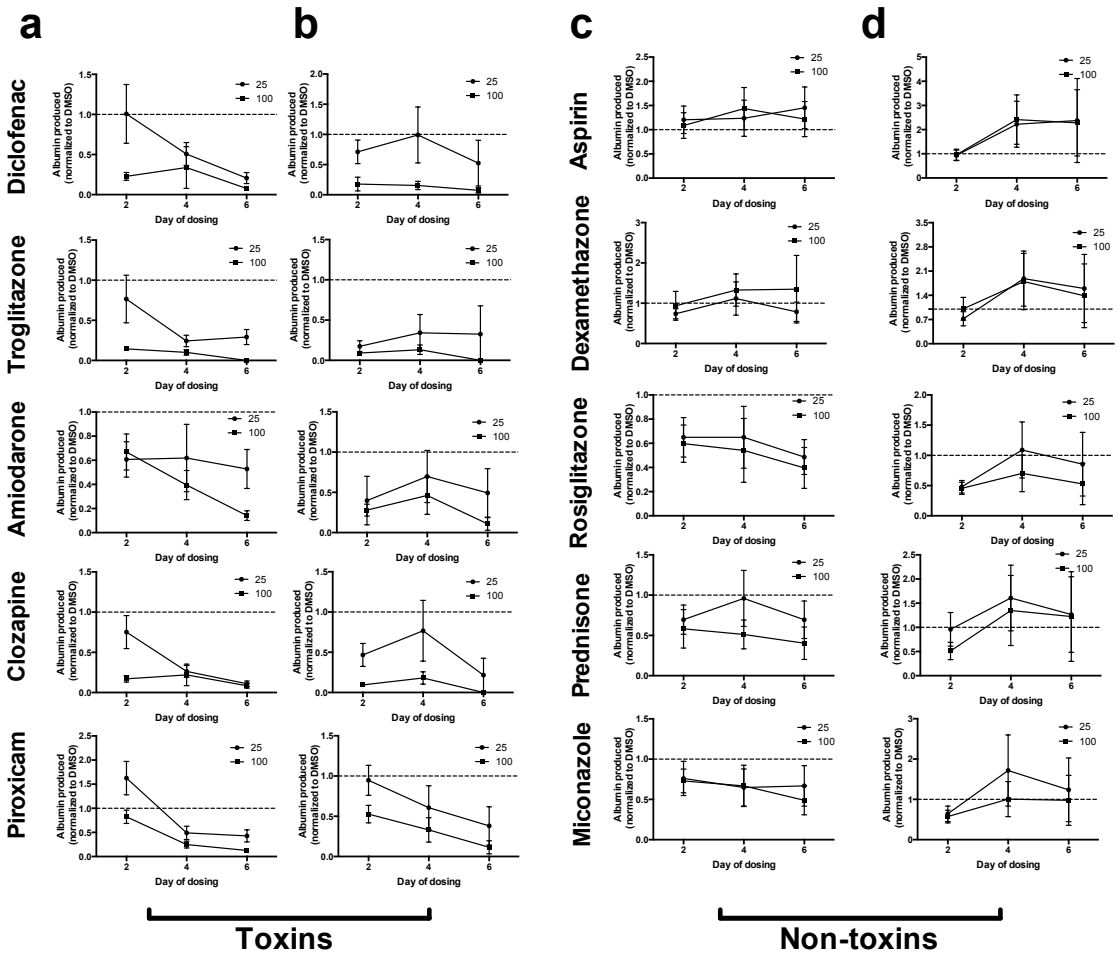

Supplemental Figure. 4.5.3. Albumin dose response curves with toxins and non-toxins in starved and non-starved cultures. Starved or non-starved MPCCs were cultured for 4 weeks and then assessed for sensitivity and specificity in a proof of concept drug toxicity screen. (a) Non-starved MPCC albumin production in response to a series of known hepatotoxins. (b) Starved MPCC albumin production in response to a series of known hepatotoxins. (c) Non-starved MPCC albumin production in response to a series of non-toxins. (d) Starved MPCC albumin production in response to a series of non-toxins. Error bars are standard deviation. All data was normalized to the vehicle, DMSO, control.

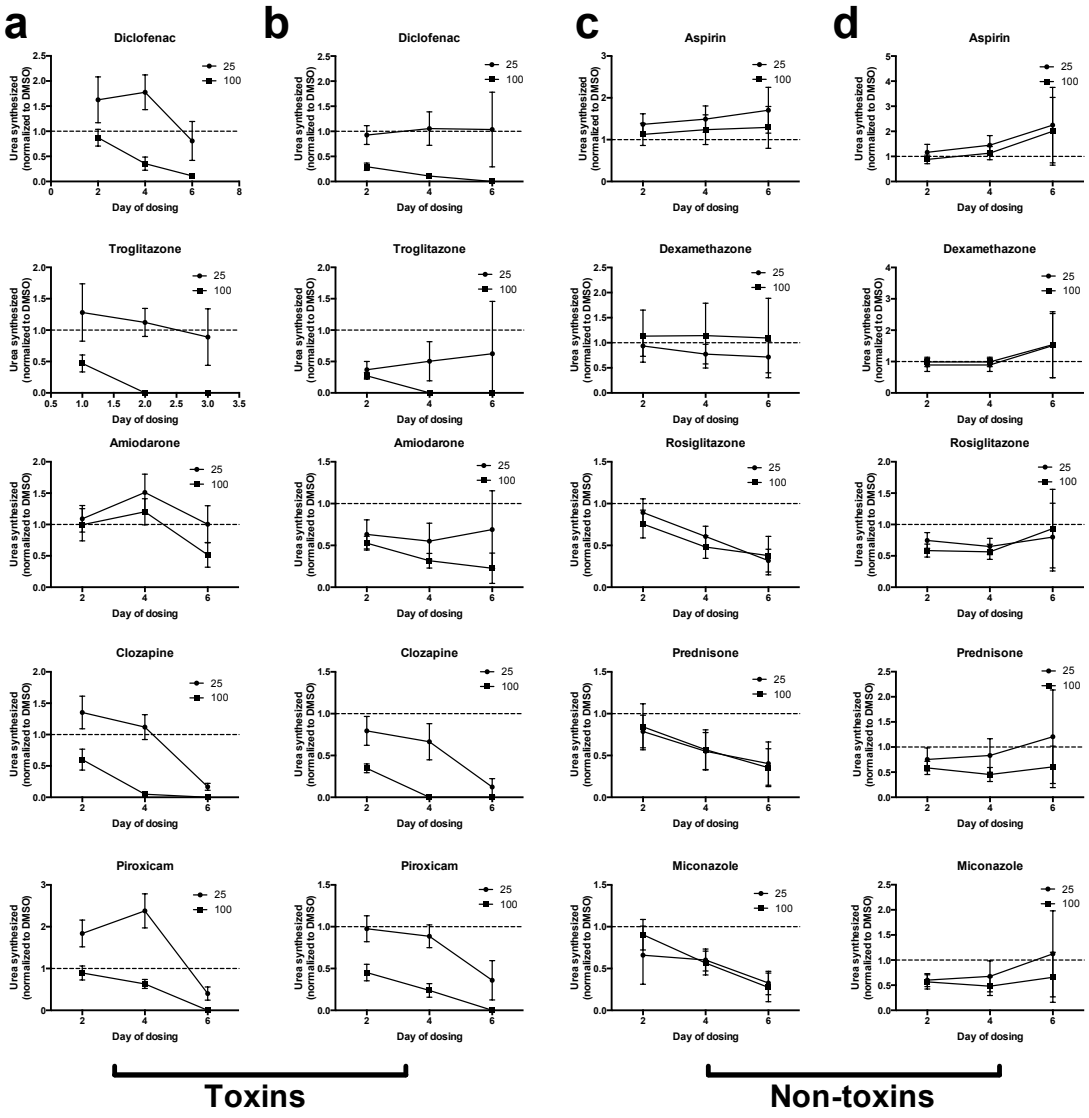

Supplemental Figure. 4.5.4. Urea dose response curves with toxins and non-toxins in starved and non-starved cultures. Starved or non-starved MPCCs were cultured for 4 weeks and then assessed for sensitivity and specificity in a proof of concept drug toxicity screen. (a) Non-starved MPCC urea production in response to a series of known hepatotoxins. (b) Starved MPCC urea production in response to a series of known hepatotoxins. (c) Non-starved MPCC urea production in response to a series of non-toxins. (d) Starved MPCC urea production in response to a series of non-toxins. Error bars are standard deviation. All data was normalized to the vehicle, DMSO, control.

References

1. DiMasi JA, Grabowski HG, Hansen RW. Innovation in the pharmaceutical industry: New estimates of R&D costs. J Health Econ. **47**, 20, 2016.

2. Onakpoya IJ, Heneghan CJ, Aronson JK. Worldwide withdrawal of medicinal products because of adverse drug reactions: a systematic review and analysis. Critical Reviews in Toxicology. **46**(6), 477, 2016.

3. Cook D, Brown D, Alexander R, March R, Morgan P, Satterthwaite G, et al. Lessons learned from the fate of AstraZeneca's drug pipeline: a five-dimensional framework. Nat Rev Drug Discov. **13**(6), 419, 2014.

4. Olson H, Betton G, Robinson D, Thomas K, Monro A, Kolaja G, et al. Concordance of the toxicity of pharmaceuticals in humans and in animals. Regul. Toxicol. Pharmacol. **32**(1), 56, 2000.

5. Takahashi Y, Soejima Y, Fukusato T. Animal models of nonalcoholic fatty liver disease/nonalcoholic steatohepatitis. WJG. **18**(19), 2300, 2012.

6. Delire B, Starkel P, Leclercq I. Animal Models for Fibrotic Liver Diseases: What We Have, What We Need, and What is Under Development. JCTH. **3**(1), 53, 2015.

7. Khetani SR, Berger DR, Ballinger KR, Davidson MD, Lin C, Ware BR. Microengineered liver tissues for drug testing. J Lab Autom. **20**(3), 216, 2015.

8. Gómez-Lechón MJ, Tolosa L, Conde I, Donato MT. Competency of different cell models to predict human hepatotoxic drugs. Expert Opin Drug Metab Toxicol. **10**(11), 1553, 2014.

9. March S, Ramanan V, Trehan K, Ng S, Galstian A, Gural N, et al. Micropatterned coculture of primary human hepatocytes and supportive cells for the study of hepatotropic pathogens. Nature Protocols. **10**(12), 2027, 2015.

10. Davidson MD, Ballinger KR, Khetani SR. Long-term exposure to abnormal glucose levels alters drug metabolism pathways and insulin sensitivity in primary human hepatocytes. Sci. Rep. **6**, 28178, 2016.

11. Norona LM, Nguyen DG, Gerber DA, Presnell SC, LeCluyse EL. Modeling Compound-Induced Fibrogenesis In Vitro Using Three-Dimensional Bioprinted Human Liver Tissues. Toxicological Sciences. 2016.

12. Bell CC, Hendriks DFG, Moro SML, Ellis E, Walsh J, Renblom A, et al. Characterization of primary human hepatocyte spheroids as a model system for drug-induced liver injury, liver function and disease. Sci. Rep. **6**, 25187, 2016.

13. Alison MR, Islam S, Lim S. Stem cells in liver regeneration, fibrosis and cancer: the good, the bad and the ugly. J. Pathol. **217**(2), 282, 2009.

14. Hatori M, Vollmers C, Zarrinpar A, DiTacchio L, Bushong EA, Gill S, et al. Time-restricted feeding without reducing caloric intake prevents metabolic diseases in mice fed a high-fat diet. Cell Metabolism. **15**(6), 848, 2012.

15. Bailey SM, Udoh US, Young ME. Circadian regulation of metabolism. Journal of Endocrinology. **222**(2), R75, 2014.

16. Yamajuku D, Inagaki T, Haruma T, Okubo S, Kataoka Y, Kobayashi S, et al. Real-time monitoring in three-dimensional hepatocytes reveals that insulin acts as a synchronizer for liver clock. Sci. Rep. **2**, 439, 2012.

17. Ching JK, Rajguru P, Marupudi N, Banerjee S, Fisher JS. A role for AMPK in increased insulin action after serum starvation. American Journal of Physiology - Cell Physiology. **299**(5), C1171, 2010.

18. Khetani SR, Bhatia SN. Microscale culture of human liver cells for drug development. Nat Biotechnol. **26**(1), 120, 2007.

19. Khetani SR, Kanchagar C, Ukairo O, Krzyzewski S, Moore A, Shi J, et al. Use of Micropatterned Cocultures to Detect Compounds That Cause Drug-Induced Liver Injury in Humans. Toxicological Sciences. **132**(1), 107, 2013.

20. Xu JJ, Henstock PV, Dunn MC, Smith AR, Chabot JR, de Graaf D. Cellular imaging predictions of clinical drug-induced liver injury. Toxicological Sciences. **105**(1), 97, 2008.

21. Godoy P, Hewitt NJ, Albrecht U, Andersen ME, Ansari N, Bhattacharya S, et al. Recent advances in 2D and 3D in vitro systems using primary hepatocytes, alternative hepatocyte sources and non-parenchymal liver cells and their use in investigating mechanisms of hepatotoxicity, cell signaling and ADME. Arch Toxicol. **87**(8), 1315, 2013.

22. Huh D, Hamilton GA, Ingber DE. From 3D cell culture to organs-on-chips. Trends in Cell Biology. **21**(12), 745, 2011.

23. Díaz-Muñoz M, Vázquez-Martínez O, Báez-Ruiz A, Martínez-Cabrera G, Soto-Abraham MV, Avila-Casado MC, et al. Daytime food restriction alters liver glycogen, triacylglycerols, and cell size. A histochemical, morphometric, and ultrastructural study. Comp Hepatol. **9**, 5, 2010.

24. Davidson MD, Lehrer M, Khetani SR. Hormone and Drug-Mediated Modulation of Glucose Metabolism in a Microscale Model of the Human Liver. Tissue Engineering Part C: Methods. **21**(7), 716, 2015.

25. Nelson W, Halberg F. Meal-timing, circadian rhythms and life span of mice. J. Nutr. **116**(11), 2244, 1986.

26. Li Q, Zhang Y, Pluchon P, Robens J, Herr K, Mercade M, et al. Extracellular matrix scaffolding guides lumen elongation by inducing anisotropic intercellular mechanical tension. Nat. Cell Biol. **18**(3), 311, 2016.

27. Halilbasic E, Claudel T, Trauner M. Bile acid transporters and regulatory nuclear receptors in the liver and beyond. Journal of Hepatology. **58**(1), 155, 2013.

28. Feldstein AE, Werneburg NW, Canbay A, Guicciardi ME, Bronk SF, Rydzewski R, et al. Free fatty acids promote hepatic lipotoxicity by stimulating TNF-alpha expression via a lysosomal pathway. Hepatology. **40**(1), 185, 2004.

29. Brandhorst S, Choi IY, Wei M, Cheng CW, Sedrakyan S, Navarrete G, et al. A Periodic Diet that Mimics Fasting Promotes Multi-System Regeneration, Enhanced Cognitive Performance, and Healthspan. Cell Metabolism. **22**(1), 86, 2015.

30. Lee S-H, Min K-J. Caloric restriction and its mimetics. BMB Rep. **46**(4), 181, 2013.

31. Kulkarni SR, Xu J, Donepudi AC, Wei W, Slitt AL. Effect of caloric restriction and AMPK activation on hepatic nuclear receptor, biotransformation enzyme, and transporter expression in lean and obese mice. Pharm. Res. **30**(9), 2232, 2013.

32. Rheinwald JG, Green H. Serial cultivation of strains of human epidermal keratinocytes: the formation of keratinizing colonies from single cells. Cell. **6**(3), 331, 1975.

33. Kim YD, Park KG, Lee YS, Park YY, Kim DK, Nedumaran B, et al. Metformin Inhibits Hepatic Gluconeogenesis Through AMP-Activated Protein Kinase-Dependent Regulation of the Orphan Nuclear Receptor SHP. Diabetes. **57**(2), 306, 2007.

34. Paul SM, Mytelka DS, Dunwiddie CT. How to improve R&D productivity: the pharmaceutical industry's grand challenge. Nat. Reviews Drug discovery. 2010.

Chapter 5

Biologically inspired cell culture medium prolongs the lifetime and insulin sensitivity of hepatocytes in micropatterned co-cultures[4]

Summary:

In chapter 4 we showed that dynamic culturing methods could prolong the lifetime, along with many other benefits, and lipid profile of hepatocytes in MPCCs. Importantly the lifetime of hepatocytes in vivo is suggested to be around 1 year and we observed clear declines in hepatocyte numbers and function with the starvation protocol described in chapter 4. The culture medium used in theses studies still has supraphysiologic levels of insulin and bovine serum, both of which could have major detrimental effects on hepatocyte insulin signaling and longevity. One alternative to using bovine serum is the use of pooled human serum and potentially reducing the level of insulin in culture medium down to physiologic levels. Human serum is commercially available and economically feasible. Therefore we developed a culture medium where bovine serum is replaced with human serum. Human serum could successfully be used to maintain MPCCs and we fortuitously found that it also enabled the use of physiologic levels of insulin without losing hepatocyte functions, as was seen with the use of bovine serum. We then assessed how this bioinspired, physiologically relevant, medium altered hepatocyte longevity, drug metabolism and insulin sensitivity over time towards developing the optimal cell culture medium for NAFLD disease model applications as well as other engineered liver tissue systems.

[4]A manuscript similar to the work described in this chapter is in preparation and will be submitted for publication shortly.

5.1 Introduction

The drug development pipeline is a long and rigorous pathway that commonly leads to hundreds of millions of dollars being wasted in pre-clinical drug screening (1). Costly issues faced during drug development include identifying efficacious therapies and verifying that those compounds will be safe in the clinic (2). Accordingly, many efforts are being put forth to develop sensitive cell-based pre-clinical screening systems that can identify efficacious and safe compounds prior to initiation of costly and dangerous phase I clinical trials (3). The advantage of such models is that they can be scaled up to high throughput formats, which enables the screening of tens of thousands of compounds simultaneously. One major area of focus is on the development of liver models since many new therapies are being developed to target liver disease while hepatotoxicity remains a major cause for post-market withdraw of compounds (4-6).

Owing to species-specific differences in drug metabolism enzymes, human-relevant systems are needed to properly model human drug metabolism/toxicity/efficacy (7). Additionally, to model human diseases, such as viral infection and fatty liver disease, human-based systems will likely be necessary since animal models are not susceptible to infection, as is the case with hepatitis C, and disease development is significantly different in humans (8). Cell-based systems, ranging from simple 2D cultures up to complex bioprinted 3D tissues, have gained the most interest for these areas of drug development. Regardless of culture setup, primary human hepatocytes (PHHs) remain the gold standard for the pharmaceutical industry since they retain the entire set of drug metabolism enzymes necessary for processing candidate compounds and they accurately predict human drug metabolism/toxicity (9). The drawback to using PHHs is that they rapidly, 24-72 hours, lose their liver phenotype *in vitro*. The liver tissue

engineering field has evolved around this issue and consequently, methods have been developed to prevent the premature decline of PHHs (10). Unfortunately, even with the major advances that have been made, hepatocyte *in vitro* functional lifetime seems to be limited to 4-6 weeks, while the in vivo lifetime is expected to be >1 year (11).

One area that has lacked substantial improvement over the years is the formulation of cell culture medium. Current culture systems either oversupply nutrients and hormones to cells while using animal-based products, such as serum, or undershoot the vast complexity of the soluble factors found in the body using chemically defined medium(12). Once the ideal liver culture system is designed, these soluble cues will be major determining factors for cell function and lifetime. Additionally, for regenerative medicine purposes, all human or synthetic based cell culture medium supplements will be necessary to prevent non-human component induced immune reactions(13), and the transmission of infectious agents (14).

Recently it has been shown that physiologic concentrations of glucose and bile acid supplementation to culture medium can prevent an insulin resistant and inflamed state from developing in hepatocytes, respectively (15,16). Inspired by this work and the remaining issues with liver cell culture, we developed a xeno-free cell culture medium with physiologically relevant concentrations of insulin and glucose to address how a more physiologically relevant medium might enhance hepatocyte lifetime and functionality. We utilized an already established long-term hepatocyte culture system to address how this xeno-free cell culture medium may provide any significant advantage over similar animal based components. In this culture system, hepatocytes are micropatterned onto collagen domains to facilitate homotypic, self-self, interactions and then surrounded by supportive 3T3-J2 murine embryonic fibroblasts, which enables important heterotypic interactions (17-19). Micropatterned co-cultures (MPCCs) have a

lifetime of 4-6 weeks and are normally cultivated in animal-based products. This provides a system to address how a xeno-free culture medium may further improve cultures that already have a significantly high level of function and lifetime. Over 4-10 weeks, we assessed how this new medium formulation affects hepatocyte morphology, lifetime, functions, transporter formation and insulin sensitivity. Additionally, we verified that this system could still be used to identify hepatotoxic and non-toxic compounds as well as drug-drug interactions.

5.2 Methods

5.2.1 Cell culture and MPCC fabrication

MPCC fabrication was carried out as described in chapter 2 and 3. Growth arresting fibroblast cultures and seeding into MPCCs was carried out as described in chapter 4. To account for potential differences in fibroblast growth and spreading between physiologic medium and traditional medium, cultures were first created and maintained in traditional medium for 4 days and then switched to their respective medium.

5.2.2 Biochemical and enzyme activity assays

Urea synthesis and glucose production were quantified using the same methods described in chapter 2 and 3. Since human serum contains significant amounts of human serum, we used an alternative protocol to quantify MPCC albumin production. Specifically, after 2 and 3 weeks of culture, cultures were washed 3 times with 1x PBS and then incubated for 24 hours in serum-free

medium. Albumin was then measured in this medium using the sandwich ELISA method described in chapter 2 and 3. To account for potential residual albumin in cell culture medium, we looked for any differences in albumin production between cultures incubated in 5%, 7.5%, and 10% serum. We found no significant differences in albumin production between these cultures, which suggested that most residual albumin had been successfully removed with the PBS washing steps prior to the 24 hour incubation period. Enzyme activity was assessed using the methods described in chapter 3 and 4.

5.2.3 Imaging and transporter visualization

Bile canaliculi (CDCFDA) and phase contrast imaging were carried out in the same fashion described in chapter 4. Importantly, bile canaliculi imaging was carried out after 4 weeks of culture in these studies.

5.2.4 Insulin resistance assay

To assess the insulin sensitivity of these cultures we utilized similar methods described in chapter 3. Cultures were first cultured in hormone-free, serum-containing medium for 24 hours, and then washed 3 times with 1x PBS to remove residual glucose. Cultures were then incubated in glucose-free medium containing 4 mM L-glutamine, 1% penicillin/ streptomycin, 1.5% HEPES buffer, 20 mM lactate and 2 mM pyruvate to and +/- 10 nM insulin. Insulin resistance was calculated by dividing the insulin-stimulated glucose output by the basal level of glucose output.

5.2.5 Drug toxicity and enzyme induction studies

Drug toxicity and enzyme induction were assessed in the same manner described in chapter 4. Importantly, in these studies, drug toxicity and enzyme induction were carried out after 2 weeks of culture, and the level of these metrics was not directly compared to traditional medium since these MPCC utilities have clearly been demonstrated in previous publications (17,25).

5.2.6 Statistical analyses

Each experiment was carried out in 2 or more wells for each condition. Two to three cryopreserved PHH donors were used to confirm observed trends. Microsoft Excel and GraphPad Prism 5.0 (La Jolla, CA) were used for data analysis and plotting data. Error bars on average values represent standard deviation (SD) across wells. Statistical significance of the data was determined using the average and SD across wells in representative experiments using the Student's *t*-test or one-way ANOVA with Dunnett's multiple comparison tests for post hoc analysis.

5.3 Results

5.3.1 Optimizing culture medium to enable proper comparison of physiologically relevant medium to traditional medium

Traditionally, hepatocyte maintenance medium utilizes bovine serum and an excessive amount of glucose as well as insulin. Bovine serum could potentially have proteins which negatively affect hepatocyte insulin pathways(20) on human hepatocytes while it could also contain pathogenic proteins or cause an immune response in humans if used for regenerative medicine purposes. Additionally, high amounts of glucose and insulin are major contributors to fatty liver disease and we have recently shown this is recapitulated in the MPCC system (15). These abnormalities in culture medium inspired us to develop a more physiologic medium that did not contain any animal products, xeno-free medium. Specifically, we formulated medium that had physiologic glucose (~5 mM), human serum (in place of bovine serum) and physiologic levels of insulin (0.5-1 pM versus the traditional 1 μM).

Since we have already shown that glucose levels can be reduced in medium without adverse effects on MPCC performance, we focused on how changing insulin levels and serum type affected hepatocyte function and longevity. Surprisingly, we found that reducing insulin to physiologic levels in MPCCs cultured with bovine serum led to declining hepatocyte urea production and lower CYP3A4 activity, whereas lowering insulin in MPCCs cultured with human serum maintained stable hepatocyte urea production and CYP3A4 activity after 3 weeks in culture (Supplemental Fig. 1). These results suggested that human serum enables culturing MPCCs in physiologic concentrations of insulin, whereas MPCCs cultured in bovine serum

decline without excessive insulin supplemented in the culture medium. Consequently, the remainder of these studies were carried out using the traditional amount of insulin (1 μM) in cultures with bovine serum containing medium, while cultures carried out in medium with human serum had physiologic (500 pM) levels of insulin.

To further optimize the medium formulation, we cultured MPCCs in different percentages of serum and assessed the effects of serum concentration on hepatocyte albumin production and urea synthesis. Within the range we tested, 5-10% serum containing medium, we found no significant change in hepatocyte function with different amounts of human serum, while we did find that 10% bovine serum seemed to be the optimal percentage of serum for MPCC albumin production (Supplemental Fig.2). Therefore, subsequent studies were carried out using 10% human and 10% bovine serum. Since fibroblasts enable hepatocyte functions in MPCCs and we wanted to get a proper comparison between physiologic medium and the traditional medium, we growth-arrested fibroblasts using mitomycin C prior to incorporation into MPCCs (Fig. 1). Growth arrested fibroblasts can still support hepatocytes while their growth and numbers should be consistent with different medium supplements.

5.3.2 Physiologically relevant medium prolongs the lifetime of hepatocytes in micropatterned co-cultures

Once the optimal medium formulations were identified, we carried out long-term studies (10 weeks) to assess the possibility of culturing hepatocytes in a xeno-free and physiologically relevant medium, where we assessed hepatocyte colony morphology, and functions over time. Surprisingly, physiologically relevant medium was not only compatible with MPCCs, but

hepatocyte colony morphology, as assessed by phase contrast imaging, showed dramatic stabilization of hepatocytes compared to traditional medium (Fig. 1). Specifically, hepatocyte morphology and island integrity were diminished by 6 weeks in traditional medium, whereas hepatocyte morphology was greatly retained up to 10 weeks using physiologically relevant medium

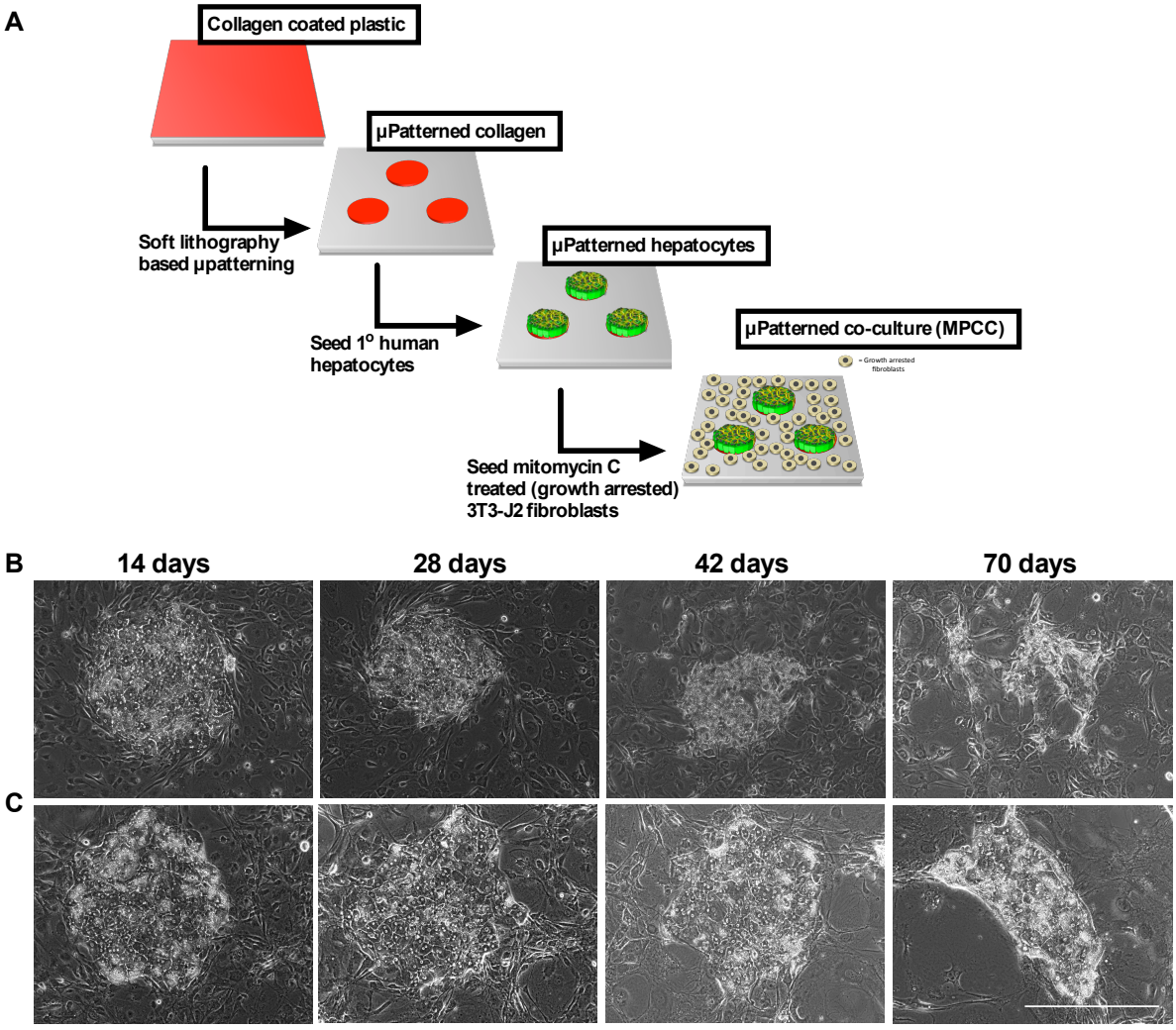

Figure 5.1. Physiologically relevant medium prolongs the lifetime of hepatocytes in micropatterned co-cultures. (A) MPCC fabrication scheme. Representative phase contrast images of MPCC hepatocyte islands in traditional medium (B) and Physiologic medium (C) over time. Scale bar represents 400 µm.

5.3.3 Hepatocyte functional lifetime is significantly longer in a physiologic medium

Along with hepatocyte morphology, hepatocyte functions were also maintained in the physiologic medium. Specifically, when we measured CYP3A4 activity in MPCCs over time we found that traditional medium enzyme activity was ~1% of 1-week levels, while physiologic medium MPCC enzyme activity was ~60% of 1-week levels (Fig. 2). CYP2A6 enzyme activity was also assessed for 8 weeks, and traditional medium CYP2A6 activity was completely absent by 62 days in culture, while physiologically relevant medium CYP2A6 levels were still 45% of 1-week levels.

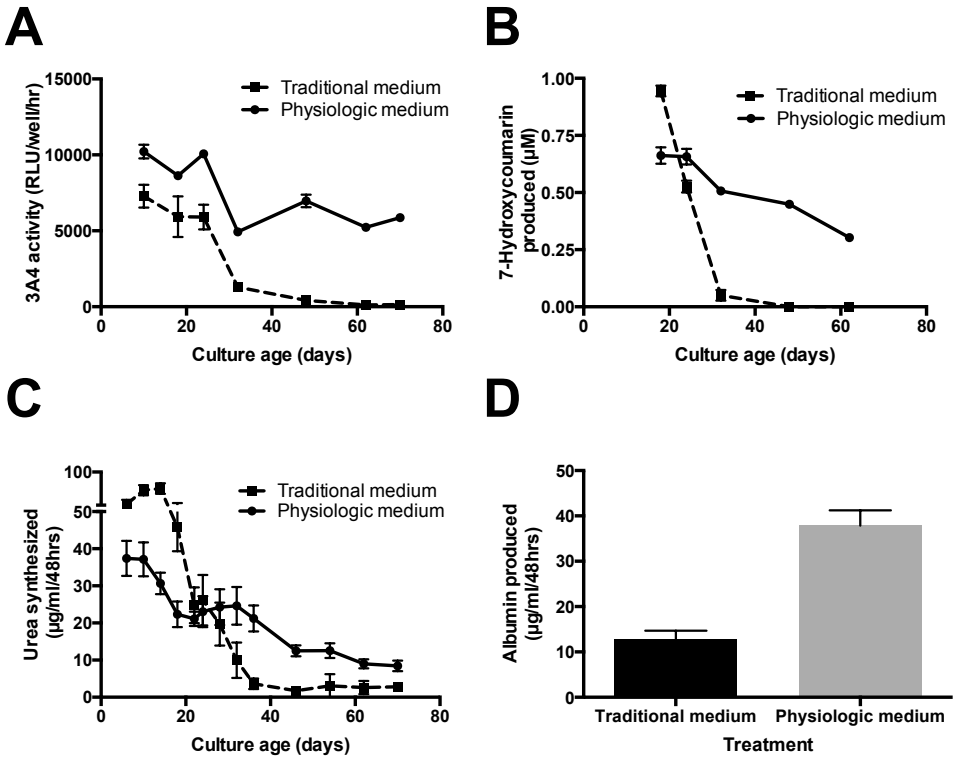

Figure 5.2. Hepatocyte functional lifetime is significantly longer in a physiologic medium. MPCCs were carried out in the traditional or the physiologic medium for 8-10 weeks and assessed for CYP3A4 (A), and CYP2A6 (B) enzyme activity. Urea synthesis (C) and albumin production (D) were assessed in cultures treated with traditional or physiologic medium over 10 weeks and at 3 weeks of culture, respectively. Error bars represent SD.

Urea synthesis was also maintained in the physiologic medium at 57% and 23% of 1-week levels at 5 and 10 weeks in culture, respectively. Alternatively, urea synthesis of MPCCs in the traditional medium was ~7% and 5% of 1-week levels by 5 weeks and 10 weeks in culture, respectively. Importantly, albumin production was ~ 3 fold higher at 3 weeks of culture in the physiologic medium relative to the traditional medium. These results suggest that physiologic medium supports a high level of hepatocyte function in MPCCs while also prolonging the lifetime of hepatocytes in culture.

5.3.4 Polarized hepatocyte transporters remain intact in physiologic medium

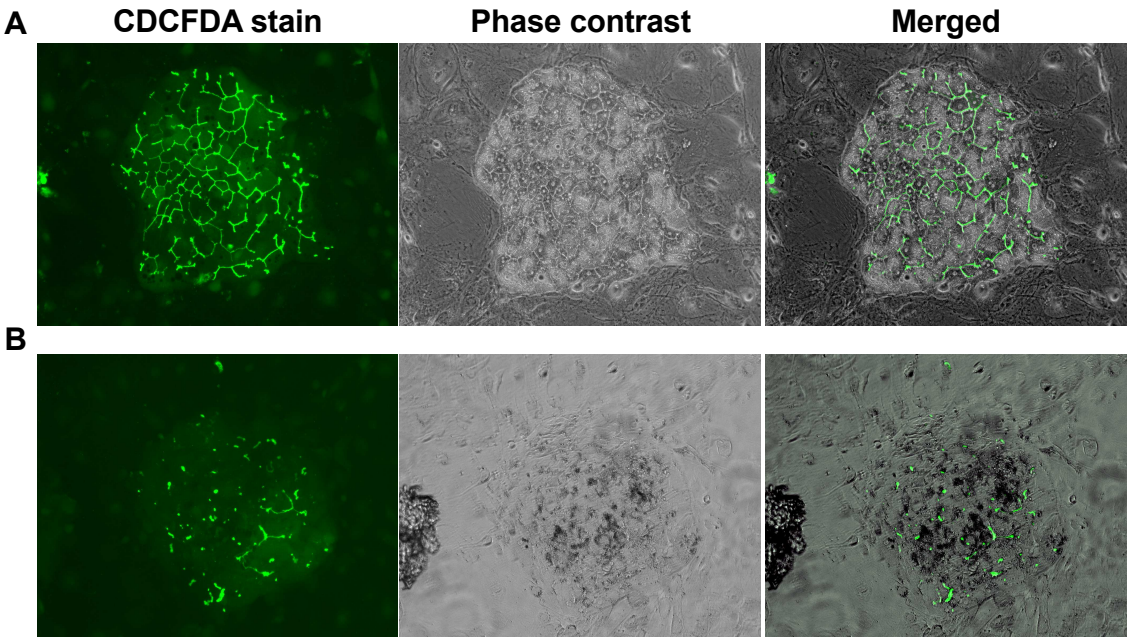

Figure 5.3. Polarized hepatocyte transporters remain intact in physiologic medium. MPCCs were cultured for 4 weeks in the physiologic (A) or traditional (B) medium and then assessed for bile canaliculi function, with CDCFDA transporter dye, and corresponding phase contrast imaging.

Since hepatocyte islands had sustained integrity in physiologic medium, we hypothesized that hepatocyte islands would have greater levels of transporter function, which requires a high

degree of homotypic hepatocyte-hepatocyte interactions (21). To probe transporter function, we used a fluorescent dye, which is selectively transported through the hepatospecific multidrug resistance-associated protein 2 and 3 (MRP2, -3). At early time points, (~2 weeks, data not shown) hepatocytes had significant transporters in all conditions, while after 4 weeks there was a significant loss of transporters in hepatocyte islands cultured in traditional medium (Fig. 3). Importantly, hepatocyte transporters were mostly retained in hepatocyte islands cultured in the physiologic medium. This loss or retention of transporters correlated with the retention of island integrity, as shown by corresponding phase contrast images. These results suggest that physiologic medium retains hepatocyte polarity and transporters over at least 4 weeks *in vitro.*

5.3.5 Hepatocyte insulin sensitivity is retained in physiologically relevant medium

One critical function of the liver is to maintain glucose levels in the blood by responding to hormones secreted from the pancreas and to a lesser extent by factors secreted from adipose tissue (22). This function of liver cells is almost always overlooked in *in vitro* liver models, although it is a key determinant of liver health. Additionally, bovine factors, such as fetuins, and high amounts of insulin could contribute to insulin resistance *in vitro* (20,23). Therefore we assessed MPCC insulin resistance after treatment with the traditional or physiologic medium over 4 weeks. Insulin resistance is calculated by dividing the insulin-stimulated glucose output from cultures by the non-insulin stimulated glucose output over 8 hours of glucose production, where completely insulin resistant cultures have a value of 1 and completely insulin sensitive cultures have a value of 0 (Fig. 4). We found that hepatocytes in the traditional medium were ~50% insulin resistant after 2 weeks and completely insulin resistant after 4 weeks of culturing

in the traditional medium. Alternatively, hepatocytes cultured in the physiologic medium were almost completely insulin sensitive, 2.5% insulin resistant, after 2 weeks of culture, and 23% insulin resistant after 4 weeks of culture. This increased rate of insulin resistance was likely from bovine serum factors since even hepatocytes cultured in physiologic insulin (~500pM) developed insulin resistance faster than cultures in human serum (Fig. S3). These results suggest that physiologic medium retains insulin sensitivity in hepatocytes longer than traditional medium.

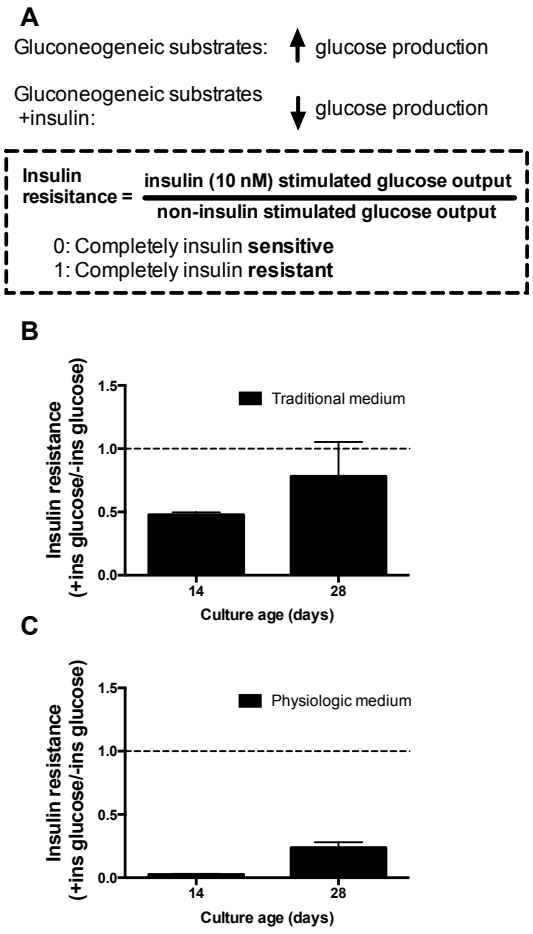

Figure 5.4. Hepatocyte insulin sensitivity is retained in physiologically relevant medium. (A) Diagram describing how to calculate insulin resistance in MPCCs. Insulin resistance after 2 and 4 weeks of culture in traditional (B) and physiologic (C) medium. Error bars represent SD.

5.3.6 Physiologically relevant medium allows for sensitive and specific hepatotoxicity screening as well as drug-drug interactions

Since these changes in medium formulation led to increased longevity, function, and hormone responses, we wanted to ensure that these cultures could also accurately predict hepatotoxins and drug-drug interactions. Therefore we carried out a drug screen with cultures after they were subjected to physiologic medium for 10 days (Fig. 5). Specifically, cultures were treated with 5 known hepatotoxins, and 5 non-toxins 2 times over a period of 5 days with increasing concentrations of C_{max} ($25*C_{max}$, and $100*C_{max}$), the average maximal drug concentration observed in patients after administering the drug. The compounds tested have previously been identified as hepatotoxins or non-toxins in comprehensive hepatotoxicity studies (24). Drug treatments were carried out in serum free medium to prevent potential drug-protein interactions. Compounds were categorized as toxic if urea synthesis in MPCC supernatants, which has recently been shown to be a more sensitive marker of liver toxicity than ATP, dropped below 50% of the vehicle (DMSO) treated control (25). After 2 treatments with toxins, MPCCs cultured in physiologic medium correctly identified all 5 hepatotoxins (diclofenac, troglitazone, clozapine, amiodarone, and piroxicam) as toxic, as shown by a concentration and time dependent decrease in urea synthesis (Fig. 5). Calculated TC_{50} values, the interpolated concentration of the drug where urea synthesis drops below 50% of the vehicle control, for the various compounds were 282 μM, 334 μM, 63 μM, 41 μM and 475 μM for diclofenac, troglitazone, clozapine, amiodarone, and piroxicam, respectively (Supplemental Table. 1). Importantly, MPCCs in physiologic medium also correctly categorized all 5 non-toxins (aspirin, dexamethasone, rosiglitazone, prednisone, and miconazole), as shown by no significant loss in urea synthesis

over time with increasing concentration of compound (Fig. 5). These results suggest that hepatocytes cultured in physiologic medium retain the ability to correctly identify potential hepatotoxins and non-toxic compounds.

To assess the potential of MPCCs in physiologic medium to predict drug-drug interactions, we treated cultures with known enzyme inducers and quantified their enzyme activity (26). Specifically, to induce CYP3A4, CYP1A2, and CYP2C9, we treated MPCCs twice with phenobarbital, omeprazole or rifampin, respectively, over 4 days in serum-free medium. Cultures were treated with the respective vehicle control, water or DMSO, as a non-induced control. Induction was carried out after 10 days of culture in the physiologic medium. MPCCs in physiologic medium showed a 3.5 (± 0.25) fold induction of CYP3A4 activity, 2.75 (± 0.24) fold induction of CYP1A2 and a 7.2 (± 1.8) fold induction of CYP2C9 activity (Fig. 5). We also found slightly higher levels of basal CYP1A2 and CYP2C9 activity in MPCCs after 3 weeks of culture in the physiologic medium compared to traditional medium (Supplemental Fig. 5). These results suggest that MPCCs cultured in physiologic medium retain the ability to identify potential enzyme induction and drug-drug interactions.

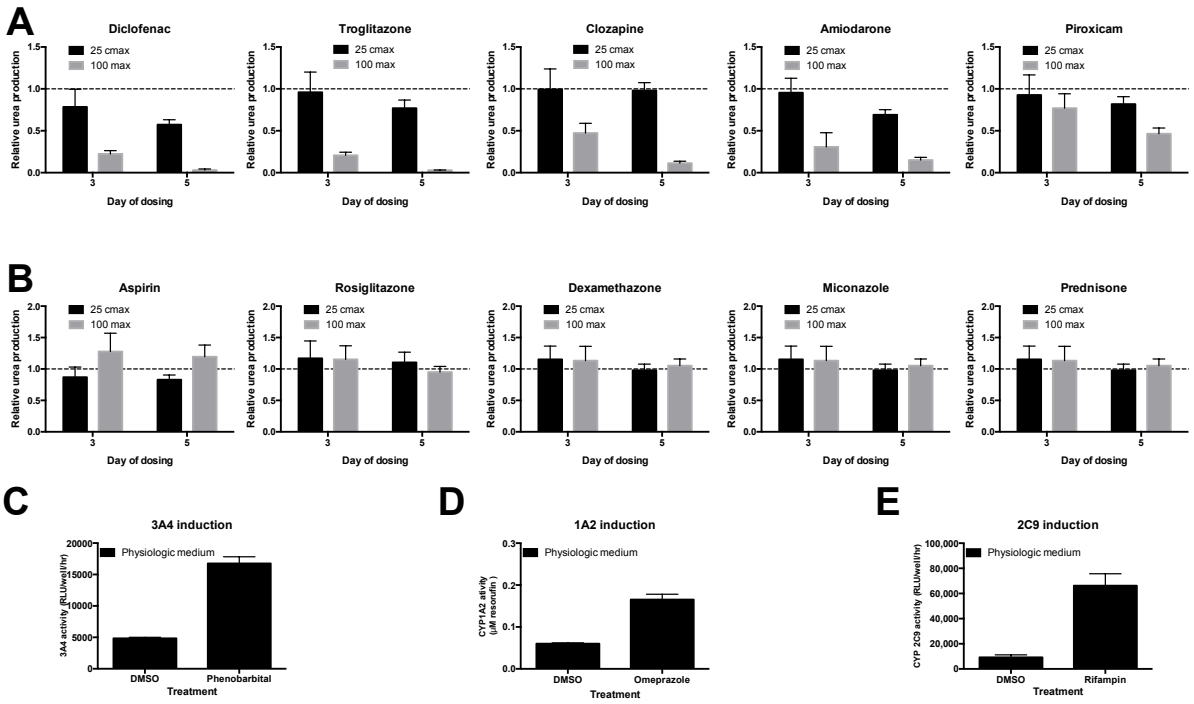

Figure 5.5. Physiologically relevant medium allows for sensitive and specific hepatotoxicity screening as well as drug-drug interactions. MPCCs were cultured in physiologic medium for 10 days and then placed in a liver toxicity screen (A,B) or assessed for induction capabilities (C-E). (A) Urea synthesis in treatments with liver toxins after the first and second drug treatment or day 3 and 5 of dosing. (B) Urea synthesis in treatments with non-toxins after the first and second drug treatment or day 3 and 5 of dosing. CYP3A4 (C), CYP1A2 (D) and CYP2C9 (E) enzyme induction with prototypical inducers. Error bars represent SD.

5.4 Discussion

Primary human hepatocytes are the gold standard for pharmaceutical drug screening and also the development of bio-artificial livers and implantable constructs for regenerative medicine applications. Since hepatocytes are inherently difficult to maintain outside of the body this poses significant hurdles for drug screening and regenerative medicine applications and any advances in maintaining hepatocytes outside the body should benefit these areas. One area of optimization that can be broadly applicable across these inherently different research fields is advancements in the medium by which nutrients and signaling proteins are supplied to cell and tissue cultures.

Inspired by recent cell culture medium modifications and the need for a medium that is free of animal components, we developed a xeno-free culture medium that better mimics the physiologic concentrations of glucose and insulin *in vivo* while maintaining the complexity of human blood profile by using pooled human serum (16). Surprisingly, we found that the physiologically relevant medium formulation we developed could not only support normal hepatocyte functions enabled by micropatterned co-cultures (MPCCs) but that it significantly prolonged the lifetime and functions of hepatocytes in this co-culturing system without losing its utility for drug screening and glucose metabolism studies.

The use of human serum, more than any other modification we made, is what enabled the long lifetime and functions of hepatocytes, as we were able to sustain hepatocytes for extended periods of time over cultures with bovine serum even with abnormal levels of insulin and glucose. Although, our overall goal was to develop a more physiologically relevant medium that would be useful for a variety of applications, including disease modeling, so we further modified the culture medium to have the ideal amount of serum, and insulin. Surprisingly, we found that by using 10% serum in our medium we could lower the amount of insulin supplemented in medium down to a physiologically relevant concentration, ~500 pM, while this amount of insulin supplementation in medium containing bovine serum as a base led to declining hepatocyte functions. Using this optimized xeno-free medium we showed that hepatocyte functions, such as drug metabolism enzyme activity, urea synthesis, and albumin production, were retained longer than traditional medium. Serum is a complex mixture of proteins, lipids, and biomolecules, and we are currently assessing how individual components of serum may prolong the lifetime of hepatocytes *in vitro.* Since bile acid and lipid profiles are unique across different species, we

suspect these components may be responsible for the prolonged longevity of human hepatocytes in human serum (27).

When human serum is supplemented for bovine serum there is a substantial change in hepatocyte morphology and this is reflected with more cuboidal cells, distinctive hepatocyte borders (between surrounding fibroblasts and hepatocyte islands), and extensive bile canaliculi. This was confirmed with hepatocyte transporter specific dye export, where the fluorescent dye accumulated in the canaliculi between hepatocytes. The hepatocyte colonies in MPCCs cultured in the physiologic medium are sustained for an unprecedented 10 weeks *in vitro*. Over the last 2 weeks of culture the island geometry begins to morph into random shapes, rather than the initial circles they were patterned in, while the loss of cells seems to be much slower than colonies in bovine serum.

One major benefit of the MPCC is that it greatly retains the ability of hepatocytes to respond to insulin(28). Unfortunately, insulin signaling studies must be carried out within the first 2 weeks of culture or else hepatocytes lose the ability to respond to insulin, which is likely due bovine serum factors, such as fetuins, and overstimulation with excessive amounts of insulin in traditional medium (15,23,29). Accordingly, hepatocytes in physiologic medium, which has low levels of insulin, greatly retained the ability to respond to insulin even after 4 weeks *in vitro*, while cultures in the traditional medium were completely insulin resistant by this time. Another possibility for the retained lifetime of hepatocytes in physiologic medium is that bovine serum has components, such as fetuins, which may cause the decreased insulin signaling (insulin resistance), which could lead to premature cell death since insulin signaling is necessary for cell survival (20,30,31). Along with this theory, hepatocyte insulin resistance occurred at a much higher rate in hepatocytes cultured with bovine serum, compared to cultures in human serum.

Additionally, even cultures in bovine serum with low insulin, which have decreased hepatic functions, also developed insulin resistance at a faster rate than cultures in human serum. This has major implications for diabetes and insulin signaling research since MPCCs, or possibly other liver cell culture platforms, could be maintained in the physiologic medium while also supplementing various factors that are implicated in insulin resistance development to ultimately identify mechanisms behind disease progression in a human-relevant system (8).

Lastly, the most widely used application of the MPCC platform is drug toxicity screening and we found that physiologic medium did not prevent the platform from correctly identifying potential hepatotoxins and drug-drug interactions (17). Since hepatocyte functions are sustained for extended periods of time in this physiologic medium, we would expect to also obtain highly sensitive drug screening results after prolonged periods of culture. This will be especially important for liver disease modeling applications where disease development takes extended periods of time to develop, such as non-alcoholic steatohepatitis (NASH), and fibrosis (32).

This medium formulation should also aid regenerative medicine efforts for multiple reasons. The most common methods of engineering liver tissue constructs to potentially replace failing livers is to fabricate and stabilize the tissue *in vitro*, and then implant the construct (33). This optimized medium should greatly enhance the stabilization of liver cells prior to implantation and also prevent them from developing disease phenotypes prior to implantation. Additionally, for the FDA to approve implantable engineered tissue constructs in the future, these tissues will need to be created using good manufacturing practices (GMP), which prevents the use of xeno-based factors(34). Our work provides a substantial advance for hepatocyte culturing while considering this aspect.

Although we have identified the critical benefits of this optimized medium, it is still unclear what soluble factors in human serum-mediate this effect. Some clear differences between human and bovine serum are the ratios of high-density lipoprotein to low density lipoprotein (HDL:LDL), as well as the amounts and species of fatty acids(35). Lipids and cholesterol have numerous effects on hepatocyte metabolism and survival, which might explain the benefits of the human serum. Another clear difference is the bile acid pool, which seems to be species specific (27). Bile acids have pleiotropic effects on hepatocytes, of which binding to nuclear receptors being a major function and this has been clearly shown to affect hepatocyte pathways and aid in maintaining differentiation of hepatocytes (36,37). Accordingly, we are currently assessing the effects of supplementing these components into hepatocyte culture medium on hepatocyte functions and longevity.

For all cell culture applications, optimized medium formulations are critical for ensuring the conclusions of studies are made in the relevant setting. For instance, based on this work we now know that the results from our past work with the MPCC model could be more representative of an insulin resistant diabetic liver rather than that of a healthy liver. Therefore we hope that the ideas presented within this work will inspire researchers to appraise their cell culture medium more thoroughly and ask if certain components could lead to abnormal experimental outcomes. Additionally, we hope that the optimized medium we developed will find utility in multiple aspects of liver cell culture and possibly in other types of cell and tissue culture.

5.5 Supplemental Figures

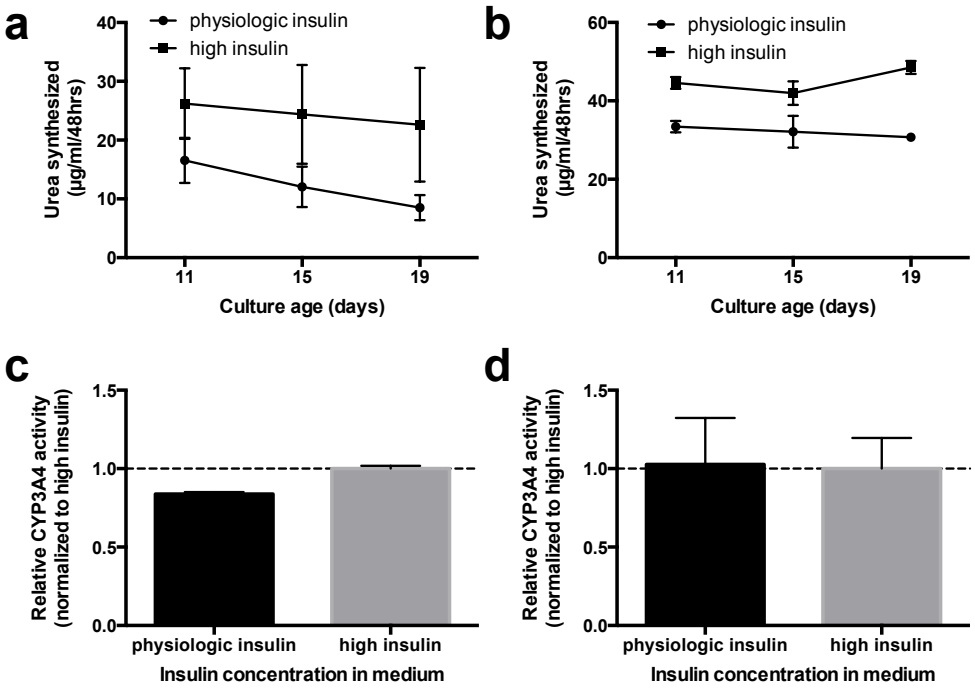

Supplemental Figure. 5.5.1. Optimizing culture medium to enable proper comparison of physiologically relevant medium to traditional medium. (a) Urea synthesis in MPCCs cultured in medium containing bovine serum and physiologic or the normal high insulin. (b) Urea synthesis in MPCCs cultured in medium containing human serum and physiologic or the normal high insulin. (c,d) 3 week relative CYP3A4 activity in MPCCs cultured in medium containing bovine serum (c) or human serum (d) and physiologic or the normal high insulin, normalized to the high insulin control. Error bars represent SD.

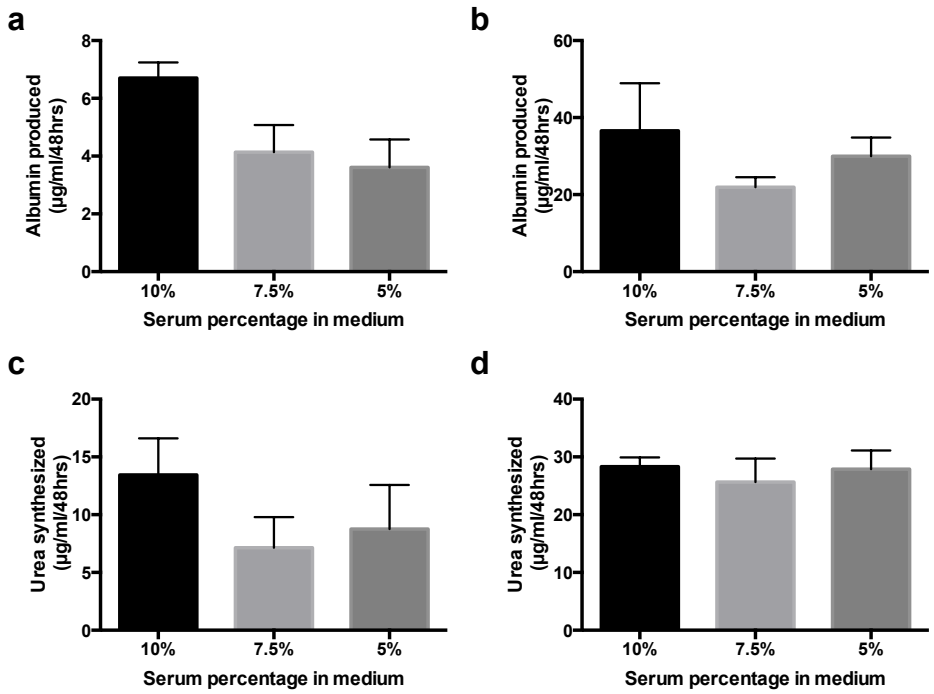

Supplemental Figure. 5.5.2. Optimization of serum concentration in cell culture medium. MPCCs were cultured in medium with different percentages of serum for 2 weeks and albumin and urea production were assessed. (a,b) Albumin production in cultures with bovine (a) and human (b) serum at different percentages. (c,d) Urea synthesis in cultures with bovine (a) and human (b) serum at different percentages. Error bars represent SD.

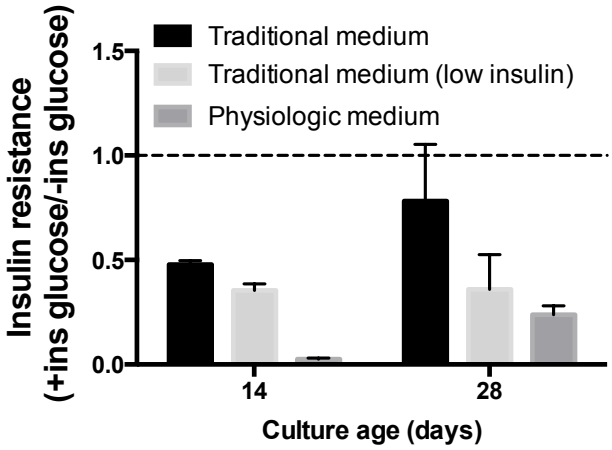

Supplemental Figure. 5.5.3 Insulin resistance over time with varying insulin concentration and serum type. MPCCs were cultured in the traditional medium, with the normal high insulin concentration or physiologic insulin concentration (low insulin), or physiologic medium and assessed for insulin resistance as described in Fig. 4. This figure shows the same data depicted in Fig. 4 for comparison. Error bars represent SD.

Supplemental Table. 5.5.1. Calculated TC_{50} values for cultures in the physiologic medium.

	Hepatotoxicity screening	
Compound tested	**Calculated TC_{50}**	**C_{max}**
Diclofenac	**282 µM**	**8.023 µM**
Troglitazone	**334 µM**	**6.387 µM**
Clozapine	**63 µM**	**0.951 µM**
Amiodarone	**41 µM**	**0.806 µM**
Piroxicam	**475 µM**	**5.135 µM**

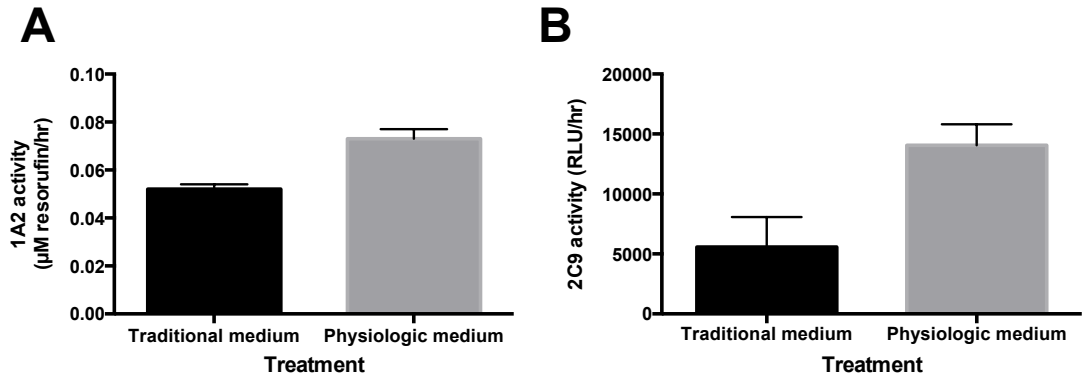

Supplemental Fig. 5.5.5. CYP1A2 and CYP2C9 activity in MPCCs cultured in the traditional and physiologic medium. MPCCs were cultured in traditional or physiologic medium for 3 weeks and assessed for CYP1A2 (A) and CYP2C9 (B) activity. Error bars represent SD.

References

1. DiMasi JA, Grabowski HG, Hansen RW. Innovation in the pharmaceutical industry: New estimates of R&D costs. J Health Econ. **47**, 20, 2016.

2. Cook D, Brown D, Alexander R, March R, Morgan P, Satterthwaite G, et al. Lessons learned from the fate of AstraZeneca's drug pipeline: a five-dimensional framework. Nat Rev Drug Discov. **13**(6), 419, 2014.

3. Bhatia SN, Ingber DE. Microfluidic organs-on-chips. Nat Biotechnol. **32**(8), 760, 2014.

4. Khetani SR, Berger DR, Ballinger KR, Davidson MD, Lin C, Ware BR. Microengineered liver tissues for drug testing. J Lab Autom. **20**(3), 216, 2015.

5. Bhatia SN, Underhill GH, Zaret KS, Fox IJ. Cell and tissue engineering for liver disease. Science Translational Medicine. **6**(245), 2452, 2014.

6. Onakpoya IJ, Heneghan CJ, Aronson JK. Worldwide withdrawal of medicinal products because of adverse drug reactions: a systematic review and analysis. Critical Reviews in Toxicology. **46**(6), 477, 2016.

7. Olson H, Betton G, Robinson D, Thomas K, Monro A, Kolaja G, et al. Concordance of the toxicity of pharmaceuticals in humans and in animals. Regul. Toxicol. Pharmacol. **32**(1), 56, 2000.

8. Hebbard L, George J. Animal models of nonalcoholic fatty liver disease. Nat Rev Gastroenterol Hepatol. **8**(1), 34, 2011.

9. Gómez-Lechón MJ, Tolosa L, Conde I, Donato MT. Competency of different cell models to predict human hepatotoxic drugs. Expert Opin Drug Metab Toxicol. **10**(11), 1553, 2014.

10. Godoy P, Hewitt NJ, Albrecht U, Andersen ME, Ansari N, Bhattacharya S, et al. Recent advances in 2D and 3D in vitro systems using primary hepatocytes, alternative hepatocyte sources and non-parenchymal liver cells and their use in investigating mechanisms of hepatotoxicity, cell signaling and ADME. Arch Toxicol. **87**(8), 1315, 2013.

11. Alison MR, Islam S, Lim S. Stem cells in liver regeneration, fibrosis and cancer: the good, the bad and the ugly. J. Pathol. **217**(2), 282, 2009.

12. Bell CC, Hendriks DFG, Moro SML, Ellis E, Walsh J, Renblom A, et al. Characterization of primary human hepatocyte spheroids as a model system for drug-induced liver injury, liver function and disease. Sci. Rep. **6**, 25187, 2016.

13. Selvaggi TA, Walker RE, Fleisher TA. Development of antibodies to fetal calf serum with arthus-like reactions in human immunodeficiency virus-infected patients given syngeneic

lymphocyte infusions. Blood. **89**(3), 776, 1997.

14. Ghani AC, Donnelly CA, Ferguson NM, Anderson RM. The transmission dynamics of BSE and vCJD. C. R. Biol. **325**(1), 37, 2002.

15. Davidson MD, Ballinger KR, Khetani SR. Long-term exposure to abnormal glucose levels alters drug metabolism pathways and insulin sensitivity in primary human hepatocytes. Sci. Rep. **6**, 28178, 2016.

16. Godoy P, Widera A, Schmidt-Heck W, Campos G, Meyer C, Cadenas C, et al. Gene network activity in cultivated primary hepatocytes is highly similar to diseased mammalian liver tissue. Arch Toxicol. 1, 2016.

17. Khetani SR, Bhatia SN. Microscale culture of human liver cells for drug development. Nat Biotechnol. **26**(1), 120, 2007.

18. Bhatia SN, Balis UJ, Yarmush ML, Toner M. Effect of cell–cell interactions in preservation of cellular phenotype: cocultivation of hepatocytes and nonparenchymal cells. FASEB J. 1999.

19. Bhatia SN, Balis UJ, Yarmush ML, Toner M. Effect of cell-cell interactions in preservation of cellular phenotype: cocultivation of hepatocytes and nonparenchymal cells. FASEB J. **13**(14), 1883, 1999.

20. Mathews ST, Srinivas PR, Leon MA, Grunberger G. Bovine fetuin is an inhibitor of insulin receptor tyrosine kinase. Life Sci. **61**(16), 1583, 1997.

21. Li Q, Zhang Y, Pluchon P, Robens J, Herr K, Mercade M, et al. Extracellular matrix scaffolding guides lumen elongation by inducing anisotropic intercellular mechanical tension. Nat. Cell Biol. **18**(3), 311, 2016.

22. Samuel VT, Shulman GI. Mechanisms for Insulin Resistance: Common Threads and Missing Links. Cell. **148**(5), 852, 2012.

23. Cook JR, Langlet F, Kido Y, Accili D. Pathogenesis of selective insulin resistance in isolated hepatocytes. Journal of Biological Chemistry. **290**(22), 13972, 2015.

24. Xu JJ, Henstock PV, Dunn MC, Smith AR, Chabot JR, de Graaf D. Cellular imaging predictions of clinical drug-induced liver injury. Toxicological Sciences. **105**(1), 97, 2008.

25. Khetani SR, Kanchagar C, Ukairo O, Krzyzewski S, Moore A, Shi J, et al. Use of Micropatterned Cocultures to Detect Compounds That Cause Drug-Induced Liver Injury in Humans. Toxicological Sciences. **132**(1), 107, 2013.

26. Silva JM, Day SH, Nicoll-Griffith DA. Induction of cytochrome-P450 in cryopreserved rat and human hepatocytes. Chemico-Biological Interactions. **121**(1), 49, 1999.

27. de Aguiar Vallim TQ, Tarling EJ, Edwards PA. Pleiotropic Roles of Bile Acids in

Metabolism. Cell Metabolism. Elsevier Inc; **17**(5), 657, 2013.

28. Davidson MD, Lehrer M, Khetani SR. Hormone and Drug-Mediated Modulation of Glucose Metabolism in a Microscale Model of the Human Liver. Tissue Engineering Part C: Methods. **21**(7), 716, 2015.

29. Samuel VT, Shulman GI. The pathogenesis of insulin resistance: integrating signaling pathways and substrate flux. Journal of clinical Investigation. **126**(1), 12, 2016.

30. Meex RC, Hoy AJ, Morris A, Brown RD, Lo JCY, Burke M, et al. Fetuin B Is a Secreted Hepatocyte Factor Linking Steatosis to Impaired Glucose Metabolism. Cell Metabolism. **22**(6), 1078, 2015.

31. Brunet A, Bonni A, Zigmond MJ, Lin MZ, Juo P, Hu LS, et al. Akt promotes cell survival by phosphorylating and inhibiting a Forkhead transcription factor. Cell. **96**(6), 857, 1999.

32. Wree A, Broderick L, Canbay A, Hoffman HM, Feldstein AE. From NAFLD to NASH to cirrhosis-new insights into disease mechanisms. Nature Publishing Group. **10**(11), 627, 2013.

33. Paschos NK, Brown WE, Eswaramoorthy R, Hu JC, Athanasiou KA. Advances in tissue engineering through stem cell-based co-culture. J Tissue Eng Regen Med. **9**(5), 488, 2015.

34. Lee MH, Arcidiacono JA, Bilek AM, Wille JJ, Hamill CA, Wonnacott KM, et al. Considerations for Tissue-Engineered and Regenerative Medicine Product Development Prior to Clinical Trials in the United States. Tissue Engineering Part B: Reviews. **16**(1), 41, 2010.

35. Haylett AK, Moore JV. Comparative analysis of foetal calf and human low density lipoprotein: relevance for pharmacodynamics of photosensitizers. J. Photochem. Photobiol. B, Biol. **66**(3), 171, 2002.

36. Sawitza I, Kordes C, Götze S, Herebian D, Häussinger D. Bile acids induce hepatic differentiation of mesenchymal stem cells. Sci. Rep. **5**, 13320, 2015.

37. Halilbasic E, Claudel T, Trauner M. Bile acid transporters and regulatory nuclear receptors in the liver and beyond. Journal of Hepatology. **58**(1), 155, 2013.

Chapter 6

Fatty acids can be used to model steatosis and insulin resistance in vitro using MPCCs[5]

Summary:

The previous chapters helped to clearly establish the benefits and limitations of the MPCC platform specifically for NAFLD-related studies. The advancements make it possible to now start developing disease models that recapitulate certain aspects of NAFLD. The major cause for lipid accumulation in NAFLD and diabetic patient livers is excessive amounts of fatty acids in the blood released from fat tissue. The most common of which is the triacylglycerol molecule, which is a high energy compound that is stored in the lipid droplet organelle of hepatocytes. Ectopic lipid accumulation within the liver has been highly correlated with insulin-resistant glucose output (ie. fasting hyperglycemia) for many years, although it is still unclear how lipid accumulation contributes to insulin-resistant glucose output from the liver. Many theories have been proposed, although these are mainly developed using animal model systems and in vivo studies, which cannot directly show how lipids contribute to hepatocyte glucose output due to confounding factors from other tissues. Therefore here we used or modified MPCC system to address how fatty acids might contribute to insulin-resistant glucose output over different times scales. Initially, we were unsure of how toxic fatty acid treatments may be to MPCCs, so we extensively studied their basic functions prior to making any conclusions about insulin-resistant glucose output. Eventually, we addressed how intracellular fatty acid pathways might contribute to insulin resistance.

[5]A manuscript similar to the work described in this chapter is in preparation and will be submitted for publication shortly.

6.1 Introduction

The liver dynamically regulates blood glucose levels to maintain nutrient homeostasis throughout the body. During times of fasting, when the insulin to glucagon ratios is low, the liver produces glucose for the body and inhibits the storage of fatty acids. Conversely, after feeding, insulin and nutrient (fatty acids and glucose) levels rise, which is followed by a reduction in liver glucose production and the storage of excess nutrients. In the fed state, insulin stimulates lipid production and storage, while inhibiting glucose production pathways (1). In type II diabetic (T2D) patients, this homeostatic function of the liver is lost, and in the face of excess nutrients, it continues to produce glucose, which leads to chronic hyperglycemia (2). This abnormal production of glucose is the hallmark feature of insulin resistance (IR) and has long been correlated with hepatic fat accumulation (3). Within the last ~20 years there have been extensive theories proposed on the potential cellular mechanisms for insulin resistance within the liver, but a unified theory still remains to be described (4,5).

The canonical insulin signaling pathway in the liver is mediated by the insulin receptor, which carries out its intracellular functions by activating the downstream kinase AKT/protein kinase B to modulate lipid and glucose metabolism (6). Activated AKT then stimulates the production and storage of lipids partly through activating mechanistic target of rapamycin (mTorc1) (7,8). Conversely, forkhead box protein O1 (FOXO1), a transcription factor that increases lipolysis gene expression such adipose triglyceride lipase (ATGL), is displaced from the nucleus after AKT phosphorylation, which limits lipid breakdown (9). The more characterized function of FOXO1 is to increase glucose output from the liver during times of fasting by increasing the expression of gluconeogenic genes and promoting the release of fatty

acids for oxidation (9-11). This process is also inhibited by insulin via AKT phosphorylation (12).

One controversial hypothesis has been the idea of "selective insulin resistance" in the liver, which suggests that the insulin-stimulated lipogenesis pathway is intact while the insulin pathway to inhibit glucose production is somehow faulty (13). Recent studies that selectively remove the canonical insulin signaling pathway in the liver have shown that the liver can still regulate blood glucose levels by responding to extrahepatic factors (14-17). Importantly, Vatner et al. showed that lipid re-esterification in the liver is regulated by substrate, fatty acid, availability and not insulin signaling, which undermines the selective IR theory by suggesting that the liver could be completely IR and still accumulate lipids (18). Conversely, Titchenell et al. recently showed that the insulin signaling pathway is required to stimulate lipid production in the liver, which also throws a wrench in the selective IR hypothesis by suggesting that the insulin signaling pathway is intact in the diabetic liver and mediates the increased de novo lipogenesis observed in patients with diabetes (19). These highly important studies are laying the groundwork for what will likely be the next generation of targets for diabetic drug therapy development.

Many of the hypotheses derived from these studies focus on how the hepatocyte responds to various nutritional and hormonal stimuli, yet researchers still struggle to study these *in vivo* phenomena in an *in vitro* setting with isolated hepatocytes due to their limited lifetime outside the body 1-3 days, and lack of response to hormonal stimuli (20,21). Furthermore, most of these studies are carried out in mouse or rat models, which do not accurately recapitulate the progression of NAFLD or insulin resistance (22). Additionally, there are critical species-specific differences between rodents and humans in drug metabolism enzymes, which will limit the

translation of therapies developed using these model systems (23). Primary human hepatocytes are the gold standard for the pharmaceutical industry since they retain all of the enzymes necessary for human drug metabolism (24). Therefore to properly model human diseases such as NAFLD or IR, and develop therapies for these ailments, we need human-relevant systems that can retain primary human hepatocytes outside of the body for extended periods.

Fortunately, methods have been developed to maintain the hepatocyte phenotype *in vitro* by co-culturing these cells with non-parenchymal cells (25). Khetani and Bhatia have expanded upon this idea by using microfabrication techniques to carefully pattern hepatocytes into optimized circular domains and then surround them with supportive fibroblasts, which enables long-term hepatocyte cultures with consistent cellular outputs (26). We have modified this micropatterned co-culture system so that it retains hepatocyte insulin sensitivity as well as healthy glucose and lipid metabolism for at least 2 weeks *in vitro* (27). Now we can finally use this system to address some of the lingering and controversial hypotheses in the diabetes research field that has been hampered by the lack of a culturing system that retains hepatocyte functions outside the body.

Here we used the modified form of the MPCC to address: 1. If hepatocytes can be treated with fatty acids to induce a state of steatosis without lipotoxicity, 2. If insulin-resistant glucose output can be induced in hepatocytes after acute or prolonged fatty acid treatment, 3. Which pathways induced by fatty acid treatment can bypass insulin signaling. We believe that our isolated approach will help clarify current misunderstandings surrounding selective IR, provide a human-relevant perspective on IR and help develop a unifying hypothesis on what drives IR glucose production in the liver. The insulin signaling pathway has been clearly shown to be altered in the diabetic liver, however, the biochemical implications of this inhibition might be

irrelevant for controlling glucose production (18). Here we show that lipid-filled hepatocytes can retain the insulin signaling pathway while displaying insulin-resistant glucose output.

6. 2 Methods

6.2.1 Cell culture and MPCC fabrication

Cell culture and MPCC fabrication were carried out as described in chapter 3. For fatty acid treatments, cultures were stabilized for 4-6 days and then treated with the various fatty acids and mixtures every other day for up to 10 days. Importantly, cultures were carried out in 5 mM glucose maintenance medium that did not have supplemented linoleic acid that is normally found in the ITS(+) supplement, specifically the (+) stands for linoleic acid and therefore we added ITS in place of this supplement.

6.2.2 Fatty acid preparation and treatments

Single and mixtures of fatty acids were complexed to BSA to increase their solubility in the aqueous medium as well as facilitate their uptake by hepatocytes. Specifically, concentrated stocks of palmitic (PA), stearic (SA), oleic (OA) and linoleic acid (LA) (all purchased from NU-CHEP PREP INC Elysian, MN) were prepared in molecular grade ethanol (Thermo Scientific). To increase the solubility of saturated fatty acids (PA and SA), fatty acid-ethanol solutions were incubated in a 70 °C water bath for 5 minutes and then 1 M NaOH was quickly added to achieve a final concentration of 0. 02 M NaOH. After adding NaOH, these solutions were incubated for

another 5 minutes at 70 °C. Concurrently, a solution of 10% w/v fatty acid-free BSA (Sigma Aldrich, St. Louis, MI), diluted in glucose-free DMEM, containing a stir bar, was warmed in a 45 °C water bath with stirring. After NaOH precipitate went into solution in the saturated fatty acid ethanol mixtures (~5 minutes), fatty acids were added to the pre-warmed BSA solution dropwise to achieve a final concentration of 3.03 mM fatty acid and 1.515 mM BSA, to achieve a 2:1 fatty acid to albumin ratio. For OA and LA, NaOH addition was not necessary and these fatty acids could be directly added to the BSA solution. For BSA controls, pure ethanol was added to BSA at the same concentration as fatty acids. These solutions were stirred overnight in the 45°C water bath sterile filtered, aliquoted and stored at -20°C.

Alternatively, two different fatty acid mixtures, 2:1 and 7:1 fatty acid to albumin mixtures containing equal molar concentrations of all four fatty acids previously used, were created. To make these mixtures, saturated fatty acids were added firsts, as previously described, and then unsaturated fatty acids were added. For the 2:1 solution, each fatty acid was added at a concentration of 0.758 mM and for the 7:1 solution each fatty acid was added at a concentration of 2.65 mM.

For fatty acid treatments, each single fatty acid solution or the 2:1 fatty acid mixture was added to cell culture medium at a concentration of 260 μM. The 7:1 fatty acid mixture was added to cell culture medium at a concentration of 910 μM. The BSA concentration was maintained at the same concentration, 130 μM, for all treatments. One important difference between the 2:1 and 7:1 treatment was that significantly more ethanol was added to the 7:1 mixture and BSA control since more fatty acid-ethanol solution was needed to make these mixtures.

6.2.3 Biochemical and enzymatic assays

All biochemical and enzyme activity assays were carried out as described in chapter 2 and 3. In-cell ELISAs for the phosphorylation of AKT, a downstream insulin signaling protein, were carried out on fixed MPCC cultures stimulated with insulin after 1 hour according to manufacturer protocols (R&D systems). Briefly, fixed cultures were first incubated in a 1% hydrogen peroxide solution in PBS for 20 minutes, washed twice with PBS and then incubated again with the peroxide solution to remove any endogenous peroxides. Fixed culture antigens were then blocked with blocking buffer (R&D systems) for 1 hour and then incubated with primary antibodies for p-AKT and total AKT (t-AKT) overnight in blocking buffer. Some cultures were incubated in only blocking buffer as a no primary control. Cultures were then washed 3 times with wash buffer (R&D systems) and then incubated with secondary antibodies containing alkaline phosphatase (AP) or horseradish peroxidase (HRP) specific for the animal the primary antibodies were raised in (R&D systems) were incubated with fixed cells for 2 hours at room temperature. Cultures were then washed 3 times with wash buffer and first incubated with a fluorometric HRP specific substrate, to detect p-AKT, for 1 hour. Next a fluorometric AP specific substrate was added to detect the level of t-AKT. The fluorescence of each of these substrates was detected using a fluorometric plate reader and the data was presented as the level of p-AKT fluorescence divided by the t-AKT fluorescence.

6.2.4 Live cell imaging, staining, and immunocytochemistry

All live cell imaging and staining were carried out as described in chapter 3 and 4. Importantly, here we also assessed mitochondrial membrane potential (MMP) using the fluorescent dye tetramethylrhodamine methyl ester (TMRM). This dye is added to serum-free cell culture medium at a concentration of 200 nM and then incubated with cultures for 15 minutes. Specifically, cultures are washed once in serum free medium, incubated in TMRM containing medium, and then washed 3 times and imaged on the EVOS FL microscope using the RFP light cube. Immunocytochemistry for FOXO1 was carried out on fixed cultured as described in chapter 3.

6.2.5 Glucose production and insulin resistance/response assays

Here we developed a new assay to assess insulin resistance and insulin responsiveness. Specifically, cultures were incubated 18-24 hours a minimal serum-free medium containing 5 mM glucose, 1% penicillin/streptomycin and 1.5% HEPES buffer and glucose-free DMEM containing 4 mM L-glutamine to essentially starve the cultures and prevent any insulin signaling that may occur with hormones present in serum. To assess insulin responsive phosphorylation of AKT (p-AKT, S473) and FOXO1 nuclear displacement we treated cultures with gluconeogenic medium (described in chapter 2 and 3) for 1 hour and then fixed the cultures with 4% PFA for 15 minutes at room temperature. To detect insulin resistance, cultures were incubated for 1 or 6 hours in gluconeogenic medium and the level of glucose production under insulin stimulation was divided by the basal level of glucose production.

6.2.6 Gene expression

Gene expression and analysis was carried out as described in chapter 3. Importantly, in these studies, basal gene expression after fatty acid treatment and insulin-responsive gene expression were assessed. To assess insulin-responsive gene expression, cultures were treated with the same protocol used to assess insulin-resistant glucose production, except at the terminal time point RNA was isolated and assessed via qPCR. The data are presented as the relative expression of each gene normalized to the same treatment's non-insulin stimulated expression level, rather than across different treatments as was carried out for basal levels of expression.

6.2.7 Inhibitor treatments

To inhibit ATGL and CPT1, we treated cultures with increasing doses of atglistatin and etomoxir. Specifically, atglistatin was first diluted in DMSO and was then diluted into gluconeogenic medium containing insulin and serially diluted to achieve the desired concentrations. A precipitate formed upon atglistatin addition to aqueous medium so this medium was incubated in a 37 degrees C water bath for 5 minutes, which solubilized the precipitate. The DMSO concentration in these studies was maintained at 0.1% w/v DMSO. For etomoxir treatments, etomoxir was first diluted in DMOS and then added to gluconeogenic medium containing insulin. The DMSO concentration used was 1.2% DMSO.

6.2.8 Statistical analyses

Each experiment was carried out in 2 or more wells for each condition. Two to three cryopreserved PHH donors were used to confirm observed trends. Microsoft Excel and GraphPad Prism 5.0 (La Jolla, CA) were used for data analysis and plotting data. Error bars on average values represent standard deviation (SD) across wells. Statistical significance of the data was determined using the average and SD across wells in representative experiments using the Student's *t*-test or one-way ANOVA with Dunnett's multiple comparison tests for post hoc analysis.

6.3 Results

6.3.1 Fatty acids are not toxic to primary human hepatocytes in MPCCs

Hepatocellular toxicity can be assessed through various metrics (28), such as mitochondrial membrane potential (MMP) and adenosine triphosphate (ATP), although these outputs can be altered with different nutritional inputs, such as fatty acids, which may artificially raise the amount of a substrate such as ATP. Additionally, in the micropatternd co-culture (MPCC) system, many of these outputs can be confounded by changes in the surrounding fibroblast population while the hepatocyte population is unchanged. Accordingly, to assess the potential toxicity of fatty acid treatments we first assessed the hepatocyte-specific outputs albumin production and urea synthesis, which have been shown to be sensitive markers of liver toxicity (29). We first stabilized hepatocytes for 4-6 days in maintenance medium, and then

began treating cultures with single fatty acids (palmitic (PA), stearic (SA), oleic (OA) and linoleic (LA) acid at a 2:1 fatty acid to albumin ratio and a concentration of ~260 μM) or a mixture of fatty acids (with equal molar contribution of PA, SA, OA, SA at a 2:1 and 7:1 fatty acid to albumin ratio and a total concentration of 260 μM or 910 μM, respectively) at a low, 2:1, and high, 7:1, fatty acid to albumin ratios to mimic physiologic and obese/diabetic ratios (30).

Past experience with known liver toxins has suggested that treatments which cause a decrease in albumin or urea levels to values lower than 50% of our vehicle control, BSA in this case, should be considered potentially toxic, and we found that none of our fatty acid treatments reduced these hepatocyte-specific outputs below 50% of the control over 10 days of treatment (Figure 1). To further confirm this, we carried out propidium iodide (data not shown), tetramethylrhodamine methyl ester (TMRM) and 5(6)-carboxy-2',7'-dichlorofluorescein-diacetate (CDCFDA) staining and confirmed a lack of cell death, retained MMP and bile canaliculi formation in hepatocyte islands after 8 days of treatment with representative fatty acid treatments (Supplemental Fig.1). These results suggest that fatty acid treatments to do not significantly altered the viability of hepatocytes in MPCCs over extended periods of treatment.

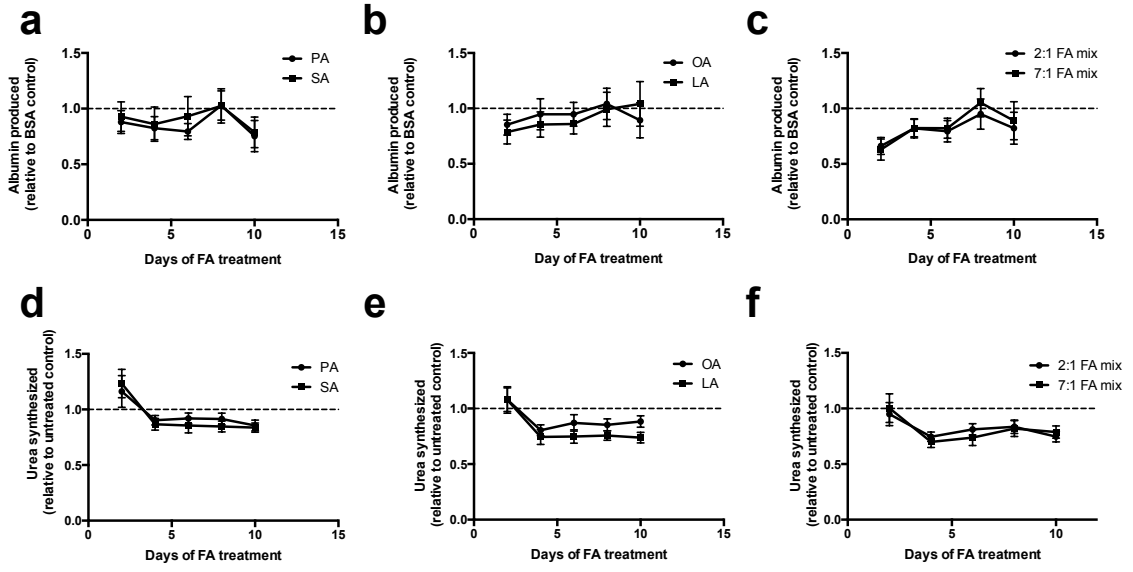

Figure 6.1. Fatty acid treatments are not toxic to hepatocytes in MPCCs. MPCCs were stabilized for 5 days and then treated with single saturated fatty acids (a,d), unsaturated fatty acids (b,e) and mixtures of fatty acids (c,f) for 10 days (n= 3-4). Albumin production (top row) and urea synthesis (bottom row) were assessed over this treatment period and normalized to the respective BSA-treated control. Error bars represent Sd. PA, SA, OA, and LA represent palmitic, stearic, oleic, linoleic acid. 2:1 and 7:1 FA mix represent fatty acid mixtures containing all four fatty acids at 2:1 or 7:1 fatty acid: BSA ratios.

NAFLD is associated with changes in drug metabolism enzymes, which could have implications for drug development efforts in this space. This encouraged us to address how 10 days of fatty acid treatment may alter MPCC CYP3A4 and CYP2A6 activity using the enzyme-specific substrates luciferin-IPA and coumarin, respectively. We found that saturated fatty acids significantly increased CYP3A4 activity, 1.3 and 1.16 fold for PA and SA respectively, while concomitantly decreasing CYP2A6 activity, to 60% and 78% of the control levels for PA and SA, respectively (Supplemental Fig. 2). Unsaturated fatty acids had no significant effect on CYP3A4 activity, while they significantly decreased CYP2A6 activity to ~80% of the BSA control. Importantly, when we incubated cultures with mixtures of fatty acids, either 2:1 or 7:1, we found that this normalized CYP3A4 and CYP2A6 activity to control levels. These results suggest that single fatty acids can alter drug metabolism enzyme activity, while mixtures of fatty acids have no considerable effect on drug enzyme activity.

6.3.2 Fatty acids can acutely push glucose production, but this glucose production is sensitive to insulin inhibition

Since fatty acid treatments can be carried out without causing hepatocyte toxicity or cell death, we first addressed the effects of acute fatty acid treatment on hepatocyte glucose output with and without insulin stimulation. Glucose production is highly retained in hepatocytes cultured in MPCCs and we have recently developed culture medium that further retains

hepatocyte insulin sensitivity (27). We found that acute treatment with a fatty acid mixture (250 μM with a 2:1 fatty acid to albumin ratio) during glucose production significantly reduced glucose output from MPCCs to ~60% of the BSA-treated control, while adding substrates for gluconeogenesis, lactate, and pyruvate, along with fatty acids increased glucose production 1.36 fold over the BSA-treated control, which had added substrates (Fig. 2). We can also measure insulin resistance (IR) in MPCCs by stimulating them with insulin while they are making glucose. We then quantify the amount of glucose in supernatants and divide the insulin-stimulated glucose output by the basal glucose output to give us a number between 0 and 1, where 0 corresponds to a completely insulin sensitive culture while 1 corresponds to a completely insulin resistant culture (Fig. 2).

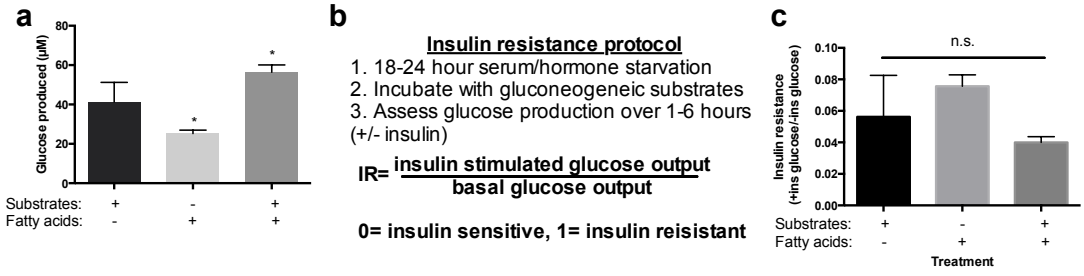

Figure 6.2. Acute fatty acid treatments stimulate glucose production that is sensitive to insulin repression. MPCCs were stabilized for 4 days and then starved overnight in serum-free medium prior to assessing glucose output and insulin resistance. (a) Glucose output with and without gluconeogeneic substrates in the presence or absence of 2:1 exogenous fatty acid mixture (250 μM) (n=3-4). (b) Insulin resistance assessment protocol and calculation. (c) Insulin resistance with and without gluconeogeneic substrates in the presence or absence of 2:1 exogenous fatty acid mixture (250 μM) (n=3-4). Error bars represent SD. * represents $p \leq 0.05$ as assessed by one-way ANOVA.

Importantly, when the same treatments were carried out in the presence of insulin (10 nM), there was no significant difference in glucose output and therefore insulin resistance. These results suggest that fatty acids can acutely increase glucose production in hepatocytes, while this fatty acid-induced glucose production is sensitive to insulin inhibition.

6.3.3 Prolonged fatty acid treatment induces steatosis and insulin-resistant glucose production in hepatocytes

Since fatty acid re-esterification is the major source of lipid accumulation in the liver during NAFLD, we assessed how prolonged fatty acid treatment contributes to lipid accumulation and insulin resistance in MPCCs. All single fatty acid treatments (PA, SA, OA, and LA) led to noticeably more neutral lipid accumulation, assessed via Nile red staining, and significantly more insulin resistance than BSA treated cultures (Supplemental Fig. 3). Importantly, the 7:1 fatty acid mixture led to extensive lipid accumulation and significantly higher levels of Nile red staining, ~2.3 fold higher fluorescence than the BSA control (Fig. 3). We also observed significantly higher insulin resistance in the fatty acid treated cultures over the BSA treated cultures after 2, ~1.8 fold, and 4 days, ~1.6 fold, of treatment. This difference in IR was still apparent after 8 days of fatty acid treatment, ~1.3 fold higher, although not significantly higher than the BSA control.

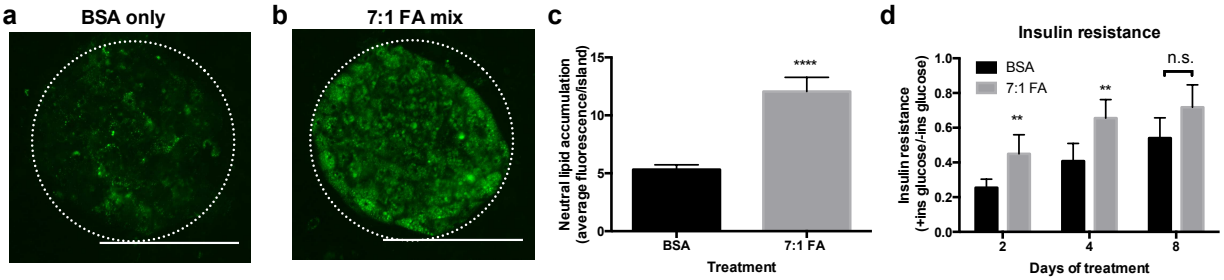

Figure 6.3. Prolonged fatty acid treatments cause steatosis and insulin-resistant glucose production. MPCCs were stabilized for 4 days and then treated with the 7:1 fatty acid mixture or the associated BSA control. (a,b) Nile red staining (green) of MPCCs treated with BSA or the 7:1 fatty acid mixture for 10 days. Circle highlights island and scale bar represents 400 μM. (c) Average Nile red fluorescence/hepatocyte island at the same time point as (a,b) (n=10 hepatocyte islands). (d) Insulin resistance after 2, 4 and 8 days of fatty acid treatment (n=3-4). Error bars represent SD. ** represents $p \leq 0.01$ as assessed by t-test between BSA and fatty acid insulin resistance at the respective time point.

Since glucose levels must rapidly adjust after ingesting a meal to maintain normoglycemia, we assessed glucose production under insulin stimulation after 1 hour. Cultures responded to insulin stimulation after 1 hour and cultures treated with 7:1 fatty acid mixture had a blunted response to insulin compared to BSA-treated cultures (Supplemental Fig. 4). Importantly, we also found that after 1 hour of insulin stimulation, MPCC protein kinase B/AKT phosphorylation (S473), was higher or the same in fatty acid treated cultures compared to BSA-treated cultures after 2 and 8 days of treatment, respectively (Supplemental Fig. 5). Overall these studies suggest that fatty acid accumulation leads to insulin-resistant glucose output in human hepatocytes over different time scales and that this insulin-resistant glucose output does not correlate with an insulin resistant signaling pathway.

6.3.4 Fatty acids lead to the retention of FOXO1 in the nucleus after insulin stimulation and downstream gene expression

Due to the abnormal drug metabolism enzyme activity levels we observed with excessive levels of single fatty acids and the significant amount of steatosis and IR observed with fatty acid mixtures, we carried out the remaining studies with the 7:1 fatty acid mixtures. Since we observed significant insulin resistance after 2 days of fatty acid treatment, we assessed hepatocyte FOXO1 nuclear to cytoplasmic (N:C) ratios with and without 1 hour of 10 nM insulin stimulation in fatty acid and BSA treated cultures (Figure 4). FOXO1 N:C ratios in BSA-pretreated cultures were significantly decreased, ~20% reduction ($n > 350$ cells across 6 separate hepatocyte islands), after insulin stimulation, while fatty acid pretreated cultures N:C ratios only decreased by ~2% ($n > 350$ cells across 6 separate hepatocyte islands). Along with increased

nuclear FOXO1, we also found that the expression of phosphoenolpyruvate carboxykinase (*PCK1*) and *ATGL* was significantly increased in MPCCs, ~7.8 and ~10 fold, respectively, after a 2-day treatment with fatty acids and normalized to the BSA-treated control (Figure 4).

We also found that MPCC gluconeogenic gene expression (*PCK1* and glucose 6 phosphatase (*G6PC*)) was responsive to insulin stimulation, and that fatty acid treated MPCC *PCK1* expression was slightly repressed when compared to BSA treated cultures, but not significantly (Supplemental Fig. 6).

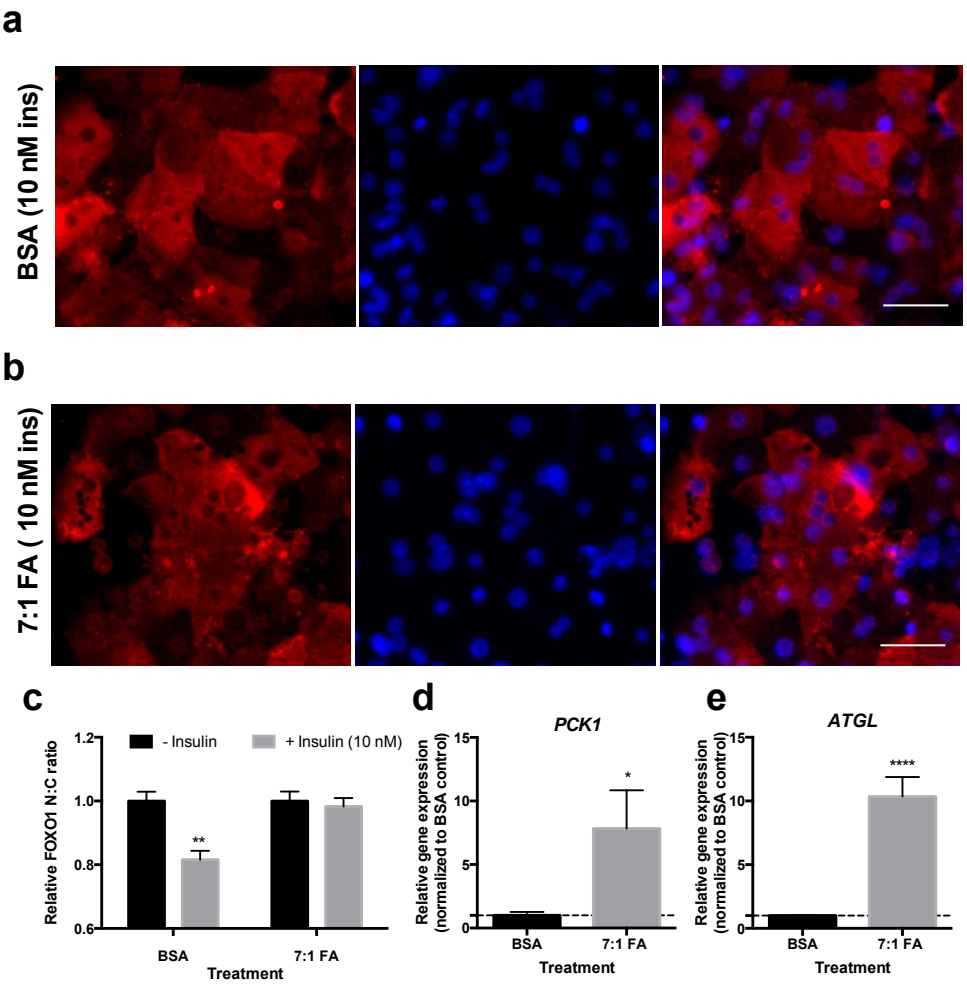

Figure 6.4. Fatty acid treatment leads to reduced FOXO1 insulin response and increased expression of FOXO1 regulated genes. (a,b) Representative FOXO1 (red, left), DAPI (blue, center) and merged channels (right) immunolabeling and staining after insulin (10 nM) stimulation in hepatocytes treated for 2 days with BSA (a) or the 7:1 fatty acid mixture (b). Scale

bar represents 50 μM. **(c)** Relative nuclear to cytoplasmic (N:C) ratios of FOXO1 fluorescence intensity after insulin stimulation in hepatocytes treated for 2 days with BSA or the 7:1 fatty acid mixture (n>300 individual hepatocytes). Basal phosphoenolpyruvate carboxykinase catalytic subunit (*PCK1*), and adipose triglyceride lipase (*ATGL*) gene expression in hepatocytes treated with BSA or the 7:1 fatty acid mixture after 2-day treatment, normalized to the BSA-treated control (n=3). Error bars represent SD. *,** and **** represent $p \leq 0.5$, ≤ 0.01 and ≤ 0.0001, respectively, assessed by a t-test between +/- insulin stimulation for (c) and a t-test between BSA and fatty acid treated cultures for (d,e).

Surprisingly, regardless of treatment, MPCC lipogenic gene expression (sterol regulatory-element binding protein 1 C (*SREBF1*), fatty acid synthase (*FASN*), and stearoyl-CoA desaturase-1 (*SCD1*)) was not responsive insulin stimulation (Supplemental Fig. 6). Last, we assessed *ATGL* expression and found that *ATGL* was significantly increased, ~1.5 fold, in fatty hepatocytes upon insulin stimulation over the non-insulin treated fatty hepatocyte control, while it was non-significantly repressed in BSA-treated cultures. These results suggest that fatty acid treatment activates FOXO1 and reduces the ability of insulin to translocate FOXO1, which likely accounts for the increased expression of FOXO1 responsive genes *ATGL* and *PCK1*.

6.3.5 ATGL and beta-oxidation drive insulin-resistant glucose production in steatotic hepatocytes

Since we observed increased *ATGL* expression after fatty acid treatment, we assessed how ATGL may affect insulin-resistant glucose production by inhibiting this enzyme with the specific ATGL inhibitor atglistatin (31). We found that increasing doses of atglistatin significantly rescued insulin-resistant glucose production in MPCCs (Fig. 6). Atglistatin treatment also reduced hepatocyte glucose output without insulin treatment (data not shown). Atglistatin did not cause overt toxicity, which was assessed by monitoring culture morphology during glucose production, and 2 days after treatment.

Once fatty acyl-CoAs are liberated from the lipid droplet by ATGL, they can either be re-esterified into glycerides or shuttled to the mitochondria for oxidation. To assess the contribution of fatty acid oxidation (FAO) to insulin-resistant glucose production, we treated cultures with the carnitine palmitoyl transferase 1 (CPT1) inhibitor, etomoxir, to effectively block fatty acid entry into the mitochondria. Similar to ATGL inhibition, we found that increasing doses of etomoxir significantly reduced insulin-resistant glucose output (Fig. 6). Etomoxir had no considerable effect on BSA treated culture glucose output, if anything it slightly increased insulin-stimulated glucose output (data not shown). Etomoxir did not cause overt toxicity, which was assessed by monitoring culture morphology during glucose production, and 2 days after treatment. These results suggest that ATGL activity and fatty acid oxidation significantly contribute to steatotic hepatocyte insulin-resistant glucose production.

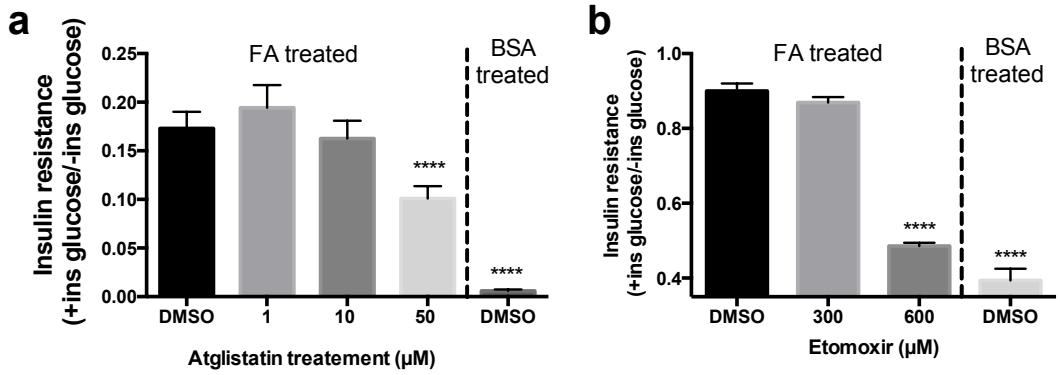

Figure 6.5. ATGL and fatty acid oxidation drive IR glucose output in steatotic hepatocytes. MPCCs were incubated with the 7:1 fatty acid mixture or BSA control for 2 days and then assessed for insulin resistance in the presence of increasing doses of atglistatin (n=4) (a) or etomoxir (n=3) (b) or the vehicle control, DMSO. Error bars represent SD. **** represents $p \leq 0.0001$ assessed via one-way ANOVA.

6.4 Discussion

With NAFLD on the rise and associated IR and type II diabetes (T2D), now is the time for engineers and biologists alike to work together to develop tools and therapies to help better understand the pathology that underlies these diseases and treat them, respectively. Unfortunately, the bioengineering community has put forth very few efforts to contribute to this field, which could potentially be due to the intimidating and heavy emphasis on signaling and metabolic pathways, which are traditionally molecular biologist specialties. Although there is a clear need for human-relevant models and ways to maintain functional and healthy liver cells outside the body. This is a great opportunity for tissue engineers to step in and contribute the vast knowledge we have on advanced cellular models. Here we developed a diseased liver cell culture model that mimics certain aspects of NAFLD and IR and can sustain this diseased state for at least 8 days *in vitro* using substrates, fatty acids, known to contribute to liver disease.

Using this disease model, we surveyed how fatty acids could potentially cause insulin-resistant glucose production in the liver. Surprisingly, we found that fatty acid treatments were not toxic to our primary human hepatocytes and that they could be treated multiple times over a period of 8 days without toxic effects. This is in sharp contrast to many primary hepatocyte experiments where abrupt apoptosis was seen (32,33). Most researchers have resorted to using cell lines for this type of work, but we clearly show here that MPCCs allow one to chronically treat hepatocytes with at least 4 major lipid species (palmitic (16:0), stearic (18:0), oleic (18:1) and linoleic (18:2) acid) at physiologically relevant concentrations (34,35).

Importantly, many in vivo studies with human samples and corresponding cell-based approaches have found that fatty acid treatments can alter drug metabolism enzymes, and we

confirmed these accounts (36-39). Although, we did find that treating MPCCs with mixtures of fatty acids, which more closely mimics the fatty acid lipid profile in the blood rather than an abnormal excess of one fatty acid, normalized drug metabolism enzyme activity back to the vehicle control levels, which suggests that fatty acids alone are likely not the major contributors to altered drug metabolism activity observed in NAFLD patients (40). We suspect that pro-inflammatory secretions, prominent in advanced NAFLD or non-alcoholic steatohepatitis (NASH), are likely the major contributors to altered drug metabolism, as they are known to alter hepatic drug metabolism and transporter activity (41). Supporting this we also found that fatty acid treatments did not disrupt bile canaliculi formation between hepatocytes, which is mediated by the localization and functional transport of the hepatic transporters multidrug resistance associated protein 2 and 3 (MRP2 and MRP3)(42).

We found that saturated and unsaturated fatty acids, either mixtures of or single treatments, led to significant lipid accumulation over 8 days of treatment and this was mirrored by increased insulin-resistant glucose production over BSA-treated controls. This insulin-resistant glucose production occurred in cultures that had intact insulin signaling pathways, as assessed by measuring the amount of phosphorylated AKT in fixed MPCCs stimulated with insulin, which suggests that a non-insulin sensitive pathway to produce glucose exists within hepatocytes.

Importantly, we showed that hepatocytes respond to insulin rapidly, within ~ 1 hour, with respect to their glucose output and over longer periods, ~ 6hrs, with respect to their gluconeogenic gene expression, *PCK1,* and *G6PC.* The liver rapidly adjusts to changes in nutrients and hormones after ingesting a meal, and we found that isolated hepatocytes in micropatterned co-cultures can respond to insulin acutely with respect to their glucose output. It

is important to note that some have speculated that cell-non-autonomous factors, such as adipose-derived fatty acids, acutely control glucose output from the liver (15,43). Accordingly, we were able to modulate glucose production in MPCCs with acute fatty acid treatments during glucose production assays via a substrate push mechanism, but this fatty acid-induced glucose production was not able to overcome insulin's inhibitory effect on glucose production. These studies suggest that fatty acids can increase glucose production in the liver through multiple pathways that are not interdependent, either excess delivery during the postprandial state and or from stored fatty acids within the liver itself.

The latter aspect of fatty acid-induced glucose production, accumulated hepatic lipid, has garnered great attention since it is strongly associated with IR, yet multiple studies have provided seemingly contradictory results on the mechanism of IR in fatty livers. Fabbrini et al. correlated the degree of steatosis with IR and others have found that reducing intrahepatic lipid accumulation, via dietary changes, can significantly enhance overall insulin sensitivity in patients (44,45). Other studies have shown that inhibiting lipolysis proteins and their co-activators, namely ATGL and comparative gene identification-58 (CGI-58), respectively, leads to increased steatosis, but retained insulin sensitivity and glucose tolerance (46-48), which suggests that regulating hepatic triacylglycerol (TAG) may be important for insulin to control hepatic glucose production. Importantly, FOXO1 regulates ATGL expression, and the overexpression of ATGL increases fatty acid oxidation (FAO), which may contribute to insulin-resistant glucose production (9,49). Here we show that fatty acid treatment alone caused increased ATGL expression and FOXO1 nuclear retention under insulin stimulation in human hepatocytes. Insulin represses *ATGL* expression in adipose tissue, yet here we found the opposite trend in fatty acid treated hepatocytes, where insulin-stimulated *ATGL* expression. Additionally,

we found that we could rescue insulin-resistant glucose output from hepatocytes by selectively inhibiting ATGL, with the small molecule atglistatin, or carnitine palmitoyltransferase I (CPTI), using etomoxir, which effectively blocks fatty acid release from hepatocyte lipid droplets and fatty acid entry into the mitochondria for oxidation, respectively (31,50). Overall these studies support a unified theory for NAFLD associated insulin-resistant glucose production, where stored fatty acids in hepatocytes are liberated by ATGL, even in the face of insulin signaling, which allows them to undergo FAO and activate glucose production through the generation of acetyl-CoA, and NADH, which allosterically activates pyruvate carboxylase and provides reducing equivalents for phosphoenolpyruvate carboxykinase (PEPCK) to carry out gluconeogenesis, respectively (51,52).

Surprisingly, lipogenic gene expression, *SREBF1*, *FASN*, and *SCD1*, in hepatocytes was not responsive to insulin stimulation in MPCCs, which may be due to a zonated phenotype that develops in hepatocytes when cultured in an incubator with atmospheric oxygen conditions. De novo lipogenesis is predominantly localized to the hypoxic perivenous zone 3 of the liver sinusoid (53). Supporting this, it has been shown that a hypoxic environment is needed for insulin stimulation of glucokinase expression in hepatocytes, and we also did not detect this transcript after insulin stimulation (54). Additionally, hepatocytes in MPCCs undergo robust gluconeogenesis, produce urea and albumin and store glycogen, all of which are thought to be part of the hyperoxic periportal zone 1 of the liver (55)

It is still unclear as to why fatty acids alone lead to FOXO1 nuclear retention. This is the first study with isolated primary human hepatocytes where insulin-stimulated FOXO1 nuclear displacement was assessed after prolonged treatment with fatty acids and steatosis establishment. We postulate that fatty acids may activate SIRT1 or its co-activator PGC1a, which would

deacetylate FOXO1 and enable its interaction with transcriptional promoters (56,57). Additional studies are needed to clarify why FOXO1 in hepatocytes seems to be less response to insulin stimulation in an environment with excess fatty acids. Another unexpected result was that insulin stimulation increased the expression of *ATGL* in fatty hepatocytes, whereas insulin is normally thought to inhibit the expression of *ATGL* (58). Since FOXO1 regulates the expression of *ATGL*, we believe this increased *ATGL* may be due to nutrient fluxes that occur upon insulin stimulation, such as increased glucose utilization, which further activates FOXO1 as we have previously seen that hyperglycemia can activate this transcription factor (27). Either way, if this occurs in vivo in fatty livers after ingesting a meal, when insulin levels rise, this could explain why NAFLD is highly correlated with insulin-resistant glucose output and predisposes patients to diabetes.

This is the first look at how human hepatocytes adapt to fatty acid fluxes over time, and we believe we are providing the field with not only important results but also a great tool to study isolated hepatocyte physiology over time in a human-relevant system. From a translational perspective, our results suggest that once the liver becomes steatotic, regardless of the lipid species causing steatosis, it is filled with fatty acids which are primed to be shuttled to the mitochondria for fatty acid oxidation, to fuel insulin-resistant glucose production. This intrahepatic lipid accumulation along with excess delivery from insulin resistant fat tissue can help explain how, regardless of insulin sensitivity, the liver continues to produce glucose in the postprandial state. The coordinated release of fatty acids, either from adipose tissue or intrahepatic stores, can be attributed to ATGL actions and our results suggest that targeted ATGL inhibition in the liver, and or fat tissue, may provide benefits for patients with NAFLD and T2D. Importantly, lipid-laden human hepatocytes can in have intact insulin signaling

pathways (p-AKT) and insulin-responsive gluconeogenesis gene expression, but still display insulin-resistant glucose production, which suggests that these metrics, although clearly correlated with IR, should not be the major determinants of efficacious therapies in the future.

6.5 Supplemental Figures

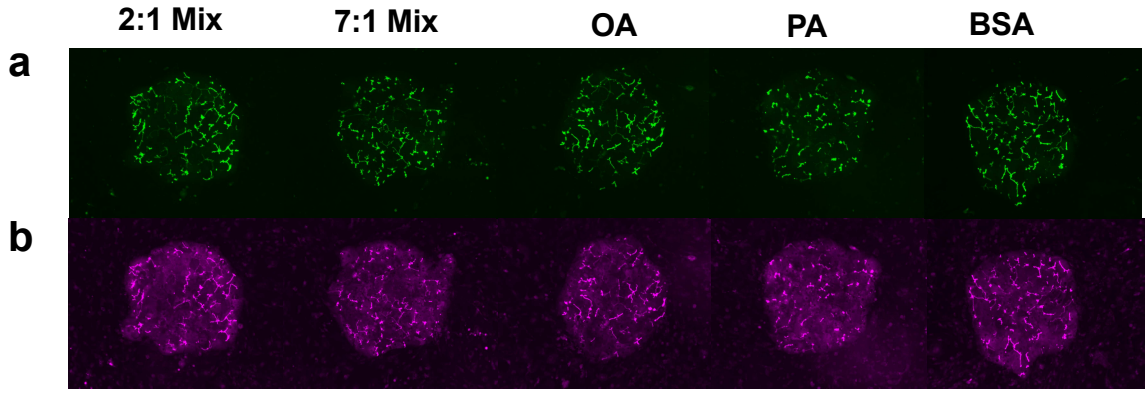

Supplemental Figure. 6.5.1. Fatty acid treatments do not alter bile canaliculi or mitochondrial membrane potential (MMP) in MPCCs. MPCCs were treated with various fatty acid treatments or the BSA control for 8 days and then assessed for bile canaliculi function (a), via fluorescent excretion of CDCFDA stain, or MMP (b) with live cell fluorescent imaging. Images show representative island staining. PA, OA and represent palmitic, and oleic acid. 2:1 and 7:1 mix represent fatty acid mixtures containing all four fatty acids at 2:1 or 7:1 fatty acid: BSA ratios.

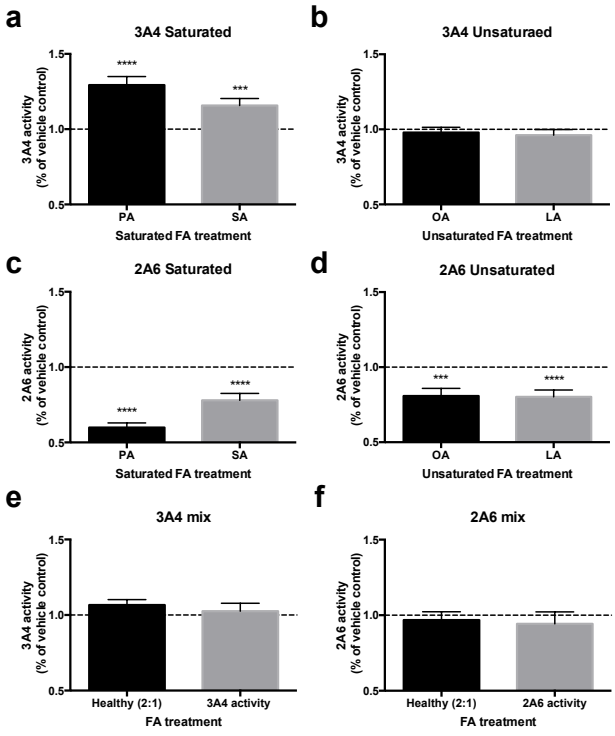

Supplemental Figure. 6.5.2. Single fatty acid mixtures alter CYP450s, while mixtures do not. MPCCs were treated with various fatty acid treatments or the BSA control for 10 days and then assessed for CYP3A4 or CYP2A6 enzyme activity function. (a,b) Relative CYP3A4 activity

assessed via L-IPA substrate incubation and subsequent luminescence, n MPCCs treated with saturated (a) or unsaturated (b) fatty acids normalized to the BSA control. (c,d) Relative CYP2A6 activity, assessed via coumarin incubation and subsequent detection of 7-hydroxy-coumarin, in MPCCs treated with saturated (c) or unsaturated (d) fatty acids normalized to the BSA control. CYP3A4 (e) and CYP2A6 (f) enzyme activity in MPCCs treated with fatty acid mixtures, normalized to the respective BSA control. PA, SA, OA, and LA represent palmitic, stearic, oleic, linoleic acid. 2:1 and 7:1 FA mix represent fatty acid mixtures containing all four fatty acids at 2:1 or 7:1 fatty acid: BSA ratios. Error bars represent SD and n=4. *** and **** represent p ≤0.001 and ≤0.0001, respectively, assessed by a one-way ANOVA.

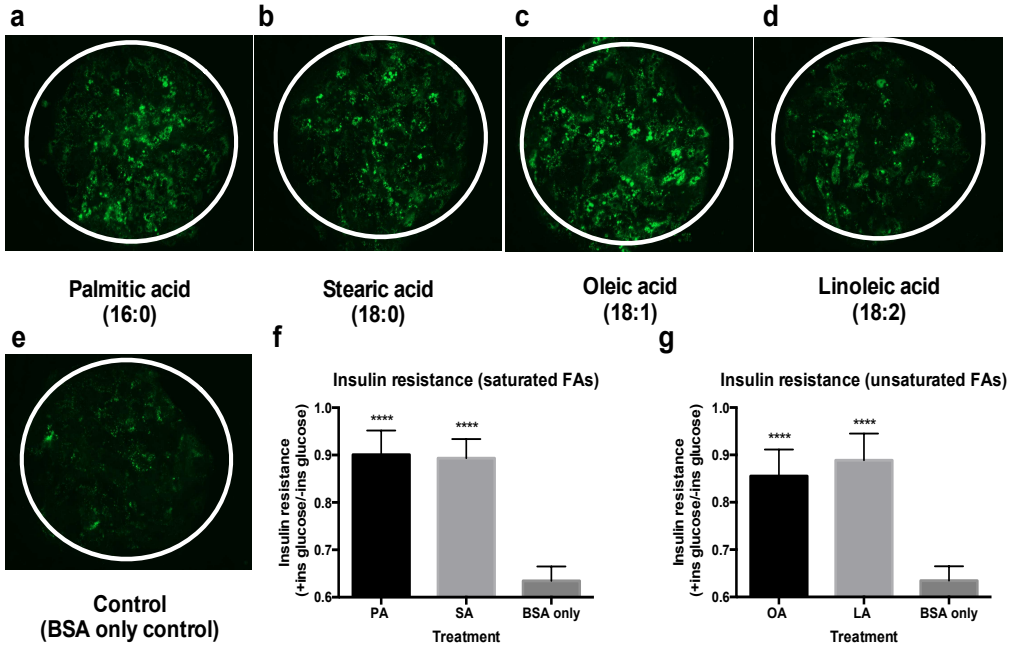

Supplemental Figure. 6.5.3 Single fatty acids induce lipid accumulation and insulin resistance in MPCCs. MPCCs were treated with various fatty acid treatments or the BSA control for 10 day or 8 days and then assessed for lipid accumulation or insulin resistance respectively. (a-e) Representative Nile red staining of hepatocyte islands after 10 days of fatty acid or BSA treatment. Circles surround hepatocyte islands. (f,g) Calculated insulin resistance in saturated (f) and unsaturated (g) fatty acid treated MPCCs. Error bars represent SD. **** represents p ≤0.0001 assessed via one-way ANOVA.

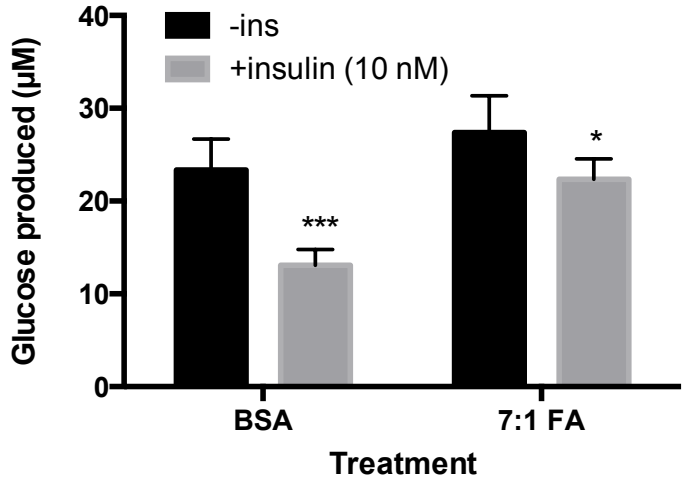

Supplemental Figure. 6.5.4. 1-hour glucose production and insulin response in MPCCs treated with BSA or fatty acid mixture for 8 days. Error bars represent SD. *,and *** represent $p \leq 0.5$, ≤ 0.001, respectively, assessed by a t-test between +/- insulin stimulation for respective treatment.

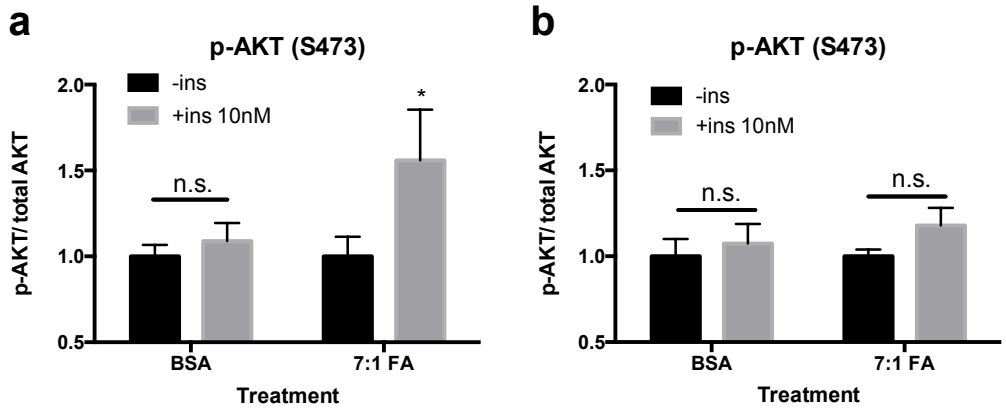

Supplemental Figure. 6.5.5. Phosphorylated AKT (p-AKT, serine 473)/ total AKT (t-AKT) in BSA and fatty acid treated cultures over time. MPCCs were treated with BSA or fatty acids for 2 (a) or 8 (b) days, starved overnight and then treated with +/- insulin for 1 hour and then fixed. In-cell ELISAs were performed to assess the level of AKT phosphorylation. Error bars represent sd. * represents $p \leq 0.5$ assessed by a t-test between +/- insulin stimulation for respective treatment.

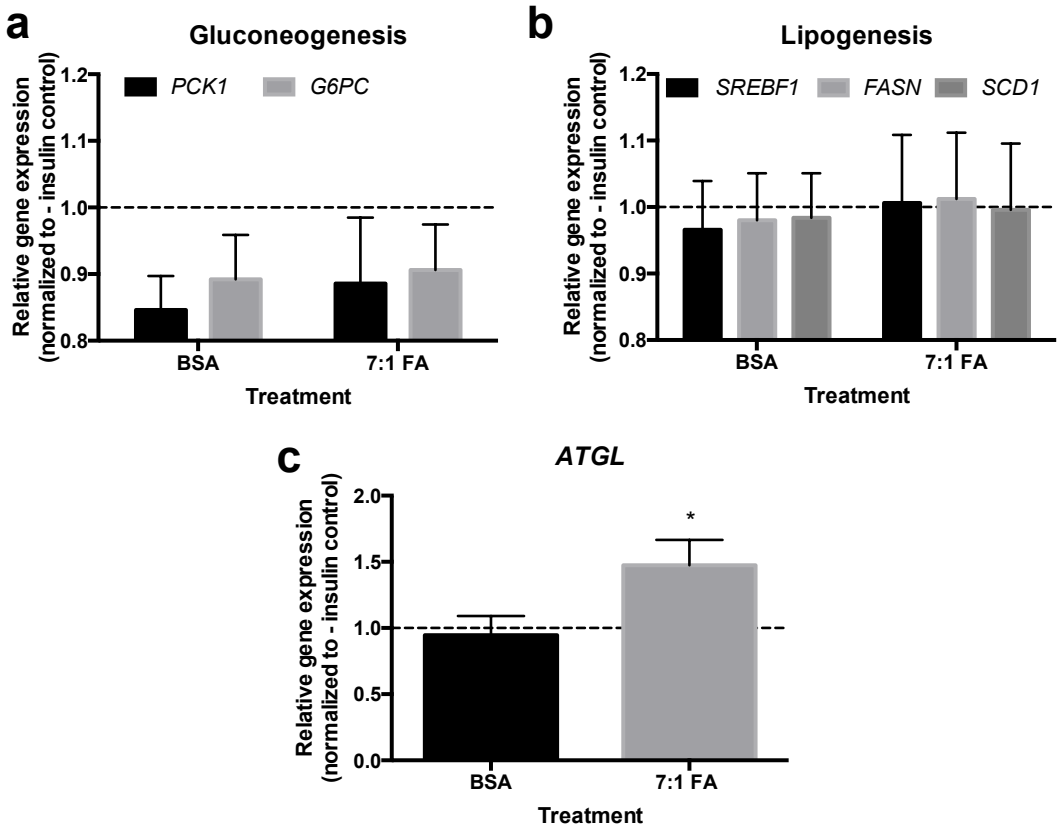

Supplemental Figure. 6.5.6. Gene expression under insulin stimulation. MPCCs were treated with BSA or fatty acids for 2 days, starved overnight, and incubated with +/- insulin for 6 hours and then RNA was collected. Gluconeogenesis (a), lipogenesis (b) and ATGL (c) expression was quantified and normalized to the non-insulin stimulated control for each treatment. Error bars represent sd. * represents $p \leq 0.5$ assessed by a t-test between +/- insulin stimulation for respective treatment.

References

1. Wilcox G. Insulin and Insulin Resistance. Clinical Biochemist Reviews. The Australian Association of Clinical Biochemists; **26**(2), 19, 2005.

2. Tayek JA, Katz J. Glucose production, recycling, and gluconeogenesis in normals and diabetics: a mass isotopomer [U-13C]glucose study. American Journal of Physiology - Endocrinology and Metabolism. American Physiological Society; **270**(4), E709, 1996.

3. Marchesini G, Brizi M, Morselli-Labate AM, Bianchi G, Bugianesi E, McCullough AJ, et al. Association of nonalcoholic fatty liver disease with insulin resistance. Am. J. Med. **107**(5), 450, 1999.

4. Samuel VT, Shulman GI. The pathogenesis of insulin resistance: integrating signaling pathways and substrate flux. Journal of clinical Investigation. **126**(1), 12, 2016.

5. Samuel VT, Shulman GI. Mechanisms for Insulin Resistance: Common Threads and Missing Links. Cell. **148**(5), 852, 2012.

6. Taniguchi CM, Emanuelli B, Kahn CR. Critical nodes in signalling pathways: insights into insulin action. Nat. Rev. Mol. Cell Biol. **7**(2), 85, 2006.

7. Laplante M, Sabatini DM. mTORC1 activates SREBP-1c and uncouples lipogenesis from gluconeogenesis. Proceedings of the National Academy of Sciences. **107**(16), 7617, 2010.

8. Li S, Brown MS, Goldstein JL. Bifurcation of insulin signaling pathway in rat liver: mTORC1 required for stimulation of lipogenesis, but not inhibition of gluconeogenesis. Proceedings of the National Academy of Sciences. **107**(8), 3441, 2010.

9. Zhang W, Bu SY, Mashek MT, O-Sullivan I, Sibai Z, Khan SA, et al. Integrated Regulation of Hepatic Lipid and Glucose Metabolism by Adipose Triacylglycerol Lipase and FoxO Proteins. CellReports. **15**(2), 349, 2016.

10. Zhang W, Patil S, Chauhan B, Guo S, Powell DR, Le J, et al. FoxO1 regulates multiple metabolic pathways in the liver: effects on gluconeogenic, glycolytic, and lipogenic gene expression. The Journal of Biological Chemistry. **281**(15), 10105, 2006.

11. Zhang K, Li L, Qi Y, Zhu X, Gan B, DePinho RA, et al. Hepatic suppression of Foxo1 and Foxo3 causes hypoglycemia and hyperlipidemia in mice. Endocrinology. **153**(2), 631, 2012.

12. Dong XC, Copps KD, Guo S, Li Y, Kollipara R, DePinho RA, et al. Inactivation of hepatic Foxo1 by insulin signaling is required for adaptive nutrient homeostasis and endocrine growth regulation. Cell Metabolism. **8**(1), 65, 2008.

13. Brown MS, Goldstein JL. Selective versus Total Insulin Resistance: A Pathogenic Paradox. Cell Metabolism. **7**(2), 95, 2008.

14. Lu M, Wan M, Leavens KF, Chu Q, Monks BR, Fernandez S, et al. Insulin regulates liver metabolism in vivo in the absence of hepatic Akt and Foxo1. Nature Medicine. **18**(3), 388, 2012.

15. Perry RJ, Camporez J-PG, Kursawe R, Titchenell PM, Zhang D, Perry CJ, et al. Hepatic acetyl CoA links adipose tissue inflammation to hepatic insulin resistance and type 2 diabetes. Cell. **160**(4), 745, 2015.

16. Titchenell PM, Chu Q, Monks BR, Birnbaum MJ. Hepatic insulin signalling is dispensable for suppression of glucose output by insulin in vivo. Nat Commun. **6**, 7078, 2015.

17. O-Sullivan I, Zhang W, Wasserman DH, Liew CW, Liu J, Paik J, et al. FoxO1 integrates direct and indirect effects of insulin on hepatic glucose production and glucose utilization. Nat Commun. **6**, 7079, 2015.

18. Vatner DF, Majumdar SK, Kumashiro N, Petersen MC, Rahimi Y, Gattu AK, et al. Insulin-independent regulation of hepatic triglyceride synthesis by fatty acids. Proceedings of the National Academy of Sciences. **112**(4), 1143, 2015.

19. Titchenell PM, Quinn WJ, Lu M, Chu Q, Lu W, Li C, et al. Direct Hepatocyte Insulin Signaling Is Required for Lipogenesis but Is Dispensable for the Suppression of Glucose Production. Cell Metabolism. **23**(6), 1154, 2016.

20. Kostadinova R, Boess F, Applegate D, Suter L, Weiser T, Singer T, et al. A long-term three dimensional liver co-culture system for improved prediction of clinically relevant drug-induced hepatotoxicity. Toxicology and Applied Pharmacology. **268**(1), 1, 2013.

21. Davidson MD, Lehrer M, Khetani SR. Hormone and Drug-Mediated Modulation of Glucose Metabolism in a Microscale Model of the Human Liver. Tissue Engineering Part C: Methods. **21**(7), 716, 2015.

22. Hebbard L, George J. Animal models of nonalcoholic fatty liver disease. Nat Rev Gastroenterol Hepatol. **8**(1), 34, 2011.

23. Olson H, Betton G, Robinson D, Thomas K, Monro A, Kolaja G, et al. Concordance of the toxicity of pharmaceuticals in humans and in animals. Regul. Toxicol. Pharmacol. **32**(1), 56, 2000.

24. Khetani SR, Berger DR, Ballinger KR, Davidson MD, Lin C, Ware BR. Microengineered liver tissues for drug testing. J Lab Autom. **20**(3), 216, 2015.

25. Guguen-Guillouzo C, Clément B, Baffet G, Beaumont C, Morel-Chany E, Glaise D, et al. Maintenance and reversibility of active albumin secretion by adult rat hepatocytes co-cultured with another liver epithelial cell type. Experimental Cell Research. **143**(1),

47, 1983.

26. Khetani SR, Bhatia SN. Microscale culture of human liver cells for drug development. Nat Biotechnol. **26**(1), 120, 2007.

27. Davidson MD, Ballinger KR, Khetani SR. Long-term exposure to abnormal glucose levels alters drug metabolism pathways and insulin sensitivity in primary human hepatocytes. Sci. Rep. **6**, 28178, 2016.

28. Kim J-A, Han E, Eun C-J, Tak YK, Song JM. Real-time concurrent monitoring of apoptosis, cytosolic calcium, and mitochondria permeability transition for hypermulticolor high-content screening of drug-induced mitochondrial dysfunction-mediated hepatotoxicity. Toxicology Letters. **214**(2), 175, 2012.

29. Khetani SR, Kanchagar C, Ukairo O, Krzyzewski S, Moore A, Shi J, et al. Use of Micropatterned Cocultures to Detect Compounds That Cause Drug-Induced Liver Injury in Humans. Toxicological Sciences. **132**(1), 107, 2013.

30. Kleinfeld AM, Prothro D, Brown DL, Davis RC, Richieri GV, DeMaria A. Increases in serum unbound free fatty acid levels following coronary angioplasty. Am. J. Cardiol. **78**(12), 1350, 1996.

31. Mayer N, Schweiger M, Romauch M, Grabner GF, Eichmann TO, Fuchs E, et al. Development of small-molecule inhibitors targeting adipose triglyceride lipase. Nat Chem Biol. **9**(12), 785, 2013.

32. Feldstein AE, Werneburg NW, Canbay A, Guicciardi ME, Bronk SF, Rydzewski R, et al. Free fatty acids promote hepatic lipotoxicity by stimulating TNF-alpha expression via a lysosomal pathway. Hepatology. **40**(1), 185, 2004.

33. Malhi H, Bronk SF, Werneburg NW, Gores GJ. Free Fatty Acids Induce JNK-dependent Hepatocyte Lipoapoptosis. Journal of Biological Chemistry. **281**(17), 12093, 2006.

34. Reaven GM, HOLLENBECK C, JENG CY, WU MS, CHEN Y. Measurement of Plasma-Glucose, Free Fatty-Acid, Lactate, and Insulin for 24-H in Patients with Niddm. Diabetes. **37**(8), 1020, 1988.

35. Puri P, Baillie RA, Wiest MM, Mirshahi F, Choudhury J, Cheung O, et al. A lipidomic analysis of nonalcoholic fatty liver disease. Hepatology. **46**(4), 1081, 2007.

36. Fisher CD, Lickteig AJ, Augustine LM, Ranger-Moore J, Jackson JP, Ferguson SS, et al. Hepatic cytochrome P450 enzyme alterations in humans with progressive stages of nonalcoholic fatty liver disease. Drug metabolism and disposition. **37**(10), 2087, 2009.

37. Donato MT. Potential Impact of Steatosis on Cytochrome P450 Enzymes of Human Hepatocytes Isolated from Fatty Liver Grafts. Drug metabolism and disposition. **34**(9), 1556, 2006.

38. Donato MT, Jimenez N, Serralta A, Mir J, Castell JV, Gomez-Lechon MJ. Effects of steatosis on drug-metabolizing capability of primary human hepatocytes. Toxicology in Vitro. **21**(2), 271, 2007.

39. Woolsey SJ, Mansell SE, Kim RB, Tirona RG, Beaton MD. CYP3A Activity and Expression in Nonalcoholic Fatty Liver Disease. Drug metabolism and disposition. **43**(10), 1484, 2015.

40. Canet MJ, Hardwick RN, Lake AD, Dzierlenga AL, Clarke JD, Cherrington NJ. Modeling Human Nonalcoholic Steatohepatitis-Associated Changes in Drug Transporter Expression Using Experimental Rodent Models. Drug metabolism and disposition. **42**(4), 586, 2014.

41. Christensen H, Hermann M. Immunological response as a source to variability in drug metabolism and transport. Front Pharmacol. **3**, 2012.

42. Zamek-Gliszczynski MJ, Xiong H, Patel NJ, Turncliff RZ, Pollack GM, Brouwer K. Pharmacokinetics of 5 (and 6)-carboxy-2 “,7 -”dichlorofluorescein and its diacetate promoiety in the liver. Journal of Pharmacology and Experimental Therapeutics. **304**(2), 801, 2003.

43. LEVINE R, FRITZ IB. The relation of insulin to liver metabolism. Diabetes. **5**(3), 209, 1956.

44. Fabbrini E, Magkos F, Mohammed BS, Pietka T, Abumrad NA, Patterson BW, et al. Intrahepatic fat, not visceral fat, is linked with metabolic complications of obesity. Proceedings of the National Academy of Sciences. National Academy of Sciences; **106**(36), 15430, 2009.

45. Petersen KF, Dufour S, Befroy D, Lehrke M, Hendler RE, Shulman GI. Reversal of Nonalcoholic Hepatic Steatosis, Hepatic Insulin Resistance, and Hyperglycemia by Moderate Weight Reduction in Patients With Type 2 Diabetes. Diabetes. **54**(3), 603, 2005.

46. Haemmerle G, Lass A, Zimmermann R, Gorkiewicz G, Meyer C, Rozman J, et al. Defective Lipolysis and Altered Energy Metabolism in Mice Lacking Adipose Triglyceride Lipase. Science. American Association for the Advancement of Science; **312**(5774), 734, 2006.

47. Wu JW, Wang SP, Alvarez F, Casavant S, Gauthier N, Abed L, et al. Deficiency of liver adipose triglyceride lipase in mice causes progressive hepatic steatosis. Hepatology. Wiley Subscription Services, Inc., A Wiley Company; **54**(1), 122, 2011.

48. Brown JM, Betters JL, Lord C, Ma Y, Han X, Yang K, et al. CGI-58 knockdown in mice causes hepatic steatosis but prevents diet-induced obesity and glucose intolerance. J. Lipid Res. **51**(11), 3306, 2010.

49. Ong KT, Mashek MT, Bu SY, Greenberg AS, Mashek DG. Adipose triglyceride lipase

is a major hepatic lipase that regulates triacylglycerol turnover and fatty acid signaling and partitioning. Hepatology. **53**(1), 116, 2011.

50. Satapati S, Sunny NE, Kucejova B, Fu X, He TT, Méndez-Lucas A, et al. Elevated TCA cycle function in the pathology of diet-induced hepatic insulin resistance and fatty liver. J. Lipid Res. **53**(6), 1080, 2012.

51. FREEDMAN AD, KOHN L. PYRUVATE METABOLISM AND CONTROL: FACTORS AFFECTING PYRUVIC CARBOXYLASE ACTIVITY. Science. **145**(3627), 58, 1964.

52. Williamson JR, Kreisberg RA, Felts PW. Mechanism for the stimulation of gluconeogenesis by fatty acids in perfused rat liver. Proc. Natl. Acad. Sci. U.S.A. **56**(1), 247, 1966.

53. Jungermann K, Kietzmann T. Oxygen: Modulator of metabolic zonation and disease of the liver. Hepatology. **31**(2), 255, 2000.

54. Roth U, Curth K, Unterman TG, Kietzmann T. The transcription factors HIF-1 and HNF-4 and the coactivator p300 are involved in insulin-regulated glucokinase gene expression via the phosphatidylinositol 3-kinase/protein kinase B pathway. The Journal of Biological Chemistry. **279**(4), 2623, 2004.

55. Chen KS, Katz J. Zonation of glycogen and glucose syntheses, but not glycolysis, in rat liver. Biochem J. **255**(1), 99, 1988.

56. Brunet A, Sweeney LB, Sturgill JF, Chua KF, Greer PL, Lin Y, et al. Stress-dependent regulation of FOXO transcription factors by the SIRT1 deacetylase. Science. **303**(5666), 2011, 2004.

57. Lim JH, Gerhart-Hines Z, Dominy JE, Lee Y, Kim S, Tabata M, et al. Oleic Acid Stimulates Complete Oxidation of Fatty Acids through Protein Kinase A-dependent Activation of SIRT1-PGC1 Complex. Journal of Biological Chemistry. **288**(10), 7117, 2013.

58. Chakrabarti P, Kandror KV. FoxO1 Controls Insulin-dependent Adipose Triglyceride Lipase (ATGL) Expression and Lipolysis in Adipocytes. Journal of Biological Chemistry. **284**(20), 13296, 2009.

Chapter 7

Engineering an *in vitro* model of non-alcoholic steatohepatitis using hepatic stellate cells and MPCCs[6]

Summary:

Given species-specific differences in drug metabolism pathways, modeling interactions between activated human hepatic stellate cells (HSCs) and primary human hepatocytes (PHHs) *in vitro* can aid in the development of therapeutics for non-alcoholic steatohepatitis (NASH) and fibrosis. However, current human liver platforms do not adequately model the negative effects of activated HSCs on the phenotype of otherwise functionally stable PHHs as occurs *in vivo*. Thus, we engineered a micropatterned tri-culture (MPTC) platform that allows stabilized PHHs to interact with activated HSCs over several weeks. Specifically, we integrated HSCs into a modified version of the MPCC containing growth-arrested fibroblasts, which was optimized in chapter 4. We could increase the severity of the NASH-like phenotype by increasing the number of HSCs we added to the culture. Furthermore, we discovered critical pathways that HSCs alter in hepatocytes to drive them into a diseased phenotype, which could have implications for understanding NAFLD disease progression. Importantly, we were also able to use this MPTC system to identify efficacious compounds that are currently in clinical trials for NASH.

[6]A manuscript similar to the work described in this chapter is in preparation and will be submitted for publication shortly.

7.1 Introduction

Non-alcoholic fatty liver disease (NAFLD) is reaching epidemic proportions in the U.S. population due to the concurrent rise in obesity and type 2 diabetes mellitus (1). While the onset of NAFLD is asymptomatic, ~5-10% of patients with NAFLD will develop non-alcoholic steatohepatitis (NASH), which is the progressive stage of NAFLD characterized by fatty liver, inflammation, and fibrosis that predisposes individuals to cirrhosis and hepatocellular carcinoma (2). During NASH, hepatocytes accumulate abnormal amounts of lipids (steatosis), swell (balloon), and display altered cytochrome-P450 (CYP450) enzyme and drug transporter activities (3,4), while pro-inflammatory macrophages and natural killer T cells accumulate in the liver (5,6). Additionally, hepatic stellate cells (HSCs), which normally store vitamin A and aid in regeneration, can become activated in NASH and differentiate into myofibroblast-like cells that secrete factors (i.e. proinflammatory cytokines, excessive collagen which leads to fibrosis) that can negatively affect hepatic functions (7), such as drug metabolism pathways (8). Since fibrosis has been identified as the major predictor of long-term outcomes in patients with NASH (9), developing novel liver models containing activated HSCs and hepatocytes should aid in the development of NASH therapeutics.

While animal models have provided important insights into NAFLD/NASH (10), significant differences across species in drug metabolism (11) and disease pathways (12) necessitate the supplementation of animal data with human-relevant *in vitro* assays for understanding species-specific cellular mechanisms and drug development. Untransformed primary human hepatocytes (PHHs) are widely considered to be the "gold standard" for building human liver models since they are relatively simple to use in medium-to-high throughput culture formats and are the closest representation of hepatic functions in the human liver (13). However,

in the presence of ECM manipulations alone, PHHs display a precipitous decline in liver functions such as CYP450 activities (14) and insulin responsiveness (15), which is likely due to the severe downregulation of the expression of a master liver transcription factor, hepatocyte nuclear factor 4 alpha or HNF4α (16). Furthermore, gene regulatory network alterations of de-differentiating hepatocytes in monolayers and to a lesser extent in 3D self-assembled spheroids resemble those of inflammatory liver diseases (i.e. cirrhosis, carcinoma, hepatitis B virus infection) (16).

In contrast to pure hepatocyte monolayers, co-culture with both liver- and non-liver-derived non-parenchymal cells (NPCs) has been long known to enhance hepatic functions *in vitro* (17). HSCs have been previously explored towards transiently enhancing hepatocyte functions in co-cultures relative to declining mono-cultures (18-22). However, these studies were not designed to model the negative effects of activated HSCs on the phenotype of otherwise *stable* and highly functional hepatocytes, as would be important for testing a novel therapeutic that alleviates such effects in NASH/fibrosis. More recently, bioprinted human liver tissues containing PHHs, HSCs, and endothelial cells were used to model drug-induced accumulation of fibrillar collagen, hepatocellular damage and transient secretion of proinflammatory cytokines (23). However, beyond testing the effects of fibrogenesis-inducing drugs, the utility of bioprinted tissues for recapitulating a progressive NASH-like phenotype (i.e. modulation of drug metabolism/transporter pathways and development of hepatic steatosis) and ameliorating it using drug candidates has not been shown. Additionally, bioprinted tissues are slow to produce and mature, and not amenable to high-throughput drug screening. Therefore, there remains a need for high-throughput culture systems that can functionally stabilize PHHs, while simultaneously

allowing for the incorporation of activated HSCs towards developing *in vitro* disease models for anti-NASH/fibrosis drug screening.

Semiconductor-driven microfabrication is useful for enhancing and stabilizing liver functions in co-cultures for several weeks by controlling the extent of homotypic interactions between PHHs and their heterotypic interactions with NPCs (24). In particular, Khetani and Bhatia organized PHHs onto collagen-coated circular domains of empirically optimized dimensions and surrounded them with 3T3-J2 murine embryonic fibroblasts (14), which are devoid of major liver functions but express hepatocyte-supporting molecules present in the liver (25). These 'micropatterned co-cultures' (MPCCs) maintain prototypical PHH morphology, secrete albumin, synthesize urea, retain polarized and functional drug transporters, and display high levels of CYP450 activities for ~4 weeks (26). Furthermore, we have shown that PHHs in MPCCs develop steatosis and selective insulin resistance following treatment with a hyperglycemic culture medium (27). However, the lack of HSCs in MPCCs limits their utility for developing NASH/fibrosis disease models. Therefore, here we engineered PHH-HSC interactions using the MPCC platform such that PHHs remained differentiated for several weeks, but could interact with HSCs at physiologically-relevant ratios. We then determined the effects of activated HSCs on diverse PHH phenotypic functions over long-term culture, identified target pathways involved in such effects, and screened key compounds and their combinations to demonstrate platform utility in drug development.

7.2 Methods

7.2.1 Hepatic stellate cell culture

Cryopreserved primary human stellate cells (HSCs) were commercially obtained from Sciencell Research Laboratories (Carlsbad, CA) and Zen-Bio (Durham, NC). HSCs were seeded onto poly-L-lysine (PLL) (Sciencell) coated flasks (20 μg/mL) and passaged 1-3 times in Sciencell proprietary stellate cell medium. One passage prior to experiments with hepatocytes, HSCs were activated by culturing in 10% vol/vol fetal bovine serum (FBS, Thermo Fisher Scientific, Waltham, MA) with high glucose Dulbecco's Modified Eagle's Medium (DMEM, Corning Life Sciences, Manassas, VA), 1% vol/vol penicillin/streptomycin (Corning), and 15 mM HEPES (Corning) on PLL-coated flasks. In some experiments, HSCs were labeled in suspension with a fluorescent PKH67 membrane dye (Sigma-Aldrich, St. Louis, MO) per manufacturer's protocols. In conditioned culture medium experiments, supernatants from pure HSC cultures were collected, sterile filtered through a 0.2 μm cellulose acetate filter, and then added to hepatocyte cultures within 1 hour following collection. In some experiments, the conditioned culture medium was spiked with a neutralizing antibody for interleukin-6 (IL-6) or an isotype-matched IgG control antibody (R&D Systems, Minneapolis, MN) prior to incubation with hepatocytes.

7.2.2 Micropatterned co- and tri-culture fabrication and drug dosing

Cryopreserved primary human hepatocytes (PHHs) were commercially obtained from Triangle Research Labs (Durham, NC). PHHs were thawed, counted and viability was assessed as previously described (27). Micropatterned co-cultures (MPCCs) were created as previously described (24). Briefly, adsorbed rat tail collagen I (Corning) was lithographically patterned in each well of a 24-well or 96-well plate to create 500 μm diameter circular domains spaced 1200 μm apart, center-to-center. PHHs selectively attached to the collagen domains leaving ~30K attached PHHs on ~85 collagen-coated islands within each well of a 24-well plate or ~4.5K attached PHHs on ~13 collagen-coated islands within each well of a 96-well plate. 3T3-J2 fibroblasts were passaged as previously described (14), and growth-arrested by incubating in culture medium containing 1 μg/mL mitomycin-C (Sigma-Aldrich) for 4 hours prior to trypsinization. These growth-arrested 3T3-J2 murine embryonic fibroblasts were seeded at ~90,000 cells per well in a 24-well plate or ~15,000 cells per well in a 96-well plate 18 to 24 hours after PHH seeding to create MPCCs. To create MPCCs with HSCs (passage 1-4) as the supportive cell type, HSCs were seeded instead of the fibroblasts at ~90,000 cells per well in a 24-well format onto adhered micropatterned PHH colonies.

To create micropatterned tri-cultures (MPTCs), activated HSCs at different numbers were mixed into a suspension of ~90,000 or ~15,000 growth-arrested fibroblasts, and then this mixture was seeded onto micropatterned PHH colonies in each well of 24-well or 96-well plate formats, respectively. For transwell® experiments, 0.4 μm polycarbonate 24-well inserts (6.5 mm diameter) were coated with collagen (100 μg/ml) and HSCs were seeded at a density of 15 x 10^3 cells/cm^2 (~5K cells/insert). The transwell inserts were placed atop pre-established MPCCs

adhered to the bottom of each well in 24-well plates. Culture medium containing ~5 mM D-glucose (Fisher BioReagents, Pittsburgh, PA) in a DMEM base (Corning) was replaced on MPCCs and MPTCs every 2 days (300 μL/well for a 24-well plate and 50 μL/well for a 96-well plate). For transwell experiments, MPCCs at the bottom of each well in a 24-well plate were cultured in 600 μL/well of culture medium, while the transwell insert on top was cultured in 50 μL/well. Other components of the culture medium have been described previously (27).
For drug dosing studies, cultures were dosed with obeticholic acid (Selleck Chem, Houston, TX) or GKT137821 (Cayman Chemical Company, Ann Arbor, MI) or a combination of the two drugs using dimethylsulfoxide (DMSO) as the vehicle solvent at 0.1% vol/vol final concentration in the culture medium.

7.2.3 Quantitative polymerase chain reaction (qPCR)

Total RNA was isolated, purified, and reverse transcribed into complementary DNA (cDNA) as previously described (27). Then, 250 ng of cDNA was added to each qPCR reaction along with the Taqman™ master mix (Thermo Fisher Scientific) and pre-designed Solaris™ (GE Healthcare Dharmacon, Lafayette, CO) or Taqman human-specific primer/probe sets according to manufacturers' protocols. The primer/probe sets were selected to be human-specific without cross-reactivity to 3T3-J2 mouse DNA; however, Taqman primer/probe sequences are proprietary to the manufacturer. Hepatic gene expression was normalized to the housekeeping gene, glyceraldehyde 3-phosphate dehydrogenase (*GAPDH*), while HSC gene expression was normalized to the housekeeping gene, hypoxanthine-guanine phosphoribosyltransferase (*HPRT)*. qPCR was performed on a MasterCycler RealPlex-2 (Eppendorf, Hamburg, Germany).

7.2.4 Biochemical assays and cell staining

Concentrations of albumin and urea in collected cell culture supernatants were assayed using previously published protocols (27). CYP450 enzyme activities were measured by first incubating cultures in substrates for 1 hour at 37°C and then detecting either the luminescence or fluorescence of metabolites using previously described protocols (27). CYP2A6 was measured by the modification of coumarin to fluorescent 7-hydroxy-coumarin (Sigma-Aldrich), and CYP3A4 was measured by cleavage of luciferin-IPA into luminescent luciferin (Promega, Madison, WI). Interleukin-6 (IL-6) secretions were quantified using a sandwich enzyme-linked immunosorbent assay (ELISA) kit (R&D Systems).

Live MPCCs or MPTCs were incubated with 2 μg/mL 5(6)-carboxy-2',7'-dichlorofluorescein-diacetate (CDCFDA) and NucBlue® (Thermo Fisher Scientific) for 15 min in serum-free culture medium at 37°C. Cultures were then washed 3X with a serum-free culture medium and imaged using the GFP (green fluorescent protein) and DAPI (4',6-diamidino-2-phenylindole) light cubes on an EVOS FL microscope (Thermo Fisher Scientific). Additionally, mitochondrial membrane potential in cells was imaged by incubating cultures with 200 nM tetramethylrhodamine, methyl ester (TMRM, Thermo Fisher Scientific) for 15 min at 37°C. Cultures were then washed 3X with serum-free medium and imaged using the RFP (red fluorescent protein) light cube. Paraformaldehyde (4% vol/vol)-fixed cultures were stained for intracellular lipids using the Nile Red dye as previously described (27).

7.2.5 Statistical analysis

Each experiment was carried out in 2 or more wells for each condition. Two to three cryopreserved PHH donors and two to three HSC donors were used to confirm observed trends. Microsoft Excel and GraphPad Prism 5.0 (La Jolla, CA) were used for data analysis and plotting data. Error bars on average values represent standard deviation (SD) across wells. Statistical significance of the data was determined using the average and SD across wells in representative experiments using the Student's *t*-test or one-way ANOVA with Dunnett's multiple comparison tests for post hoc analysis.

7.3 Results

7.3.1 Engineering an MPCC platform containing HSCs

Cryopreserved PHHs were first seeded onto micropatterned collagen islands, and then growth-arrested 3T3-J2s or primary HSCs activated by prior passaging on tissue culture plastic in serum-supplemented culture medium (28,29) or a combination of both NPCs were seeded at different densities the next day onto micropatterned PHHs (**Fig. 1a-e**). PHH islands retained their shape and morphology for at least 2 weeks when the 3T3-J2s were present in the culture (90K 3T3-J2s: 30K PHHs in each well of a 24-well format) in the presence or absence of HSCs. On the other hand, in co-cultures containing PHHs and only HSCs (90K HSCs: 30K PHHs), uncontrolled HSC growth led to the loss of hepatic morphology and island integrity. Furthermore, albumin secretion, urea synthesis and CYP3A4 activity in MPCCs containing 3T3-

J2s were ~3.1 fold, ~7.8 fold and ~47 fold higher, respectively, after ~2 weeks as compared to HSC-containing MPCCs (**Fig. 1f vs. Fig. 1g**). These results suggest that HSCs cannot stabilize PHH functions to the same extent as the 3T3-J2 fibroblasts.

Growth-arrested 3T3-J2s (90K cells in a 24-well format) were co-mixed with HSCs at different densities (1.25K, 2.5K or 5K cells) and this NPC mixture was seeded onto pre-established micropatterned PHH colonies (30K cells). The 2.5K HSCs with 30K PHHs corresponds to the approximate ratio in the human liver (i.e. 5% HSCs and 60% PHHs of the total number of cells in the liver) (24). In such micropatterned tri-cultures (MPTCs), hepatic albumin and urea secretions did not vary significantly with different numbers of HSCs (**Fig. 1h**),

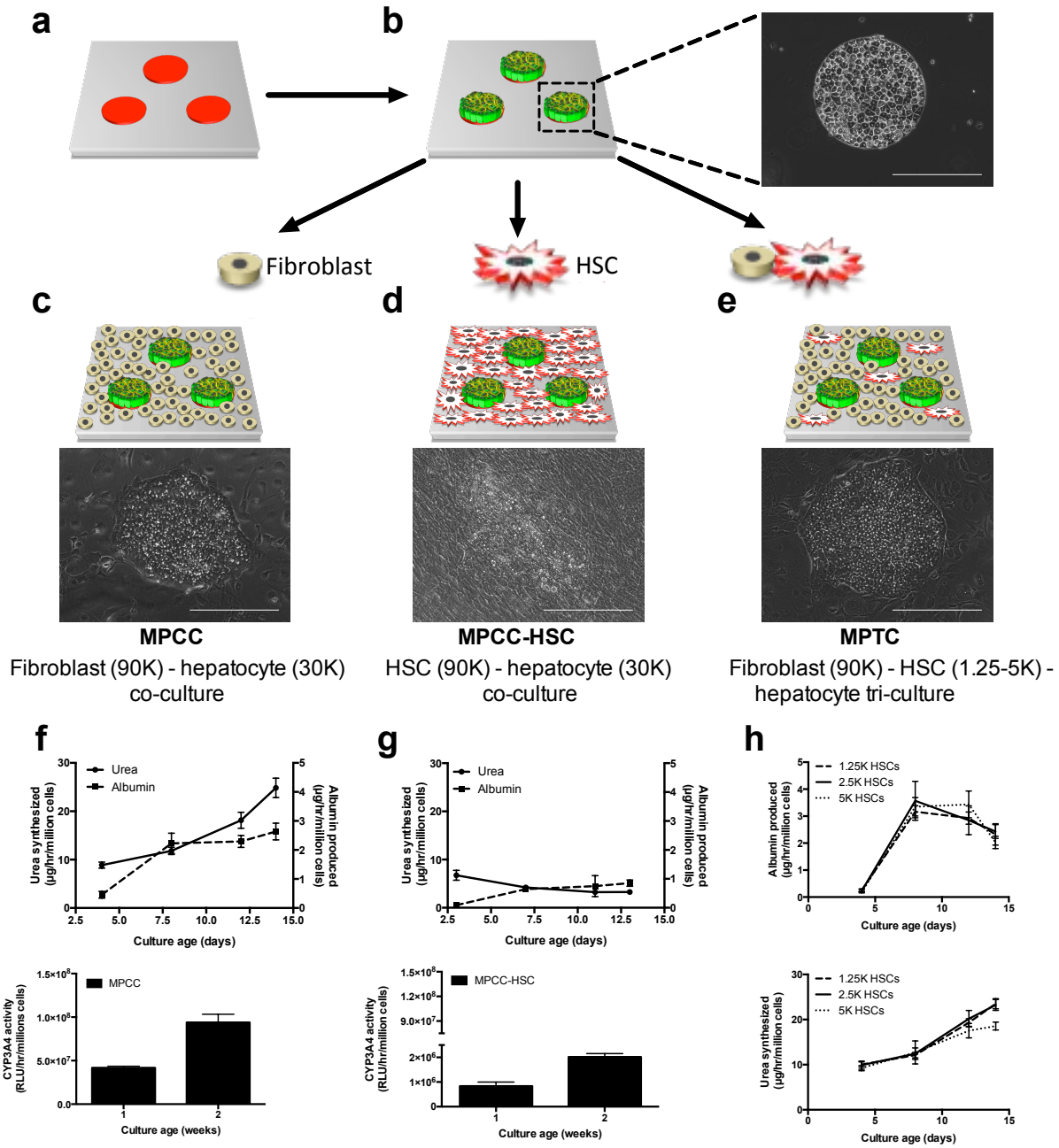

Figure 7.1. Engineering micropatterned co-cultures (MPCCs) and micropatterned tri-cultures (MPTCs) containing hepatic stellate cells (HSCs). (a) The creation of MPCCs starts with the patterning of extracellular matrix (ECM) proteins (e.g. collagen) into each well of a tissue culture polystyrene plate. **(b)** Primary human hepatocytes (PHHs) then selectively attach to the ECM domains. Phase contrast image on the day of seeding is shown. **(c)** 3T3-J2 fibroblasts are seeded the next day to create MPCCs. Phase contrast image after 7 days of culture is shown. **(d)** HSCs can be seeded instead of the 3T3-J2 fibroblasts to create MPCC-HSCs (phase contrast image on day 7 is shown). **(e)** Growth-arrested 3T3-J2s can be co-mixed with HSCs at ratios that are at or near physiologic with the PHHs to create MPTCs (phase contrast image on day 7). The 2.5K HSCs with 30K PHHs in a 24-well format corresponds to the approximate ratio in the human liver (i.e. 5% HSCs and 60% PHHs of the total number of cells in the liver). **(f)** Albumin

and urea secretion in standard MPCCs (with only 3T3-J2s and PHHs) is shown on top, while CYP3A4 activity is shown at the bottom. **(g)** A similar set of graphs as panel 'f' except data from MPCC-HSCs is shown. **(h)** Albumin (top) and urea (bottom) secretion in MPTCs that contain HSCs at different numbers. The data for the HSC-free control (i.e. MPCCs) is shown in panel 'f'. Similar trends were observed in multiple PHH and HSC donors. Error bars on average values represent SD (n=3 wells). Scale bars on images represent 400 μm.

and were similar to the secretions measured in MPCCs (**Fig. 1f**). Fluorescent PKH67-labeled HSCs were observed around and on top of PHH islands that were stained for mitochondrial membrane potential (**Fig. 2a-b**). Therefore, the inclusion of activated HSCs within a growth-arrested 3T3-J2 monolayer enabled high/stable levels of albumin and urea in PHHs over at least 2 weeks and did not compromise the ability of HSCs to interact with PHHs.

7.3.2 Activated HSCs downregulate hepatic CYP450/transporter functions and cause steatosis

In MPTCs, CYP3A4 (**Fig. 2c**) and CYP2A6 (**Fig. 2d**) enzyme activities were increasingly downregulated with increasing numbers of activated HSCs as compared to the HSC-free MPCC control. Specifically, at the HSC:PHH ratio of 2.5K:30K (physiological seeding ratio), CYP3A4 was downregulated by ~89% and CYP2A6 was downregulated by ~70% after 2 weeks relative to MPCCs. Downregulation of CYP3A4 activity in MPTCs was also observed after 1 week (**Fig. S1**). Such a downregulation in hepatic CYP450 activities occurred with a concomitant increase in mRNA transcripts for HSC activation markers, *LOX* (lysyl oxidase) and *COL1A1* (collagen type I alpha I), as compared to HSC gene expression prior to seeding into tri-cultures (**Fig. 2e**), suggesting that HSCs get further activated within MPTCs.

Consistent with the downregulation of hepatic CYP450 activities, transcripts for nuclear receptors, *NR1I2* (nuclear receptor subfamily 1, group I, member 2, also known as pregnane X

receptor or *PXR)* and *NR1I3* (nuclear receptor subfamily 1, group I, member 3, also known as constitutive androstane receptor or *CAR*) showed significant downregulation (by ~70%) in MPTCs relative to MPCCs (**Fig. 2f**). Such downregulation of nuclear receptor transcripts also correlated with a downregulation (by ~92%) of CYP3A4 transcripts in MPTCs as compared to MPCCs.

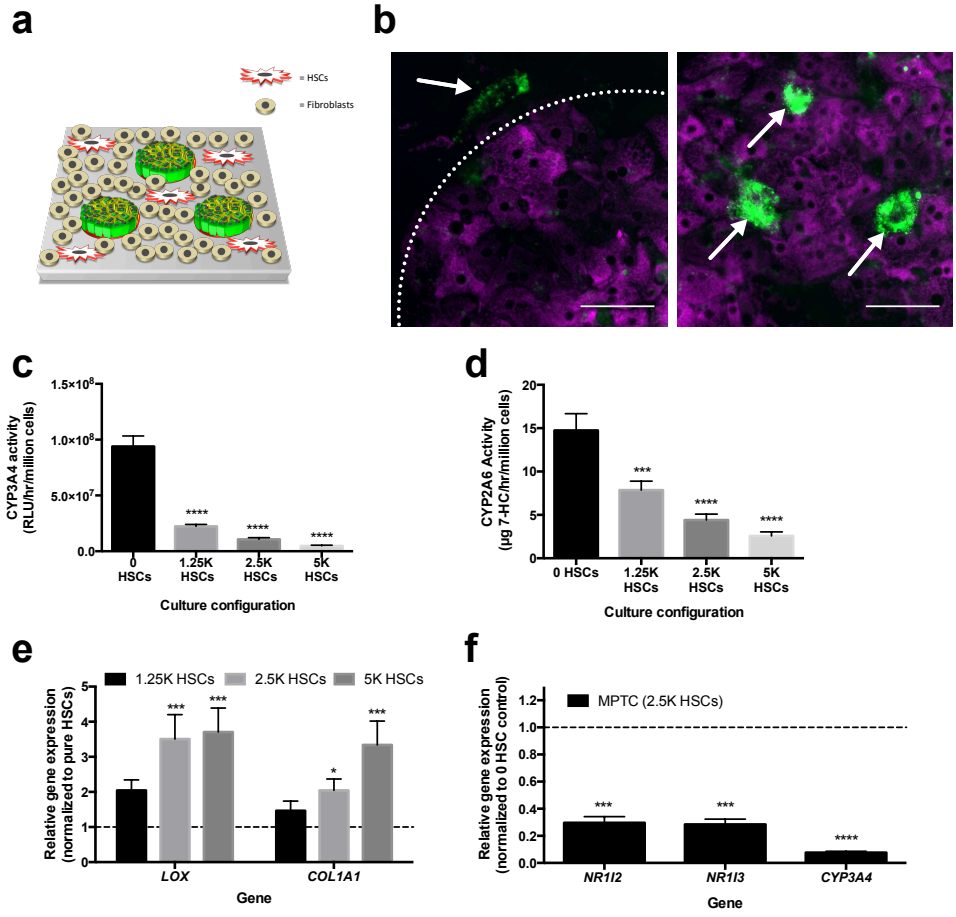

Figure 7.2. Activated hepatic stellate cells (HSCs) cause downregulation of drug metabolism pathways in primary human hepatocytes (PHHs). (a) Schematic of the micropatterned tri-cultures (MPTC) model with PHH colonies that are surrounded by a mixture of growth-arrested 3T3-J2 fibroblasts and HSCs at different ratios with PHHs. **(b)** HSCs (labeled with PKH67 green dye) are observed to be interacting around (left image) and on top (right image) of PHH islands labeled with a mitochondrial membrane potential dye (magenta). HSC:PHH ratio in these MPTCs was 5K:30K cells. **(c)** Downregulation of CYP3A4 activity in MPTCs (week-2 time point) as a function of the number of HSCs seeded initially into the model. Similar trends were seen at other time points (see Fig. S1). The '0 HSC' control is the micropatterned co-culture (MPCC) containing PHH colonies surrounded by only 3T3-J2 fibroblasts. **(d)** Similar data as panel 'c', but CYP2A6 activity is shown. **(e)** HSCs in MPTCs

(week-2 time point) display increased gene expression of activation markers (lysyl oxidase or *LOX* and collagen, type I, alpha 1 or *COL1A1*). Data is normalized (dotted line) to HSC gene expression immediately prior to seeding into MPTCs. **(f)** Gene expression of drug metabolism pathways in MPTCs cultured with 2.5K HSCs (physiologic ratio with 30K PHHs). Week 2 time-point is shown, but trends were observed over multiple weeks. Data is normalized (dotted line) to HSC-free MPCCs. *CYP3A4*: cytochrome P450 3A4; *NR1I2:* nuclear receptor subfamily 1, group I, member 2, also known as pregnane X receptor or *PXR*; and, *NR1I3*: nuclear receptor subfamily 1, group I, member 3, also known as constitutive androstane receptor or *CAR*. Similar trends were observed in multiple PHH and HSC donors. Error bars on average values represent SD (n=3 wells). * $p \leq 0.05$, *** $p \leq 0.001$, and **** $p \leq 0.0001$. In all panels, statistical significance is displayed relative to the HSC-free MPCC control condition. Scale bars on images represent 80 μm.

Transwell cultures, containing MPCCs on the bottom well and HSCs in the insert, allowed us to isolate hepatocyte-only functions/gene expression and compare responses to MPTCs (**Fig. S2**). In such a transwell format, we confirmed that while hepatic albumin secretion and urea synthesis were not affected significantly, the gene expression of *PXR*, *CAR*, and *CYP3A4* as well as the activity of CYP3A4 were severely downregulated in MPCCs in the presence of activated HSCs as compared to the MPCCs cultured with cell-free transwell inserts. The MPTC data, as well as that obtained from transwell cultures, suggests that the addition of activated HSCs to MPCCs leads to a severe downregulation of multiple drug metabolism pathways in otherwise functionally stable hepatocytes (as assessed by albumin and urea secretion). Since we observed downregulation of hepatic CYP450 activities and an increase in HSC activation markers as a function of HSC density in MPTCs, we proceeded to utilize the physiologic seeding ratio for HSCs and PHHs (2.5K HSCs: 30K PHHs) for all subsequent studies unless otherwise noted.

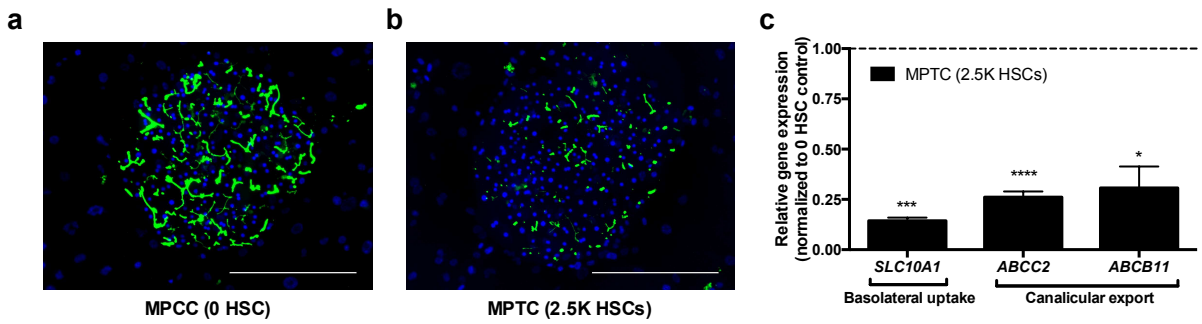

Figure. 7.3. Activated hepatic stellate cells (HSCs) cause downregulation of drug transporter pathways in primary human hepatocytes (PHHs). (a) Representative image of a PHH island in micropatterned co-cultures (MPCCs) with 3T3-J2 fibroblasts after 13 days in culture showing export of fluorescent dye into the bile canaliculi between PHHs (see methods for additional details). Nuclei are stained with Hoescht 33342. **(b)** Similar image as in panel 'a' except micropatterned tri-cultures (MPTCs) containing 2.5 K HSCs and 3T3-J2 fibroblasts around the PHH colonies are shown (day 13 of culture). **(c)** Gene expression of hepatic transporters in MPTCs relative to the HSC-free MPCC control. Data from week 2 cultures is shown, but trends were observed for multiple time points. *SLC10A1*: also known as sodium/taurocholate co-transporting polypeptide (NTCP, involved in basolateral uptake); *ABCC1*: ATP-binding cassette, sub-family C, member 2, also known as multi-drug resistance associated protein 2 (MRP2, involved in canalicular export), and, *ABCB11*: also known as bile salt export protein (BSEP, involved in canalicular export). Similar trends were observed in multiple PHH and HSC donors. Error bars on average values represent SD (n=3 wells). * $p \leq 0.05$, ** $p \leq 0.01$, *** $p \leq 0.001$, and **** $p \leq 0.0001$. In panel 'c', statistical significance is displayed relative to the HSC-free MPCC control condition. Scale bars on images represent 400 μm.

We observed a significant loss of bile canaliculi structures between adjacent PHHs in MPTCs relative to PHHs in MPCCs as assessed by the active excretion of fluorescent 5 (and 6)-carboxy-2',7'-dichlorofluorescein (CDF) dye into bile canaliculi presumably by MRP2 (multidrug resistant-like protein 2) and MRP3 (30) (**Fig. 3a-b**). Additionally, transcripts of several hepatic transporters were significantly modulated in MPTCs relative to MPCCs (**Fig. 3c**). The basolateral uptake transporter, *SLC10A1* (solute carrier family 10 member 1, also known as sodium/taurocholate co-transporting polypeptide or *NTCP*), was downregulated by 86%, while the major ATP-binding cassette (ABC) canalicular transporters, *ABCC2* (also known as multi-

drug resistance associated protein 2 or *MRP2*) and *ABCB11* (also known as bile salt export protein or *BSEP*), were downregulated by 70-74% in MPTCs as compared to MPCC controls.

Finally, after ~8-9 days, PHHs in MPTCs accumulated cytoplasmic vesicles at a greater rate/level than PHHs in MPCCs (**Fig. 4a**). After 13 days, a majority of the PHHs in MPTCs had vesicle accumulation, which was identified to be neutral lipids (i.e. acylglycerols and cholesterol esters) via Nile red staining (**Fig. 4b**). The level of lipid accumulation also directly correlated with the initial number of HSCs seeded into MPTCs. Importantly, MPTCs had reduced expression of the bile acid-sensitive receptor, *NR1H4* (nuclear receptor subfamily 1 group H member 4, also known as farnesoid X receptor or *FXR*) (**Fig. 4c**), which regulates transporter as well as glucose and lipid homeostasis (31). Transwell experiments to isolate PHH gene expression also showed severe downregulation of transporter (*SLC10A1*, *ABCC2*, and *ABCB11*) (**Fig. S3**) and *NR1H4* gene expression in MPCCs cultured with HSC-containing inserts as compared to MPCCs cultured with cell-free inserts (**Fig. S4**). These data sets suggest that activated HSCs decrease transport flux as well as induce lipid accumulation in PHHs.

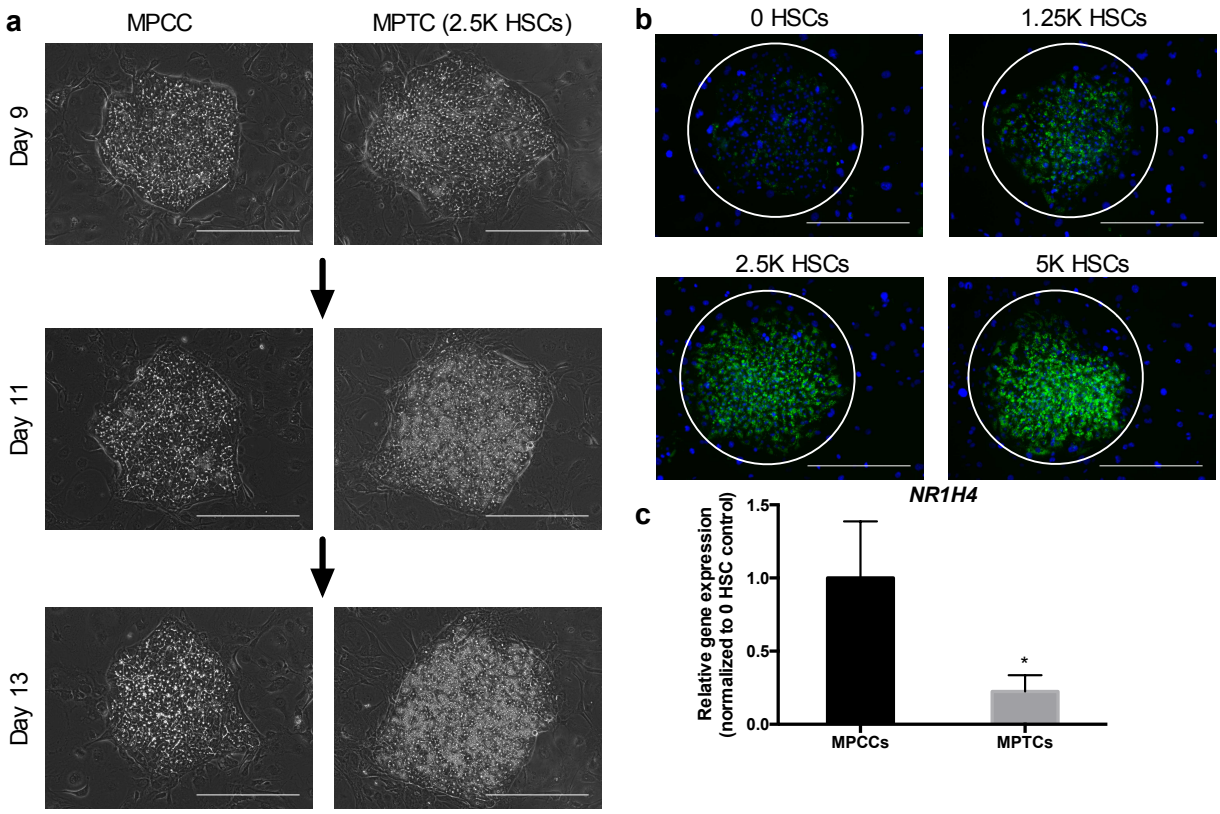

Figure 7.4. Activated hepatic stellate cells (HSCs) cause steatosis in primary human hepatocytes (PHHs). (a) Phase contrast images of micropatterned co-cultures (MPCCs) (left) and micropatterned tri-cultures (MPTCs) (right) at days 9, 11, and 13 of culture. The PHH islands within MPTCs accumulate vesicles over time. **(b)** Representative Nile red (neutral lipids) stained PHH islands in MPCCs (0 HSCs) and MPTCs with 1.25 K, 2.5 K and 5K seeded HSCs after 2 weeks of culture. Thus, the accumulating vesicles observed in phase contrast images were verified to be neutral lipids. Circles outline PHH islands. **(c)** *NR1H4* (nuclear receptor subfamily 1 group H member 4, also known as farnesoid X receptor or *FXR*) expression in MPCCs and MPTCs after 2 weeks of culture. Similar trends were observed in multiple PHH and HSC donors. Error bars on average values represent SD (n=3 wells). * $p \leq 0.05$. Scale bars on images represent 400 μm.

7.3.3 HSC-derived paracrine factors are involved in the downregulation of hepatic functions

Activated HSCs are known to secrete inflammatory cytokines that can negatively modulate hepatic functions (8). Thus, we assessed interleukin 6 (IL-6) protein levels in the supernatants of MPCCs and MPTCs. While MPCC supernatants were devoid of detectable levels of IL-6, this cytokine was detected at increasing levels in MPTC supernatants (**Fig. S5**).

Additionally, *IL-6* expression was not detected in MPCCs cultured with HSC-containing transwells, while *IL-6* was highly expressed in pure HSCs (**Fig. S6**), suggesting that IL-6 detected in MPTC supernatants is secreted by the activated HSCs. Therefore, we assessed the contribution of HSC-derived paracrine factors alone in the downregulation of CYP3A4 activity in MPCCs. Activated HSCs were cultured in separate wells alongside MPCCs. Then, the HSC-conditioned supernatants were filtered to remove cell contaminants and added to MPCCs with each medium exchange every 2 days (**Fig. 5a**). We observed a significant downregulation of CYP3A4 activity in MPCCs (by 99% after 13 days in culture) that were treated with activated HSC-conditioned culture medium as compared to non-conditioned MPCCs (**Fig. 5b**). After ~2 weeks of treatment, hepatic steatosis and loss of bile canaliculi structures were also observed (**Fig. S7**). IL-6 protein levels were found to increase in activated HSC-conditioned supernatants over time as the cells grew to confluence (**Fig. 5c**).

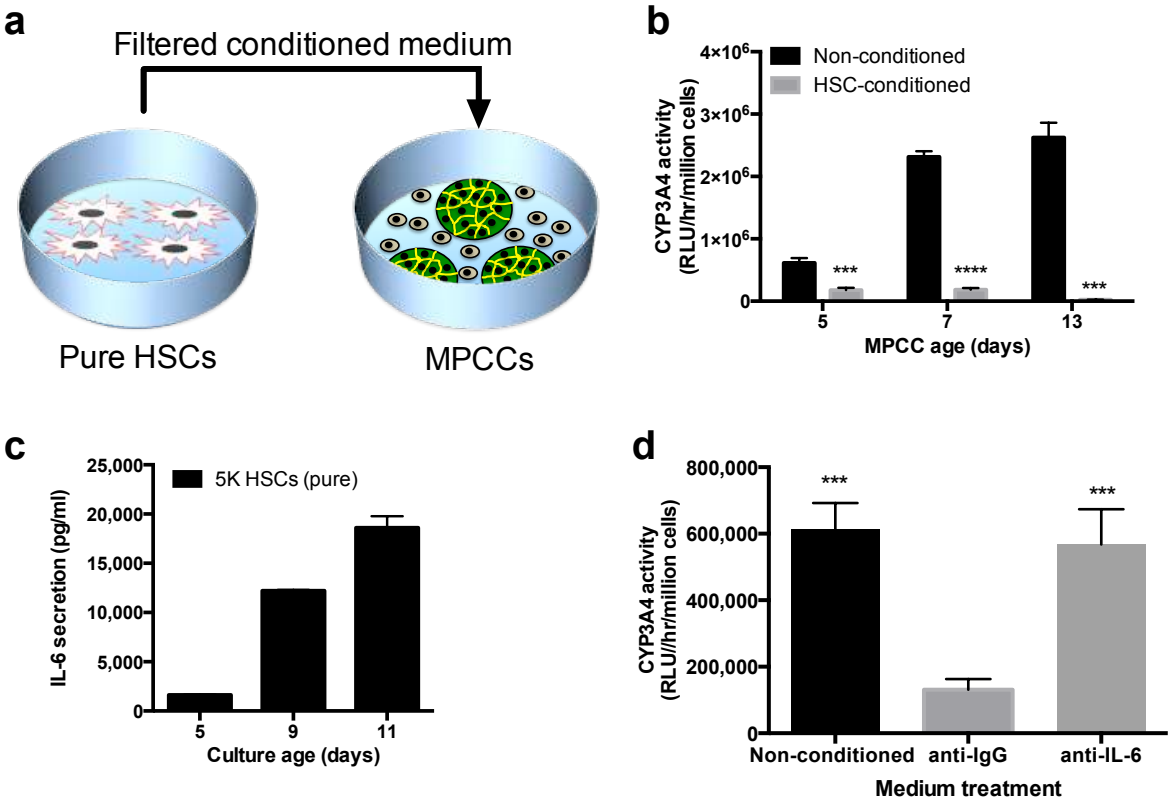

Figure 7.5. Conditioned culture medium from activated hepatic stellate cells (HSCs) causes downregulation of CYP3A4 in primary human hepatocytes (PHHs) through interleukin-6 (IL-6) signaling. (a) Pure HSCs were cultured on collagen-coated tissue culture polystyrene concurrently to micropatterned co-cultures (MPCCs) containing PHHs colonies surrounded by 3T3-J2 fibroblasts in separate wells of a 24-well plate format. Conditioned culture medium from the HSC cultures (initial seeding density of 5K cells per well) was filtered to remove cell contaminants and transferred to MPCCs every 2 days for ~2 weeks. **(b)** CYP3A4 activity in MPCCs that were either incubated with HSC-conditioned culture medium or non-conditioned culture medium (n=3 wells, except n=2 wells for conditioned MPCCs on day 13 of culture). **(c)** IL-6 levels in HSC-conditioned culture medium over time as the HSCs grew to confluence. **(d)** HSC-conditioned culture medium was spiked with either an anti-IL-6 neutralizing antibody or its isotype-matched anti-IgG antibody control. MPCCs on day 3 of culture were then incubated with these conditioned media for 48 hours and CYP3A4 activity was assessed on day 5 of culture. Similar trends were observed in multiple PHH and HSC donors. Error bars on average values represent SD (n=3 wells except where otherwise noted). 'ns' not significant, and *** $p \leq 0.001$. Statistical significance is displayed relative to the non-conditioned MPCC control.

Importantly, a neutralizing antibody against IL-6 ameliorated the effects of activated HSC-conditioned culture medium on CYP3A4 activity in MPCCs, while an isotype control antibody,

anti-IgG, had no considerable effect (**Fig. 5d**). These results support the idea that activated HSCs can downregulate liver drug metabolism pathways partly through IL-6 secretion.

We also incubated pure PHH monolayers with conditioned culture medium from activated HSCs to determine the effects on PHHs alone without the presence of the growth-arrested fibroblasts. CYP3A4 activity in PHH monolayers was significantly downregulated in the presence of activated HSC-conditioned culture medium as compared to the non-conditioned control (**Fig. S8**). However, PHH monolayers displayed a severely de-differentiated morphology after 6 days in culture with CYP3A4 activities that were ~10 fold lower than activities measured in MPCCs.

7.3.4 NADPH oxidase (NOX) inhibition and farnesoid X receptor (FXR) activation rescue PHH functions in the presence of activated HSCs

In MPTCs, we observed an increase (relative to MPCC controls) in the gene expression of *NFE2L2* (nuclear factor, erythroid 2 like 2 or *Nrf2*), which is a transcription factor involved in oxidative stress signaling (32) (**Fig. S9**). Reactive oxygen species (ROS) generated via NOX1 and NOX4 enzymes can mediate fibrogenic pathways in HSCs (33) and hepatocytes (34). We did not detect the expression of either *NOX1* or *NOX4* in MPCC controls, but both were detected in pure activated HSC cultures with *NOX4* expression being higher than *NOX1* (**Fig. S9**). However, only *NOX4* gene expression was detected in MPTCs, likely due to contribution from the activated HSCs at the physiological seeding ratio. Since the inhibition of NOX1&4 with the small molecule GKT137831 has shown anti-fibrotic effects in mouse models of NASH (34), we hypothesized that incubating MPTCs with GKT137831 could alleviate the hepatic dysfunctions observed due to the presence of activated HSCs. Furthermore, FXR is a major regulator of

hepatocyte metabolism and bile production/transport that is downregulated in NASH patients (31). Activation of FXR via obeticholic acid (OCA, a semi-synthetic bile acid analog agonist for FXR) has shown positive effects in ameliorating lipid accumulation and fibrosis in patients with NASH (35). Since we observed a strong downregulation of *NR1H4* (FXR) gene expression in hepatocytes, we hypothesized that treatment of MPTCs with OCA could alleviate the hepatic dysfunctions observed. Finally, we explored the effects of combining these two compounds on hepatic dysfunctions.

We first determined the effects of the drugs on albumin and urea secretion, sensitive markers of hepatotoxicity (36), in MPTCs fabricated in a high-throughput 96-well plate format (**Fig. 6a**). Drug doses that did not cause a significant downregulation of albumin and urea secretions (**Fig. S10**) were also tested on PHH functions that are severely affected in MPTCs. We found that GKT137831, but not OCA, helped rescue CYP3A4 activity in MPTCs to ~81% and ~60% of MPCC controls after 4 and 10 days of treatment, respectively, as compared to DMSO-treated MPTC controls (**Fig. 6b**). Such a rescue in CYP3A4 activity was not due to nuclear receptor-mediated induction as GKT137831 did not induce CYP3A4 activity in MPCC controls (**Fig. S11**). A similar rescue of CYP3A4 activity was observed with the GKT137831+OCA mixture as with GKT137831 alone. On the other hand, OCA, but not GKT137831, caused a partial recovery of bile canaliculi (**Fig. 6c**) and reduced steatosis (**Fig. 6d**) in hepatic colonies within MPTCs. The GKT137831+OCA drug mixture also caused partial recovery of bile canaliculi and a reduction in steatosis in MPTCs; however, the effects were not enhanced over OCA alone.

Gene expression analysis was also conducted on drug-treated MPTCs to compare and contrast with the aforementioned functional effects. Consistent with the rescue of CYP3A4

activity, GKT137831, but not OCA, caused a ~1.4 fold increase in *NR1I2* (*PXR*) expression, while GKT137831+OCA caused a ~1.9 fold increase in *NR1I2* expression in MPTCs relative to DMSO-treated controls (**Fig. 6e**). The expression of *ABCC2* showed different trends as compared to the functional trends observed with the recovery of bile canaliculi. In particular, GKT137831, but not OCA, caused a ~1.9 fold increase in *ABCC2* (*MRP2*) expression, while

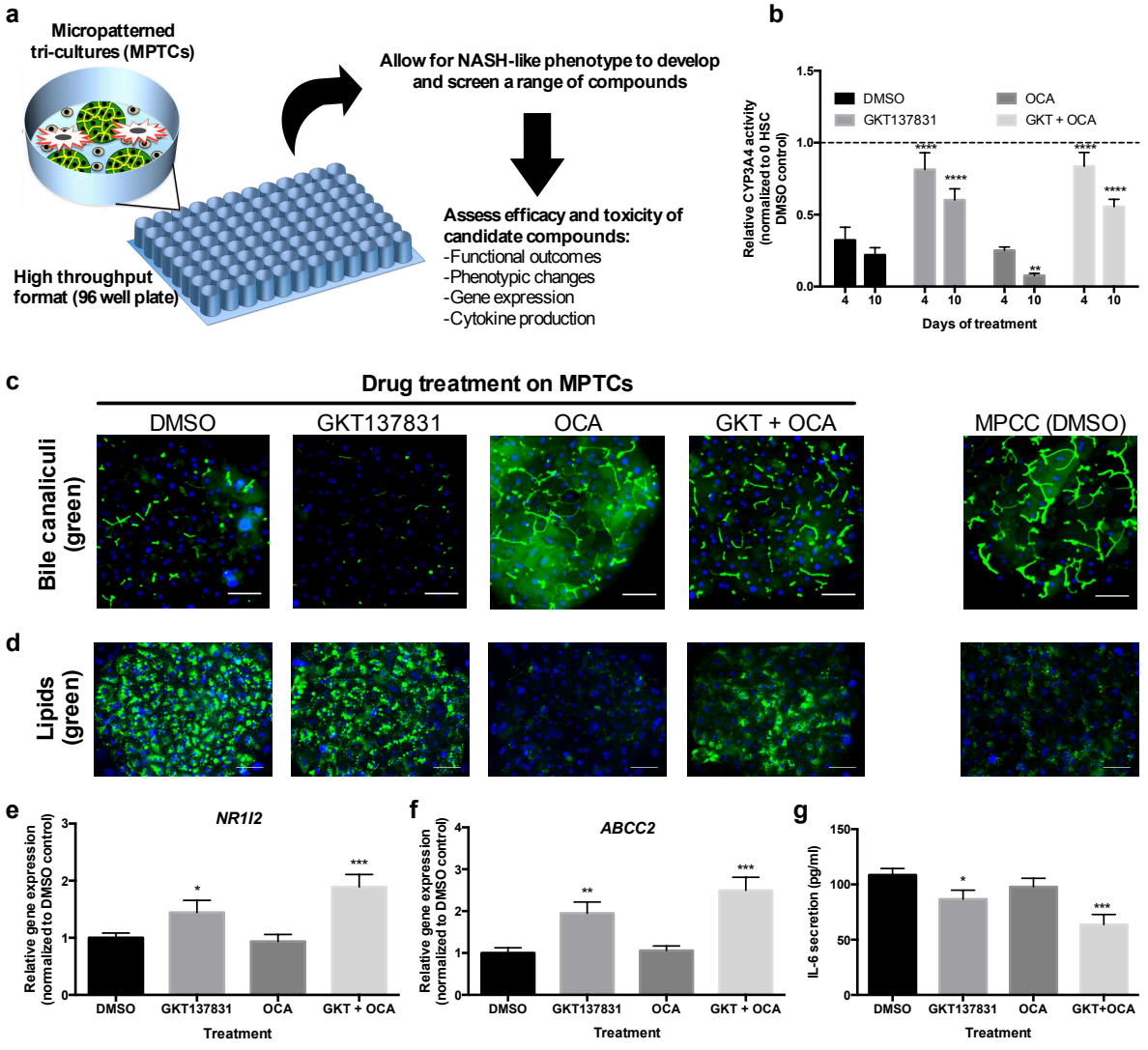

Figure 7.6. Simultaneous inhibition of NADPH oxidase 4 (NOX4) and activation of farnesoid X receptor (FXR) rescues hepatocyte phenotype in the presence of activated hepatic stellate cells (HSCs). (a) Schematic showing how MPTCs in a higher-throughput 96-well plate-based format can be used for investigating the effects of drugs on PHH functions that are affected by activated HSCs. **(b)** CYP3A4 activity in micropatterned tri-cultures (MPTCs) treated for 4 and 10 days with either vehicle solvent (dimethylsulfoxide or DMSO), GKT137831,

obeticholic acid (OCA) or a mixture of both drugs (GKT137831+OCA). Data is normalized to CYP3A4 activity in HSC-free micropatterned co-culture (MPCC) controls (dashed line) (n=5 wells). **(c)** Functional bile canaliculi or lack thereof in MPTCs as visualized by transport of fluorescent (green) dye into the canaliculi between PHHs. MPTCs were treated with drugs or their combinations for 12 days. The MPCC control treated with DMSO is shown to the far right of the image panel for reference. **(d)** Nile red (neutral lipids, green) staining of primary human hepatocytes (PHHs) in MPTCs treated with drugs and their combinations for 12 days. The MPCC control treated with DMSO is shown to the far right of the image panel for reference. **(e)** *NR1I2* (nuclear receptor subfamily 1, group I, member 2, also known as pregnane X receptor or *PXR*) gene expression in MPTCs treated as described in panel 'b' for 12 days. Data is normalized to a DMSO-treated MPTC control (n=3 wells). **(f)** Gene expression as in panel 'e', except *ABCC2* (ATP-binding cassette transporter, family c, member 2, also known as multi-drug resistance associated protein 2 or *MRP2*) is shown (n=4 wells). **(g)** Interleukin-6 (IL-6) levels in MPTC supernatants treated with individual drugs and their combination for 6 days (n=3 wells). Similar trends were observed in multiple PHH and HSC donors. Error bars on average values represent SD (n=3-5 wells as indicated for each panel above). * $p \leq 0.05$, ** $p \leq 0.01$, *** $p \leq 0.001$, and **** $p \leq 0.0001$. In panels 'b', 'e', 'f' and 'g', statistical significance is displayed relative to the DMSO-treated MPTC control at the respective time point. Scale bars on images represent 80 μm.

GKT137831+OCA caused ~2.5 fold increase in *ABCC2* expression in MPTCs relative to DMSO-treated controls (**Fig. 6f**).

Finally, OCA reduced IL-6 levels by ~10% (albeit statistical significance was not reached across all HSC donors), GKT137831 reduced IL-6 levels by ~20%, and GKT137831+OCA reduced IL-6 levels by ~40% in MPTCs relative to DMSO-treated controls (**Fig. 6g**). Therefore, the abovementioned functional and gene expression trends suggest that GKT137831+OCA was more effective than the individual drugs in alleviating the key hepatic dysfunctions, potentially due to a greater reduction in IL-6 levels. However, neither the drugs nor their combination caused a significant reduction in HSC activation markers, *LOX* and *COL1A1*, in MPTCs (data not shown).

7.4 Discussion

We developed and characterized a high-throughput micropatterned tri-culture (MPTC) platform that recapitulates key hepatic dysfunctions observed in NASH/fibrosis due to activated HSC-derived factors. Studies with prototypical drugs suggest MPTC utility for screening novel anti-NASH/fibrosis therapeutics. In contrast to previously developed liver models, MPTCs offer advantages such as a high-throughput 96-well format for screening, stabilization of PHH functions (i.e. CYP450s and transporters) independently of HSCs, and the ability to modulate diverse PHH functions (including the development of steatosis) via increasing numbers of activated HSCs as occurs in progressive steatohepatitis.

In our first attempt to develop a model containing activated HSCs *and* functionally stable PHHs, we replaced 3T3-J2s with activated HSCs (assessed by *LOX* and *COL1A1* expression) as the supportive cell type surrounding micropatterned PHHs within MPCCs. However, hepatic functions in MPCCs containing HSCs as the sole NPC were significantly blunted, and PHH islands lost morphology/integrity with overgrowing HSCs. Nonetheless, we confirmed findings by others that HSCs can enhance some PHH functions (i.e. albumin, CYP3A4) over time in culture relative to declining PHH monolayers (18-22). Our previous results indicated that urea secretion and CYP3A4 activity in MPCCs containing 3T3-J2s are ~70% and ~50% of levels observed in fresh PHHs, respectively(37), while albumin secretion recovers to physiologically-relevant levels (14). Therefore, in contrast to HSCs, 3T3-J2s enhance/stabilize PHH functions to levels that are closer to physiological outcomes.

Since 3T3-J2s support high levels of PHH functions, we postulated that we could add HSCs into MPCCs (with PHHs and growth-arrested 3T3-J2s) at physiologic ratios to the number of PHHs to develop a model in which the negative effects of activated HSCs on the phenotype of

otherwise functionally stable PHHs can be measured and modulated with drugs. Once we identified the appropriate range of HSCs that could be incorporated into MPTCs without compromising a differentiated PHH phenotype (as assessed by albumin and urea secretions), dramatic changes in certain PHH functions were observed that scaled with the increasing numbers of activated HSCs in MPTCs over time. Consistent with clinical findings in patients with NASH/fibrosis (3,4), PHHs displayed a significant loss in the activities of enzymes that metabolize and transport xenobiotics/biomolecules, while the transcription factors responsible for controlling these pathways were also altered in MPTCs as compared to MPCC controls. Importantly, the gene expression of *PXR*, a nuclear receptor that regulates liver transporters and metabolic pathways (38), was downregulated in MPTCs. Accordingly, CYP3A4 and CYP2A6 activities were severely downregulated in MPTCs. CYP3A4 metabolizes ~50% of prescribed medications, including lipid-lowering statins that may help reduce the chances of cardiovascular complications in patients with NAFLD (39), while CYP2A6 is involved in the metabolism of nicotine (40) and the cancer drug, tegafur (41). Lastly, dye transport into hepatic bile canaliculi was noticeably diminished in MPTCs, and such correlated with the downregulation of key transporters (*NTCP, MRP2,* and *BSEP*). Altered CYP450/transporter activities could have major implications for drug development efforts in this disease space.

An increase in the number of activated HSCs within MPTCs correlated with an increase in hepatic steatosis. Previously, paracrine signaling between HSCs and hepatocytes has been shown to mediate ethanol-induced steatosis in mice through increasing lipogenesis (42). Our study constitutes the first time that HSCs have been shown to induce steatosis in PHHs in the absence of ethanol treatment, which could be useful to develop targeted therapies against

NAFLD since recent studies have shown that HSC-altering therapies can have efficacious outcomes in patients with NAFLD (43).

In order to confirm that the aforementioned dysfunctions measured in the supernatant and via gene expression in MPTCs were specific to PHHs, we incubated pre-established MPCCs with transwell inserts containing activated HSCs, which allowed paracrine signaling between the cell types while enabling assessment of cell-specific responses. Indeed, while albumin and urea secretion were not affected, CYP3A4 activity and the expression of key genes (*CYP3A4, PXR, CAR, NTCP, MRP2,* and *BSEP*) were severely downregulated in MPCCs cultured with HSC-containing transwell inserts as compared to MPCCs cultured with cell-free inserts. However, in contrast to the transwell configuration, MPTCs allow for modeling of both cell-cell contact and paracrine signaling between stabilized PHHs and activated HSCs as occurs *in vivo*.

Paracrine factors from activated HSCs in pure cultures (i.e. in the absence of PHH influence) were sufficient to significantly downregulate CYP450/transporter activities and cause steatosis within MPCCs when compared to the non-conditioned control. Since IL-6 levels are increased in livers of patients with NASH (44), and IL-6 can cause downregulation of multiple nuclear receptors in intestinal ischemic/reperfusion injury (45), we investigated the role of this cytokine in the paracrine effects of activated HSCs on PHH functions. We observed increased IL-6 secretion in pure HSC cultures and MPTCs over time. Blocking IL-6 with a neutralizing antibody led to a rescue of CYP3A4 activity in MPCCs treated with HSC-conditioned culture medium relative to non-conditioned MPCC controls. HSCs can produce a multitude of signaling molecules (46) that may also be involved in modulating diverse PHH functions, and thus a thorough molecular profiling of HSC-conditioned culture medium is important for future work.

Nonetheless, our studies with IL-6 demonstrate MPTC utility for developing therapeutics that can block the activity of one or more secreted factors from activated HSCs in NASH/fibrosis.

As in MPCCs, we observed significant downregulation of CYP3A4 activity when short-term *pure* PHH monolayers were treated with activated HSC-conditioned culture medium as compared to non-conditioned controls. These results suggest that HSC secretions can directly affect hepatic CYP3A4 instead of indirectly through the 3T3-J2s in MPTCs. Furthermore, albumin/urea secretion levels in MPTCs, even with increasing numbers of HSCs, were similar to MPCCs, which suggests that the ability of the fibroblasts to support a differentiated PHH phenotype is not affected by HSC contact and/or paracrine signaling. Such an outcome allows the same hepatocyte-stabilizing strategy to be used across conditions and their controls, something that is not possible with declining PHH monolayers. Ultimately, MPTCs constitute a more suitable model than PHH monolayers for fundamental studies and drug screening due to the higher levels and long-term stability of PHH functions.

Since we observed an upregulation of *NFE2L2* (Nrf2, involved in oxidative stress) and *NOX4* in MPTCs, we treated the cultures with GKT137831, a selective dual inhibitor of NOX1&4 (34), which are ROS-generating enzymes involved in liver fibrosis (43). NOX4 levels are increased in livers of patients with NASH, and hepatocyte-specific deletion of NOX4 or treatment with GKT137831 can ameliorate fibrosis in mouse models of NASH (43). In MPTCs, a non-toxic dose of GKT137831 increased the expression of *PXR* and rescued CYP3A4 activity, which was not due to nuclear receptor-mediated CYP3A4 induction as observed with other drugs such as rifampin (47). Since we found that *NOX4* was expressed in MPTCs and pure HSC cultures but not in MPCCs, it could be that HSCs inhibit drug metabolism pathways in PHHs via

the generation of ROS via *NOX4*. We plan to further elucidate the role of ROS and NOX4 in MPTCs in future studies.

We also observed that FXR, a bile acid-sensitive nuclear receptor that regulates hepatocyte metabolism and bile production/transport (48), was downregulated in MPTCs and MPCCs incubated with HSC-containing transwell inserts relative to MPCCs that were devoid of HSC influence. FXR was shown to be downregulated in livers of patients with NASH (31), and activating it via OCA can ameliorate lipid accumulation and fibrosis in such patients (35). Thus, here we incubated MPTCs with a non-toxic dose of OCA and found a significant reduction in the steatosis and restoration of some of the bile canaliculi within PHH colonies. Others have also shown that FXR activation can inhibit lipogenesis and upregulate transporters within hepatocytes (49), while FXR expression is inhibited by IL-6 (45). Thus, HSCs may cause hepatic steatosis in MPTCs by altering lipogenesis/beta-oxidation pathways and/or inhibiting transporter flux, which is also associated with steatosis development (50). Since neither GKT137831 nor OCA alleviated all three types of hepatic dysfunctions observed in MPTCs, we treated the cultures with a combination of the two drugs. The GKT137831+OCA treatment significantly alleviated all three types of hepatic dysfunctions and reduced IL-6 levels by ~40% in MPTCs relative to vehicle-treated controls; however, neither the drugs individually nor their combination reduced HSC activation markers (*LOX* and *COL1A1*) in MPTCs. Thus, the MPTC platform allows for better discrimination of the effects of different drug types on the phenotype of PHHs and activated HSCs, and can be used to discover efficacious drug combinations and ultimately, novel drug classes.

While activated HSCs play a critical role in negatively affecting key hepatic functions and causing fibrosis in NASH, this disease can also be modulated by Kupffer macrophages

(KMs), liver sinusoidal endothelial cells (51) and natural killer T cells (6). The MPCC platform was designed to be 'modular' such that controlled interactions between PHHs and different NPCs can be studied without significant changes to PHH homotypic interactions on the micropatterned ECM domains, which are critical for the proper formation of bile canaliculi. For instance, KMs can be cultured atop pre-established MPCCs to study the effects of KM activation on hepatic CYP450s (52). This model can also be useful to study how pro-inflammatory KMs/macrophages further activate HSCs as has been observed previously (28). In the future, combining all of the liver NPCs in the same microfabricated platform while also maintaining PHH stability (i.e. CYP450s) could be beneficial for modeling more complex cell-cell interactions in NASH and allow screening for therapeutics that target different cell types.

In conclusion, we engineered a platform useful for investigating and therapeutically modulating the negative effects of activated HSCs on functionally stable PHHs as observed in NASH/fibrosis. Ultimately, coupling liver models with other tissue types on a microfluidic chip will allow a systems level exploration of NASH/fibrosis progression.

7.5 Supplemental Figures

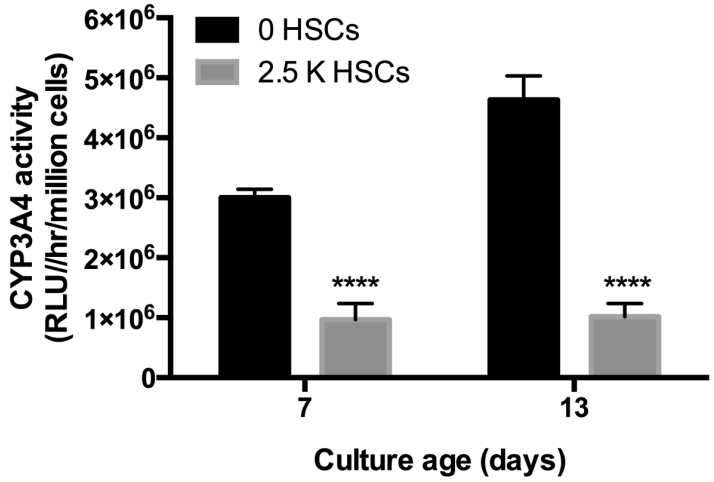

Supplemental Figure. 7.5.1. Activated hepatic stellate cells (HSCs) cause downregulation of CYP3A4 activity in primary human hepatocytes (PHHs). Micropatterned tri-cultures (MPTCs) contain PHH colonies that are surrounded by a mixture of growth-arrested 3T3-J2 fibroblasts and activated HSCs (see Figure 1 of the main manuscript for fabrication schematic). The 2.5K HSCs with 30K PHHs in a 24-well format corresponds to the approximate ratio in the human liver of 1 HSC to 12 PHHs (i.e. 5% HSCs and 60% PHHs of the total number of cells in the liver). Downregulation of CYP3A4 activity in MPTCs is shown over time relative to the HSC-free micropatterned co-culture (MPCC) control containing PHH colonies surrounded by 3T3-J2 fibroblasts only. Similar trends were seen with multiple PHH donors and multiple HSC donors. Error bars on average values represent SD (n=5 wells). **** $p \leq 0.0001$ relative to the micropatterned co-cultures (MPCC) control.

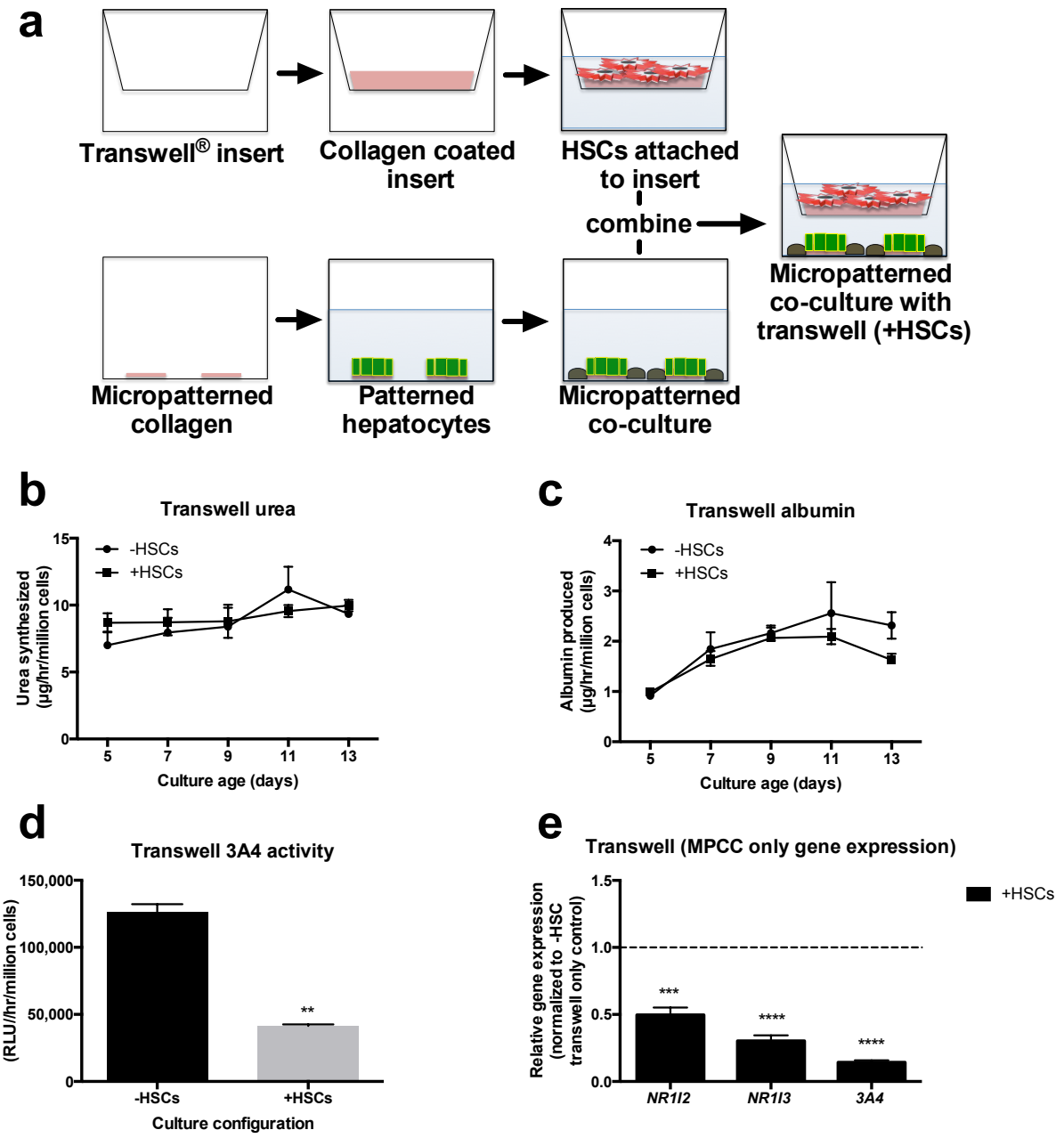

Supplemental Figure. 7.5.2. Paracrine signaling between activated hepatic stellate cells (HSCs) and primary human hepatocytes (PHHs) in a transwell® configuration leads to downregulation of CYP3A4 activity and gene expression in PHHs. (a) Schematic depicting the process used to fabricate transwell tri-cultures containing micropatterned co-cultures (MPCCs) of PHHs and 3T3-J2 fibroblasts on the bottom of the well and activated HSCs cultured in the insert placed on top within 1-2 days following the separate establishment of both MPCCs and HSC cultures. **(b)** Urea levels over time in supernatants of MPCCs cultured with either HSC-containing inserts or cell-free inserts (n=3 wells). **(c)** Albumin secretion over time for the same conditions as those shown in panel 'b' (n=3 wells). Neither albumin nor urea levels were significantly different in the conditions tested. **(d)** CYP3A4 activity after 2 weeks of culture for the same conditions as those shown in panel 'b' (n=2

wells). **(e)** Gene expression is shown after 2 weeks of culture in MPCCs cultured with HSC-containing inserts. Data is normalized to gene expression in MPCCs cultured with cell-free inserts (n=3 wells). *CYP3A4*: cytochrome P450 3A4; *NR1I2:* nuclear receptor subfamily 1, group I, member 2, also known as pregnane X receptor or *PXR*; and, *NR1I3*: nuclear receptor subfamily 1, group I, member 3, also known as constitutive androstane receptor or *CAR*. Glyceraldehyde 3-phosphate dehydrogenase (GAPDH) was used as the housekeeping gene. Similar trends were observed in multiple PHH and HSC donors. Error bars on average values represent SD (n=2-3 wells as indicated above for each panel). ** $p \leq 0.01$, *** $p \leq 0.001$, and **** $p \leq 0.0001$. In panels 'd' and 'e', statistical significance is displayed relative to the HSC-free MPCC control condition.

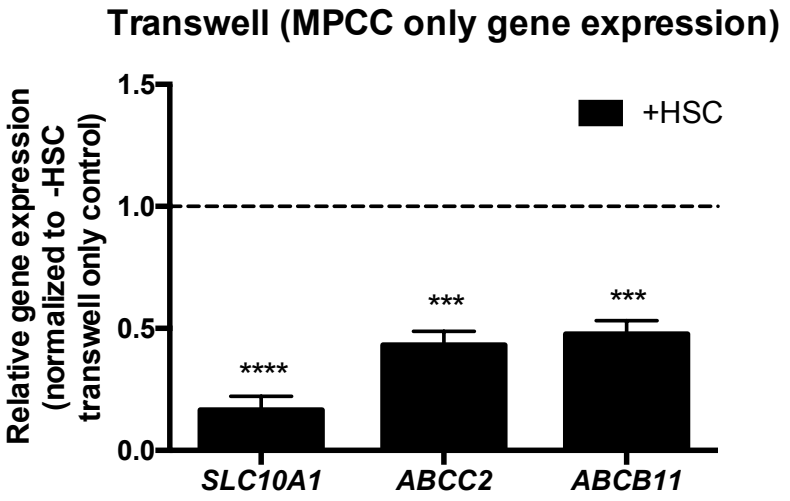

Supplemental Figure. 7.5.3. Paracrine signaling between activated hepatic stellate cells (HSCs) and primary human hepatocytes (PHHs) in a transwell configuration leads to downregulation of transporter gene expression in PHHs. Transwell tri-cultures containing micropatterned co-cultures (MPCCs) on the bottom of the well and HSC-containing inserts on top were fabricated as shown in supplemental figure 2a. Gene expression values of key transporters are shown after 2 weeks of culture in MPCCs cultured with HSC-containing inserts. Data is normalized to gene expression in MPCCs cultured with cell-free inserts. *SLC10A1*: also known as sodium/taurocholate co-transporting polypeptide (NTCP, involved in basolateral uptake); *ABCC1*: ATP-binding cassette, sub-family C, member 2, also known as multi-drug resistance associated protein 2 (MPR2, involved in canalicular export), and, *ABCB11*: also known as bile salt export protein (BSEP, involved in canalicular export). Glyceraldehyde 3-phosphate dehydrogenase (GAPDH) was used as the housekeeping gene. Similar trends were observed in multiple PHH and HSC donors. Error bars on average values represent SD (n=3 wells). *** $p \leq 0.001$, and **** $p \leq 0.0001$. Statistical significance is displayed relative to the HSC-free MPCC control condition.

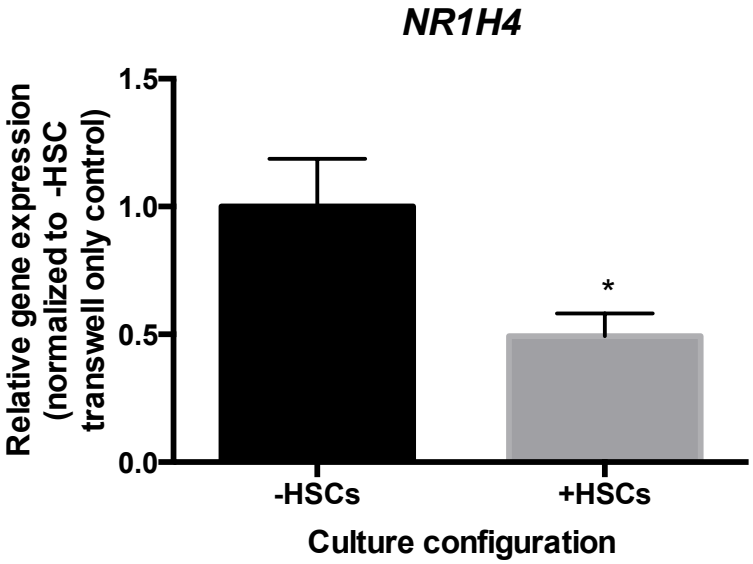

Supplemental Figure. 7.5.4. Paracrine signaling between activated hepatic stellate cells (HSCs) and primary human hepatocytes (PHHs) in a transwell configuration leads to downregulation of *NR1H4* (nuclear receptor subfamily 1 group H member 4, also known as farnesoid X receptor or *FXR*) gene expression in PHHs. Transwell tri-cultures containing micropatterned co-cultures (MPCCs) on the bottom of the well and HSC-containing inserts on top were fabricated as shown in supplemental figure 2a. *NR1H4 (*FXR) gene expression is shown after 2 weeks of culture in MPCCs cultured with HSC-containing inserts. Data is normalized to gene expression in MPCCs cultured with cell-free inserts. Glyceraldehyde 3-phosphate dehydrogenase (GAPDH) was used as the housekeeping gene. Similar trends were observed in multiple PHH and HSC donors. Error bars on average values represent SD (n=3 wells). * $p \leq 0.05$. Statistical significance is displayed relative to the HSC-free MPCC control condition

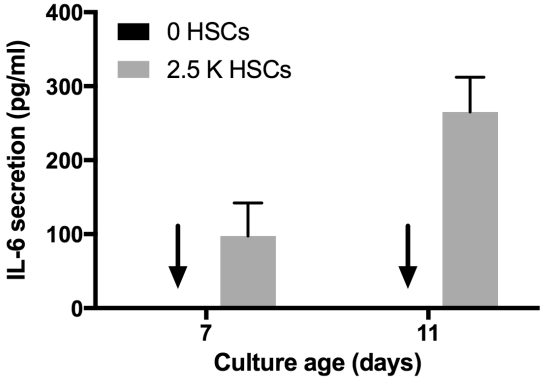

Supplemental Figure. 7.5.5. Interleukin-6 (IL-6) protein levels increase over time in supernatants from micropatterned tri-cultures (MPTCs) but were not detected in supernatants from micropatterned co-cultures (MPCC). MPTCs (containing 2.5K hepatic stellate cells) and MPCCs (devoid of hepatic stellate cells) were created as described in figure 1 of the main manuscript. Arrows indicate undetectable IL-6 protein in MPCC supernatants. Error bars on average values represent SD (n=3 wells).

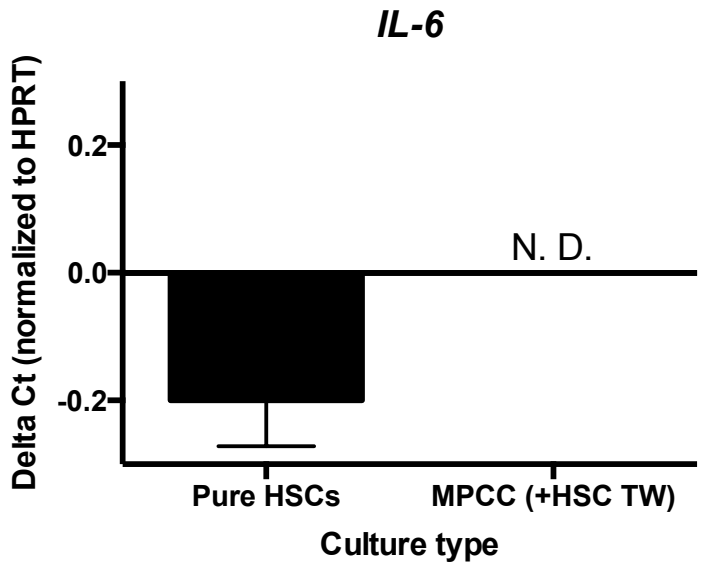

Supplemental Figure. 7.5.6. Interleukin-6 *(IL-6)* transcripts were detected in pure cultures of activated hepatic stellate cells (HSCs) but not detected in micropatterned co-cultures (MPCCs) cultured with HSCs in the transwell configuration. Transwell tri-cultures containing micropatterned co-cultures (MPCCs) on the bottom of the well and HSC-containing inserts on top were fabricated as shown in supplemental figure 2a. *IL-6* gene expression is shown after 2 weeks of culture in pure HSCs and MPCCs cultured with HSC-containing transwell (TW) inserts on top. Data is normalized to the housekeeping gene, hypoxanthine-guanine phosphoribosyltransferase (*HPRT*), via the delta Ct method. While *IL-6* was highly expressed in pure HSC cultures, it was not detected in MPCCs with HSC-containing transwell inserts on top. Error bars on average values represent SD (n=3 wells).

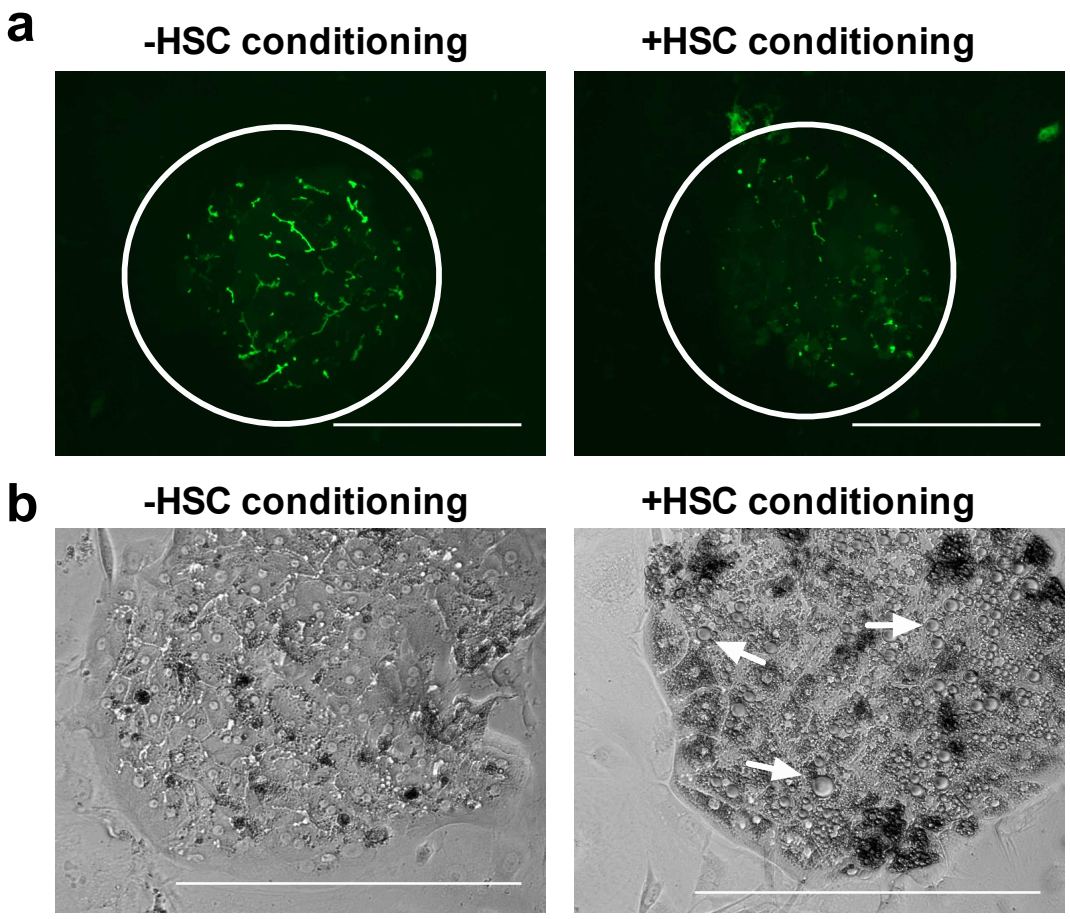

Supplemental Figure. 7.5.7. Conditioned culture medium from activated hepatic stellate cells (HSCs) causes loss of bile canaliculi and leads to steatosis in primary human hepatocytes (PHHs) within micropatterned co-cultures (MPCCs). Pure HSCs were cultured on collagen-coated tissue culture polystyrene concurrently to MPCCs containing PHHs colonies surrounded by 3T3-J2 fibroblasts in separate wells of a 24-well plate format. Conditioned culture medium from the HSC cultures (initial seeding density of 5K cells per well) was filtered to remove cell contaminants and transferred to MPCCs every 2 days for ~2 weeks. **(a)** Representative images of a PHH island in MPCCs (denoted by the white circle) after 2 weeks in culture showing export of fluorescent dye into the bile canaliculi between PHHs (see methods for additional details). Fewer functional bile canaliculi were detected in PHHs within MPCCs that were incubated with HSC-conditioned culture medium (right image) as compared to PHHs within MPCCs that were incubated with non-conditioned culture medium. **(b)** Similar conditions as in panel 'a' except phase contrast micrographs of PHH islands within MPCCs are shown. Macrovesicular steatosis (white arrows) is visible in PHHs within MPCCs that were incubated with HSC-conditioned culture medium (right) as compared to PHHs within MPCCs that were incubated with non-conditioned culture medium. The scale bars represent 400 μm.

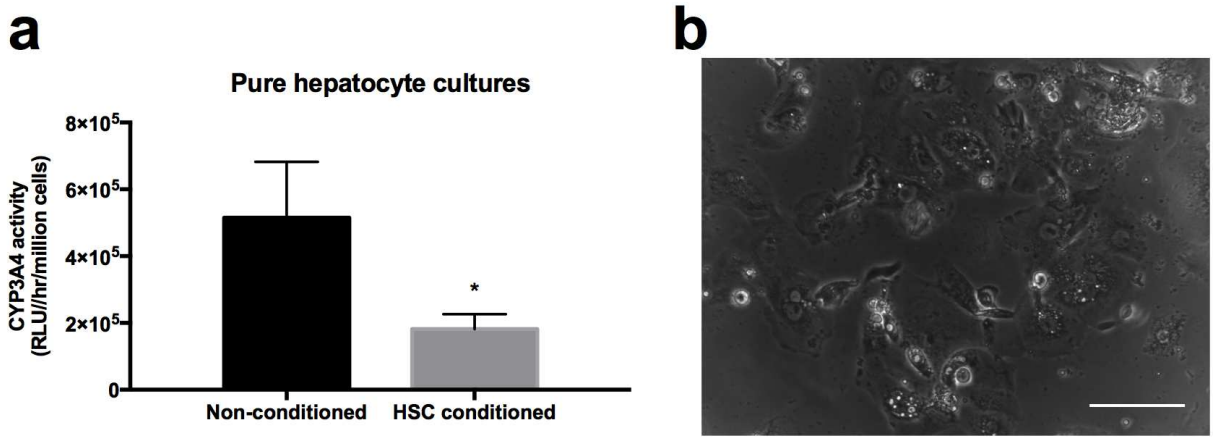

Supplemental Figure. 7.5.8. Conditioned culture medium from activated hepatic stellate cells (HSCs) leads to the downregulation of CYP3A4 activity in pure primary human hepatocyte (PHH) monolayers. Pure HSCs (initial density of 5K cells per well) were cultured on collagen-coated tissue culture polystyrene concurrently to pure PHH monolayers (seeded on collagen-coated tissue culture polystyrene at 1.05M cells/cm^2) in separate wells of a 24-well plate format. Conditioned culture medium from the HSC cultures was filtered to remove cell contaminants and transferred to PHH monolayers every 2 days for 6 days. **(a)** CYP3A4 activity in PHH monolayers (at day 6 of culture) that were either incubated with HSC-conditioned culture medium (n=5 wells) or non-conditioned culture medium (n=2 wells). **(b)** Representative phase contrast image of PHH monolayer after 6 days in culture. Error bars on average values represent SD (n=2-5 as indicated above for each panel). * $p \leq 0.05$ relative to non-conditioned control. Scale bar on image represents 80 μm.

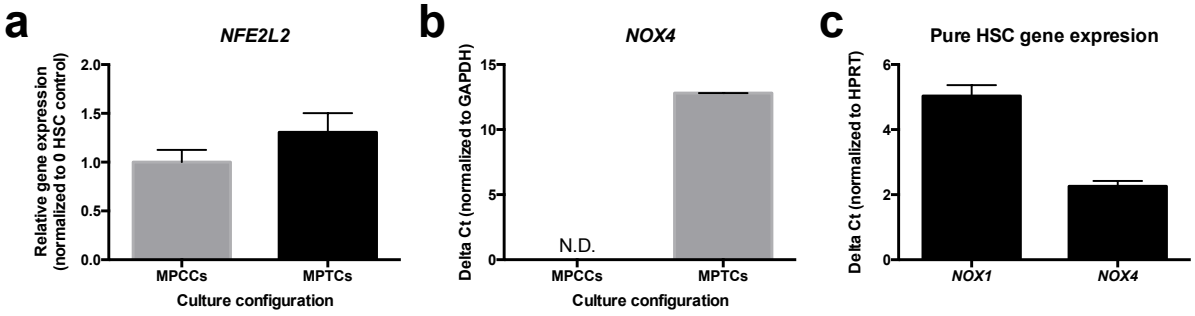

Supplemental Figure. 7.5.9. Oxidative stress-related signaling in micropatterned co-cultures (MPCCs), micropatterned tri-cultures (MPTCs), and pure cultures of activated hepatic stellate cells (HSCs). MPCCs containing primary human hepatocytes (PHHs) and 3T3-J2 fibroblasts, and MPTCs containing PHHs, 3T3-J2 fibroblasts, and 2.5K HSCs were created as described in figure 1 of the main manuscript. **(a)** Nuclear factor Erythroid 2 like 2 (*NFE2L2,* also known as Nrf2) gene expression after 2 weeks of culture in MPTCs (n=2 wells) normalized to MPCC controls (n=3 wells). **(b)** Delta Ct levels of NADPH-oxidase 4 (*NOX4*) gene expression in MPTCs and lack of *NOX4* gene expression in MPCCs (N.D., not detected) after 2 weeks of culture. *NOX1* was not detected in MPCCs or MPTCs (not shown). **(c)** Delta Ct levels of *NOX1*

and *NOX4* gene expression in pure HSC cultures after 2 weeks in culture (n=3 wells). Note the significantly higher expression (lower Delta Ct) of *NOX4* relative to *NOX1*. Glyceraldehyde 3-phosphate dehydrogenase (GAPDH) was used as the housekeeping gene for panels 'a' and 'b', while hypoxanthine-guanine phosphoribosyltransferase (*HPRT*) was used as the housekeeping gene for panel 'c'. Error bars on average values represent SD (n=2-3 wells as indicated above for each panel).

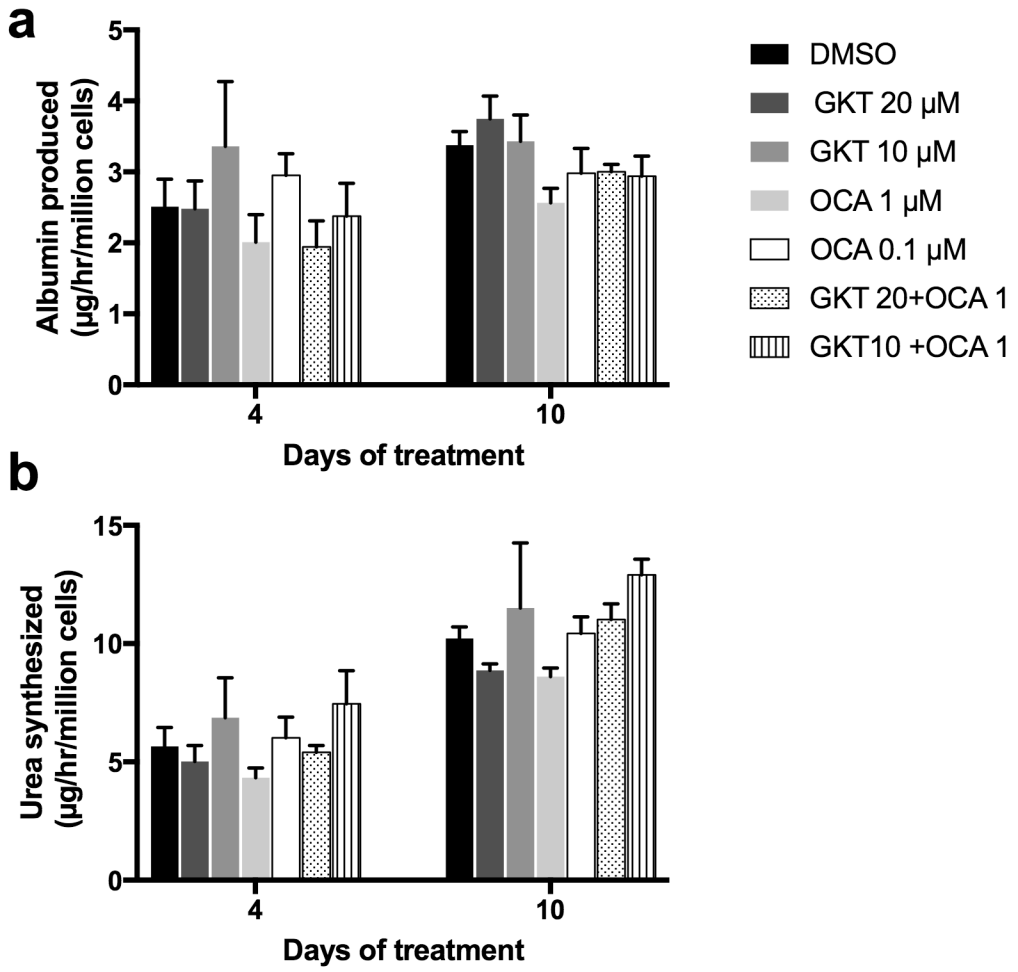

Supplemental Figure. 7.5.10. Albumin and urea secretions (as markers of hepatotoxicity) in micropatterned tri-cultures (MPTCs) treated with drugs and their combinations. (a) Albumin secretion over time in MPTCs (containing micropatterned primary human hepatocytes, growth-arrested 3T3-J2 fibroblasts, and 2.5K hepatic stellate cells) treated with vehicle control (dimethylsulfoxide, DMSO), two doses of GKT137831 (GKT), two doses of obeticholic acid (OCA), and a mixture of both GKT (20 µM and 10 µM) and OCA (1 µM) at the indicated doses. **(b)** Dosing as in panel 'a' except urea synthesis from MPTCs is shown. Error bars on average values represent SD (n=3 wells).

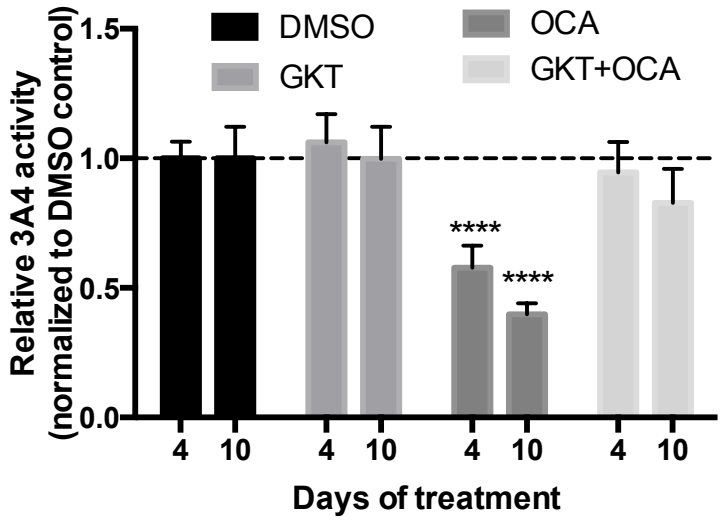

Supplemental Figure. 7.5.11. CYP3A4 activity in micropatterned co-cultures (MPCCs) treated with individual drugs, drug combination, and the vehicle control. CYP3A4 activity over time in MPCCs treated with vehicle control (dimethylsulfoxide, DMSO), 20 μM GKT137831 (GKT), 1 μM obeticholic acid (OCA), and a mixture of both GKT (20 μM) and OCA (1 μM). Data is normalized to the CYP3A4 activity measured in DMSO-treated MPCCs. Error bars on average values represent SD (n=5 wells). **** $p \leq 0.0001$ relative to vehicle control for the respective time point.

References

1. Chalasani N, Younossi Z, Lavine JE, Diehl AM, Brunt EM, Cusi K, et al. The diagnosis and management of non-alcoholic fatty liver disease: practice Guideline by the American Association for the Study of Liver Diseases, American College of Gastroenterology, and the American Gastroenterological Association. Hepatology. p. 2005–23, 2012.

2. Calzadilla Bertot L, Adams LA. The Natural Course of Non-Alcoholic Fatty Liver Disease. **17**(5), 2016.

3. Merrell MD, Cherrington NJ. Drug metabolism alterations in nonalcoholic fatty liver disease. Drug Metab. Rev. **43**(3), 317, 2011.

4. Hardwick RN, Fisher CD, Canet MJ, Scheffer GL, Cherrington NJ. Variations in ATP-Binding Cassette Transporter Regulation during the Progression of Human Nonalcoholic Fatty Liver Disease. Drug metabolism and disposition. **39**(12), 2395, 2011.

5. Wree A, Broderick L, Canbay A, Hoffman HM, Feldstein AE. From NAFLD to NASH to cirrhosis-new insights into disease mechanisms. Nature Publishing Group. **10**(11), 627, 2013.

6. Syn W-K, Oo YH, Pereira TA, Karaca GF, Jung Y, Omenetti A, et al. Accumulation of natural killer T cells in progressive nonalcoholic fatty liver disease. Hepatology. **51**(6), 1998, 2010.

7. Puche JE, Lee YA, Jiao J, Aloman C, Fiel MI, Muñoz U, et al. A novel murine model to deplete hepatic stellate cells uncovers their role in amplifying liver damage in mice. Hepatology. **57**(1), 339, 2013.

8. Friedman SL. Hepatic Stellate Cells: Protean, Multifunctional, and Enigmatic Cells of the Liver. Physiological Reviews. **88**(1), 125, 2008.

9. Angulo P, Kleiner DE, Dam-Larsen S, Adams LA, Bjornsson ES, Charatcharoenwitthaya P, et al. Liver Fibrosis, but No Other Histologic Features, Is Associated With Long-term Outcomes of Patients With Nonalcoholic Fatty Liver Disease. Gastroenterology. **149**(2), 389, 2015.

10. Hebbard L, George J. Animal models of nonalcoholic fatty liver disease. Nat Rev Gastroenterol Hepatol. **8**(1), 34, 2011.

11. Shih H, Pickwell GV, Guenette DK, Bilir B, Quattrochi LC. Species differences in hepatocyte induction of CYP1A1 and CYP1A2 by omeprazole. Hum Exp Toxicol. **18**(2), 95, 1999.

12. Teufel A, Itzel T, Erhart W, Brosch M, Wang XY, Kim YO, et al. Comparison of Gene Expression Patterns Between Mouse Models of Nonalcoholic Fatty Liver Disease and Liver Tissues From Patients. Gastroenterology. **151**(3), 513, 2016.

13. Godoy P, Hewitt NJ, Albrecht U, Andersen ME, Ansari N, Bhattacharya S, et al. Recent advances in 2D and 3D in vitro systems using primary hepatocytes, alternative hepatocyte sources and non-parenchymal liver cells and their use in investigating mechanisms of hepatotoxicity, cell signaling and ADME. Arch Toxicol. **87**(8), 1315, 2013.

14. Khetani SR, Bhatia SN. Microscale culture of human liver cells for drug development. Nat Biotechnol. **26**(1), 120, 2007.

15. Davidson MD, Lehrer M, Khetani SR. Hormone and Drug-Mediated Modulation of Glucose Metabolism in a Microscale Model of the Human Liver. Tissue Engineering Part C: Methods. **21**(7), 716, 2015.

16. Godoy P, Widera A, Schmidt-Heck W, Campos G, Meyer C, Cadenas C, et al. Gene network activity in cultivated primary hepatocytes is highly similar to diseased mammalian liver tissue. Arch Toxicol. 1, 2016.

17. Bhatia SN, Balis UJ, Yarmush ML, Toner M. Effect of cell–cell interactions in preservation of cellular phenotype: cocultivation of hepatocytes and nonparenchymal cells. FASEB J. 1999.

18. Riccalton-Banks L, Liew C, Bhandari R, Fry J, Shakesheff K. Long-term culture of functional liver tissue: three-dimensional coculture of primary hepatocytes and stellate cells. Tissue Engineering. **9**(3), 401, 2003.

19. Lee S-A, No DY, Kang E, Ju J, Kim DS, Lee S-H. Spheroid-based three-dimensional liver-on-a-chip to investigate hepatocyte-hepatic stellate cell interactions and flow effects. Lab on a chip. **13**(18), 3529, 2013.

20. Krause P, Saghatolislam F, Koenig S, Unthan-Fechner K, Probst I. Maintaining hepatocyte differentiation in vitro through co-culture with hepatic stellate cells. In Vitro Cell Dev Biol - Animal. **45**(5-6), 205, 2009.

21. Wong SF, No DY, Choi YY, Kim DS, Chung BG, Lee S-H. Concave microwell based size-controllable hepatosphere as a three-dimensional liver tissue model. Biomaterials. **32**(32), 8087, 2011.

22. Thomas RJ, Bhandari R, Barrett DA, Bennett AJ, Fry JR, Powe D, et al. The effect of three-dimensional co-culture of hepatocytes and hepatic stellate cells on key hepatocyte functions in vitro. Cells, tissues, organs. **181**(2), 67, 2005.

23. Norona LM, Nguyen DG, Gerber DA, Presnell SC, LeCluyse EL. Modeling Compound-Induced Fibrogenesis In Vitro Using Three-Dimensional Bioprinted Human Liver Tissues. Toxicological Sciences. 2016.

24. Khetani SR, Berger DR, Ballinger KR, Davidson MD, Lin C, Ware BR. Microengineered liver tissues for drug testing. J Lab Autom. **20**(3), 216, 2015.

25. Khetani SR, Szulgit G, Del Rio JA, Barlow C, Bhatia SN. Exploring interactions between rat hepatocytes and nonparenchymal cells using gene expression profiling. Hepatology. **40**(3), 545, 2004.

26. Lin C, Shi J, Moore A, Khetani SR. Prediction of Drug Clearance and Drug-Drug Interactions in Microscale Cultures of Human Hepatocytes. Drug metabolism and disposition: the biological fate of chemicals. **44**(1), 127, 2016.

27. Davidson MD, Ballinger KR, Khetani SR. Long-term exposure to abnormal glucose levels alters drug metabolism pathways and insulin sensitivity in primary human hepatocytes. Sci. Rep. **6**, 28178, 2016.

28. De Minicis S, Seki E, Uchinami H, Kluwe J, Zhang Y, Brenner DA, et al. Gene expression profiles during hepatic stellate cell activation in culture and in vivo. **132**(5), 1937, 2007.

29. Olsen AL, Bloomer SA, Chan EP, Gaça MDA, Georges PC, Sackey B, et al. Hepatic stellate cells require a stiff environment for myofibroblastic differentiation. AJP: Gastrointestinal and Liver Physiology. **301**(1), G110, 2011.

30. Zamek-Gliszczynski MJ, Xiong H, Patel NJ, Turncliff RZ, Pollack GM, Brouwer K. Pharmacokinetics of 5 (and 6)-carboxy-2 “,7 -”dichlorofluorescein and its diacetate promoiety in the liver. Journal of Pharmacology and Experimental Therapeutics. **304**(2), 801, 2003.

31. Min H-K, Kapoor A, Fuchs M, Mirshahi F, Zhou H, Maher J, et al. Increased hepatic synthesis and dysregulation of cholesterol metabolism is associated with the severity of nonalcoholic fatty liver disease. Cell Metabolism. **15**(5), 665, 2012.

32. Kim J, Keum Y-S. NRF2, a Key Regulator of Antioxidants with Two Faces towards Cancer. Oxidative medicine and cellular longevity. **2016**, 2746457, 2016.

33. Lan T, Kisseleva T, Brenner DA. Deficiency of NOX1 or NOX4 Prevents Liver Inflammation and Fibrosis in Mice through Inhibition of Hepatic Stellate Cell Activation. PLoS ONE. Public Library of Science; **10**(7), e0129743, 2015.

34. Jiang JX, Chen X, Serizawa N, Szyndralewiez C, Page P, Schröder K, et al. Liver fibrosis and hepatocyte apoptosis are attenuated by GKT137831, a novel NOX4/NOX1 inhibitor in vivo. Free Radic. Biol. Med. **53**(2), 289, 2012.

35. MD PBAN-T, MD RL, MD PAJS, MD PJEL, Van Natta MHS ML, MD MFA, et al. Farnesoid X nuclear receptor ligand obeticholic acid for non-cirrhotic, non-alcoholic steatohepatitis (FLINT):a multicentre, randomised, placebo-controlled trial. The Lancet. Elsevier Ltd; **385**(9972), 956, 2015.

36. Khetani SR, Kanchagar C, Ukairo O, Krzyzewski S, Moore A, Shi J, et al. Use of Micropatterned Cocultures to Detect Compounds That Cause Drug-Induced Liver Injury in Humans. Toxicological Sciences. **132**(1), 107, 2013.

37. Berger DR, Ware BR, Davidson MD, Allsup SR, Khetani SR. Enhancing the Functional Maturity of Induced Pluripotent Stem Cell-Derived Human Hepatocytes by Controlled Presentation of Cell-Cell Interactions In Vitro. Hepatology. **61**(4), 1370, 2015.

38. Bitter A, Rümmele P, Klein K, Kandel BA, Rieger JK, Nüssler AK, et al. Pregnane X receptor activation and silencing promote steatosis of human hepatic cells by distinct lipogenic mechanisms. Arch Toxicol. **89**(11), 2089, 2014.

39. Tziomalos K, Athyros VG, Paschos P, Karagiannis A. Nonalcoholic fatty liver disease and statins. Metabolism: clinical and experimental. **64**(10), 1215, 2015.

40. Tyndale RF, Sellers EM. Variable CYP2A6-mediated nicotine metabolism alters smoking behavior and risk. Drug metabolism and disposition. **29**(4), 548, 2001.

41. Yamamiya I, Yoshisue K, Ishii Y, Yamada H, Chiba M. Effect of CYP2A6 genetic polymorphism on the metabolic conversion of tegafur to 5-fluorouracil and its enantioselectivity. Drug metabolism and disposition: the biological fate of chemicals. **42**(9), 1485, 2014.

42. Jeong W-I, Osei-Hyiaman D, Park O, Liu J, Bátkai S, Mukhopadhyay P, et al. Paracrine Activation of Hepatic CB1 Receptors by Stellate Cell-Derived Endocannabinoids Mediates Alcoholic Fatty Liver. Cell Metabolism. **7**(3), 227, 2008.

43. Bettaieb A, Jiang JX, Sasaki Y, Chao T-I, Kiss Z, Chen X, et al. Hepatocyte NADPH Oxidase 4 Regulates Stress Signaling, Fibrosis, and Insulin Sensitivity During Development of Steatohepatitis in Mice. Gastroenterology. Elsevier Ltd; 1, 2015.

44. Wieckowska A, Papouchado BG, Li Z, Lopez R, Zein NN, Feldstein AE. Increased Hepatic and Circulating Interleukin-6 Levels in Human Nonalcoholic Steatohepatitis. Am J Gastroenterology. **103**(6), 1372, 2008.

45. Ogura J, Terada Y, Tsujimoto T, Koizumi T, Kuwayama K, Maruyama H, et al. The Decrease in Farnesoid X Receptor, Pregnane X Receptor and Constitutive Androstane Receptor in the Liver after Intestinal Ischemia-Reperfusion. J Pharm Pharm Sci. **15**(5), 616, 2012.

46. Trasino SE, Tang X-H, Jessurun J, Gudas LJ. A retinoic acid receptor β2 agonist reduces hepatic stellate cell activation in nonalcoholic fatty liver disease. J Mol Med. Springer Berlin Heidelberg; **94**(10), 1143, 2016.

47. Rae JM, Johnson MD, Lippman ME, Flockhart DA. Rifampin is a selective,

pleiotropic inducer of drug metabolism genes in human hepatocytes: studies with cDNA and oligonucleotide expression arrays. The Journal of pharmacology and experimental therapeutics. **299**(3), 849, 2001.

48. Teodoro JS, Rolo AP, Palmeira CM. Hepatic FXR: key regulator of whole-body energy metabolism. Trends Endocrinol. Metab. **22**(11), 458, 2011.

49. de Aguiar Vallim TQ, Tarling EJ, Edwards PA. Pleiotropic Roles of Bile Acids in Metabolism. Cell Metabolism. Elsevier Inc; **17**(5), 657, 2013.

50. Figge A, Lammert F, Paigen B, Henkel A, Matern S, Korstanje R, et al. Hepatic overexpression of murine Abcb11 increases hepatobiliary lipid secretion and reduces hepatic steatosis. The Journal of Biological Chemistry. **279**(4), 2790, 2004.

51. Marrone G, Shah VH, Gracia-Sancho J. Sinusoidal communication in liver fibrosis and regeneration. Journal of Hepatology. **65**(3), 608, 2016.

52. Nguyen TV, Nguyen TV, Ukairo O, Ukairo O, Khetani SR, Khetani SR, et al. Establishment of a hepatocyte-kupffer cell coculture model for assessment of proinflammatory cytokine effects on metabolizing enzymes and drug transporters. **43**(5), 774, 2015.

Chapter 8

Conclusions and future work

8.1 Conclusions

This dissertation methodically developed healthy and diseased in vitro culture platforms that can be used for various applications but were inspired by the need for human-relevant metabolic liver disease models. This was done by first developing methods to measure and quantify hepatocyte health and disease and then using those methods to constantly re-appraise the health status of hepatocytes in this culture system. This relentless pursuit of the healthiest cells possibly led to the identification of physiologically relevant ways to improve cell health. These include normoglycemic culture medium, dynamic serum and hormone removal (ie. starvation), normoinsulinemia as well as the use of human serum. After identifying these retrospectively simple factors that dramatically improved cell function and health, one major conclusion that could be drawn is that researchers should always question every component found in the medium that is suggested for their cell type, and have a clear reason why that component is necessary. Regardless, the advancements made with these culture medium alterations and practices made it possible to develop the disease models that inspired this entire dissertation. These models consisted of a NAFLD mimic model where exogenous fatty acids were used to induce a steatotic state, which could then be probed for pathways and enzymes responsible for the detrimental symptoms of type II diabetes. Additionally, the modified MPCC was amenable to the incorporation of another liver cell, the hepatic stellate cell, which allowed

for the development of an in vitro model of NASH. Importantly, we were able to screen this model for efficacious therapies and we believe this system holds great promise for identifying therapies to alleviate this fatal disease. Overall the advances described within lay the groundwork for substantial and important future studies.

8.2 Future work

8.2.1 Periodic starvation

The dramatic changes we observed by simply starving our MPCCs could not have been predicted a priori and it raises the question of how a more physiologically relevant fasting and feeding cycle may benefit hepatocyte functions and lifetime over the static starvation protocol we developed. Current work in out lab is geared towards developing microfluidic devices that allow the user to dynamically tune all components that are administered to cultures housed within these chips. One great application for such technology would be to systematically oscillate every component in our cell culture medium to identify which factors, when administered dynamically, can further boost the lifetime and health of hepatocytes. Insulin, glucagon, and glucose are known the fluctuate in the body, so this would be a great starting point.

We are also still unclear about why the starvation protocol increased the lifetime of our cultures over metformin-treated cultures. We suspect that the lack of excess nutrients found in serum during the starvation period allow the hepatocytes to activate more starvation pathways than what is activated via metformin treatment (ie. AMPK). Another possibility is that, as the

insulin resistance studies in chapter 5 showed, bovine serum ultimately has detrimental effects on hepatocytes over time. It will be important to assess how starvation benefits hepatocytes over non-starved cultures using the physiologic medium developed in chapter 5.

8.2.2 Physiologic medium and human serum

As mentioned in chapter 5, the physiologic medium formulation greatly enhanced various outputs from hepatocytes, but this was mostly enabled by the use of human serum, as these benefits were still seen in cultures maintained in human serum containing high levels of insulin. This suggests that human-specific factors may be critical to the dramatic enhancement in longevity that was observed by the use of human serum. Identifying these factors should enable the development of a fully defined serum-free medium that still enables high levels of hepatocyte functions. This will be especially beneficial for regenerative medicine efforts. The top human-specific candidates are lipid species, and bile acid/salt species.

Arachidonic acid is found in high levels in human plasma and it is known to activate AMPK, which we have previously shown is correlated with increased hepatocyte lifetime. As shown in chapter 7, bile acids, or synthetic derivatives, can have substantial effects on hepatocyte transporters. Specifically, obeticholic acid (OCA) treated cultures had increased transporter levels over DMSO-treated MPCC controls and bile acids have also been shown to activate AMPK and increase the level of transporter expression. Importantly, we did assess AMPK activation in cultures treated with human serum and observed less AMPK activation than bovine serum treated cultures.

Ultimately, screening the human serum lots we identified as beneficial for hepatocyte longevity should unlock the critical factors needed for gaining the benefits of the human serum. Lipidomics, metabolomics, and proteomics approaches could be used to compare human serum to bovine serum lots that we have validated with MPCCs over long-term culture. This comprehensive approach would eventually lead to identifying the critical factors for reverse engineering a defined serum replacement.

8.2.3 Studying insulin resistance in MPCCs

The highly insulin sensitive MPCC model developed throughout this dissertation should greatly enhance diabetes researcher abilities. Researchers that have been restricted to using animal models for all of their studies can finally confirm the trends they observe in their in vivo disease models with isolated human cells. Additionally, one great direction for this work is to use the same factors we identified as important for maintaining insulin sensitivity to create a rodent based hepatocyte model that is highly insulin sensitive. This would enable researchers to isolate hepatocytes from their genetically modified mouse/rat strains and confirm the trends observed in vivo with isolated cells.

This system also holds great promise for understanding the role of cell-cell interactions in insulin resistance development. Specifically, Kupffer macrophages have been shown essential in the development of insulin resistance in animal models. It would be interesting to incorporate macrophages into this system and see how different types of macrophages, either proinflammatory, M1, or anti-inflammatory, M2, macrophages modulate hepatocyte glucose output under insulin stimulation. Additionally, it could be interesting to assess how hepatic

stellate cells modulate hepatocyte insulin sensitivity since they cause massive lipid accumulations in hepatocytes and secrete IL-6, which is hypothesized to cause insulin resistance through activation of STAT3.

Ultimately, this system will be very useful for understanding organ-organ interactions. Specifically, a large body of evidence currently suggests that the adipose tissue is the major regulator of liver glucose output. Coupling the lab's current expertise in microfluidics with other researchers that have engineered adipose tissue mimics could enable some of the first highly functional liver-adipose-on-a-chip platforms.

8.2.3 Developing a high throughput model of liver fibrosis

Since hepatic stellate cells (HSC) were successfully incorporated into MPCCs, the next logical step is to assess the system's ability to model fibrosis. One unfortunate aspect of a 2D system like the MPCC is that the cultures reside on plastic, which is exceptionally stiff, compared to the liver, and likely activates HSCs without any additionally soluble cues since these cells are mechanosensitive. Studies will need to be carried out to first see if co-culturing HSCs with fibroblasts, as they are in MPTCs, prevents their activation over plastic alone. Additionally, prototypical fibrotic stimuli, such as transforming growth factor –beta (TGFb), will need to be tested on MPTCs to see if HSC activation markers can be further increased over the basal level in maintenance medium. This will be essential to have a model that mimics aspects of fibrosis and could eventually identify pro-fibrotic drugs.

Another area for development could be in the medium formulation as various factors found in the hepatocyte maintenance medium could lead to HSC activation. One factor left out of the

medium that is essential for HSC quiescence is vitamin A, and its addition could potentially reduce HSC activation in MPTCs. Additionally, if MPCCs could be created on compliant substrates, such as soft polyacrylamide gels, HSCs on this substrate might have a completely quiescent phenotype, which would allow for the development of a fibrotic response from a non-activated state.